

# **The Emergence of Social Hierarchy in Prehistory**

**Application of Fractal Analysis on  
Archaeological Settlement Plans**

Hallvard Bruvoll

Thesis submitted for the Degree of  
**Philosophiae Doctor (PhD)**

August 2023

Department of Archaeology, Conservation  
and History  
Faculty of Humanities



**UNIVERSITY  
OF OSLO**



# **Abstract**

English abstract here

Remember to add abstracts

Furholt, Grier, et al. (2020), Furholt, Müller, et al. (2020), Furholt, Müller-Scheeßel, et al. (2020) are three different publications. Furholt, Grier, et al. (2020), Furholt, Müller, et al. (2020), Furholt, Müller-Scheeßel, et al. (2020) are the same three publications in the same order. gfdsdfgs , Get on with it!



# **Sammendrag**

Norsk oversettelse av Abstract over. Trenger ikke være på ny side



# Preface

Add acknowledgements here



# Contents

<b>Abstract</b>	<b>iii</b>
<b>Sammendrag</b>	<b>v</b>
<b>Preface</b>	<b>vii</b>
<b>List of Figures</b>	<b>xi</b>
<b>List of Tables</b>	<b>xiii</b>
<b>I Frameworks</b>	<b>1</b>
<b>1 Introduction</b>	<b>3</b>
1.1 Background of the study . . . . .	3
1.2 Research question and objectives . . . . .	4
1.3 Defining hierarchies . . . . .	6
1.4 What is social hierarchy? . . . . .	9
1.5 Main findings here? . . . . .	11
1.6 Research ethics . . . . .	11
1.7 Structure of the thesis . . . . .	11
<b>2 Theoretical framework: Complexity and Fractals</b>	<b>13</b>
2.1 Very short introduction to Complexity Theory / Dynamical Systems Theory .	13

2.2	Very short introduction to Fractals and Fractal Analysis . . . . .	14
2.3	Very short introduction to micro-macro approaches in social theory . . . . .	16
<b>3</b>	<b>Material and data: social complexity in the European Neolithic</b>	<b>19</b>
3.1	Studying social hierarchy in archaeology and prehistory. . . . .	19
3.2	The Linear Pottery culture complex . . . . .	22
3.3	The Cucuteni-Trypillia culture complex . . . . .	23
3.4	Reading site plans from geomagnetic imagery . . . . .	23
3.5	Synthetic data . . . . .	24
<b>II</b>	<b>Size distributions</b>	<b>25</b>
<b>4</b>	<b>House sizes and social meaning</b>	<b>27</b>
4.1	Interpreting house-size differences . . . . .	27
4.1.1	House size and household organisation . . . . .	30
4.1.2	House size and wealth . . . . .	32
4.2	Distribution types and their underlying mechanisms . . . . .	35
4.2.1	Normal distributions and the Central Limit Theorem . . . . .	38
4.2.2	Exponential distributions and constant rates of growth and decay . . .	42
4.2.3	Log-normal distributions and Gibrat's law . . . . .	46
4.2.4	Power-law distributions, preferential attachment and hierarchy . . . .	52
4.2.5	Some variants of power-law distributions . . . . .	62
4.3	Fitting heavy-tailed distributions in archaeology . . . . .	65
<b>5</b>	<b>Methods: Distribution fitting</b>	<b>69</b>
5.1	Modelling heavy-tailed distributions . . . . .	70
5.2	Testing for false positive power-law tails . . . . .	73

5.3	False positives from data aggregation . . . . .	82
5.4	Summary of methodological procedure and tests . . . . .	85
<b>6</b>	<b>Results: Distribution fitting</b>	<b>89</b>
6.1	Settlements . . . . .	89
6.2	Quarters/neighbourhoods . . . . .	99
6.3	Temporal samples (Vráble) . . . . .	105
6.4	Summary of findings . . . . .	112
<b>III</b>	<b>Settlement Plans</b>	<b>115</b>
<b>7</b>	<b>Village planning in prehistory</b>	<b>117</b>
7.1	Settlement layout and social structure . . . . .	117
7.2	The geometries of conscious planning vs. emergent behaviour . . . . .	118
7.3	Fractal image analysis in archaeology . . . . .	118
<b>8</b>	<b>Methods: Fractal image analysis</b>	<b>119</b>
8.1	Calculating fractal dimension and lacunarity . . . . .	119
8.2	Effects from image size, element size and element count . . . . .	124
8.3	Effects from density and size distribution . . . . .	129
8.4	Quantification of self-similarity and random noise . . . . .	135
8.5	Summary of procedure and tests . . . . .	139
<b>9</b>	<b>Results: Image analysis</b>	<b>145</b>
9.1	Settlements . . . . .	146
9.2	Quarters/neighbourhoods . . . . .	149
9.3	Temporal samples (Vráble) . . . . .	153
9.4	Summary of findings . . . . .	156

<b>IV</b>	<b>Synthesis</b>	<b>159</b>
<b>10</b>	<b>Discussion: Social complexity in Linear Pottery and Trypillia settlements</b>	<b>161</b>
<b>11</b>	<b>Discussion: Fractal Analysis and Archaeological data</b>	<b>163</b>
11.1	Distribution fitting . . . . .	163
11.2	Image analysis . . . . .	165
11.3	Concluding remarks? . . . . .	166
<b>12</b>	<b>Conclusion and Outlook</b>	<b>167</b>
12.1	Things I would like to have done, but that didn't fit into this study . . . . .	167
12.2	Concluding remarks . . . . .	167
<b>References</b>		<b>169</b>
<b>Appendix</b>		<b>185</b>
<b>A</b>	<b>This is my first appendix</b>	<b>187</b>
<b>B</b>	<b>This is my second one</b>	<b>189</b>

# List of Figures

4.1	My short caption . . . . .	29
4.2	Example curves of the probability density function (PDF) of four common distribution types: normal (blue, $\mu = 50, \sigma = 8$ ), exponential (red, $\lambda = 0.1$ ), log-normal (green, $\mu = 3, \sigma = 0.5$ ) and power-law (purple, $\alpha = 3, x_{min} = 1$ ), in linear (a) and logarithmic scales (b). Parameter values are arbitrary and x-axis is truncated at $2 < x < 100$ for readability. The power-law distribution is the only to form a straight line when both scales are logarithmic	37
4.3	The same distributions as in Figure 4.2, but with the complementary (right-tail) cumulative distribution function (cCDF), in linear (a) and logarithmic scales (b), with $0 < x < 80$ for readability . . . . .	38
4.4	Exponential distribution of $y = \lambda^x$ with rate ( $\lambda$ ) fluctuating randomly and uniformly between 0.75 and 1.4, i.e. with a mean rate of approx. 1.08, over 40 periods ( $x$ ) from an initial value of 1. The plots figure 100 individual runs of the distribution, with linear (a) and logarithmic (b) y-axis. Over time, y-values at any given x are expected to be log-normally distributed by the Central Limit Theorem . . . . .	48
4.5	Density function of y-values from Figure 4.4 at $x = 40$ , with linear (a) and logarithmic (b) x-axis, following a typical log-normal distribution . . . . .	49
4.6	a: Exponential growth of 100 samples drawn from a normally distributed initial population ( $\mu = 10, \sigma = 2$ ), all following the same sequence of uniformly distributed rates ( $0.75 < \lambda < 1.4$ ). b: Over time, $\mu$ and $\sigma$ values change, but the distribution remains normal. Scales are linear . . . . .	50

- 4.7 Examples of power-law distributions with different scaling exponent ( $\alpha$ ) values on logarithmic axes, showing how this parameter reflects change over orders of magnitude. For a model with  $\alpha = 3$  (blue), a decrease in probability  $p(x)$  of 3 orders of magnitude (powers of 10), e.g. from 0.1 to 0.0001 corresponds to an increase in the size of  $x$  of 1 order. For a model with  $\alpha = 1.5$ , the same decrease in probability corresponds to an increase in  $x$  of 2 orders of magnitude. The models appear linear in logarithmic space, but are in reality highly non-linear, as illustrated by the grid . . . . . 54
- 4.8 A power-law distribution of sizes arranged in discrete levels, illustrating its characteristic scale invariance. From the largest element on top and downwards, sizes decrease while numbers (frequencies) increase, both exponentially but in opposite direction, generating a hierarchical fractal structure where the same shapes are recognised at different scales . . . . . 55
- 5.1 Synthetic data series drawn from four different distribution types: exponential ( $\lambda = 0.125$ ), log-normal ( $\mu = 0.3$ ,  $\sigma = 2$ ), power-law ( $\alpha = 2.5$ ) and stretched exponential/Weibull ( $shape = 0.5$  and  $scale = 3$ ), all with  $n = 100$  data points and  $x_{min} = 15$ . Plot equivalent to Fig.5a in Clauset et al. (2009), with deviations due to random fluctuations only. Scales are logarithmic, and all four series appear as roughly straight lines, though only one is a true power law . . . . . 75
- 5.2 Selected tail models for the same synthetic data sets, each with four sample sizes ( $n = 10^1, 10^2, 10^3, 10^4$ ). For each tail model,  $x_{min}$  is set at the value which gives the best power-law fit. Point size indicates fraction of data points thus included in the tail model. For power-law distributions, all samples are correctly identified, while this is the case only for large samples ( $n > 10^2$ ) of log-normal and exponential samples, smaller samples being interpreted as having power-law or stretched exponential tails . . . . . 76

5.3	Boxplot of all the synthetic data sets, overlaid (in red) with the data points interpreted as power-law tails. X axis is logarithmic – however the log-normal distributions do not appear symmetric since they are truncated with a lower threshold. Note that especially for log-normals and power laws, larger samples give longer tails. If the model predicts a probability of having a value of 10.000 or more as only 1 in 10.000 or 0.01%, a sample size of 10.000 will probably allow for one such value . . . . .	77
5.4	cCDF plot of 36 synthetic log-normal distributions with parameter values $1 \leq \mu \leq 6$ and $0.5 \leq \sigma \leq 3$ . Each distribution is generated with $n = 1000$ data points, but rendered here as lines for clarity. Scales are logarithmic . . . . .	79
5.5	Interpreted tail models of the same log-normal distributions. 19 of 36 distributions have tails that are best modelled as power laws. Symbol size indicates fraction of the data included in the tail, with $x_{min}$ parameter set for best possible power law fit. See text for details . . . . .	80
5.6	Boxplot of the same 36 synthetic log-normal distributions, overlaid (in red) with data points included in tails interpreted as power laws. The power-law tails stretch across the log-normal data in a range from 0.3% (3 data points out of 1000) to 23.5% . . . . .	81
5.7	Twenty series of sequentially aggregated log-normal distributions, starting with 100 data points and 100 more added for each iteration. Parameter values for every group of 100 data points are fixed at $\mu = 4.5$ and $\sigma = 0.4$ (a) or uniformly fluctuating between $4 < \mu < 5$ and $0.3 < \sigma < 0.5$ (b). Both settings give distributions that resemble those of Neolithic house-size distributions. Red lines indicate power-law tails. The series overlap to a large extent, so y axis is plotted with rank rather than normalised cCDF to facilitate readability. Scales are logarithmic . . . . .	84
5.8	The same aggregated distributions as above in box-plots, illustrating how the data ranges increase much more slowly with sample size than expected for log-normal distributions. Sample size is 100 for iteration 1 and increases by 100 to 2000 in iteration 20. Fluctuating parameter values (b) increase variance and the probability of finding power-law tails (red points). X axis is logarithmic	85

6.1	House sizes of the 13 analysed settlements, arranged according to median house size. Red dots represent houses with size $\geq x_{min}$ within distribution tails interpreted as power laws. X axis is logarithmic . . . . .	90
6.2	Analysed house-size distributions for whole settlements. a) Distributions with identified power-law tails. For clarity, only the tails (house sizes $\geq x_{min}$ ) are coloured and connecting lines are added within each settlement. The grey frame represents the extent of panel b. b) House-size distributions without power-law tails. Two settlements are atypical with their absence of large houses. Scales are logarithmic . . . . .	91
6.3	Power-law distributed houses at Vráble (Linear Pottery), arbitrarily grouped to three levels using the Jenks optimisation method integrated in QGIS for readability. Figure made by author with data from Müller-Scheeßel et al. (2020)	95
6.4	Power-law distributed houses at Maidanetske (Trypillia), grouped to three levels with Jenks optimisation. The levels are arbitrary but overlap well with the typological distinction between mega-structures (dark blue) and other houses. Hierarchical scaling includes far more houses than the mega-structures, and is distributed across the settlement. Figure made by author with data from Ohlrau (2020) . . . . .	96
6.5	Power-law distributed houses at Nebelivka (Trypillia), grouped into four arbitrary levels with Jenks optimisation, the two largest of which are overlapping with the typological levels of the “Mega-structure” and the “Assembly Houses”. Figure made by author with data from Hale (2020) . . . . .	97
6.6	Power-law distributed houses at Moshuriv (Trypillia), grouped arbitrarily into three size categories using Jenks optimisation. Made by author with data from Ohlrau (2020) . . . . .	98
6.7	House-size distributions of individual quarters for Nebelivka and neighbourhoods for Vráble, arranged according to median house size. Red dots indicate houses of size $\geq x_{min}$ in cases where the distribution tail was interpreted as a power law. X axis is logarithmic . . . . .	100

6.8	Survival function of the same house-size distributions of quarters/neighbourhoods. Coloured dots represent houses within power-law tails. Three series were not interpreted as power laws. Scales are logarithmic . . . . .	101
6.9	Power-law distributed houses in quarters D to G in Nebelivka, fitted by quarter (top) and for the settlement as a whole (bottom). Quarter-wise distribution fitting does not identify hierarchical scaling in quarter E, though many of the houses there are included in the power-law model for the whole settlement. Size categories are arbitrary (three levels with Jenks optimisation) and values differ between quarters. Legend values correspond to quarter F. Figure by author with data from Hale (2020) . . . . .	104
6.10	House-size distributions at single time samples for the entire settlement at Vráble (a) and the South-West neighbourhood only (b). Red dots indicate houses with power-law distributed size. Only distributions including more than 10 houses are represented. In plot b, the single largest house of each sample is also excluded. X axis is logarithmic . . . . .	107
6.11	Survival function of the same house-size distributions of time samples for Vráble (a) and Vráble SW only excluding the largest house of each sample (b). Coloured dots represent houses within power-law tails. Power-law tails persist despite the gradual breaking down of the data set. Scales are logarithmic	109
6.12	Vráble at three temporal samples, with house sizes above $x_{min}$ grouped into three arbitrary classes by Jenks optimisation. Parameter values differ slightly between time samples (see table), and the legend categories refer to the 5130 sample. Counter-clockwise shift in house orientation is used as proxy for construction date . . . . .	112
8.1	Effects from image size, element count and element size on fractal dimension and lacunarity. Density is fixed at 0.25 for all images. Number labels represent iteration within each series. Image size is variable in the upper and lower series, house size in the upper and the vertical series, and house count in the vertical and the lower series. The three corner images are identical for two series each. Images are selected here to prevent overlaps . . . . .	125

8.2	Different image sizes and house sizes, with $N = 4$ and density = 0.25. Resulting fractal dimension ( $D$ ) and mean lacunarity ( $L\_mean$ , plot a) and exponent lacunarity (plot b). Images are numbered by iteration . . . . .	126
8.3	Variable element count ( $N$ ) and image size, with constant house length of 10 pixels and density at 0.25. Resulting fractal dimension ( $D$ ) and mean lacunarity ( $L\_mean$ , plot a) and exponent lacunarity ( $L$ , plot b). Images are numbered by iteration . . . . .	127
8.4	Variable house count ( $N$ ) and house size, with fixed image size of $420^2$ pixels and density at 0.25. Resulting fractal dimension ( $D$ ) and mean lacunarity ( $L\_mean$ , plot a) and exponent lacunarity ( $L$ , plot b). Images are numbered by iteration . . . . .	129
8.5	Fractal dimension and mean lacunarity of images with identical size and layout, but with densities varying with linear increments from 0.05 to 1. Number labels represent iteration, and images are selected to prevent overlaps . . . . .	131
8.6	Fractal dimension and lacunarity measures on the same 20 images with varying density. Because of pixelation the first image was rounded up to be identical to the second, with density = 0.01. Number labels represent iterations . .	132
8.7	Fractal dimension and mean lacunarity of images with identical size, layout and density but with varying size distributions of single elements, from uniform (image 1) to log-normal with $\sigma = 0.9$ (image 20), in linear increments of $\sigma$ from 0. Number labels represent iteration, and images are selected here to prevent overlaps . . . . .	133
8.8	Fractal dimension and lacunarity estimates of the whole image series, with 729 square points varying in size distribution from uniform (log-normal with $\sigma = 0$ ) to log-normal with $\sigma = 0.9$ . For each image, sizes were normalised so that they together covered 25% of the total image area, notwithstanding some overlaps causing image density to descend to a minimum of 0.242. Label numbers indicate iteration . . . . .	134

8.9 Fractal dimension and mean lacunarity of images of identical size, layout and density, but with degrees of hierarchical clustering, from no clustering (image 1) to high clustering in two levels, where the space between clusters represent 8% of the superior level's total length and the points start to percolate (image 20). Number labels represent iteration, and images are selected to prevent overlaps . . . . .	136
8.10 Fractal dimension and lacunarity measures on the same images with varying degrees of spatial clustering, and fixed image size, density, element count and size distributions. Number labels represent iteration . . . . .	137
8.11 Different degrees of random spatial noise . . . . .	138
8.12 Estimates of fractal dimension ( $D$ ) and mean lacunarity (plot a) and exponent lacunarity (plot b), of 20 images with increasing degrees of added random spatial noise. Number labels represent iteration . . . . .	139
8.13 The first and last images of the clustering, size distribution and noise series, as well as images 8, 10 and 12 of the density series, showing how only small increments in density – here from 0.16 (im. 8) to 0.36 (im. 12) – generate changes in fractal dimension and lacunarity that are larger than those induced by the whole range of the other variables. Density image 10 is identical to image 1 of the three other series, and has density value 0.25 . . . . .	141
8.14 Fractal dimension and lacunarity estimates of all synthetic images analysed in this chapter. $L_{mean}$ and $L$ show largely similar distributions but with some marked differences. See text for details. The grey frame in plot a shows the extent of Figure 8.13 . . . . .	142
9.1 Fractal dimension and mean lacunarity (plot a) and exponent lacunarity (plot b) for all 46 images analysed in this chapter. Values are presented as a data table in Appendix #add ref . . . . .	146

9.2	Settlements plans quantified through their fractal dimension ( $D$ ) and mean lacunarity ( $L\_mean$ , plot a) and house count ( $N$ ) and density (plot b). In plot b, scales are logarithmic, and the y axis is reversed, in order to obtain as similar results as possible to those shown in plot a. The settlements of Talne 3 and Horný Oháj had images that were smaller than the lower threshold proposed in the previous chapter . . . . .	147
9.3	Plans of the same settlements, plotted by $D$ and $L\_mean$ . Image sizes are not internally to scale – size differences are reduced to facilitate readability, as the mega-sites are in reality orders of magnitude larger than the smallest ones	148
9.4	$D$ and $L\_mean$ residuals for the same settlements after subtracting expected values due to image density alone, modelled on the synthetic images with variable density presented in Chapter 8. See #table for details . . . . .	150
9.5	Fractal dimension ( $D$ ) and mean lacunarity ( $L\_mean$ , plot a) and house count ( $N$ ) and density (plot b) of the plans of separate Nebelivka quarters and Vráble neighbourhoods. The image size of Nebelivka E was below the lower threshold of 260*260 pixels. Axes in plot b are logarithmic, with the y-axis reversed, in order to reproduce the spread in plot a . . . . .	151
9.6	Plans of Nebelivka quarters and Vráble neighbourhoods, placed according to fractal dimension ( $D$ ) and mean lacunarity ( $L\_mean$ ). Image sizes are transformed to allow for better visibility of smaller images. The two layout types representative of Trypillia (Nebelivka) and Linear Pottery (Vráble) settlements largely overlap . . . . .	152
9.7	Fractal dimension and mean lacunarity estimate residuals after controlling for effects from density, on the same quarter and neighbourhood images. Values expected from density are modelled on the density series of synthetic images in the previous chapter, see #table . . . . .	153
9.8	Fractal dimension ( $D$ ) and mean lacunarity ( $L\_mean$ , plot a) and house count ( $N$ ) and image density (plot b) of the site plan of the Linear Pottery settlement of Vráble, subset into 15 coeval time samples with 20 year intervals. Axes in plot b are logarithmic and with reversed y axis in order to emulate plot a . . .	154

9.9	The temporal development of Vráble (Linear Pottery), as seen through the fractal dimension ( $D$ ) and mean lacunarity ( $L_{mean}$ ) of coeval samples of its settlement plan. Images are selected here to prevent overlaps . . . . .	155
9.10	Fractal dimension and mean lacunarity residuals after controlling for effects from image density, following the models presented in #Tab. in the previous chapter. . . . .	156



# List of Tables

6.1	short caption . . . . .	93
6.2	Results of distribution fitting on separate quarters at Nebelivka and neighbourhoods at Vráble, arranged by tail model and parameter. Par1 and Par2 indicate $\mu$ and $\sigma$ for log-normal distributions, and T_Par1 is $\alpha$ for power-law and $\lambda$ for exponential tail distributions. Gini index is calculated on the entire sample . . . . .	102
6.3	Distribution analysis results for Vráble, subdivided into time samples with coeval houses, arranged chronologically. The analysis was also done on the South-West neighbourhood separately, where the single largest house for each sample was excluded. In both series, only samples consisting of 10 houses or more were analysed. Par1 and Par2 are $\mu$ and $\sigma$ for log-normal and normal distribution models. T_Par1 is $\alpha$ for power-law and $\lambda$ for exponential tail models. Tail_P is the proportion of data points (N) in the tail model (N_Tail), or N_Tail/N. Gini index is calculated on the entire sample distribution . . . . .	110
8.1	Linear models of fractal dimension ( $D$ ), exponent lacunarity ( $L$ ) and mean lacunarity ( $L_{mean}$ ) with the log-transformations that give the best fit, evaluated by the coefficient of determination ( $R^2$ ). The third model can be written in power-law form as $L_{mean} = 0.862 * density^{-0.61}$ . . . . .	142



# **Part I**

## **Frameworks**



# Chapter 1

## Introduction

### 1.1 Background of the study

- Studying social hierarchy in prehistory through fractal analysis of settlement plans
- In Europe, the Neolithic is the long and messy transition period between mobile hunter-gatherer groups in the Palaeo- and Mesolithic, and the first city states in the Bronze (Aegean) and Iron Ages (Mediterranean and Central Europe)
- Early farming economy, influence from the Near East.
- Large variety in scale and content of archaeologically defined culture groups. Single farmsteads and small hamlets in many phases – some with hardly any settlement evidence at all **examples mid-neo, use Shennan (2018)**. Other phases include exceptionally large settlements, probably hosting populations of several thousand inhabitants, like at Maidanetske in central Ukraine around 3.800 BCE (see 3.3). While in some settings, like in Linear Pottery society in much of continental Europe north of the Alps towards 5.100 BCE (see 3.2), the dead were buried in simple pit graves, with very little distinction in treatment between individuals, in other phases some individuals were buried with tremendous amounts of precious goods like in Varna, Romania, or under colossal burial mounds like in Carnac, France, both in the mid-5th millennium (Shennan, 2018)**check ref.**
- Seen at a very large scale – across the continent and through the Holocene – the development of society from small scale and relatively egalitarian towards large scale

and more hierarchical seems evident (though not to everyone, see Graeber & Wengrow (2021) and Section ??). When we look more closely however, this evolution is anything but linear, as both population sizes and levels of hierarchical organisation seem to fluctuate considerably, sometimes over short time spans as from the Trypillia **C2 to D1??, check this**, when the so-called mega-sites are abandoned and their former inhabitants regroup into much smaller settlements during a transition of maybe only **check and ref** years.

- In many cases, the level of social hierarchisation and complexity in a given Prehistoric society is very hard for researchers to evaluate, since many indicators of such structures are either lost from the archaeological record, or were never included in the first place [Perreault (2019); Section 3.1]. Archaeological traces that are often interpreted as signs of social complexity and hierarchy may furthermore be deceiving. Seemingly monumental structures were in many cases built through small additions over centuries, rather than in one colossal construction campaign [**example, Carnac alignments? Danish megaliths?**]. In many megalithic burial contexts, it may be impossible to know how large a segment of the society that had access to such inhumations (**rephrase**).
- New methods for investigating hierarchy: fractal analysis. Borrowed from other disciplines, not much tested in archaeology. Example from human geography, use:(Batty, 2005; Batty & Longley, 1994; D'Acci, 2019; Jahanmiri & Parker, 2022; Lagarias & Prastacos, 2021; Tannier & Pumain, 2005) (say what fractal analysis does, don't explain what it is here)(explain just the word fractal and cite section).

## 1.2 Research question and objectives

The overall goal of the present study is to test and assess the utility of fractal analysis techniques as tools for studying hierarchical social organisation in prehistoric societies. Two methodological approaches are under special scrutiny: the distribution fitting approach and the image analysis approach (C. T. Brown et al., 2005; C. Brown & Liebovitch, 2010). These are applied to architectural data series from well-preserved and documented archaeological samples within Neolithic Linear Pottery and Trypillia contexts, as well as to synthetic data series. This thesis is thus not to be considered a culture-historic study of Linear Pottery or

Trypillia society, but mainly a methodological study with two case studies. However, results from the proposed analyses of these cases may also contribute, as side-effects, to their respective fields of research.

For the distribution fitting approach, house-size distributions within settlements are modelled following a given procedure, and the retained model (the best fit) is interpreted in terms of social generating mechanisms. In particular, it is argued here that so-called power-law distributions reflect hierarchical structure, so that the identification of these within the studied samples may indicate the presence of some social hierarchisation process which warrants further interpretation.

With the image analysis approach, the spatial layouts of archaeological and synthetic settlement plans are analysed through the calculation of fractal dimension and lacunarity – summary statistics which serve as quantifications of irregular spatial patterns or image textures. I argue here that geometrically irregular settlement plans are indicative of relative independence between households, while settlements that develop within geometrically regular grids indicate stronger overarching social structures, with a continuous range of possibilities in-between. The goal here is to test to which extent quantitative measures like fractal dimension and lacunarity may help differentiating between varying degrees of planning in prehistoric settlements.

While both these methodological approaches are well developed and integrated to other disciplines (Jahanmiri & Parker, 2022; e.g. in urban science, see Lagarias & Prastacos, 2021), their usage in archaeology have so far remained anecdotal (Diachenko, 2018). A further overall goal of this thesis is to identify and explore possible constraints in the nature of archaeological data that may limit the applicability of fractal analysis methods within this discipline. For example, does fractal analysis of settlement plans require a data quality that would be practically unattainable in archaeological settings? But also inversely, as it is impossible to explore all potential applications within the framework of one doctoral thesis, suggestions for future research are provided in the last chapter.

## 1.3 Defining hierarchies

The term *hierarchy* is central to the present study. Though commonly used in daily speech, defining the word is not as straight-forward as one might think, so some clarification on how it is understood here might be needed. In a volume dedicated to exploring the meanings and uses of hierarchy as a study object within a range of natural and social sciences, Denise Pumain provides a panorama of definition nuances, but also highlighting the characteristics that are commonly found in most cases (Pumain, 2006). Among these characteristics are:

- A pyramidal organisation of elements, ordered by a very unequal size distribution of a certain quality or variable, from a few large elements on top to many small elements at the bottom
- When seen as a system, the whole is constituted of sub-systems, which are again constituted of sub-sub-systems, and so forth. These can either be ordered into clearly distinguished levels (stratified), or in other cases be scaled in a continuum (branched or tree structure)
- In physical, biological and social hierarchical systems, the structure is often accompanied by a flow of energy, material, information or control in one or both directions between the top and bottom levels

Hierarchies are found in humanly constructed classification and taxonomical systems, where morphological distinctions are considered more important or fundamental at the higher end of the hierarchy, while being more detailed or specific at the lower end. Many hierarchical social systems, like religious (from Greek *hieros* – sacred, and *archē* – government), military or corporate organisations, include strongly reinforced regulations of subordination, which in modern society has led to somewhat negative connotations to both hyper-rational and despotic rule(Pumain, 2006, pp. 5–6). While one prevalent explanation for the frequency of hierarchical structures in nature and society is indeed that they “represent the best solution for many optimisation problems” (*ibid.* p.7), that does in no way mean they need to be consciously planned. On the contrary, in most cases hierarchies seem to emerge spontaneously, often from growth processes with systems splitting into sub-systems once they reach a certain critical size limit. There is also no compulsory link between social hierarchies and despotism, as

it matters little to the overall structure whether the top element is elected for a limited period or born into an inherited leading position. More detail on how hierarchical structures emerge and how they can be described as fractals, is given in Chapter 2. A further discussion on the specifics of social hierarchies is given below in Section 1.4, and on the differences between spontaneously emergent versus consciously planned structures in Chapter 7.

A possible confusion with a somewhat different meaning of the term hierarchy should however be mentioned already here. If hierarchical structures are abundant in nature in both physical (inert) and biological systems, social hierarchies on the other hand – understood as intra-species populations of individuals organised in pyramidal hierarchical, i.e. multi-level relationships to each other – seems to be almost exclusively found among human groups. At the same time, a different type of hierarchy is frequently described by biologists which is common among animals, namely *dominance hierarchies*, also known as pecking order (Strauss et al., 2022). These structures are hierarchical in the sense that there is difference in rank between group members, and they also seem to emerge spontaneously in the animal populations where they are described. But unlike social hierarchies, these are purely *linear*, in the sense that each group member is situated in rank above one part of the group and below the rest, so that the whole group forms a rank chain in the form  $A > B > C \dots n$ . The rank of an individual will typically decide their access to food and reproduction relative to the other members, and may be settled and resettled in a number of ways depending on the species and population under study, but typically involving some level of violence or threat and subordination in face-to-face encounters (Strauss et al., 2022).

A classic example – perhaps most of all in popular culture – is dominance hierarchy among wolves, led by an alpha male (e.g. Cafazzo et al., 2016; Packard, 2003). Though it has been much discussed whether or not this trope model actually fits wolves (see Mech, 1999; Muro et al., 2011), any reported dominance hierarchies among larger groups of wolves and stray dogs are linear rather than pyramidal, even when they are illustrated as pyramidal (e.g. Fig.1 in Rodríguez et al., 2017). Similar social organisation systems are found among a wide variety of species – mammals, birds, fish, particularly but not only among group-hunting carnivores – and are generally interpreted as an evolutionary mechanism (Strauss et al., 2022, with references). Cases of branching, multi-level social hierarchies among animals are on the other hand extremely rare, but have been reported to operate among hamadryas baboons in Ethiopia, with “clan leaders” forming relays of information flow and decision making between

the “one-male units” within a total population (“band”) of about 200 individuals (Schreier & Swedell, 2009). Eusocial insects like ants and wasps provide a more well-known example of hierarchical organisation among animals (Shimoji & Dobata, 2022), also indicating – if it should be necessary – that it is not a matter of cognitive abilities or brain size, but rather of social function (e.g. building a hive or a village together) and population size above a certain threshold.

The reason to dwell upon this qualitative distinction between linear and pyramidal hierarchies, is that the prevalence of the former in nature is sometimes put forward as an argument for social hierarchies among hunter-gatherer groups in the Palaeo- and Mesolithic [find precise reference here -> Graeber, if else strawman, Hayden 2007, pp. 231-6]. In their large-scope volume of the emergence of social inequality around the world over the Holocene, Flannery and Marcus (2012, pp. 37–39, 58–60) apparently saw the need to explain away the dominance hierarchy seen among other great apes as something that among human foragers was relegated to spirits and ancestors (FINISH THIS SENTENCE)

**fill in this one.** While it is a good point that there is no reason there couldn’t be linear dominance hierarchies among small forager groups, and that such systems hardly can be described as egalitarian by those who live them, we cannot assume that pyramidal social hierarchies have always been part of human culture, but rather that they – much like agriculture – at some point came to be as historical phenomena.

Bottom line hierarchy: pecking order/linear dominance hierarchy may be prevalent in any part of human prehistory, but could also be very hard to study from material remains. Branching (i.e. fractal) hierarchies as well as social stratification should leave material traces, and are most probably related to population size (see below), and thus less likely to be found within pre-Neolithic societies. They should be regarded as historically situated phenomena – much like agriculture, pottery, writing or the steam engine – justifying the search for and explanation of their possible origins (*contra* e.g. Graeber & Wengrow, 2021). The issue of the universality or particularity of social inequality and hierarchy is discussed in more detail **in the final chapters of this thesis (specify)**.

- Inequality Kohler & Smith (2018), Midlarsky (1999), Price & Feinman (2010), Price & Feinman (1995), Flannery & Marcus (2012). The difference between the concepts of social hierarchy and social inequality lies in the former relating to social and/or po-

political organisation and the distribution of power, while the latter to economy and the distribution of wealth or income. Societies where these two are completely unrelated may be theoretically conceivable – that is, where wealth does not entail power and *vice versa* – but historically they have tended to go hand in hand, albeit not necessarily in a straightforward way. HERE discuss a bit on delegated power, democracy, taking turns etc., and such systems being impeded by wealth (lobbying, corruption++). Keep it simple, point is to prepare for the interpretation of Trypillia mega-sites as *both* egalitarian and hierarchical (and maybe LBK as *both* unequal and unstratified..).

## 1.4 What is social hierarchy?

- Political assumptions – all hierarchical social structures are not despotic top-down rule. Democracies can also be very hierarchical. Matter of scale rather than political system Graeber & Wengrow (2021), Zimmermann (2012b), p. 255. But, tendencies? Use Pumain (2006), also Furholt, Grier, et al. (2020). Use Redhead & Power (2022): status and leadership, multiple overlapping networks. Emergence of hierarchies: “Positions in the dominance hierarchy is determined by a combination of attributes of individuals, stochastic processes, and social context” Strauss et al. (2022).
- Nested and non-nested social hierarchies, hierarchical hunter-gatherers? Hamilton et al. (2007), Whitridge (2016) (or use in Chapter 11?)
- Biologically defined thresholds to group size? Dunbar’s number and controversies, Dunbar (2023), B. West et al. (2023) (add published papers). Scalar stress G. A. Johnson (1982), Alberti (2014), Zhou et al. (2005). Also Carneiro (1986), Dubreuil (2010)
- Temporal dynamics of social hierarchies: cyclicity (Peters & Zimmermann, 2017), saw-tooth waves (Scheidel, 2017), punctuated equilibrium (Gould, 2007). Archaeo. example South Sweden Neo/BA: Nordquist (2001). Transitions villages to urban: Birch (2014)
- Tools for classifying societies, or evolutionary model? Discussion of A. Johnson & Earle (1987), Testart (2005), Service (1971), T. K. Earle (1997).
  - Lineage and Chiefdom societies T. Earle (2002), Sahlins (2020)

An additional category of social structure, which has had a certain success in archaeology, was described by Claude Lévi-Strauss as *house societies* (Lévi-Strauss, 1982). Here a house is a social unit, often centred around a material estate but also involving titles, heirlooms, land ownership, rights to hunting grounds etc. and where membership is not determined from genealogy in a systematic manner, as is the case with more regularly structured lineage or clan societies. House membership may be gained through more competitive social action, privileging those that possess the resources to engage in activities such as gift exchange and *potlatch*-style feasting. This opens up for more complex configurations, and house membership will often entail a certain level of prestige. Inheritance may furthermore follow (male) descent or (female) affinity – that is from grand-father to grand-son via mother – in a pragmatic way depending on which option is in the best interest of the house, as long as it can be justified in more or less precise kinship-related terms. A segment of society of varying size will not afford to partake in this competition, and as a result, house societies can be viewed as being in a somewhat unstable transition state between lineage and class societies. Lévi-Strauss originally pinned the term on Kwakiutl society in the American north-west coast (as described by Franz Boas), but argued for its generality by associating it with the feudal system of medieval Europe. The concept has since been applied to a wide range of cases from ethnography (especially in the South-East Asian and Pacific regions), as well as to prehistoric contexts **insert examples**, reflecting a relevance that extends far beyond European feudalism. Ian Kuijt (2018) recently provided an interpretation of Neolithic Çatalöyük where he proposed that

Refs. house societies [Joyce & Gillespie (2000), Bnf; Beck (2007); Kuijt (2018); Lévi-Strauss (1982); Bickle et al 2016 (reload in Zotero)].

•

- Anti-evolution critique in Yoffee (1993), Yoffee (2005), Fontijn & Brück (2013), Kienlin & Zimmermann (2012), Lund et al. (2022), Furholt, Grier, et al. (2020). Review in Dubreuil (2010). Anarchistic critique/heterarchy: Crumley (1995), Haude & Wagner (2019), Graeber & Wengrow (2021). Paleaeolithic social inequality: Honoré (2022), also Testart (2012), Testart (1982)
- I need to address gender inequality somewhere, mainly to say that this thesis is not about gender inequality. Start from Gaydarska et al. (2023), and cite A. Augereau for

the LBK.

## 1.5 Main findings here?

Maybe leave to the end, and fill in, like abstract.

## 1.6 Research ethics

- Social complexity and evolution. Are less complex societies simple? Is that a bad thing?
- Open science and open-source scripts
- Terminology and spelling (British English for text. For geographical place names, Slovak special characters are kept as far as possible, even though it can be a pain in the xxx to render in Rmarkdown on Windows OS, and the 2010 Ukrainian National transliteration system with only ASCII characters and no soft sign)
- Abstracts in Slovak and Ukrainian (and not only in Norwegian)

## 1.7 Structure of the thesis

This thesis is structured as a monograph in four parts. In the first part the overall framework of the study is exposed, with the general introduction above, the overarching theoretical framework in Chapter 2, and the background of the study material in Chapter 3. Parts II and III are devoted to each their methodological approach to the material: Part II to the study of hierarchy in size distributions, and Part III to the quantification of image textures. Each of these parts consists of three chapters, the first of which – Chapters 4 and 7 – exposes the theoretical and interpretative background of the applied methods and their relevance to archaeology. The following chapters – Chapters 5 and 8 – detail the technical specifics of the two approaches and their implementation in this study, and the last chapters within these parts – Chapters 6 and 9 – provide the actual analyses and summaries of results. In Part IV, the findings are summarised and further discussed. Chapter 10 gives an attempt of interpreting the results in the

context of the culture-historical setting of the European Neolithic, while Chapter 11 reviews the possibilities and limitations of the fractal analysis framework in archaeology. Concluding remarks and suggestions for further study are given in Chapter 12.

Some readers might react to an apparent deviation from the academic tradition of devoting a separate chapter to research history. This is a deliberate choice, not to suggest that historiography is unimportant, but rather as a result of the fundamentally interdisciplinary scope of the study. In fact, there is very little extant history of applying fractal analysis in archaeology – the few studies that, to my knowledge, have been done in this direction are discussed primarily in Sections 4.3 and 7.3. Fractal analysis itself holds a research history of its own (see Section 2.2), and so does the study of Linear Pottery (Section 3.2) and Trypillia societies (Section 3.3), not to mention the general study of social complexity in prehistory (mainly Section 3.1). In short, instead of trying to shoehorn these parallel histories into a clearly delimited but rather hybrid chapter, I have opted for what I believe to be a more useful approach, namely to fit them in more seamlessly where they belong, in the various associated theory and methods chapters.

An additional note should be made here regarding the writing style of the different parts and chapters. It is my belief that a major obstacle for fractal analysis methods to become more integrated into the standard tool kits of archaeological research, is the excessively technical nature of much of the associated literature. Archaeology as a discipline remains profoundly rooted in the Humanities, as seen in the inbuilt structure of teaching, research and funding institutions in most (at least European) countries. Fractal analysis is derived from pure mathematics, and most applications so far have been developed within the natural sciences. Archaeologists who are trained within a humanistic scholarly tradition cannot be expected to hold a skill level of mathematics more advanced than what is achieved in high school, and code programming is hardly taught at all within the walls of Humanities faculties. Technical details regarding the methods and analyses applied in this thesis are therefore – as much as possible – limited to the devoted Chapters 5 and 8, and readers who are interested in these may also refer to the #online code repository for more details and reproducibility **cite repository**. In the rest of the thesis I have opted for a more narrative approach, in an attempt to invite a somewhat larger audience of archaeologists into the fascinating complexities of fractals.

END Chapter

# **Chapter 2**

## **Theoretical framework: Complexity and Fractals**

### **2.1 Very short introduction to Complexity Theory / Dynamical Systems Theory**

Lit. use Daems (2021), Baden & Beekman (2016), Ross & Steadman (2017), Smith (2011) and Bentley & Maschner (2008).

For Dynamical Systems, use Devaney (2020), but don't go into detail.

Describe complexity, dynamical systems, chaos, feedback loops, criticality, emergence. Scale G. B. West (2017) NA

Social complexity is more than social hierarchy, and all societies – whether they are classified as simple or complex within a social evolutionary framework – can arguably be studied as complex systems, since they always consist of various sub-systems and populations of individuals acting and interacting in a variety of ways (Daems, 2021, p. 6). The sense of social complexity that is traditionally understood in archaeology, derived from social evolution theory, is somewhat narrower and relates more to the specific characteristics of organisational scale (i.e. hierarchy) than to complexity per se. Studying the scale of social organisation from a complex systems perspective rather than from a social evolutionist one holds several advantages:

1. The switch from discrete evolutionary stages to continuous spectra allows for more nuanced evaluation of the society in question, avoiding false binaries like simple-complex
2. The complex systems approach arguably has a stronger explanatory power than the more classificatory social evolution schemes
3. Complexity theory offers a better alternative for ethical reasons, as it avoids the underlying colonial and eurocentric connotations associated with classifying societies into simple and complex

As a further elaboration on the latter point, an analysis of a society from a complexity theoretical viewpoint is not a matter of establishing whether or not the society can be characterised as a complex system. When the scale of social organisation is the object of study – as in the present thesis – the word hierarchy is both more accurate and, if not neutral, at least more balanced than social complexity, since it is not obvious whether or not it is a good thing for a society to be characterised as hierarchical. The study of the dynamics of social hierarchy over time is thus not a story of progress, as the 19th century studies of social evolution too often were.

[@hamilton2007].

Mention the most common applications in archaeology, as discussed in Daems (2021), p. 13: network science, settlement scaling, cultural evolution and agent-based modelling.

## 2.2 Very short introduction to Fractals and Fractal Analysis

Lit. use B. B. Mandelbrot (2021), Falconer (2013) (general), also C. Brown & Liebovitch (2010), C. T. Brown et al. (2005) and Diachenko (2018) (for archaeology)

The term *fractal* was pinned by the French-American mathematician Benoît Mandelbrot (1924-2010), from the latin word *fractus* meaning broken or irregular, to describe patterns that because of their apparent limitless complexity defied concise description within the framework of Euclidean geometry (Falconer, 2013, pp. 116–120). Such patterns – both theoretical and empirical – had been described and analysed by mathematicians and researchers within other disciplines since the end of the 19th century, but were mostly regarded

as curiosities and exceptions, and Mandelbrot was the first to link all these previous studies within a unified theoretical framework (B. B. Mandelbrot, 1975, 2021).

In one influential paper, drawing on previous work by mathematician Lewis Fry Richardson, Mandelbrot (1967) argued that a rugged linear feature like a coastline cannot be fully described through traditional geometry with a set of line segments, since this would result in a curve of infinite complexity. More importantly, he showed that the traditional measure of lines – the length – will inevitably depend on the scale of observation when applied to a coastline. If measured in kilometres, a coastline will always appear shorter in total length, than if it is measured in metres, since smaller bays and inlets can then also be accounted for. But this phenomenon continues seemingly without limit, since the same coastline measured in centimetres will appear much longer, and in millimetres far longer again, and so on. Length as a measure of rugged linear features thus seems inadequate, which may become a problem in practical settings when comparing coastlines between countries that operate with different measurement units and procedures. The same problem occurs when describing irregular patterns in the plane (like island or continent outlines) with area or in three-dimensional space (like clouds or galaxies) with volume. As a solution, Mandelbrot proposed the use of the *fractal dimension* as a descriptive tool for characterising such patterns.

Fractals as hierarchy

Self-similarity and scale invariance

Processes/mechanisms that produce fractals:

- Cascading bifurcations and confluences (splitting or merging - tree structure/arborescence/branching, and relation to size. Terminology borrowed from biology and fluid dynamics (including turbulence/turbulent flow)

The role of randomness - tidy and messy fractals (romanesco broccoli are not more fractal than regular broccoli, only more regular. Also: a system may be both random and deterministic, often only depending on scale of observation (chaos).

The relationship with (self-organised) criticality and chaos: deterministic *and* unpredictable

Fractals embedded in

- Space (hence “fractal geometry”): geomorphology, plants, ocean and wind currents, galaxies, also human constructed features (see Chapter xx for details)

- Time series: earthquakes, finance (not applied in this study, though should be done later)
- Networks/abstract: hierarchical organisations, income distributions, word counts, 1/f or pink noise, www. Barabási & Albert (1999) etc. (see Chapter xxx for details). Fractal social networks: B. West et al. (2023).
- Pure mathematics: Julia and Mandelbrot sets, strange attractors (don't go into details!)

No, not everything is fractal: e.g. Central Limit Theorem

Fractal analysis for studying irregular phenomena (methods described in more detail Chapters xxx), and thus as a tool for quantitative empirical research.

- Fractal dimension (explain without math here, with math in chapter 7, box-counting in chapter 8)
- Lacunarity (same)

## 2.3 Very short introduction to micro-macro approaches in social theory

- Lévi-Strauss and Structuralism
- Braudel and World Systems
- Giddens and Structuration Theory
- Delanda and Assemblage Theory

For social hierarchies, he refers to Weber's classification of legitimization strategies, as being founded on sacred tradition, personal charisma or rational bureaucracy (see also Graeber & Wengrow, 2021, pp.). Delanda furthermore places Bourdieu's concept of *habitus* on the mid-range between micro and macro processes, as an explanation of social action that is not entirely individual dependent, but not emergent properties of society-as-a-whole either.

- Latour and Actor-Network Theory

## 2.3. VERY SHORT INTRODUCTION TO MICRO-MACRO APPROACHES IN SOCIAL THEORY

---

What these approaches all have in common, is that they are entirely qualitative (**check**).

- That's not a problem in itself.
- Quant approach is both possible for the stated purpose, and desirable for reasons of comparative analysis.
- Data deluge (refer to chap. on geomagn data). The goal here is to establish a quantitative framework for studying social complexity and hierarchy in archaeological/prehistoric settings. Further articulating fractal analysis with existing social theoretical approaches is not the primary goal here, as it could constitute a separate research project. In the present thesis, bla bla.

END chapter.



# Chapter 3

## Material and data: social complexity in the European Neolithic

### 3.1 Studying social hierarchy in archaeology and prehistory.

Grave goods

Burial monuments

Architecture Rathje & McGuire (1982) – social stratification (qualitatively) through architecture and burials (and life expectancy). Short but to-the-point article.

The denominator problem

The use of ethnography

Other approaches (osteological, isotopes, craft specialisation [refs](#))

This project: house-size distributions and settlement layouts (details in subsequent chapters), just very short argumentation.

Comparative approach: Neolithic technology (not bronze axes), wood and wattle-and-daub architecture, (near) complete settlement plans/extensive documentation: Trypillia and Linear Pottery

For this project I opted for the use of houses and built environments as proxy for social hierarchy. In this way I hope to largely avoid the denominator problem associated with burials.

## CHAPTER 3. MATERIAL AND DATA: SOCIAL COMPLEXITY IN THE EUROPEAN NEOLITHIC

---

While it is true that for many archaeological culture groups in late prehistory habitats are poorly preserved and hard to discover, leaving us still with a limited understanding of them (the case in many Michelsberg, Corded Ware and Bell Beaker groups, only to mention a few **check**), in groups where habitats are well preserved, there is little reason to suspect that the available record would not cover the whole range of social statuses if these societies were hierarchical. Unlike burials, every individual in a sedentary society – with few exceptions like homeless persons in more recent urban contexts – will normally have at least one fixed place to stay overnight, and these homes will in most cases be constructed within the same fundamental framework of techniques and building materials, depending more on culture specific traditions and environmental factors than on social status (**citation?**). As an example, in a society where mudbrick is the main building material, like in the Neolithic Near East and Anatolia, nearly all constructions are made in mudbrick, regardless of the social status of the inhabitants. In Europe north of the Alps, wattle-and-daub construction was the almost exclusive building technique for any architectural feature from the early Neolithic until the Roman conquest, and well into the Middle Ages north of the *limes*. One can of course enumerate exceptions, but more importantly houses are in any stratified society also a marker of social status, which can be exhibited in a range of ways, from decorations, use of more precious raw materials as well as size. That is precisely the reason for using houses as a proxy for social status and hierarchy in archaeological settings. But the point here is that there should be little taphonomic differentiation between groups of high and low status within a given archaeological context, at least in prehistory, and at least not as much as can be expected for burials, meaning that we can expect to find samples of houses that are representative of the social structure of the archaeological culture in question. On sites where there is taphonomical loss of architectural structures, as long as the overall building tradition is homogeneous, there is no reason this loss should affect one segment of the society more or less than others.

Some caveats do remain, however, for the use of houses as proxy of social status. Firstly, there may be a documentation bias favouring larger houses, since they may be easier to discover both during excavation and in remote-sensing surveys (**citation?**). In samples with very skewed house-size distributions, there may also be a further taphonomic bias towards large houses, since smaller houses – being far more numerous – are statistically in greater risk of being affected by post-depositional disturbances. Both of these biases are hard to evaluate empirically, though computer modelling could potentially give indications of their importance.

### 3.1. STUDYING SOCIAL HIERARCHY IN ARCHAEOLOGY AND PREHISTORY.

This, however, is not within the scope of the present study.

A second, and maybe more important issue, is that of the contemporaneity of houses. When the goal is to investigate the social structure of a settlement as reflected in its architecture – be it through the size distribution of buildings or their spatial layout – all the analysed features should ideally have been in use at the same point in time. This is however very hard to achieve in most archaeological settings, and many researchers choose to either ignore the issue, or to accept a temporal resolution that is far wider than what their research questions should logically allow for (Perreault, 2019). One way of limiting this problem is to select study samples with little to no stratigraphic overlap, which might indicate short occupation span, though as shown below this indicator can also be deceiving. For both study areas selected for this thesis – the Linear Pottery in south-west Slovakia and the B2/C1 Trypillia of central Ukraine – settlement plans show very little overlap between houses, even though some of them probably developed over more than three centuries, as shown by radiocarbon dates and modelling (see below). Such settlement plans may be impossible to differentiate into separate coeval time samples without precise dating of construction and abandon of every individual house, counting in the thousands on the Trypillia mega-sites (an alternative method is presented only for the Linear Pottery settlements in Section 3.2). On the other hand, the fact that there is so little overlap between houses despite temporal differences clearly illustrates how these settlement plans emerged over time, not as a *tabula rasa* in each generation but rather with new constructions respecting the location and orientation of older ones long after abandonment. Though such practices are indeed interesting, it is not at all obvious, however, to which extent they may reflect or even relate to social factors such as hierarchy. With settlement types with much higher degree of stratigraphic overlap, like the tell sites of the Balkan and Near Eastern Neolithic traditions, it may be easier to distinguish more or less coeval occupation phases, but they are again harder to document extensively – because of the high density of archaeological finds and features, excavation surfaces typically cover only very small portions of the settlement, while remote sensing performs less well and not allowing for temporal disentanglement of constructed features (#citation). In any case, the issue of temporal resolution of the data and its influence on analytical results is crucial, and will be discussed repeatedly throughout this thesis, with a summary in Chapter 11.

Comparative technology

Meaning of “house”

## 3.2 The Linear Pottery culture complex

General intro to the culture: Bickle & Whittle (2013); Whittle & Bickle (2014).

Formation, characteristics – striking difference from earlier Mesolithic cultures, hence the term “Neolithic Revolution” pinned by Vere Gordon Childe for the seemingly abrupt transition to agriculture in continental Europe with what he called the Danubian Ia [ref](#). Whittle (2022), check with Trigger!

expansion trajectory: east: Saile (2020),

Questions of contact and even creolisation with local hunter-gatherer groups in the margins of the Linear Pottery settlement area – Limbourg and La Hoguette pottery groups in northern France and Belgium, Swifterbandt in the Netherlands??, Ertebølle in northern Germany??, Bug-Dniestr in Ukraine and Moldova (Saile, 2020) – as well as with other already established Neolithic groups in central France (Roussot-Larroque, 2022) and the lower Danube (Saile, 2020), remain hotly debated

End of LBK as collapse? The whole culture as an adaptive cycle: Gronenborn et al. (2014).

Organisation of Linear Pottery society: egalitarian or hierachic? Cemeteries: Jeunesse (2022), check Gaydarska et al. (2023) and Augereau (2021). Linear Pottery architecture and house construction

origin of the longhouse: Bánffy & Höhler-Brockmann (2020), Coudart (2015), Last (2015)

house typology, construction, and use: Modderman et al. (1970), Coudart (1998)

house orientation: “origin” hypothesis: Bradley (2001)

Number of coeval houses in LBK villages, evaluated to a mean of 5, sd. 3 (Coudart, 1998, p. 91). Furthermore, based on ethnographic analogies she estimated a typical Linear Pottery village of 3 to 8 houses (of which 1 or 2 longer than 22 m), to include on average approximately 150-260 inhabitants, though fewer (up to around 80 people) for the smallest hamlets of 3 houses.

Patrilocality in LBK based on Sr isotopes: Hrnčíř, Vondrovský, et al. (2020) (read this more carefully), and other data (check) Schiesberg (2016).

The Žitava valley and research project

### 3.3 The Cucuteni-Trypillia culture complex

General intro to the culture

Recent dating, see Harper et al. (2023), Shatilo (2021).

Trypillia architecture and house construction

Pickartz et al. (2019), pp. 1649-50: “unburnt” and “eroded” are misleading labels, since highly burnt and even vitrified material regularly found during excavation of these. Probably reflecting houses that are constructed with less daub, without an oven installation, and/or without raised clay platform, thus causing significantly weaker magnetic signals. These houses may in fact represent entirely different social functions from regular houses, but there is as for now no consensus as to what this may be (e.g. artisanal, storage etc.)

Trypillia social organisation: current debate

Side note on Varna: Lichardus (1991; also Gimbutas), as discussed in Kadrow (2013), proposed that the social inequality observed at Varna in the mid-5th millennium, was already then adopted from pastoral North Pontic steppe cultures (*check this and delete if unsure*); cf. Chapman et al. (2006) – three social levels interpreted from grave goods, but not clear if these are really discrete or constructed on a continuum. The term *fractal* is here used purely as a metaphor for complex personhood structures, rather in opposition to the described social hierarchy.

The B2/C1 and the mega-sites of the Southern Bug – Dnieper interfluvium The urbanism debate: Comparison with Uruk in Müller and CHECK; low-density urbanism for Nebelivka: check for refs. in Ohlrau (2022), p. 91 cc. Mega-sites as *anomalocivitates*: Ohlrau (2022) and Sindbæk (2022).

### 3.4 Reading site plans from geomagnetic imagery

Caveats: fill in here.

Pickartz et al. (2021) fds

Say where the shapefiles come from here. Müller-Scheeßel et al. (2020); Hale (2020); Ohlrau (2020) (double-check in my article)

### **3.5 Synthetic data**

And why I'm not (this time) relying on ethnographic data.

Don't go into technicalities here, just the reasoning.

## **Part II**

### **Size distributions**



# Chapter 4

## House sizes and social meaning

### 4.1 Interpreting house-size differences

In archaeology there are two recurrent and seemingly contradicting assumptions underlying interpretations of house-size differences within a society. In studies where the goal is to provide population size estimates, this is often calculated from living area, where the square metres per inhabitant is modelled from ethnographic analogies. The population of a village is then found by summing together those of every house (e.g. Coudart, 1998, pp. 79–80). A simpler and probably more simplistic version of this is to consider a  $\text{m}^2/\text{inhabitant}$  proportion that is constant no matter the size, and thus calculate the population directly from the total living area of the village (**give examples**). This mean value is generally obtained from multiple ethnographic parallels. With this assumption – that every inhabitant requires a similar amount of living space – the size of a house effectively reflects its number of inhabitants. The second assumption, which is more frequently seen in studies focussing on wealth inequality and social stratification, is that house-size differences are expressions of differences in some sort of wealth or power (**give examples**). In this view, a larger house would have belonged to a wealthier household, capable of procuring more raw materials and activating a larger labour force for its construction and maintenance, in which case there would be significant disparities in living space per individual. Even though there is not necessarily any contradiction between these two interpretations from an anthropological point of view, most archaeologists seem to be unable to consider both possibilities simultaneously (Wilk, 1983). From a methodological point of view, each of these assumptions will tend to mask our ability

to see traces in the archaeological data relating to the other assumption – that is, with existing methods we cannot convincingly provide estimations of both population size and level of social inequality from the same data, even though house sizes frequently form the basis of both argumentations. Far from proposing a solution to this issue, my argument here is that a variety of social institutions known from ethnography and historical sources can explain some level of correlation between the two variables. Dowry and bride price are geographically and temporally widespread practices that link number of offspring (daughters, sons or both, depending on cultural context) with wealth. Clan leaders may draw upon kinship ties and dependencies in order to obtain the workforce needed to construct a larger house (**citation needed**). In agricultural societies, land ownership is often seen to correlate with household size, since land owners tend to attach workers and servants to them, people who themselves in turn tend to come from landless households (Netting, 1982; Wilk & Rathje, 1982, p. 629). Nevertheless, if the notion of wealth is at all to be applied meaningfully to non-capitalistic societies, it should designate cases where there is significant and persistent material disparities between members of a population, and not simply point to different household sizes where wealth is proportional. House sizes could thus potentially reflect a somewhat more complex culture-specific interplay between household size and wealth, meaning that for a given house size, one could assume a range of possible values of the two parameters (Figure 4.1). This relationship between household size, wealth and house size should be studied more in detail empirically through the available ethnographic data, rather than reducing its complexity to a mean surface area per inhabitant for the entire population. Such a study, however, lies beyond the scope of the present thesis. Here I will largely leave aside the question of population and household size, focussing on distribution types of house-size data, arguing that the most unequal distribution type considered here – the power-law distribution – is unlikely to emerge only from random differences in household size and standard marital patterns, favouring thus interpretations relating to systemic wealth and/or power differences.

Even though the goal here is not to investigate household sizes but to focus on the material aspect of house-size distributions, some fundamental issues of terminology should be addressed. The use of the word *house* (in the wider material sense rather than the Lévi-Straussian sense, see Section 1.4) is indicative of an underlying assumption that the building in question was in use primarily for domestic purposes – essentially, a fixed architectural unit where someone would spend their nights at least most of their time, and in many cases also cook and eat their

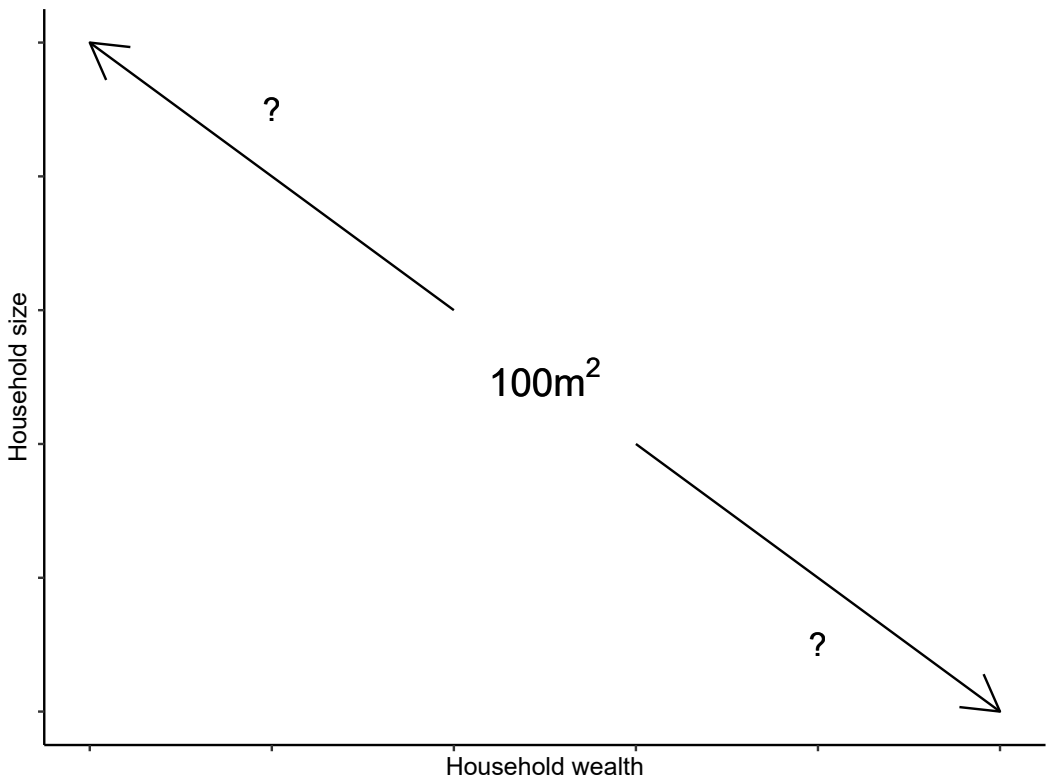


**Figure 4.1:** House size can be interpreted in terms of number of inhabitants (household size) or material wealth of the inhabitants, but the exact relationship between these two variables remains poorly understood and is probably both complex and culturally contingent. Any given house size within a distribution can thus result from a combination of effects from the two. In many cultural contexts household size and wealth may furthermore be directly correlated

main meal during the day – though proving this directly is not always straightforward in archaeology. For the cultural contexts discussed here – the Linear Pottery and Trypillia groups in the Neolithic-Chalcolithic – there is however little evidence for buildings with specific non-domestic (e.g. economic, religious or administrative) purposes, with the probable exception of the so-called mega-structures or assembly houses in the Trypillia mega-sites, which are discussed more in detail below. This lack of evidence does not imply that there was no specialised economic, religious or administrative activity in these societies, as ethnography and history clearly shows that such activity must reach a certain degree of specialisation before it materialises in distinct buildings devoted exclusively for these functions. Artisans, shamans and chiefs could be specialised to some extent but still perform their activity at their domestic home or more diffusely outdoors or without any fixed location (e.g. Costin, 1991, p. 25; Kahn, 2021). It is in any case of common usage to speak of houses when discussing architectural units in Neolithic Europe and other prehistoric contexts, maybe because of a lack of a better generic word, but this usage should not prevent archaeologists from recognising

other non-domestic functions of buildings whenever there is evidence for it. The *household* is furthermore the designation of all the people, genealogically related or not, usually (though not necessarily) living under the same roof or within the same architectural unit, constituting a functional whole economically and socially, and potentially including more than a single family unit, as well as servants or slaves, depending on the context (Wilk & Rathje, 1982, p. 620). The emphasis for defining a household is thus more on its economic and social function than on co-residence and kinship relations, which are somewhat more variable. In the following, I go into some more detail as to how household organisation as well as wealth are known to influence house size.

#### 4.1.1 House size and household organisation

The focus on houses and households in archaeology – as opposed to larger units of analysis like whole settlements, cultures and periods – started to attract momentum by the end of the 1970s, with the work of Wilk & Rathje (1982) often cited as the original manifesto of its validity and importance, pinning “Household Archaeology” as an independent genre of study. In their view, the household could be understood as the most abundant activity group in any society, despite considerable variations as to its importance relative to other types and scales of social groupings. They defined it by their *social*, *material* and *behavioural* constituent elements, that is, its members and their relations, the dwelling and other possessions, and the activities it performs. The material element is of course the only one directly accessible to archaeologists, and the task for researchers would be to reconstruct the social and behavioural elements from the material. This realisation led to ambitious comparative projects of mapping the variability of houses and their occupants in different parts of the world and socio-economical contexts, with inferences onto prehistoric contexts built upon existing ethnographic literature (e.g. Murdock, 1949) as well as new ethno-archaeological observations (Blanton, 1994; e.g. Wilk, 1983).

One of the main characteristics of households is their *size*, which, according to Wilk & Rathje (1982), to some extent is determined by the scale of the production activities that fall within their organisational sphere. In societies where large scale complex tasks necessitating the simultaneous cooperation of many hands are organised at the household level, the optimal household size will be accordingly large. Such activities can include agricultural tasks like

irrigation or terracing, as well as house construction. However, when large-scale activities are necessary only once or twice a year, as with seasonal large game hunting or intensive fisheries, they tend to be organised at a community level by many households working together temporally. In such contexts, households can be smaller as their daily activities can be performed by a smaller number of people (Wilk & Rathje, 1982, p. 623; see also Hamilton et al., 2007 CHECK#). Furthermore, ethnography has repeatedly shown that large households performing complex activities often need a head coordinator for the activities to run smoothly. However, the set of activities organised at the household level in a society and thus determining the optimal household size, will affect all households similarly unless there is some economic differentiation between them. In societies where households are economically more or less self-sufficient, their size differences should be expected to be random (i.e. normally distributed, see Section 4.2.1).

Kinship studies within anthropology have shown over the last decades that in most societies, contrarily to common misconception, kin affiliation is *not* simply a matter of biological relatedness. In an attempt of grouping together all possible justifications for kinship ties, Marshall Sahlins (Sahlins, 2013) defined kinship as “mutuality of being” – that some real or imagined substance is shared, and that this substance is not necessarily genes, as is mostly the case in modern Western societies (with adoption as the main exception). A variety of non-genetic foundations of kinship are widely accepted in different cultures, like sharing of name, time or place of birth or childhood, food source, shared experiences, blood ties, and so on. At the same time, archaeology as a whole has arguably been very slow in taking this diversity of kinship configurations into account, far too often taking for granted the modern Western (especially post-war 20th century) ideal of patrilineal nuclear families as the default configuration for all of human history (Ensor, 2021). That being said, anthropological kinship studies such as that represented by Sahlins typically shows little concern with material culture, and are mostly silent on the question of who – at the end of the day, quite literally – sleeps under the same roof, making it hard to interpret domestic architecture in terms of kinship structure and social organisation. The recent comeback of kinship studies in archaeology has been far more focussed on linking isotope and aDNA data with social structures, largely fuelled by the rapid developments of the related methodologies.

- Kinship and households: who lives in a house? Ensor (2013), Ensor et al. (2017).. archaeology: , Madella (2013), Joyce & Gillespie (2000), Carsten & Hugh-Jones (1995),

Hofmann & Smyth (2013), Kramer (1982)

### 4.1.2 House size and wealth

Wilk and Rathje pointed to the important role of households in inter-generational transmission of wealth in many societies (1982, pp. 627–631). Specifically, following Murdock (1949) and other ethnographers, they argued that as populations grow, land tenure tends to institutionalise at the household – and later individual – level around the moment when agricultural land becomes more scarce than labour. Before this – in pioneer phases of agricultural development – land is readily available and if there is any concept of land ownership at all, it usually lays at the community level. Once the agricultural land in a region is saturated, rights to use it will tend to be transferred within households, and children from households with extensive rights have a greater incentive to stay within or close to it, while children from households with less land rights are more likely to emigrate. Further population pressure will tend to limit partition of inheritance between siblings, so that land ownership over time is transmitted within a smaller and smaller fraction of the population. This situation is also shown to entail stratified (and parentally arranged) marriage, further entrenching social stratification.

Maya here!

Kahn (2021) describes an example from eastern Polynesia of agricultural expansion and intensification developing over 400 years from the initial colonisation before social stratification starts to become materialised in differential architecture. In later phases, she links the appearance of specialised buildings devoted to communal assemblies, rituals as well as residential and ritual buildings for elites with the emergence of complex chiefdoms. Though quantitative measures of house size are not presented in the study, it clearly demonstrates that elite architecture was consistently larger than that of commoners in the prehistoric Society Islands. However, she also identifies types of houses of special economic function like workshops, and points out that these can be hard to distinguish from common residential houses archaeologically simply by looking at size (Kahn, 2021, pp. 90–91). In such cases – where there is a range of non-residential building types – it may be of little use to analyse house-size distributions as single blocks. It may then be necessary to first group buildings into functional types based on internal structure and finds inventories, given that this information is available. This issue concerning the prerequisites of data input for the analyses done in this thesis,

is further discussed in Chapter 11. It should also be noted that interpretations regarding the social structure of pre-contact Polynesian societies are greatly aided by near-contemporary written accounts from the first European explorers in the region, and house floor levels are often well-preserved due to the relatively recent dates of the structures (10<sup>th</sup> to 18<sup>th</sup> centuries CE) – both factors being in stark contrast to the central European Neolithic, where the spatial organisation and sizes of houses are often nearly the only information available.

Regarding the domestic architecture of clan leaders and chiefs, several studies have highlighted how elites both have the material means and the socio-economic incentives to build houses that are more monumental than those of commoners HAYDEN1997++. Others have warned that this should not lead archaeologists to systematically interpret large buildings as evidence of elite-based top-down social hierarchies, since there are also ethnographic examples of monumental buildings being constructed collectively by more egalitarian communities for assemblies or other communal activities. Referencing a range of ethnographic and archaeological examples, Goodale et al. (2021) point out that the act of constructing a monument may be organised and to some extent coerced by a leader, or equally by a collective group. In both cases the intended function of the finished building will serve in the interest of the one or those who initiated the project. This is furthermore valid at all social scales – the construction of a residential building is initiated and driven by those who wish to live in it, and the construction of a ritual building for the village like an assembly house is initiated and driven by the entire village. Furthermore, the construction of a palace in a state society is initiated by the leader and financed through the tribute collected throughout their effective territory. Consequently, buildings should be expected to somewhat reflect the scale of their social importance through the level of effort put into their construction, so that in a hierarchically organised society (be it top-down coercive or bottom-up collective), this effort should also be hierarchically distributed in its buildings. I argue here that building size is the best (and often the only) available proxy to this construction effort (see Section 4.2.4 below for more discussion on this point).

Do clan leaders have bigger houses? check Haude & Wagner (2019), Bradley (2013), Wilk (1983). Smith (1987).

- General tendencies for Pueblo contexts: Dohm (1990)

P. Květina and J. Řídký point out both architecture (construction, size, orientation) and settle-

ment layout as possible distinctive features between Big Men (achievement-based) and Chief societies, arguing that the former type may be recognised by a dispersed intra-settlement layout combined with uniform architecture, while the latter type would tend towards more regular settlement layout and more marked differences in architecture (Květina & Řídký, 2019, p. 13). EXPAND UPON THIS.

- Schiesberg 2010 2016, go through refs in Zotero, family size and houses for the LBK.

Functional difference:

- Ethnography of initiation houses, communal/assembly houses, ritual houses, including Barley (2011), Godelier (1986), Wilk (1983), Fraser (1968), Haude & Wagner (2019)

Some factors other than household size and wealth have been suggested and empirically reported to systematically influence house size (Wilk, 1983, p. 101). Among these are:

- Mobility – Seasonally mobile groups tend to build smaller dwellings than more sedentary groups (Porčić, 2012)
- Post-marital residence – Houses in matrilocal societies tend to be larger on average than in patrilocal societies (Hrnčíř, Duda, et al., 2020; Porcic, 2010)
- Climate – Houses are smaller in cold circumpolar or mountainous regions because of the cost of heating
- Duration of residence – Households that have been established at a location for a long time or are well integrated in the community tend to have larger houses (Wilk, 1983)
- Material use and technology – All building materials have associated constraints and costs, and innovations can lead to larger constructions at lower costs

Of these factors, only the duration of residence will have a direct influence on house-size difference *within* communities. Mobility, residence patterns and climate are more constant factors affecting entire communities and will thus affect the average house size, but not the level of inequality. Access to building materials and technology on the other hand may be differentiated in stratified societies, and lead to unequal house sizes as a materialisation of wealth.

A related factor that may lead to a certain under-representation of the wealthiest households, is the construction of multi-floored houses, unless this feature is recognised archaeologically and included in the calculation of house sizes. For the case studies presented in this thesis however, building materials and techniques are not noticeably differentiated between small and large houses, and the possibility of multi-floored houses is only a minor issue that has been discussed in Chapter 3.

Lastly, in his ethnographic comparison between egalitarian and more ranked contemporary Maya village communities in Belize, Wilk (1983, pp. 111–114) also pointed to social norms potentially *preventing* differences in public display of wealth even when such differences existed. He linked such norms to the openness of the village economies – in closed self-sufficient villages there was greater mutual dependence between households, and wealth display was strongly discouraged, potentially sanctioned with witchcraft, whereas in villages with more open economies household wealth was more readily displayed through house size and the quality of construction materials.

## 4.2 Distribution types and their underlying mechanisms

The main question in this part of the thesis is on the nature of house-size differences in the studied contexts, and to explain them either as being due to random fluctuations or as a material expression of a more structural inequality, or something in-between. In statistical terms, this is a question of distributions. A distribution is a mathematical model of the spread of data along a variable or axis, and it can be modelled on empirical data as a succinct description, or used to predict unobserved data (e.g. future developments, or, in the case of archaeology, data that is lost to taphonomy). In theory, there is an infinite number of possible distributions, as there is no limit to how many parameters one can include to fit the data. It is however generally considered good practice in statistics to limit the number of parameters and identify the simplest possible model that gives a good fit, since a larger number of parameters can often lead to a better fit, but at the same time be harder to explain in terms of underlying mechanisms. Adding many parameters only to achieve a marginally better fit is referred to as *overfitting* (#ref?), and for most real-world contexts there is a limited number of model types that can be considered reasonable candidates. In cases where we are interested in inequality or uneven distributions of data (so-called *skewed* distributions), the most likely distribution models are

those that can be described as *heavy-tailed*, meaning that on typical graphical representations (like density/PDF plots or histograms) they will show a characteristic stretch of some of the data towards the right end of the x-axis, while most of the data remains on the left side (Figure 4.2). The opposite orientation is also possible in theory, in which case the distribution can be referred to as left-tailed. It is important to keep in mind however, that not all distributions are heavy-tailed, and that other distributions also model the spread of data across a variable, but result from very different underlying mechanisms. Identifying the most likely distribution model for a data series is therefore crucial for understanding how the data could have been generated. And though it is true that one model type can have multiple different explanations – in an archaeological setting for example, many different social behaviours can lead to the same material outcome, an issue known as *equifinality* – excluding one or more model types for the observed data can help limiting the number of plausible interpretations considerably.

Distributions can be represented graphically in a number of ways, most commonly in a coordinate system with the variable on the x-axis and its density, or *probability density function* (PDF), on the y-axis (Figure 4.2). Often, and in many of the sources cited in this part of the thesis (e.g. Clauset et al., 2009), the PDF is denoted by  $p(x)$ , reading as *the probability of  $x$* , or simply  $f(x)$  (*the function of  $x$* ). It gives the probability for a drawn sample ( $X$ ) of falling within a given arbitrarily short range of the distribution, written  $Pr(x \leq X < x + dx)$ . By definition, the area between the PDF curve and the x-axis sums to 1. For reasons that are further discussed in Chapter 5, heavy-tailed distributions, and power laws in particular, are instead often represented with their *cumulative distribution function* (CDF), which is the integral of the PDF (inversely the PDF is the derivative of the CDF; Figure 4.3). Similarly to the PDF, the CDF is often denoted as  $P(x)$ , depending on disciplinary tradition. It indicates the probability of a random sample value being equal to or lower than the function value, or  $Pr(X \leq x)$ . Furthermore, the specific version of the CDF used for plotting heavy-tailed distributions, is the *complementary* or upper tail CDF (sometimes referred to as the *survival function*, or denoted cCDF), which is  $1 - CDF$  or  $P(X \geq x)$ , indicating the probability that a random sample is higher than the function value. Both axes on such cCDF plots are traditionally set on logarithmic scales, usually  $\log_{10}$  for readability. To avoid confusion, in this thesis I refer to PDF and cCDF for density and distribution functions respectively (except in equations, where I use  $p(x)$  and  $P(x)$  respectively), and all PDFs are plotted on linear scales and cCDFs on  $\log_{10}$  scales, unless otherwise stated. Apart from scales on plots, whenever I

refer to logarithms (i.e. in calculations), I imply natural logarithms, that is  $\ln$  or  $\log_e$  where the base number  $e \approx 2.718$ .

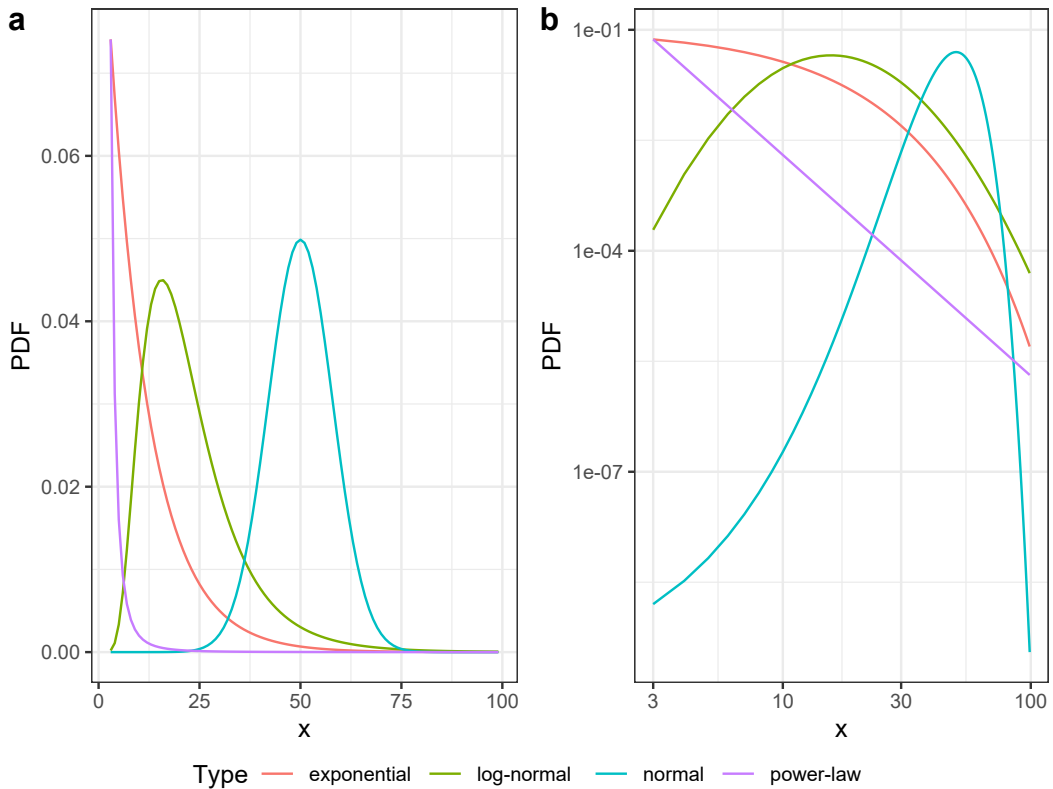


**Figure 4.2:** Example curves of the probability density function (PDF) of four common distribution types: normal (blue,  $\mu = 50$ ,  $\sigma = 8$ ), exponential (red,  $\lambda = 0.1$ ), log-normal (green,  $\mu = 3$ ,  $\sigma = 0.5$ ) and power-law (purple,  $\alpha = 3$ ,  $x_{min} = 1$ ), in linear (a) and logarithmic scales (b). Parameter values are arbitrary and x-axis is truncated at  $2 < x < 100$  for readability. The power-law distribution is the only to form a straight line when both scales are logarithmic

In the following, I present briefly the main distribution types that will be discussed further in the following chapters, with special focus on the *power-law distribution*, which is the model type associated with fractals and structural hierarchy. All of these distributions are modelled on continuous univariate data series (see N. L. Johnson, 1994 for more detailed presentations). Even though their mathematical definitions may seem complicated to non-initiated readers, most of the distribution types discussed in this thesis are readily implemented in standard statistical software, including Microsoft Excel, allowing for a more straight-forward use of them. For this thesis, I used base *R* functions for calculating PDFs and cCDFs, and for random number generation for normal, log-normal and exponential distributions (R Core Team, 2023), and equivalent functions from the *powerLaw* package for power-law and Weibull/stretched exponential distributions (Gillespie, 2015).

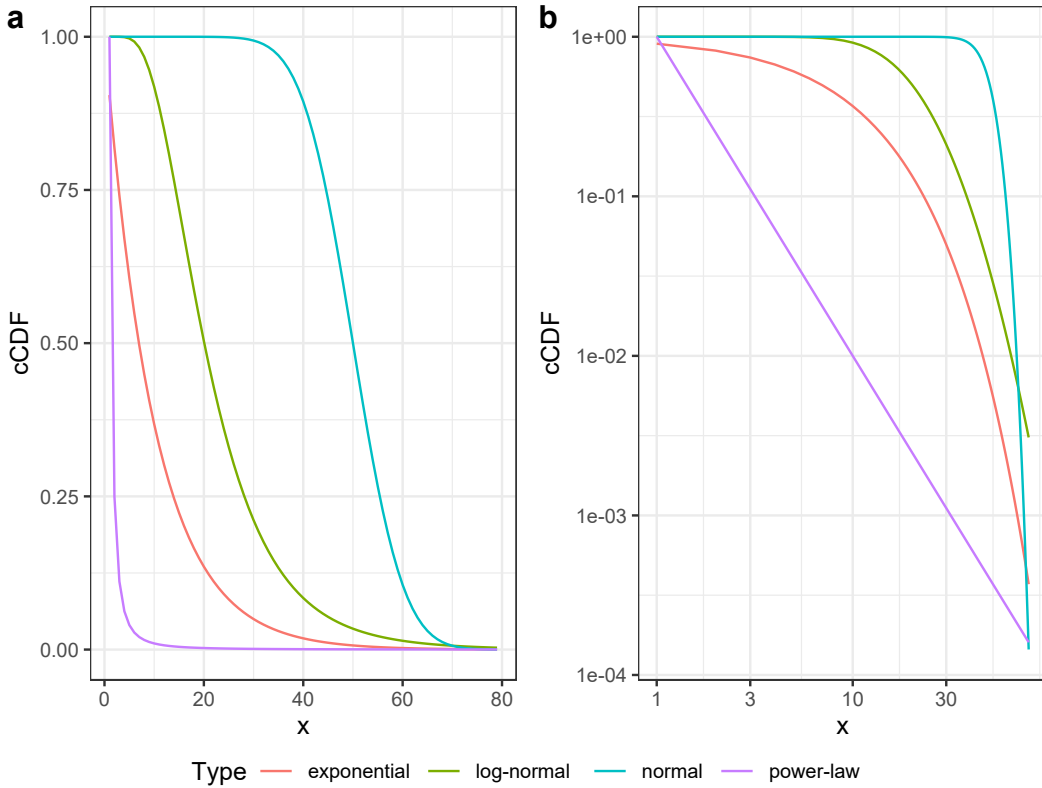


**Figure 4.3:** The same distributions as in Figure 4.2, but with the complementary (right-tail) cumulative distribution function (cCDF), in linear (a) and logarithmic scales (b), with  $0 < x < 80$  for readability

#### 4.2.1 Normal distributions and the Central Limit Theorem

One of the distribution models that are the most commonly referred to and well-known, is the *normal distribution*, also known as the “Bell Curve” due to the characteristic bell shape of its PDF (Figure 4.2a), or Gaussian after mathematician C.F. Gauss who contributed to its exploration in the early 19<sup>th</sup> century. Its characterising parameters are the *mean* (denoted  $\mu$ , *mu*) and *standard deviation* ( $\sigma$ , *sigma*), and the PDF is defined mathematically as

$$p(x) = \frac{1}{\sqrt{2\pi}\sigma} e^{-(x-\mu)^2/2\sigma^2} \quad (4.1)$$

where  $e$  (*Euler's number*) and  $\pi$  (*pi*) are mathematical constants (N. L. Johnson, 1994, pp. 80–88). This distribution is centred around its mean, with dwindling amounts of data spread outwards to either side. The mean – commonly known and widely used in daily speech – is the sum of all observations divided by number of observations, or

$$\mu = \left( \sum_{i=1}^n x_i \right) \frac{1}{n}. \quad (4.2)$$

The spread of the data from the mean is defined by the standard deviation, which is the square root of the mean of all squared deviations from the overall mean, or

$$\sigma = \sqrt{\left( \sum_{i=1}^n (x_i - \mu)^2 \right) \frac{1}{n}}. \quad (4.3)$$

Mathematically, the square of the standard deviation,  $\sigma^2$ , or *variance*, is simpler, but since it is also less intuitive, I refer here to the former whenever possible. The standard deviation can be thought of as the mean of all deviations, positive or negative, from the overall mean.

The great importance the normal distribution has to a wide range of phenomena is explained through the *Central Limit Theorem* (CLT), according to which the sum of random variables tends to a normal distribution as the number of variables increases towards infinity, under certain conditions (N. L. Johnson, 1994, pp. 85–88). More specifically, if  $X_1, X_2, \dots, X_n$  are independently drawn and identically distributed (condition referred to as *i.i.d*) random variables or samples, their sum will be normally distributed in the limit as  $n$  tends to infinity, or

$$\lim_{n \rightarrow \infty} \sum_{i=1}^n X_i = \mathcal{N}. \quad (4.4)$$

The sum may be standardized in some way to avoid infinite numbers, but in practice  $n$  will always be limited, so the resulting distribution will always also be approximately normal at best. The original distribution of the random variables (i.e. that of the *population*) does not need to be normal for the theorem to hold, but can be any distribution as long as its variance is finite. The normal distribution (referred to as the *sample distribution* in this context) is related to the population distribution of the random variables (samples), in that the mean of the population equals the mean sum of the sample distribution divided by  $n$ , and the standard deviation of the sample distribution, referred to as the standard error  $s$ , equals the standard deviation of the population divided by the square root of  $n$ , or  $s = \frac{\sigma}{\sqrt{n}}$ , meaning that  $s$  is reduced with higher  $n$  (i.e. larger sample size). A common variant of the CLT is that the distribution of sample means, rather than sums, are normally distributed, in which case the

mean of the sample distribution equals the mean of the population distribution.

In more laypersons' terms, the total weight of a box of strawberries is the sum of the weights of the strawberries it contains (subtract the weight of the box itself, and assume the same number of berries per box for the sake of argument). In the packaging facility, a large population of strawberries are continuously distributed randomly into boxes of the same size. The berries in the factory (the population) have weights that follow some distribution with limited variance – some are bigger than others, but there are upper and lower limits to how much a strawberry can weigh – and all the berries in the boxes are drawn from this same population (so identically distributed). New berries are shipped to the facility all the time, and berries are not sorted according to size but randomly mixed, so if one box by chance gets filled with only very large berries, that does not affect the weight of subsequent boxes (each box is the sum of  $n$  independently drawn sample berries  $X$ ). Under these circumstances, the weight of boxes of  $n$  berries (i.e. the sum of the berries' weights, the sample distribution) will be normally distributed by the Central Limit Theorem.

Some details here are crucial: the distribution of the strawberry weights themselves will, with higher  $n$ , tend towards that of the population, which is not necessarily normal. The theorem is only valid for summary measures like sums or means, and not for the observations directly. If the strawberries at the facility are mostly large (heavy) and with only smaller proportions of small berries, this skewed distribution will be reflected in strawberry boxes of a certain size ( $n$ ), but since the influence of this distribution is the same on all boxes of the same size, their overall weights (or mean weights) will be normally distributed. Furthermore, if we draw some boxes from one producer and some from another producer who has significantly larger or smaller berries, the samples are then drawn from different populations and are thus not identically distributed, and the sample distribution will not necessarily be normal (colloquially referred to as “comparing apples and oranges”). Similarly, if there is an overall trend of boxes becoming heavier over the season, then samples from across the season will not be normally distributed. If however, we compare the mean box weights from multiple seasons, these will again be normally distributed, unless there is also a multi-year trend of strawberries becoming larger or smaller. In other words, the i.i.d. condition of the CLT means that the samples are drawn at random, with no important underlying trends. As a side note, there is a substantial body of research on the conditions under which normal distributions can emerge *without* the i.i.d. condition being met (see N. L. Johnson, 1994, pp. 87–88 for details and

further references).

Also important to note is that the number of samples  $X_n$  (boxes of sample size  $n$  in the example above) does not matter to the shape of the sample distribution, other than to the resolution of the curve or binwidth of the histogram when plotting, and the weight of a single sample can be modelled as a probability following a distribution. The normal curve of the sample distribution can be entirely defined by the population  $\mu$  and  $\sigma$ , and sample size  $n$ . In many practical settings however, the parameter values of the population distribution (and even its type of distribution) are unknown, in which case more samples are needed in order to model a sample distribution and from there infer the parameter values of the overall population. This is the case when statistical tests like Student's t-test or ANOVA are applied for examining the relations between samples and populations.

In other cases,  $n$  (sample size) can be unknown, but assumed to be approximately the same for all  $X_n$  (samples), like in the somewhat more abstract cases where each of the  $n$  variables contained in  $X_n$  are of different nature – or stated otherwise, when the size of  $X_n$  is the sum of many different and independent causes. In the case of a normal house-size distribution within a given cultural setting (like a village), one can assume that the same number of causes affect the size each house takes when constructed, but to varying degrees (colloquially we often say *factors* for such causes, though in this setting one should strictly speaking prefer *terms*, *summands* or *addends*, since they add up rather than multiply). Say that house size in a given context results from the cumulative effects of household size, inherited wealth, soil quality, exposure to sun, wind or flooding, artisan specialisation, raw material availability in the year of construction and many more variables. Each of these may have separate probability distributions – e.g. the wealth distribution may be heavy-tailed while household size may be normal and symmetric – but as long as the overall population, so to speak, of contributing causes is distributed in the same way to all households, and that none of the variables dominates the effect of the others, and the value of each variable is independent from the values of the other variables, their sums expressed in house sizes should be normally distributed by the CLT. Such a distribution is then an expression of *random difference*, and in the case of house sizes, there would be no particular reason as to why a few houses would be bigger than all the others, just as a few houses would also be smaller, while most would be centred around the mean size. But again, if samples are drawn from *different* populations, e.g. houses from different villages or cultural contexts – where the probability distributions

of the underlying variables are categorically different – the i.i.d. condition is not met, and the distribution of house sizes is unlikely to be normal. Likewise if the population contains grades, i.e. is grouped, or where the different variables are correlated between them, e.g. if wealthier households are also larger households and have more access to raw material and better quality soils, and so on, their house sizes may also become disproportionately large and deviate from normal expectations.

A final caveat for normal house-size distributions that may be mistaken for skewed ones, is the case when there are no significant differences between house sizes, except for one that has a clearly different function – as in the ethnographic cases of community houses and men's houses discussed above. Then it makes little sense to interpret the resulting slight skewness of the distribution as a sign of social inequality in itself (notwithstanding gender inequalities). As a rule of thumb, to avoid such misinterpretations, it is useful to test whether isolating the single largest house changes the retained model when performing distribution fitting.

#### 4.2.2 Exponential distributions and constant rates of growth and decay

The exponential distribution is – next to the normal – one of the most widely applicable distribution models. In its simplest form, it is a function of a positive random variable  $x$  where some base number (usually  $e \approx 2.718$ , for compound continuous growth) is raised to the power of  $-x$ , in other words when  $x$  has the probability density

$$p(x) = e^{-x}.$$

This simple form is called the *standard* exponential distribution, and in most practical applications there will also be a *rate* parameter  $\lambda$  (*lambda*), so that the density function becomes

$$p(x) = \lambda e^{-\lambda x}. \tag{4.5}$$

In the case of the standard version,  $\lambda = 1$  and can be left out. The negative rate in the exponent is the actual rate that determines the shape of the distribution, whereas the rate multiplier to the base is a *normalising constant* which assures that the area under the curve adds up to 1, and thus that the values shown on the y-axis are probabilities. This constant

can be thought of as the y-intercept of a linear model, since at  $x = 0$  the function gives  $\lambda e^0 = \lambda 1$ . This is seen more clearly if we take the logarithm of the exponential density function,  $p(\log(x)) = \log(e) (-\lambda x) + \log(\lambda) = -\lambda x + \log(\lambda)$ , which is a linear model with slope  $-\lambda$  and  $\log(\lambda)$  as y-intercept. As a rule of thumb, an exponential distribution can thus also be recognised as a straight line on a plot with one linear and one logarithmic axis. A wide variety of more complex forms have been formulated, and the distribution type is furthermore generalisable to both the Gamma and Weibull distributions (N. L. Johnson, 1994, pp. 494–499). Note that the simple form presented here may also have more complex notations in specialised statistical literature, *cf.* Eq. 19.1 in N. L. Johnson (1994), which is equivalent to the density function above given that  $\sigma^{-1} = \lambda$  and  $\theta = 0$  (Clauset et al., 2009, p. 664; see also N. L. Johnson, 1994, pp. 522–523).

Exponential distributions have the highest probability (so the most data) at low values of  $x$ , and ever lower probabilities towards the right end of the curve (Figures 4.2a and (ref?)(fig:04-cCDF)a), with the rate of decrease determined by  $\lambda$  – the higher the rate value the steeper the curve falls off from left to right, and inversely low  $\lambda$  values give more heavy-tailed distributions. The type of setting which is most commonly modelled as an exponential distribution, is that of “events recurring at random in time” (N. L. Johnson, 1994, p. 494). If  $x$  represents the duration in time between events (or duration of single events) that occur continuously and independently from each other, with a constant average rate of  $\lambda$  events per unit of time, it can be modelled as an exponential distribution. An important feature of the underlying process (a so-called Poisson point process), is that it is memoryless, meaning that the duration between events  $X_1$  and  $X_2$  does in no way affect the duration between  $X_2$  and  $X_3$ , as all durations are drawn independently from the distribution with the same average rate  $\lambda$ . The example of such a process that may be the most familiar to archaeologists, is the radioactive decay of the  $^{14}\text{C}$  isotope with its average decay rate  $\lambda \approx 0.00012$  or 0.012% per year. With a rate that is low and using years as the time unit, it is more useful and intuitive to work with the *half-life* measure, or the time it will take on average for the initial quantity to be halved, which for  $^{14}\text{C}$  is about 5730 years. The half-life (the median of the distribution) is given by  $\log(2)/\lambda$ , solving for  $x$  in the cCDF function  $e^{-\lambda x} = 1/2$ , where the normalising constant in the PDF is replaced with 1 (and therefore omitted in multiplication) for the initial quantity or y-intercept. If we replace  $1/2$  with the remaining proportion of  $^{14}\text{C}$  in the organic material of an ancient artefact, compared to the expected amount in the same material when alive, we can use the

same equation to solve for the approximate year when the organic material died, which is the principle behind radiocarbon dating. In a radioactive decay process, a total amount of individual unstable isotopes are present from the start (here the death of an organic material), and their individual lifetimes until decay are exponentially distributed. As an additional metric of exponential random variables, the mean  $\mu$  or *expected value* is given as the reciprocal of  $\lambda$ , so that  $\mu = 1/\lambda$  and  $\lambda = 1/\mu$ . The mean is larger than the half-life, and for  $^{14}\text{C}$  decay, this corresponds to  $\mu \approx 1/0.00012 \approx 8267$  years.

The exponential distribution can also model many processes that are closer to an everyday human scale than  $^{14}\text{C}$  decay. Expanding from the example used for normal distributions, let  $\lambda$  be the average risk for a strawberry of being harvested within a week  $x$ . As the weeks go by (as  $x$  increases), the cumulative risk of being picked grows exponentially, so that there are very few berries that are older than a few weeks, and the mean age of the berries in the field is  $1/\lambda$ . The berries are furthermore picked by a harvesting machine that is unable to aim for a certain size category, and the berries grow linearly (which may be a rather poor approximation, but for the sake of argument). The harvested berries are also continuously replaced by new berries which start growing at the same pace, so the field is always renewed. Under these circumstances, the lifetime of a strawberry during which it grows is exponentially distributed, and the probability of surviving  $x$  weeks follows Equation (4.5). The example illustrates how exponential functions model repeated multiplication or multiplicative processes, since the  $x$  in the exponent means “multiplied  $x$  number of times”. The rate  $\lambda$  (technically  $e^{-\lambda}$  in the case of continuous decay) is multiplied with itself  $x$  number of times (keep in mind that  $(a^b)^c = a^{bc}$ ). Multiplying the rate for each new step in time means that the value of  $\lambda$  is applied to the current value of  $x$  rather than to the initial value. For example, let  $\lambda$  be  $1/5$  or  $0.2$ , so that there is a  $20\%$  risk of being harvested within a week, and thus  $80\%$  chance of being left in the field. The expected lifetime of a strawberry is then 5 weeks, and the probability of surviving 6 weeks or more is  $P_X(6) = e^{-(1/5)6} \approx 0.301$  or  $30.1\%$ , while that of surviving 7 weeks or more is  $P_X(7) = e^{-(1/5)7} \approx 0.247$  or  $24.7\%$ , corresponding to a relative decrease in probability of  $\frac{(0.301 - 0.247)100}{0.301} \approx 18\%$ , equal to  $1 - e^{-1/5}$ . Note that using the rate directly as the base, rather than as exponent of  $e$ , will give the same results as a (discrete) geometric distribution, in which case the reduction would be exactly the rate between each period. The difference lies in what is termed compound and simple interest in economics. For all the purposes discussed in this thesis, the continuous exponential distribution (with  $e^{-\lambda}$  as base to  $x$ ) is deemed more

appropriate than the discrete geometric distribution.

From an archaeological point of view, the essential point from the strawberry example above is that this process will also materialise in the size distributions of each single harvest, of all the strawberries at the depot, as well as the strawberries in a finished box for sale, all of which will be exponentially distributed (unless there is some additional sorting process involved). Of course, this does not change the fact that the box weights, as well as the mean strawberry size per box will be normally distributed, as previously shown. When it comes to house sizes, several scenarios involving growth could explain an exponential distribution. Let house size ( $x$ ) be directly dependent on household size, so that each inhabitant has a constant average number of  $\text{m}^2$  of roofed space. Say that the households grow exponentially at some rate, that is they increase in size by a factor of  $\lambda_1$  each cycle of some unit length ( $y$ ). At the same rate, the households also extend their houses proportionally to their growth, or replace their house altogether with a bigger house, and lastly, for each new cycle a new household is added to the village with newcomers, so that the total number of households follows  $y$  linearly. If all new households start at some minimal size  $x_{min}$ , the size  $x$  of a house after  $y$  cycles will equal  $x_{min}e^{\lambda_1 y}$ , and we can solve for its age (time since establishment of the household) as  $y = \frac{\log(x) - \log(x_{min})}{\lambda_1}$ . Here I use  $x_{min}$  for  $\theta$  in N. L. Johnson (1994), p. 494, following Clauset et al. (2009), p. 664. In other words, this context would generate an exponential house-size distribution of coeval houses in a village, where the largest houses are those of the households which were the first to settle in the village.

This model is of course not very realistic. For example, households cannot grow without limit, so the larger they become, the higher the probability that they split into two or more factions (see Alberti 2014 and Johnson 1982, and Section 1.4). The splitting of households itself can in fact also generate an exponential distribution. Let the households in a village grow linearly – say they each have a constant surplus of 1 person per year (persons who arrive or are born – persons who leave or die = 1) – but they also run a risk of  $\lambda_2$  (e.g. of 5%) of disintegrating and being replaced by a minimal sized household ( $x_{min}$ ) each year ( $y$ ), no matter their current size. House sizes are then linearly correlated with their age (or time since establishment of the household) so that  $y = x - x_{min}$  (disregarding the constant of  $\text{m}^2/\text{inhabitant}$ ). However, over time, the probability that a household continues to exist without splitting, will decrease exponentially, and we can write the survival function for households (and therefore their sizes) as  $P(X > x) = e^{-\lambda_2 y}$ , or  $e^{-\lambda_2(x-x_{min})}$ .

But again this model is not very satisfactory, particularly since it assumes purely linear population growth, which is unlikely in most cases. It would also seem likely that the probability of splitting of households would not be the same across the range of sizes, but rather be concentrated around some upper threshold, determined by the social structure between the inhabitants or by material or ecological constraints (or a combination). Common for both of the models above, is that one aspect is well described as exponential, but this aspect is only one out of many in the complex process which may underlie the house-size distribution of a settlement. Intuitively, it would also seem strange to have the whole range of houses in a settlement to scale exponentially, since it would imply that single house sizes would be ever closer and closer to each other all the way down to the smallest house in the village. Adding the  $x_{min}$  parameter does change this situation though, as it could then apply to cases within some upper class in which household size and/or wealth would increase to some fixed rate over time, not affecting the size of the main part of the settlement's households, which could well be normally distributed. Or the two models above could be combined to one, pulling exponentially in opposite directions (note that the two rates,  $\lambda_1$  and  $\lambda_2$  are positive and negative respectively). In both cases, the resulting house-size distribution would no longer be exponential, and these common combination distributions – the log-normal and the power law, both of which are heavy-tailed – are presented in more detail below.

Another issue with exponential distributions resulting from growth or decay in time, from the archaeological point of view, is that the time-averaging that so often infiltrates our analyses because of the difficulty of distinguishing temporally coeval data sets, may very well influence the observed data distribution. This influence is much more challenging to evaluate theoretically however, so in this thesis it is instead addressed empirically through simulation in Section ??.

### 4.2.3 Log-normal distributions and Gibrat's law

One of the main candidate models for heavy-tailed continuous distributions is the log-normal, defined as a variable  $x$  of which the logarithm is normally distributed. Adapted from Equation (4.1), its density function can be written (following the notation in Mitzenmacher, 2004, p. 229) as

$$p(x) = \frac{1}{\sqrt{2\pi}\sigma x} e^{-(\log(x)-\mu)^2/2\sigma^2}. \quad (4.6)$$

The  $\mu$  (mean) and  $\sigma$  (standard deviation) parameters are usually understood as the equivalent values associated with the normal distribution of  $\log(x)$ . It can be thought of as a combination of the normal and the exponential distributions, and like these, it has been shown to apply well to a wide range of natural and social phenomena, from the growth of organisms in biology to the pricing of options in finance N. L. Johnson (1994). One implication of  $\log(x)$  being normally distributed, is that the density curve of  $x$  will appear as a normal bell curve when plotted with a logarithmic scale on the x-axis (Figure 4.5). With linear scales, the curve is skewed with the mode to the left and a tail of high values to the right. More technically, the (natural) logarithm of a variable ( $x$ ) is the variable of exponents that may raise  $e$  to the values of  $x$ . A linear increment in a variable of exponents – say from 1 to 2 – will, with the same base, correspond to an exponential increment in powers (the result of exponentiation), as  $e^1 \approx 2.718$  and  $e^2 \approx 7.389$ . Thus, if the exponents of  $e$  that correspond to the values of  $x$  are normally distributed, then  $x$  itself will resemble an exponentially stretched normal distribution, which is a log-normal distribution.

Since exponents represent repeated multiplication and normal distributions result from random additive processes (see above), log-normal distributions may be most easily understood as resulting from random multiplicative processes. The product rule of logarithms states that the logarithm of a product of numbers equals the sum of the logarithms of those same numbers. This can be expressed as  $\log(ab) = \log(a) + \log(b)$ . Then, since the sums of many random numbers are normally distributed according to the Central Limit Theorem, the logarithm of the product of many random numbers (that is, these numbers multiplied together) should also be normally distributed (see e.g. Newman, 2005, pp. 347–348 for more elaboration).

The product of many random numbers is typically the result of a growth or decay process where the rate fluctuates randomly. A convenient example, following Newman (2005, p. 348), is that of a financial investment. If an initial value ( $a$ ) is invested in stocks that generate a return ( $e^\lambda$ ) which fluctuates randomly from year to year with a finite variance, the return  $y$  after  $x$  years will follow a wiggly exponential curve, or  $y = ae^{\lambda x}$  (Figure 4.4). After some years, the value of  $y$  will follow a log-normal probability distribution (Figure 4.5). If several persons start investing the same amount in stocks at the same time, then after a period, say

of 10 years, most of them will have earned returns of comparable size, centred around some mean return, while the earnings of the top investor may be several orders of magnitude higher, simply by chance. This assumes however that everyone invests randomly in the stock market, which is rarely the case. More scrupulous investment strategies may reduce the effects of chance and thus the spread of final returns, but this effect may again be countered by the risk-willingness of investors. In either case the resulting distribution after a given time period will be log-normal, which explains why this model is a central tool in financial analyses (e.g. see Mitzenmacher, 2004, p. 236 for its use in the Black-Scholes option pricing model).

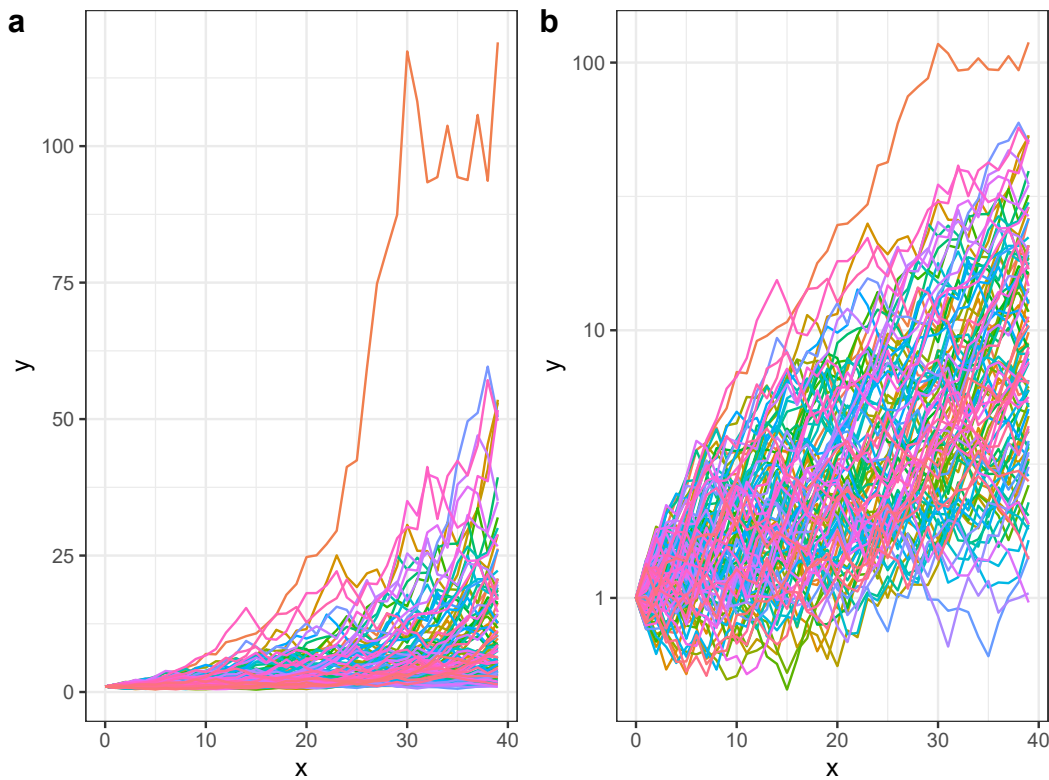


**Figure 4.4:** Exponential distribution of  $y = \lambda^x$  with rate ( $\lambda$ ) fluctuating randomly and uniformly between 0.75 and 1.4, i.e. with a mean rate of approx. 1.08, over 40 periods ( $x$ ) from an initial value of 1. The plots figure 100 individual runs of the distribution, with linear (a) and logarithmic (b) y-axis. Over time,  $y$ -values at any given  $x$  are expected to be log-normally distributed by the Central Limit Theorem

This process is known as *Gibrat's law*, after the French engineer Robert Gibrat who was the first to demonstrate its wide applicability, offering a mathematical explanation of the skewed size distributions that had frequently been observed by economists (Gibrat, 1930). Gibrat argued that the log-normal distribution was better fit for modelling firm sizes and salaries than the one already proposed by Pareto (i.e. the power law, see below), since it could account for the entire size range and not only the tail, and since it was theoretically better founded, as

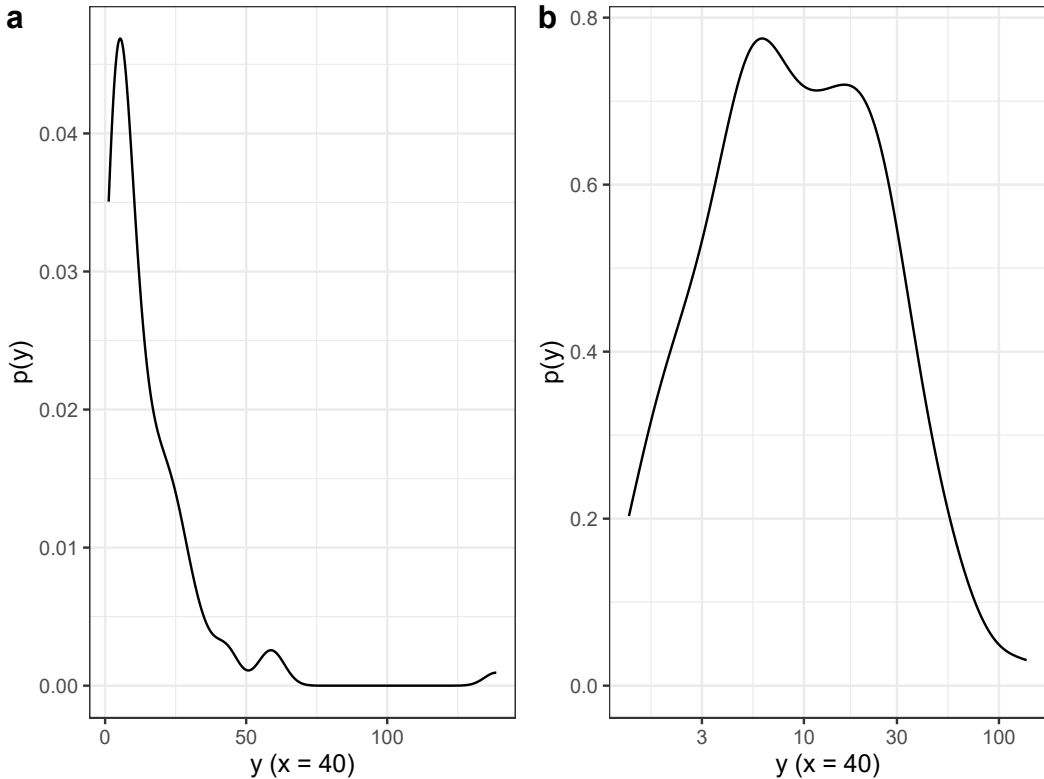


**Figure 4.5:** Density function of  $y$ -values from Figure 4.4 at  $x = 40$ , with linear (a) and logarithmic (b) x-axis, following a typical log-normal distribution

Pareto's original model was purely empirical. He termed the model the *law of proportionate effect*, since it emerges – as shown above – when proportionate growth rates are independent of absolute size. This essentially means that growth is exponential (size at any given time is multiplied with a rate, so proportional) rather than linear (additive), and that the range of possible rates is not determined by absolute size. Note however that there must be some randomness in the rate for the growth to result in a log-normal distribution. If the rate is *exactly* the same for all samples, or if it follows the exact same sequence of random rates, the initial distribution will remain the same over time, even though any initial spread will be scaled up or down according to the rates (Figure 4.6). In most economic settings, though there are overall trends that may affect everyone in a population (of firms, employees, cities etc.) at large scales, there are also many smaller factors that will affect individuals differently, causing random variation.

The modern financial market is of course not directly applicable to the Neolithic, but a number of multiplicative processes involving random fluctuations may also be relevant to Neolithic social structure or economy. One obvious example would be that of crop yields over time. Assuming that crop cultivation in a village is organised at a household level, and that house-

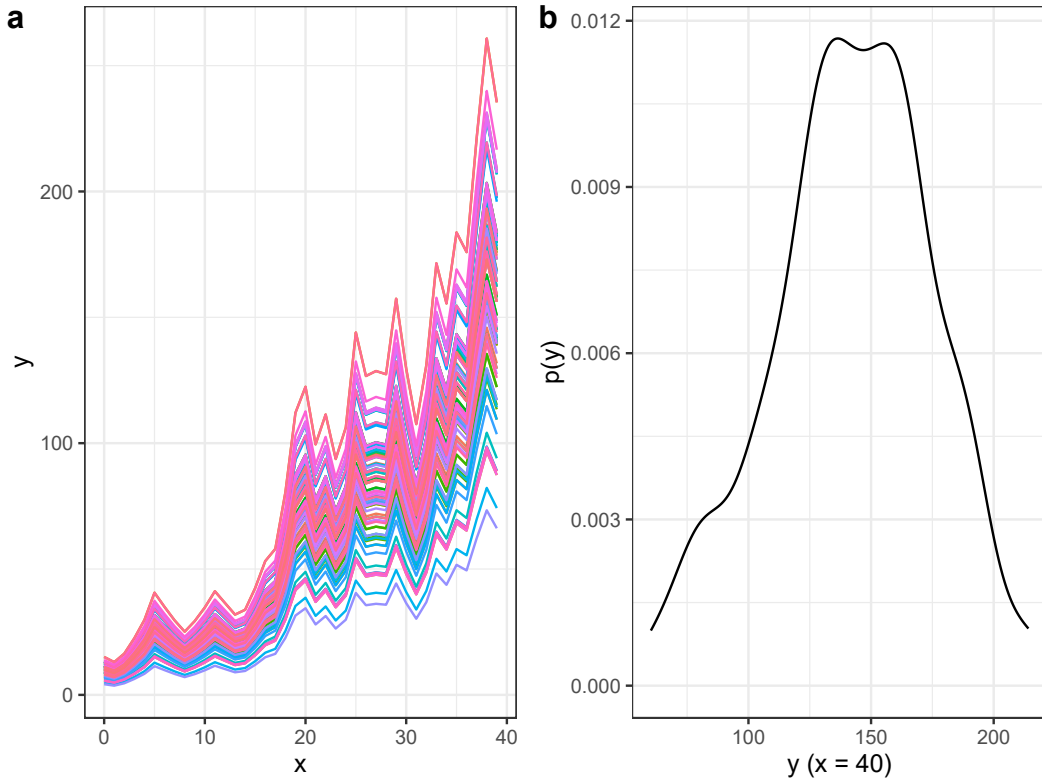


**Figure 4.6:** a: Exponential growth of 100 samples drawn from a normally distributed initial population ( $\mu = 10$ ,  $\sigma = 2$ ), all following the same sequence of uniformly distributed rates ( $0.75 < \lambda < 1.4$ ). b: Over time,  $\mu$  and  $\sigma$  values change, but the distribution remains normal. Scales are linear

holds grow their crops at separate locations in the vicinity, random differences in soil quality, sunlight, water, exposure to disease and so on, would arguably generate normally distributed yields in one year (the yield volume being the sum of many random effects). But given that the yield the year after also depends on the current yield through the size of the surplus that will be available for sowing, a randomly large yield one year will have better chances of producing an even larger yield the next year, and so on, in the same way a large financial return of a lucky investor one year is more likely to reach an even higher return later if reinvested. Supposing again that house size reflects household size linearly, and that larger yields can sustain larger households, this process could explain the emergence of a log-normal house-size distribution in a village over time.

For Neolithic crop cultivation it is in many cases more reasonable to assume that cultivation took place very close to or even within the village, in which case the conditions for yield volume would be very similar between households (#ref needed?). Cultivation could also be organised collectively rather than at the single household level, or as a combination depend-

ing on the crop. In such cases, a good or a bad harvest would affect all households equally, and skewed distributions would not emerge easily (#Ref. to Kohler 2018). However, even in such scenarios, small random differences in the initial sowing volumes of individual households could grow exponentially over time and produce a log-normal distribution of household yields, though with smaller spread between the highest and lowest values.

A somewhat different mechanism for explaining skewed house-size distributions within Linear Pottery settlements in particular, was proposed by Sara Schiesberg (2010). Assuming a stable population over time, with number of children per woman surviving to reproductive age being Poisson distributed with  $\lambda = 2$  (with ever decreasing probability of larger numbers of surviving siblings), and the probabilities of having given ratios of male and female children following a binomial distribution, the combined probability of having  $x$  male children surviving to reproductive age would follow a skewed log-normal-like (though discrete) distribution. Schiesberg observed this theoretical distribution of male siblings to be analogous to the empirical house-size distribution of excavated Linear Pottery settlements on the Aldenhoven plateau in North Rhine-Westphalia, Germany, arguing that there were gaps in the continuous size distribution that fitted with the discrete limits between numbers of male siblings. The correlation was furthermore explained as a result of a mainly patrilocal residence pattern, where house size would be a function of number of sons in an extended family (patrilocality being the most widely accepted residence pattern for the Linear Pottery culture, see Section 3.2). The same pattern could have emerged as a function of number of daughters in the case of matrilocal residence. Though Schiesberg did not model the observed house-size distribution explicitly as a log-normal, her model and the underlying process closely resemble the Gibrat's law described above. A (discrete) Poisson distribution with low rate can well approximate a (continuous) exponential, and a (discrete) binomial can approximate a (continuous) normal – so a combination of the two (by multiplication of exponential and normal probabilities) will equally approximate a log-normal. Thus, simply by the social practice of patrilocal post-marital residence, a skewed house-size distribution would emerge spontaneously, without the presence of any additional structural inequality between community members. In this case, a log-normal distribution would be present in a settlement from its onset, and the skewness could or could not become more pronounced over time, depending on other factors like whether crop surplus would be distributed within the community or kept within households.

A last mechanism that is sometimes referred to in statistical literature as causing log-normal

distributions, is that of random additive processes involving variables that by their nature cannot take on negative values, such as weights, heights or densities of physical entities (e.g. N. L. Johnson, 1994, p. 239). While (two-parameter) log-normal distributions only can have positive values (N. L. Johnson, 1994, p. 208), normal distributions will often also have positive probabilities below zero, depending on  $\mu$  and  $\sigma$  values, and are then poor models of such quantities. A house, as an example, cannot have negative size, but will always be larger than some lower threshold above zero, and should thus also be more adequately modelled as log-normal than normal, even if the distribution looks symmetrical. This will in turn allow for more accurate estimates of other derived parameters, like the confidence limits for the coefficient of variation. However, in cases of symmetrical distributions where  $\mu$  is much higher than  $\sigma$ , there is little practical reason to prefer a log-normal model over a normal one, as the probabilities of values below zero will be infinitesimally low.

#### 4.2.4 Power-law distributions, preferential attachment and hierarchy

A variable  $x$  is power-law distributed when its probability follows the power of itself with a fixed exponent  $\alpha$ , so that  $p(x) \propto Cx^{-\alpha}$  (Clauset et al., 2009, p. 662). Such distributions decrease very quickly as  $x$  increases, and are thus highly skewed, but the probability never reaches 0 – it is said to be *asymptotic* – meaning that they are also very heavy-tailed (Figures 4.2a and 4.3a). Furthermore, a power law can only take positive values, and there is always a minimal threshold  $x_{min} > 0$  above which the function holds. The exponent  $\alpha$ , often termed *scaling exponent* or *scaling parameter*, will usually lie in the range  $0 < \alpha < 3$ , though values below 1 are considered rare special cases, when considering size or frequency distributions (Newman, 2005, pp. 331–332). Low exponent values give more heavy-tailed distributions and *vice versa*, so power laws with a high scaling exponent (around 3 or above) are those that in practice will be more easily mistaken for other less skewed distributions like exponential or log-normal distributions (Figure 4.7). As with the previously discussed distribution models, the power law is also usually associated with a normalising constant (here denoted  $C$ ), a factor that ensures that the area under the curve of the PDF sums to 1, and which here is defined as  $(\alpha - 1)x_{min}^{\alpha-1}$  (Clauset et al., 2009, pp. 664–665). Applying the product rule of exponents, the power-law PDF or density function can be expressed as

$$p(x) = \frac{\alpha - 1}{x_{min}} \left(\frac{x}{x_{min}}\right)^{-\alpha}. \quad (4.7)$$

In the cCDF or survival function, again the normalising constant is replaced with 1, but rather than left out it is written in the exponential form  $(\frac{x}{x_{min}})^1$  which equals 1 when  $x = x_{min}$ , so that

$$P(x) = \left(\frac{x}{x_{min}}\right)^{-\alpha+1} \quad (4.8)$$

in the notation of Clauset et al. (2009), Eq. 2.6, equivalent to the more complex notation in Newman (2005), Eq. 4.

As shown in Figures 4.2b and 4.3b above, power-law PDFs and cCDFs hold the special property of appearing linear when plotted with logarithmic x and y axes (or equivalently when x and y values are log-transformed). This can be shown by log-transforming the simple functional form above, so that  $\log(p(x)) = (-\alpha)\log(x) + \log(C)$ , which is a linear model with y-intercept  $\log(C)$  and slope  $-\alpha$ . Power functions are in this way similar to exponential functions, with the difference that the variable  $x$  is here in the base rather than in the exponent, causing the graph to be linear only when *both* axes are logarithmic (as opposed to one axis for exponential functions). Because of this property, the most common method for estimating  $\alpha$  since the first formulation of the model and until recently (Clauset et al., 2009; Stumpf & Porter, 2012) was to plot the data on logarithmic axes, perform a least squares linear regression and estimate the slope (see Chapter 5).

The main reason for the great attention that has been given to power-law distributions over the years (see below), is its property of *scale invariance*, meaning that the distribution will appear the same no matter the scale in which it is being observed (see chapters 1 and 2 of G. B. West, 2017, pp. 1–78 for a general non-technical introduction to scaling in science). Figure 4.7 shows the relation between change in the variable being modelled ( $x$ ) and its function value (here the PDF function) as a constant proportion of exponents (i.e. a linear relation between two vectors of logarithms). This means that for a power-law distributed variable, a change of scale (zooming in or out on the x-axis, changing order of magnitude no matter the base number) will always result in a proportional change of order of magnitude of the probability or frequency modelled on the y-axis. If  $x$  represents a size related variable, and  $y$  a

frequency (probability in the PDF, rank in the CDF, or absolute frequency), this proportional relation in logarithms generates a self-similar hierarchy, where the same structure of sizes and frequencies is repeated across different scales (Figure 4.8). Thus, even though fractal structures are most often associated with geometric shapes in physical space – like the shapes of plants, rivers or clouds – they can be equally present in non-geometric variables, like income or wealth, magnitude of events, sizes of cities or nodes in networks. Such structures are, as with physical fractals, recognised by their abrupt skewness or high level of inequality, by their hierarchically distributive mode of functioning, and their statistical signature which is the power law. This connection between power-law distributions in general and fractals was first recognised and expanded upon by Mandelbrot (e.g. 1997; short summary in 1982, pp. 341–348).

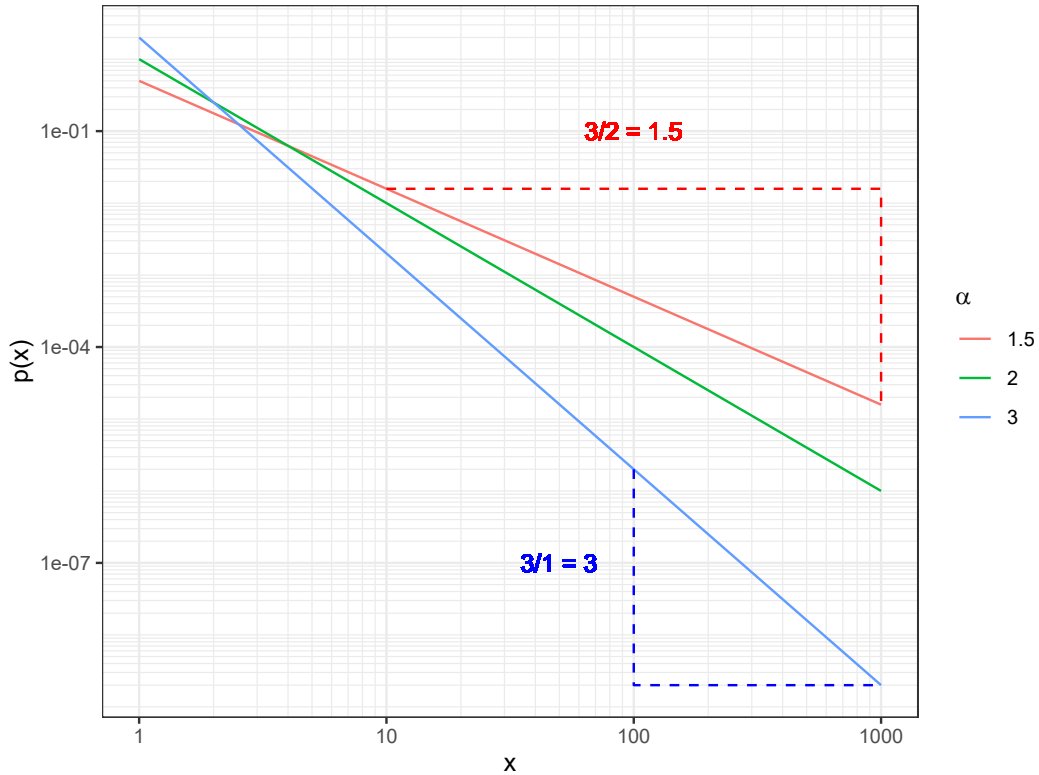


**Figure 4.7:** Examples of power-law distributions with different scaling exponent ( $\alpha$ ) values on logarithmic axes, showing how this parameter reflects change over orders of magnitude. For a model with  $\alpha = 3$  (blue), a decrease in probability  $p(x)$  of 3 orders of magnitude (powers of 10), e.g. from 0.1 to 0.0001 corresponds to an increase in the size of  $x$  of 1 order. For a model with  $\alpha = 1.5$ , the same decrease in probability corresponds to an increase in  $x$  of 2 orders of magnitude. The models appear linear in logarithmic space, but are in reality highly non-linear, as illustrated by the grid

As already mentioned, the power-law distribution was first formulated by Italian economist Vilfredo Pareto as a model of wealth inequality (1896). Over the 20<sup>th</sup> century it saw an increas-

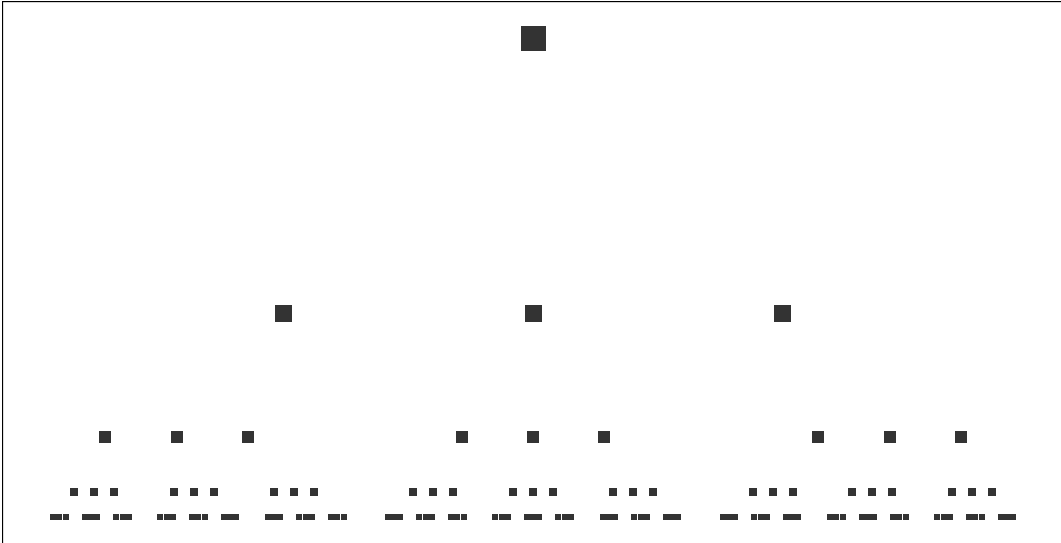


**Figure 4.8:** A power-law distribution of sizes arranged in discrete levels, illustrating its characteristic scale invariance. From the largest element on top and downwards, sizes decrease while numbers (frequencies) increase, both exponentially but in opposite direction, generating a hierarchical fractal structure where the same shapes are recognised at different scales

ing number of applications in a wide variety of fields in natural and social sciences, modelling phenomena from magnitudes of earthquakes and sizes of moon craters to the intensity of wars, frequency of family names and citations of scientific papers (see Mitzenmacher, 2004; Newman, 2005 for detailed overviews). The idea that the power law could be a suitable model for city sizes was seemingly first proposed in a short paper by Auerbach (1913), though it is often attributed to Zipf (1949), through which it has become known to and sometimes applied by archaeologists (see Section 4.3). The first influential attempt at an explanatory model of power-law distributions – which at first were primarily descriptive, one of the main critiques against Pareto – was made by Udny Yule (1925), who sought to explain the observed size distribution of genera by number of species. Yule’s model (here following the notation in Newman, 2005, pp. 340–342) involves a set of  $n$  genera consisting of a variable  $k$  number of species each. During a discrete time step interval, a constant  $m < n$  number of new species are added to the existing genera by speciation, so that some but not all genera will grow to  $k + 1$  in each time step. The probability for each genus of receiving a new species in a given time step is proportional to  $k$  or the number of species it already includes, since a speciation

is more likely to happen in an already large group of species than in a small group. Finally, for each time step one new species is sufficiently different to be considered a new genus on its own, so that  $n$  increases linearly by 1 for each step. Under these conditions, over time  $k$  will follow a heavy-tailed distribution with a power-law tail – or strictly speaking a discrete version of it known as the Yule distribution (see Simon, 1955).

The precise mathematics involved in this model are quite complex for non-specialists, especially in the version presented by Yule before modern stochastic theory was developed, but even more recent and concise formulations will involve some level of calculus (Mitzenmacher, 2004, pp. 230–233; Newman, 2005). The essential is however to note that the mechanism it describes – now known as *the Yule process* – is relatively simple and transferable to many natural as well as social settings. The heavy-tailed distribution of species will emerge even in the simplest scenario starting with one genus  $n_1$  consisting of a single species ( $k = 1$ ), and one added species to existing genera per time step ( $m = 1$ ). Then the single genus will have probability  $p(n_1) = 1$  of receiving the new species  $m$  so that it gets  $k = 2$ , while the new genus  $n_2$  starts at  $k = 1$ . In the next time step a new species will be given to one of these two genera, but  $n_1$  has twice as high probability of receiving it as  $n_2$  – that is, probabilities are  $2/3$  and  $1/3$  respectively. In other words, the probability for any genus  $n_i$  with  $k_i$  species of winning the round (so to speak) and being attributed with the extra species, is given by  $k_i / \sum k$ , or the fraction of the total amount of species (in the given time step) that the genus already has. The main difference here with the above described Gibrat's law – which also involves proportional growth – is that in the Yule process the growth is not distributed evenly across the system. There is an additional selecting process that over time gives more to those that already have, thus according a disproportionate advantage to anyone who gets even the slightest advantage by chance from the offset – which is why this is often referred to as a *rich-get-richer* process when applied to economics.

In fact, the Yule process having been recognised more or less independently within a number of disciplines over the years, it has come to be known by a plethora of different appellations, sometimes hiding the fact that they describe similar underlying mechanisms. The term *feedback loop* is derived from acoustics, describing the bothering situation when the sound from an on-stage monitor feeds into the microphones and back to the monitors, and so on, thus very quickly generating a sound so strong and high that it overturns the system. The sound going into the microphones is proportionally amplified to the volume of the sound coming

out of the monitor, so that the stronger the input, the stronger the output and by consequence the next input, and so on. Another term, derived from attempts in sociology to explain the power-law distribution of citation frequencies of academic papers, and more generally the rewarding systems in academia, is the *Matthew effect*, alluding to a passage in the Gospel of Matthew (25:29): “*For unto every one that hath shall be given, and he shall have abundance; but from him that hath not shall be taken away even that which he hath*” (Merton, 1968). A typical manifestation of such a process is when a prestigious research grant is attributed to a researcher based on academic merit, whereupon this in turn opens up numerous doors allowing for even higher career achievements, while the second best candidate, although having arbitrarily close merits to the first before the grant, afterwards will have disproportional difficulties of following their pace in career development. For paper citations, one analogous explanation is that a paper that already has many citations, is more likely to be found in literature searches and be cited again than a similar paper with less citations (Newman, 2005, p. 341). In other words, the probability of a new citation is proportional to the citations the paper (or its author) already has, but disproportional to the quality of the paper when compared to other papers of similar quality. The equivalent of the Yule process that has possibly received the most attention within social sciences since the turn of the millennium, is that of *preferential attachment*, first defined in a widely discussed study in network analysis by Barabási & Albert (1999). They were the first to identify scale-free networks of links between websites in the then young World Wide Web, where a few sites were reported to have very high numbers of links to them, while the vast majority of sites only have very few. Their explanation of how such networks emerge – strikingly similar to Yule’s explanation of speciation in biological genera – was that as new websites are made and the internet grows, these will tend to link (or preferentially attach) to existing websites that already have many links to them. It should be noted however that around 2010 there was a significant shift towards a more rigorous methodology that would be expected to accompany claims of power-law distributions in empirical data, leading to many previous claims being either weakened or fully rejected [Clauset et al. (2009); Stumpf & Porter (2012); Chapter 5].

A range of other more or less related power-law generating mechanisms and processes have been proposed (Mitzenmacher, 2004; Newman, 2005). Those that specifically relate to the magnitudes of events distributed in time may be of particular use in archaeology, though they have seemingly received little attention so far. Among these are approaches focussed on phase

transitions and critical phenomena, like *self-organised criticality* or SOC (Bak et al., 1987; Bak, 2013). This process models dynamical systems that continuously grow up until a certain critical point, at which it self-regulates downwards to stability through a collapse that is power-law distributed in size and frequency, before resuming the growth process again. The classic illustration of this model is that of a sand pile with a continuous addition of grains on top of it. Once the pile grows to its critical point where its slope becomes too steep, a sand avalanche is triggered and the pile stabilises again. The vast majorities of these avalanches are expected to be small in scale, but from time to time much larger avalanches appear. As the pile grows bigger, the critical point is also gradually raised, since a larger system can generally tolerate larger stresses before it needs to self-regulate. According to the theory behind such systems, the location of the critical point can be predicted with some accuracy, but the magnitude of the stabilising event that occurs when the system reaches this point, is impossible to predict beyond the power-law probability distribution it follows, i.e. that most events will be small but there is also a chance they will be several orders of magnitude bigger. The magnitude of the event is determined by the exact grain of sand in the pile that is the first to yield and thus triggering the chain reaction, but the scale of the potential consequences for the different grains varies greatly. The mechanism is said to be highly sensitive to initial conditions, or *chaotic*, similarly to how negligible initial differences in paper citations or website links over time can lead to disproportionately large differences, while it being virtually impossible to predict at the onset exactly *which* paper or website will come out on top Gleick (1987).

There are of course many ways in which the phenomena described here can be transposed to prehistoric social settings (see Section 4.3 below for examples of how this has been done). One important aspect of social processes that are known to generate power-law distributions, is that they often involve some sort of repeated competition, where actors who win once are more likely to win again later, thus cumulating their advantage. When the variable being modelled is house size, with the underlying assumption that this is a material reflection of wealth and/or power, and the distribution is recognised as a power law, the perhaps most straightforward interpretation is that of the emergence of a social hierarchy. The temporal process of this emergence could look something like the following. Let there be an initial population of households living within a social system that for this purpose can be described as egalitarian (that is, ignoring factors like gender inequality, random differences between households, heterarchical differentiations between kin groups etc.). If, for any reason, a competitive dom-

inance process is triggered, a household that initially holds a random slight advance over others may gain a dominant position over them, as clan leader or chief household. The leader or leading house may then gain certain privileges and duties related to tribute and redistribution of goods, thus strengthening the ties of dominance between them and the group of dominated households. There is however an upper limit to how many households that can be effectively dominated by a single household, so this relation would be unlikely to define the entire population of households. On the other hand, the same process could play out throughout the population, generating a set of leaders or leading houses each dominating a similar group of households – a situation that could be compared to the *house societies* described by Lévi-Strauss [-Lévi-Strauss (1982); Section 1.4]. If the social, and by extension political, competition continues, it will play out between these house or clan leaders, so that the one that by chance has an arbitrarily small advantage over the others may gain dominance over all of them and thus also their dominated households, and so on up to state societies (e.g. T. K. Earle, 1997; A. Johnson & Earle, 1987). As with the examples of the Yule process and preferential attachment discussed above, at any level of competition – e.g. between chiefs to become king – actors who find themselves further down the hierarchy, like clan leaders, have disproportionately lower chances of reaching that level, though in theory it is not impossible. Furthermore, the power-law relationship between leaders at different levels is recognised in that from any level to the next the number of leaders decreases exponentially while their dominance (the sum of households they each dominate) increases exponentially. The fact that most households remain at a bottom level with more random (*sensu* normal or log-normal) differences between them, does not change the fact that the leadership structure is hierarchical and power-law distributed – meaning that the entire distribution of dominance in the population has a power-law *tail*, as expected for most empirical settings.

There are some critical issues with such a model of the emergence of social hierarchy. Firstly, if house sizes are only *symbolic* materialisations of dominance – meaning that they do not in practice need to be large enough to actually fit all the people they dominate hierarchically – the distribution of these house sizes would have a much shorter spread than what is expected in systems where there is a more concrete physical flow between elements, like oxygen in blood vessels. There is no natural proportion between decision-making power and square metres of floor space, and it seems likely that absolute house sizes in practice would be more constrained by building materials and techniques, which are also subject to change over time.

Furthermore, several authors mention as a rule of thumb that a power-law tail should span at least two orders of magnitude in order to be accepted (C. Brown & Liebovitch, 2010, p. 53; e.g. Stumpf & Porter, 2012, p. 666). For a settlement where the bulk of houses are around 50 m<sup>2</sup> on average this would imply that the largest house (in a hierarchy of largest houses) would need to be in the order of 5.000 m<sup>2</sup> – comparable to the Pantheon in Rome or the Hagia Sophia in Istanbul – which, in addition to effectively excluding any prehistoric context, also seems as an unnecessary strict requirement for recognising hierarchy through house sizes. It is easily conceivable that smaller size differences could equally well be perceived as expressions of large social difference, e.g. if houses that are double the size of the average house (so 100 m<sup>2</sup>) belong to clan leaders and double that again (200 m<sup>2</sup>) to the chief. In that case, the size distribution would be more difficult to distinguish from a log-normal one, and if still interpreted as a power law, the scaling exponent ( $\alpha$ ) should be expected to take on a value considerably higher than what is usually expected for natural systems.

Another issue in need of empirical investigation, is how large a social hierarchy needs to be before it can be recognised as a power law, or over how many levels it needs to span. The rule of thumb of an interval of two orders of magnitude could be interpreted as two levels of scale (the base number of 10 is of course entirely arbitrary), which in social terms could translate to at least a complex chiefdom (i.e. a system of commons, intermediate chiefs and a chief of chiefs, A. Johnson & Earle, 1987, #ADD PAGES). A system with only a single leader or leading house per settlement as described above, could potentially not be recognised as hierarchical within a distribution fitting framework, even though it may have been lived and felt very much as a hierarchy for the people involved. A large social hierarchy will furthermore often span all settlements across a geographical area forming a settlement hierarchy, in which case studying house-size distributions within single settlements may be misleading. The overall scale of the hierarchy – whether it concerns houses in a settlement or settlements in a regional polity – is best understood from the largest element, and if this is missing from the data for whatever reason, interpretations in terms of social system will tend to underestimate the scale at hand. Luckily for archaeologists however, the largest settlements, as well as the largest houses, are usually the ones that are both best preserved and the easiest to discover, so that more often it is rather the lower end of the distribution that suffers from missing data, which has less importance to the interpretation of hierarchy (#REF?). It should also be kept in mind that in many – maybe most – hierarchical social contexts, the hierarchy may be highly

organic and volatile, and there does not always need to be any discernible discrete levels. I would argue that even in social systems where discrete levels of hierarchy are clearly defined – like in the feudal system of medieval Europe – the hierarchy expressed through the material culture of the involved actors does not always need to tell the same story as the social hierarchy expressed through their titles of nobility.

It should also be noted that there are social situations that do not involve competition of power but that still can generate power-law size distributions. Most importantly is what can in a sense be seen as the opposite of the top-down hierarchy model described above, namely a bottom-up hierarchy, which structurally speaking can be very similar, or even exist as part of the former in a continuous dialectic tension (Furholt, Grier, et al., 2020). Anarchic or democratic societies can form complex (i.e. multi-scale) community structures based on clan or kinship structures (Hamilton et al., 2007; Haude & Wagner, 2019, pp. 89–100), and if these structures are materialised in communal houses devoted to political assemblies or rituals, there is little reason to assume that the house-size distributions of such societies should be distinguishable from those of more top-down hierarchical contexts. An archetypical (pre-modern) example of such hierarchically structured democracies is the Iroquois League in the Great Lakes region during early European colonisation (Graeber & Wengrow, 2021, pp. 481–492; e.g. Haude & Wagner, 2019, pp. 127–131), but contemporary Western bureaucratic democracies are also highly hierarchical (De Landa, 2006, pp. 67–91). In any such cases, distribution fitting can allow for identifying the hierarchical structure, but not the actual type of government and to which extent its authority is based on bottom-up or top-down legitimacy. This qualitative aspect must still be investigated through other strands of evidence, like find inventories and symbolic representation within the large buildings. Building size itself will play a different role in democratic systems compared to autocratic ones, though the outcome will often be similar. In the former, communal buildings are by their very nature meant to be accessible and used by large parts of the community, and will therefore often need to be larger than common houses, while in the latter, leaders and high ranking people will be motivated to build houses for their private use that are larger than what they actually need, simply as a means to express their authority. In both cases the hierarchy is materialised in the house-size distribution, even though the absolute relationships between size and social importance may be culturally contingent. Exploring such specificities with hierarchical scaling in material culture has been one of the main motivations for this thesis.

In sum, the important characteristics of power-law generating systems, are that they are *complex*, meaning that they function or operate over several *scales* or orders of magnitude, which again implies that they exhibit *self-similarity* and can be described as *fractals* or *hierarchies*. Furthermore, they are rarely consciously planned, but rather tend to *emerge* spontaneously with growth, as a result of self-regulation and iterated responses to growth, like splitting or feedback that are proportional to size. Finally, even though such systems can be described as fully deterministic, they are also highly sensitive to initial conditions, i.e. they exhibit *chaos*, so that the magnitudes of single outcomes or trajectories can in practice be impossible to predict or forecast into the future, while the system as a whole can be well described, as well as explained backwards in time. Evidence of power-law distributed house sizes should be considered as a clear sign of a hierarchical social structure, though the exact nature of the structure – and specifically whether it is autocratic or democratic, or something in-between – needs to be argued from complementary evidence.

#### 4.2.5 Some variants of power-law distributions

A note must be made regarding terminology on power laws and some closely related distributions. Contrarily to normal, log-normal and exponential distributions, power-law distributions are not defined in a uniform way across all the disciplines where they are applied. Despite all claims of ubiquity, they remain special cases in many contexts, are not systematically taught in basic introductions to mathematics or statistics, and their broadened understanding seems to have suffered from long-standing discipline-specific traditions of defining them. Archaeologists who borrow theory and method from different fields therefore run the risk of talking past each other and not seeing the bigger picture of common phenomena described in different ways. Two alternative and more or less parallel ways of describing power-law distributions run under the names *Pareto* and *Zipf distributions*, after the first researchers who became known to define them under their specific parametrisations.

The so-called Pareto distributions form a group of distribution types with varying numbers of parameters, and are most often associated with applications in economics and finance (Pareto was an economist and his major works were on wealth and income distributions, see Chapter 20 in N. L. Johnson, 1994; Pareto, 1896). Comparing with the power-law definitions given above (Equations (4.7) and (4.8)), it is important to note that Pareto distributions are defined

as survival functions, i.e. cCDFs (complementary cumulative distribution functions) or the proportion of the distribution that is *higher* than a sample  $X$ . The scaling exponent for a Pareto distribution (N. L. Johnson, 1994 confusingly note this as  $a$ , p. 573, but here I prefer to use  $\beta$  for clarity) thus has the value of the power-law exponent  $\alpha - 1$ , or in negative values  $-\beta = -\alpha + 1$ , meaning that Pareto plots have a less steep slope than their power-law counterparts. Accompanying their use in applied economics is the appellation of the “80-20 rule”, a rule of thumb stating e.g. that in a company 80% of sales will typically go to 20% of clients as a result of the very skewed distribution. This specific rule corresponds to a power-law distribution where  $\alpha \approx 2.1$  or  $\beta \approx 1.1$  (Newman, 2005, p. 334).

Zipf law distributions, often referred to as “rank-frequency” or “rank-size” plots or rules, are most associated with linguistics, due to Zipf’s work showing that word counts (as well as city sizes) tend to follow power laws (Arshad et al., 2018; Zipf, 1949). Only some minor plotting conventions differ Zipf plots from Pareto plots, but again this influences systematically the value of the calculated scaling exponent. While Zipf distributions are also cumulative, they are not normalised to 1, meaning that absolute size ranks are plotted instead of probabilities. Furthermore, these are plotted on the x axis rather than the y axis, with the implication that the distribution is *discrete* rather than continuous. The y axis (the actual variable being measured) can in principle be discrete or continuous, but the most commonly cited cases are discrete, i.e. count data, like the number of inhabitants in a city or the number of times (frequency) a word appears in a text. The scaling exponent of a Zipf law (or a Zipf exponent, denoted  $q$  e.g. in Arshad et al., 2018, p. 78) can thus be expressed as

$$q = 1/\beta = 1/(\alpha - 1). \quad (4.9)$$

The fact that there does not seem to be any consensus on which character to use for the different parameters is an additional difficulty to handle when comparing studies that apply these different approaches. In his extensive review of these three separate research traditions, Mark Newman (a physicist; the power law is the most common variant within the natural sciences) admits that this inconsistent nomenclature “causes much confusion in the literature” (2005, p. 327), which I will claim is a polite understatement. For clarity, throughout this thesis I only refer to the scaling parameter of the power law as defined in Equation (4.7), which I denote  $\alpha$ , no matter the graphical representation of the distribution (most of the plots here are

cCDF plots, and could thus be qualified as Pareto plots). The value of  $\alpha$  is furthermore only calculated directly on the data using the maximum likelihood method described in Chapter 5, and is thus not dependent on the type of plot chosen for graphical illustration.

As already mentioned, regular power laws are asymptotic so that as  $x$  approaches infinity,  $y$  goes arbitrarily close to 0 without ever reaching it. This in itself acts as a limit to its usefulness for modelling most real-world phenomena which are of finite size, even though the power law may be a good approximation over some range of the system. In other words, in a power-law model of house sizes, no matter the value of  $\alpha$ , the probability of a house measuring a trillion square metres is certainly negligible, but still technically above 0. Several solutions have been proposed to this problem, allowing the model to end somewhere at  $x < \infty$ . Among the main candidates are the *power law with exponential cutoff*, the *stretched exponential* and the *parabolic fractal* distributions. The first one is – as the name indicates – a power law with an additional exponential factor, which turns the function increasingly (exponentially) downwards as  $x$  gets higher (see Clauset et al., 2009, p. 664 for precise definition). The second is a type of exponential distribution, similar to the one described above (Equation (4.5)), but where the  $x$  exponent is raised to a power constant  $0 < c < 1$ , giving a survival function  $P(x) = e^{-(x/x_{min})^c}$ , resulting in a tail which is heavier than that of a regular exponential distribution but thinner than that of a regular power law (Clauset et al., 2009, p. 664; Laherrère & Sornette, 1998). This survival function or cCDF of a stretched exponential is furthermore equivalent to that of the *Weibull distribution*, a well studied model type that is widely implemented in statistical software, making it easier to include in analyses compared to the more piecewise power law with exponential cutoff (comp. N. L. Johnson, 1994, p. 629 ff.).

Finally, the so-called parabolic fractal distribution has been proposed as a quadratic function model on log-transformed values of size to rank (Zipf plot), to account for cases where the distribution follows a parabola of constant curvature on a log-log plot (Laherrère, 2000). Jean Laherrère – working for a large oil company modelling the size distribution of oil reserves – noted how studies that claim to show power-law distributions in empirical data often tend to explain away the curvature of the distribution in log-log plots, e.g. by focussing on shorter ranges of the tail, or by constructing composite distribution models. While the log-normal model forms a parabola on log-log plots of its PDF (Figure 4.2), none of the above discussed models have this characteristic for their survival functions. A quadratic function is a simple polynomial including a squared term of the variable, of the type  $f(x) = ax^2 + bx + c$ . The

use of the term *fractal* here relates to the shape of the distribution being evaluated with log-log transformations, so that the function is interpreted as a power law with an additional squared factor,  $a$  and  $b$  both representing scaling exponents. With quadratic functions, the coefficient to the squared term (here  $a$ ) determines the curvature of the model, while  $c$  has the role of y-intercept as with linear models. The model can furthermore be interpreted as a power law where the scaling exponent  $\alpha$  is continuously increased with higher  $x$ , in other words where  $\alpha$  corresponds to the derivative of the parabola at any given  $x$ , forming a continuous spectrum characteristic of multifractals (see e.g. Harte, 2001). Though this model seems to have much potential both for modelling and explaining self-affine phenomena within finite systems, it is relatively recent and not easily applicable without specialist knowledge in statistics and programming, and is not further included in this thesis. Future studies would be warranted, e.g. applying the analyses proposed in Laherrère (2000) and Laherrère & Sornette (1998) for modelling sizes and frequencies of undiscovered and/or lost archaeological sites within given regions.

## 4.3 Fitting heavy-tailed distributions in archaeology

The distribution fitting approach adopted in this thesis is inspired by a relatively small number of previous studies in archaeology. Though the relationship between households and house sizes had already been thoroughly studied more generally by archaeologists and anthropologists since at least the 1970s [see Section 4.1], the earliest quantitative study of prehistoric house-size distributions accompanied with theoretical arguments for interpreting power laws as signatures of multi-level social complexity, was perhaps a study by Herbert Maschner and Alexander Bentley published 20 years ago (Maschner & Bentley, 2003). They presented a well-argued case for hierarchical scaling between households in a study area on the Alaska Peninsula, apparently discernible in several periods of the region's prehistory, and explained this as the result of an elite emerging from various (though unidentified) competitive socio-economic practices. The study could today be criticised for methodological shortcomings – the authors relied on least squares fitting on log-transformed binned data, they did not systematically propose more than one model for the data, nor propose any quantitative way of selecting the best fits, and their data sets seem to have been severely time-averaged, rendering any claims of hierarchical scaling between households potentially meaningless. All of

these issues have been thoroughly addressed in subsequent studies (see Chapter 5). The general analytical procedure and rationale however, remains highly innovative and would merit far more attention than it has received. In my view, this study represented the first turn beyond the study of size *averages* towards a theoretically informed study of size *distributions* in household archaeology (#Check this sentence again after writing the top of the chapter).

This approach was further explored by C. Brown et al. (2012) and expanded upon by Strawinska-Zanko et al. (2018), who identified a shift from less heavy-tailed distributions (exponential) to power-law distributions (Pareto) of house sizes in the Maya region approximately coinciding with the pre-Classic/Classic transition, which is traditionally considered the onset of state-level organisation. Following political scientist Manus Midlarsky (1999), Strawinska-Zanko et al. (2018) argued that this transition to a power-law distribution of wealth (proxied through house sizes) could be explained as resulting from increasing competition for agricultural land ownership following population growth. Furthermore, they identified a trend towards more pronounced inequality, both through lower  $\alpha$  values and higher Gini indices, until the end of the Classic period, with an abrupt shift to more equal distribution in the post-Classic (higher  $\alpha$  and lower Gini). Despite the inclusion of only four settlements in this case study, it remains highly interesting since the overall economic and demographic development of the Classic Maya is very well documented from a range of other approaches and intensive research. The study also contributed with detailed discussion of methodological issues, comparing the performance of different procedures. In a study by Crabtree et al. (2017) a similar analysis was performed on data from the Mesa Verde region in the American South-West over the 7<sup>th</sup> to 13<sup>th</sup> centuries CE. This cultural context is also very extensively documented, and holds the additional advantage of a fine-grained temporal sequence supported by dendrochronology, allowing for detailed analyses of near-coeval features. With the same motivation of using distribution models as proxies for underlying generative mechanisms, the authors systematically compared best fit log-normal and power-law models of settlement sizes as well as the sizes of *kivas* – a special category of communal ritual structures – across the study area. Though the results were not entirely unanimous, both indicators pointed towards a settlement hierarchy in the Pueblo II phase from ca. 1030-1140, centred around Chaco Canyon receiving tribute from surrounding areas, which again is coherent with the current understanding of the period based on other strands of evidence. Furthermore, they implemented preferential attachment mechanisms

into an agent-based model of the regional socio-demographic development accordingly, largely reproducing the observed temporal patterns. This also seems to have been the first archaeological study consistently performing distribution fitting by maximum likelihood estimation rather than least squares, and comparing the fit of different models quantitatively. For this they used the same R package *poweRlaw* that is used here in the following chapters (Gillespie, 2015).

The analysis of the size distribution of special communal structures across a region, as was done by Crabtree et al. (2017), is in some sense a bridge between analyses of house-size and settlement-size distributions. #GROVE2011 from here.

- Zipf law in archaeology, then A law (distribution) is not a law (of nature), see Grove (2011) for review of the long-lasting confusion in archaeology (e.g. Hodder (1979)), also “rank-size rule”
- Zipf law and Settlement Scaling theory, Bettencourt (2021), Gomez-Lievano et al. (2012), Lobo et al. (2020), Duffy (2015) Connection with Central Place Theory, e.g. Müller-Scheeßel (2007), Chen (2011). Why I’m not doing settlement scaling in this study.
- SOC in archaeology, see (Bentley & Maschner, 2001; Diachenko & Sobkowiak-Tabaka, 2022; Zhukov et al., 2016).
- Not fitting distributions in archaeology, just assuming they are heavy-tailed, or avoiding the question: ex. Brink (2013) (could include lots more!)

END chapter



# Chapter 5

## Methods: Distribution fitting

In this chapter I go into some more detail around the methods used in Chapter 6, and the reasoning underlying my choices of methods. As mentioned earlier (Sections 1.2 and 4.2.4), I consider power-law distributions as a statistical signature of hierarchical structures, and wish to test whether such structures may be reasonably shown to exist among houses in European Neolithic villages, or if house sizes in these contexts are better explained by other non-hierarchical models. Results from these analyses add to current debates surrounding the development of social and political organisation in the Neolithic, and to the question of the emergence of stratified societies more broadly. Furthermore, and as also mentioned in Section 4.2.4, the methodological procedure leading to claims of power-law distributed data is not entirely straightforward, and is an issue that has undergone important developments in recent years, often leading to refutations of earlier claims. It is therefore critical to be explicit as to the methods being applied in studies like this one, and not simply report results obtained in some unspecified way through obscurely documented software.

In the following I will present the methodological procedure applied in the distribution fitting on house sizes done in Chapter 6, followed by a series of tests of this procedure on synthetically generated data, with the goal of obtaining a more detailed view of the accuracy and limits of the method. Due to limited space and for simplicity, I will concentrate on the choices of methods and procedure, and not on the under-the-hood functioning of different statistical tools like maximum likelihood estimation and calculation of the Akaike information criterion. For more details on these there is a number of good introductory volumes, some of which – like Shennan (2008) and Baxter (2003) – are also specifically aimed at archaeologists.

## 5.1 Modelling heavy-tailed distributions

The standard method for fitting power-law models to empirical data throughout the 20<sup>th</sup> century was through least squares linear regression on log-transformed x and y values (e.g. Harrison, 1981; Mitzenmacher, 2004), the same way exponential and log-normal models could be fit more easily to data by log-transforming x values. Conscious about the still frequent lack of statistical training among archaeologists, C. T. Brown et al. (2005) and C. Brown & Liebovitch (2010) presented the log-linear regression method as sufficient because of its simplicity of application compared to more sophisticated methods. C. Brown & Liebovitch (2010) furthermore provided a detailed discussion around how to plot the data in order to obtain the most accurate parameter estimates. The central problem with fitting power-law models to data, is that power-law distributions characteristically have an overwhelmingly large proportion of the data at lower values, while the scarce high values are typically several orders of magnitude higher. Density plots of empirical data (with the PDF on the y axis) require binning, so that the plotted data points in reality correspond to bar heights in a histogram. The applied bin width will furthermore have a heavy influence on the appearance of the plot, where small bin widths are best to represent the many low values and large bin widths are best for the few high values. Brown and Liebovitch proposed multi-scale PDFs, combining histograms of different bin widths before performing regression, which they showed give better results on synthetic data (2010, Chapter 2). Logarithmic binning – increasing bin width exponentially so that points appear to be spaced as constant increments on a log-transformed x axis is also a possibility that has been proposed (Newman, 2005, pp. 325–326). Plotting the cCDF instead of the PDF has the advantage of avoiding the bin-width issue altogether, since y values then are a function of the rank of each data point. This also allows for using all the data and not reducing it into bins, and is shown on synthetic data to give more accurate  $\alpha$  estimates (i.e. absolute slope of cCDF +1, see Eq. (4.9)). However, the inconvenience with fitting the power-law model to the cCDF, as pointed out by C. Brown & Liebovitch (2010), is that it does not necessarily form a straight line, but will in particular be curved when  $\alpha \leq 1$ , making it more difficult to distinguish visually from other heavy-tailed distributions.

From the early 2000s, physicists and mathematicians started to criticise the frequent use of log-linear regression methods for modelling power laws, since they were shown to introduce systematic biases to the parameter estimates no matter the adopted plotting method, and calls

for the use of more robust methods like maximum likelihood estimation (MLE) were put forth (e.g. Newman, 2005, pp. 325–327; Stumpf & Porter, 2012). A new methodological tool kit was proposed by Clauset et al. (2009), which has since seemingly become the new gold standard for fitting heavy-tailed distributions. One of their main critiques of earlier practices, came from the recognition that in nearly all real-world contexts where power laws are claimed to exist, this behaviour only kicks in from some lower threshold or  $x_{min}$  in the terminology of Clauset et al. (2009). In earlier studies the value of this threshold was simply set by guessing from the looks of the plot and trying to fit a line covering as much as possible of the data. More formally, this also impeded proper normalising of the distribution. The method proposed by Clauset et al. (2009) consisted in testing a range of different  $x_{min}$  values and picking the one that gave the best MLE fit to the data by minimising the KS or Kolmogorov-Smirnov statistic (the largest observed distance between the model and the data), and was reported to perform very well on synthetic data. Next they tested the plausibility of the power-law model through bootstrapping, i.e. generating a large number of synthetic random data sets with the same estimated parameter values, each time measuring the KS statistic compared to the ideal model. The fraction of runs giving a KS statistic higher than that of the empirical data gives the  $p$ -value, which they argued should lead to a rejection of the power-law hypothesis when  $p < 0.1$ . They estimated the number of bootstrapping runs necessary for robust  $p$ -values being between 1.000 and 10.000, which for a few data series is not dramatic, but for larger numbers of data series quickly becomes computationally intensive. But most importantly, they argued that the bulk of previous studies claiming to find power laws in empirical data never actually tested and compared their model with alternative models, which they argued should be done even in convincing cases where a power-law model could not be excluded as a good fit through bootstrapping. The method they proposed for comparison and selection between competing models, was Vuong’s log-likelihood pairwise comparison test, though pointing out that any good statistical model selection method could serve this purpose (see Clauset et al., 2009, p. 663 for an overview of their “recipe for analysing power-law distributed data”). These methods were later implemented with functions and documentation in the R package *poweRlaw* (Gillespie, 2015), which has been used and cited in at least some archaeological studies since (Crabtree et al., 2017; Haas et al., 2015).

For the present study I have largely chosen to follow the instructions advocated by Clauset et al. (2009), but with a few modifications, for reasons that are discussed in more detail

below. Early experiments with the *poweRlaw* package indicated that the proposed bootstrapping procedure possibly represented a slight overkill in the present context, requiring much computing time with relatively limited gains. Furthermore, the pairwise model comparison using the Vuong's log-likelihood test appeared good but somewhat tedious, requiring a nested algorithm eliminating competing models one by one. Therefore I decided instead to opt for testing all candidate model simultaneously using the Akaike Information Criterion (AIC), or rather the version of it designed to correct for small sample sizes – the AICc. The AIC score is also calculated from the log-likelihood of each model, and indicates which of the candidates accounts for the given data with the most weight. While not implemented in the *poweRlaw* package, it is a frequently used statistical tool implemented in a number of accessible R packages. Here I used the *AICmodavg* package (Mazerolle, 2023) because of its useful functions for manually tackling the differences in how base R and *poweRlaw* models are coded. I also tested using the Bayesian Information Criterion (BIC) on the data sets, but quickly came to the conclusion that the AICc was sufficient for the types of models being used here, with maximum two parameters. The tested model types for the distribution tails were power law, log-normal, exponential and stretched exponential/Weibull, all of which were fitted using the *poweRlaw* package.

Having defined the best possible power-law model to the data series and selected the best candidate model for the distribution tail from the same  $x_{min}$  value applying the above procedure, I went on to test for the best model of the whole data series, without setting a lower threshold. This excludes per definition the power-law model, and I also excluded the Weibull distribution since it is more general and can mimic other models without providing very useful theoretical explanations. The Weibull distribution – much like the gamma distribution – can be a very handy tool for modelling empirical data when the goal is to use a single model type for data series with multiple types of shape, or for prediction in many practical settings, but it has much more limited explanatory power since it lacks a broad theoretical generative mechanism like the Central Limit Theorem or preferential attachment. The reason for including it when comparing tail models is that it provides a good power-law-like approximation with finite variance, i.e. it allows for upper bounds. The tested models for the whole data range were therefore the normal, log-normal and exponential distributions, all fitted with MLE using the broad and well established *MASS* package (Venables & Ripley, 2002), and selected with AICc as with the distribution tails.

## 5.2 Testing for false positive power-law tails

The difficulty of comparing power-law models with other common candidate models (like log-normal or exponential), is that they, unlike the others, by definition need a specified lower bound above 0, denoted  $x_{min}$ . Comparison of multiple models with AIC scores is only meaningful when done over the same range of data (this also applies to the Vuong's log-likelihood test for pairs of models proposed by Clauset et al., 2009). However, comparing multiple models over the range in a data set which has already been recognised as providing the best possible fit for a power-law model, gives this latter model a potential advantage over the other ones. Log-normal models, for instance, can explain the entire range of a data distribution, where a power law can in most cases only explain the highest values in the distribution tail. The fact that these two model types have frequently and for a long time represented competing explanations for the same empirical data sets, may reflect this apparent incomparability between them (e.g. Bee et al., 2011; Gibrat, 1930; Harrison, 1981; Mitzenmacher, 2004; Sheridan & Onodera, 2018). One can suspect then that this procedure of distribution fitting and model selection would favour power-law models unreasonably. At the same time, one of the main findings of the Clauset et al. (2009) study, was that power-law behaviour was only confirmed beyond reasonable doubt in one out of 24 empirical data sets which had been reported as power-law distributed in earlier studies, leaving the impression that the methodology would be conservative rather than lenient. In many cases however, the study remained inconclusive, especially regarding comparisons between power-law and log-normal models to empirical data sets (comparisons between power-law and other models were generally more conclusive). The authors admitted "*In general, we find that it is extremely difficult to tell the difference between log-normal and power-law behaviour. Indeed, over realistic ranges of x the two distributions are very close, so it appears unlikely that any test would be able to tell them apart unless we had an extremely large data set*" (Clauset et al., 2009, p. 689). Extremely large data sets are of course a luxury that is rarely afforded in archaeology, and if these two models are that close in many situations, one can ask whether picking one over the other really matters in the end. This question is further developed in Chapter 11.

The reliability of this methodology can to some extent be assessed using synthetic data. A first question to address is whether sample size affects the selected distribution model for the tail, and if so what size should be considered a minimum for the results to be reliable. In Figure

5.1, using random number generator functions in base R (R Core Team, 2023) and with the *poweRlaw* package (Gillespie, 2015), I reproduced Fig. 5a in Clauset et al. (2009), namely examples of a power-law, a log-normal and an exponential distribution, with the addition here of a stretched exponential, illustrating how they all can look roughly linear on log-log plots with their survival functions/cCDFs. Using the same parameter values, but with four different sample sizes (10, 100, 1.000 and 10.000) on each model, these test distributions were run through the distribution fitting algorithm described above (Figs. 5.2 and 5.3). The power law was correctly identified no matter the sample size, but for the smallest sample size ( $n = 10$ ) all other distribution types also gave power-law tails. For  $n \geq 1000$  all distribution types were correctly identified also in their tails, while for  $n = 100$  this was only the case for the stretched exponential and the power law. These results are in agreement with the analysis based on p-values obtained from bootstrapping presented by Clauset et al. (2009, p. 676 ff.), but the method opted for here is far less computationally intensive. Selecting the best model alternative directly based on AICc is also a less complex operation compared to the sequence of first bootstrapping and then performing pairwise comparisons of log-likelihood as proposed by Clauset et al. (2009). The inconvenience with the method proposed here, is of course that there is no guarantee that any of the models tested for are in reality appropriate – we only find out *which* one of them is the *most* appropriate. The p-value approach in (Clauset et al., 2009) does allow for positively rejecting hypotheses that clearly do not fit the data. However, early experiences (not presented in further detail here) gave the impression that this made little practical difference, at least on the data sets analysed in this thesis. Most sample sizes are in the order of 100 or lower, in which cases bootstrapping remained inconclusive, while it was still interesting to have an indication of which model that gave the best fit. The results shown in Figure 5.2 indicate that for sample sizes below ca. 100 power-law interpretations should be treated with care, and should not be trusted as  $n$  approaches ca. 10.

However, it must be noted that in order to generate the non-power-law distributions with a defined lower threshold as done here (and in Clauset et al., 2009), a much larger number of data points is in reality needed if we also consider those falling below that same threshold. For example, to get 1000 data points with values above  $x = 15$  following the log-normal distribution shown in Figure 5.1, they need to be filtered out from a total distribution almost ten times larger. When considering entire data distributions without lower bounds, as is usually the case e.g. when analysing archaeological house-size distributions, the sample size will

potentially also need to be much larger for correct model selection, although exactly *how* much larger should depend on the type of distribution and parameter values of the data. Similarly, when Clauset et al. argued that with the MLE method for estimating  $\alpha$  in a power-law model, sample sizes around  $n \geq 50$  would usually be enough for the estimates to be within 1% accurate (2009, p. 669), sample size is here referring to the number of data points actually being considered when fitting, which is  $n > x_{min}$  only. For this number to be 50 or higher, the total size of the distribution could often need to be 500 or higher, which is far more than most of the house counts per village in this study. This matter of sample size is a question that is perhaps less relevant to physicists and mathematicians, but that may be of crucial importance to archaeologists who regularly suffer from limited amounts of data.

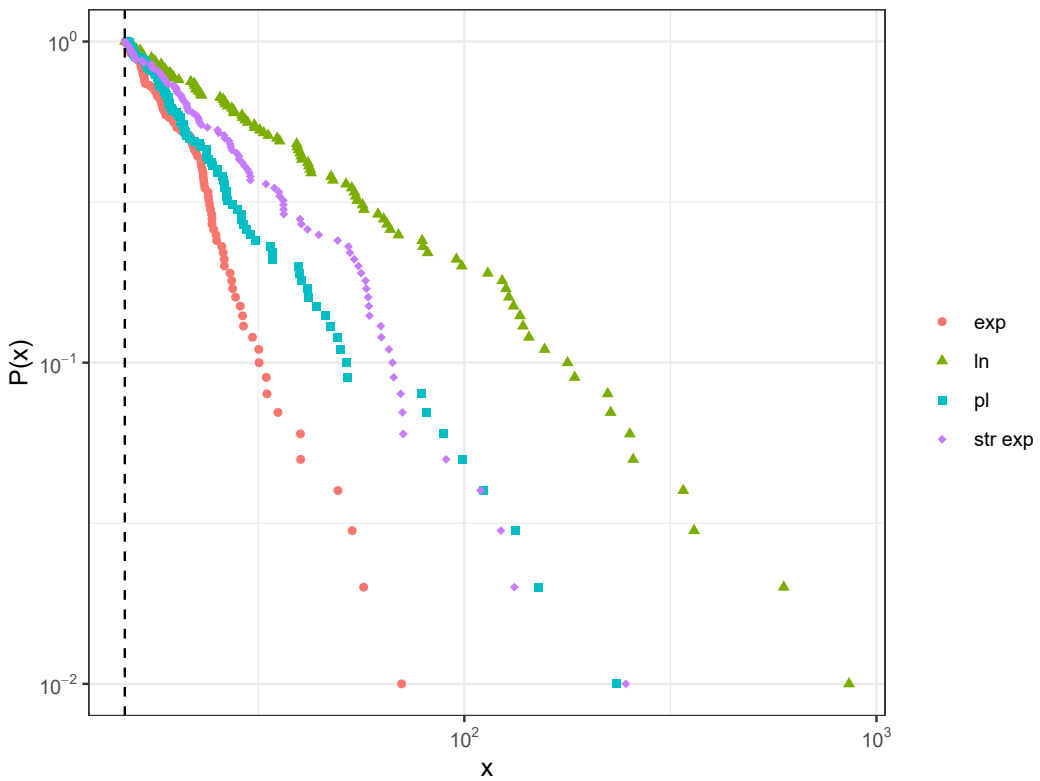


**Figure 5.1:** Synthetic data series drawn from four different distribution types: exponential ( $\lambda = 0.125$ ), log-normal ( $\mu = 0.3, \sigma = 2$ ), power-law ( $\alpha = 2.5$ ) and stretched exponential/Weibull (shape = 0.5 and scale = 3), all with  $n = 100$  data points and  $x_{min} = 15$ . Plot equivalent to Fig.5a in Clauset et al. (2009), with deviations due to random fluctuations only. Scales are logarithmic, and all four series appear as roughly straight lines, though only one is a true power law

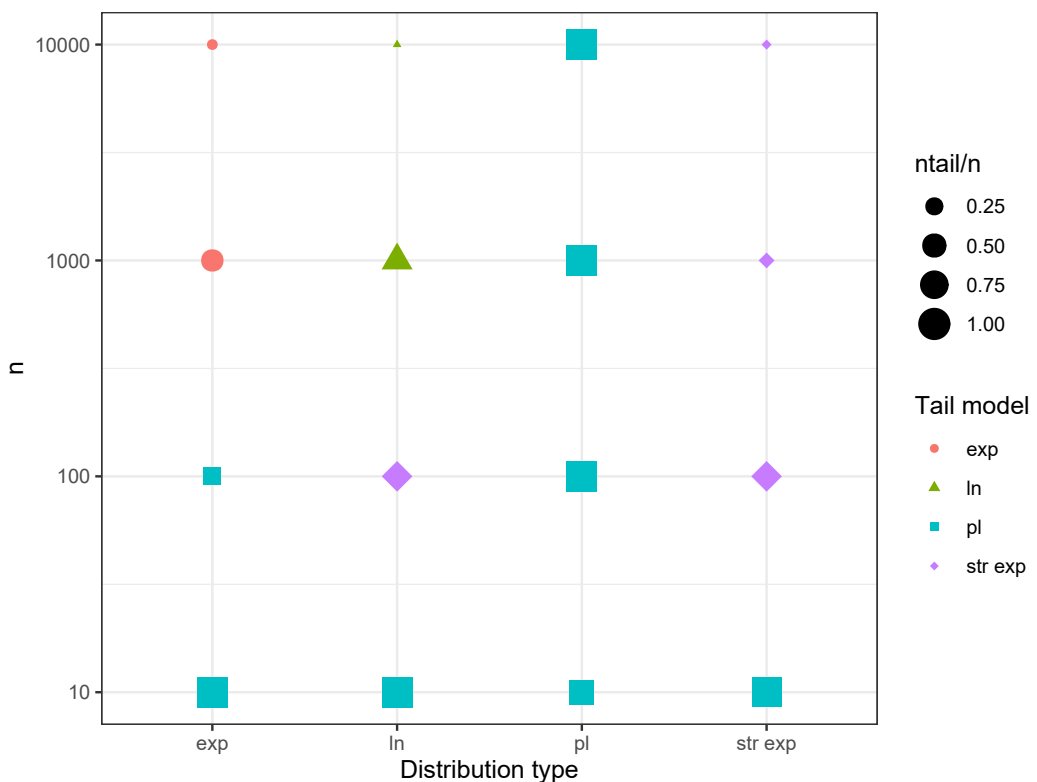


**Figure 5.2:** Selected tail models for the same synthetic data sets, each with four sample sizes ( $n = 10^1, 10^2, 10^3, 10^4$ ). For each tail model,  $x_{min}$  is set at the value which gives the best power-law fit. Point size indicates fraction of data points thus included in the tail model. For power-law distributions, all samples are correctly identified, while this is the case only for large samples ( $n > 10^2$ ) of log-normal and exponential samples, smaller samples being interpreted as having power-law or stretched exponential tails

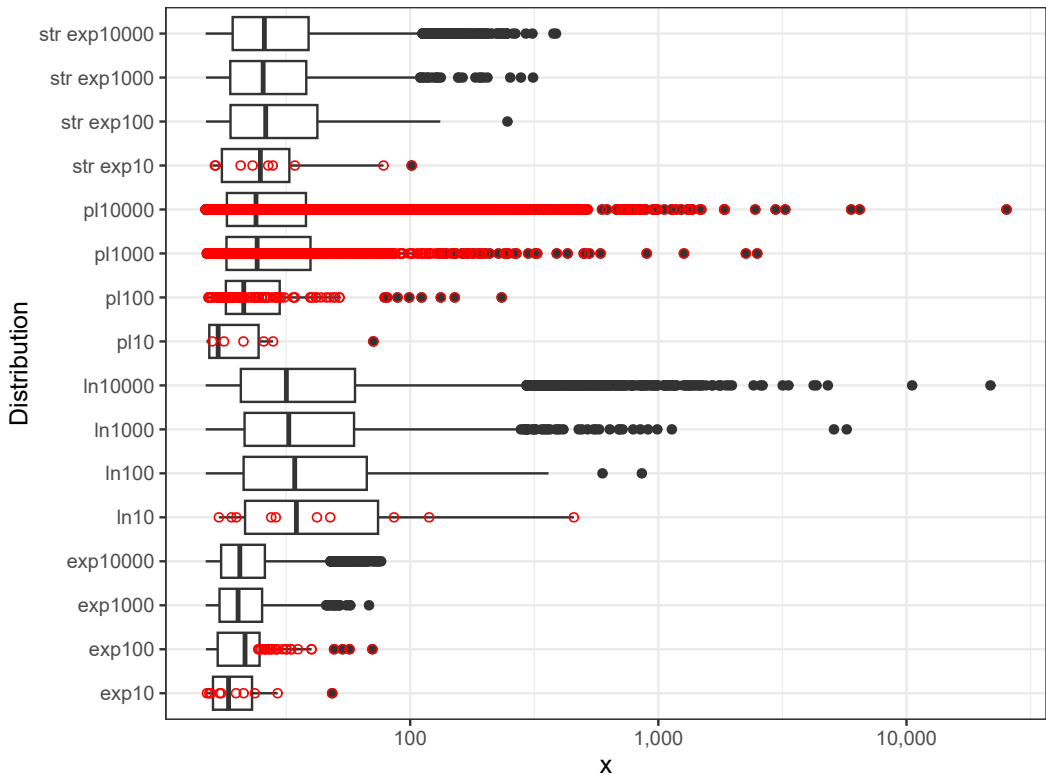


**Figure 5.3:** Boxplot of all the synthetic data sets, overlaid (in red) with the data points interpreted as power-law tails. X axis is logarithmic – however the log-normal distributions do not appear symmetric since they are truncated with a lower threshold. Note that especially for log-normals and power laws, larger samples give longer tails. If the model predicts a probability of having a value of 10.000 or more as only 1 in 10.000 or 0.01%, a sample size of 10.000 will probably allow for one such value

A second question more specifically related to the selection between log-normal and power-law models, is whether certain parameter combinations increase the likelihood of log-normal distributions being incorrectly interpreted as power laws. In his extensive review of power-law generating mechanisms, Newman (2005, pp. 347–348) showed algebraically how log-normal distributions can be mistaken for power laws especially when the range of the data that is being analysed is short, and when the value of  $\sigma$  is high. More specifically, since the PDF of a log-normal on log scales is a quadratic function – i.e. a parabola – sufficiently smaller sections of this will be nearly indistinguishable from straight lines, and can thus be well modelled as a power law (Figure 4.2b). The curvature of the function is characterised by its quadratic term, which is a fraction with  $x$  in the numerator and  $\sigma$  in the denominator, written  $-\frac{(\ln x)^2}{2\sigma^2}$ , essentially causing a flatter curvature with higher values of  $\sigma$  since this term then will vary more slowly with  $x$  (see Eq. 84 in Newman, 2005 for more details). The difficulty of distinguishing the two model types empirically undoubtedly lies in the close relationship between them, both being defined as some enhanced exponential distribution (Mitzenmacher, 2004). Figure 5.4 shows the cCDF plot of 36 synthetically constructed log-normal distributions, with  $\mu$  values ranging from 1 to 6 in integer increments, and  $\sigma$  values from 0.5 to 3 in increments of 0.5, each with sample size  $n = 1000$  and no truncation (i.e.  $x > 0$ ). When plotted this way (with the survival function of the variable), low  $\sigma$  values generate angular curves, while high  $\sigma$  values generate more parabolic curves.

Running these distributions through the distribution-fitting and model-selecting algorithm, more than half of them are interpreted with a power-law tail (19 of 36, Figures 5.5 and (ref?)(fig:05-ln-pl)). These are seemingly spread throughout the parameter space, with the only clear pattern being that for the highest  $\sigma$  values, the power-law tails cover only smaller fractions of the data.

What are we then to conclude from these preliminary tests? Clearly, it is a challenge to confidently distinguish between log-normal and power-law distributed data in the high ends of distributions, as noted in the beginning of this section. If the proposed methodological procedure seemingly serves well to identify power-law distributions when that is what they really are (i.e. there are no false negatives), it also seemingly identifies these erroneously in the tails of log-normal distributions half of the time, irrespectively of the log-normal parameter values, and with (for archaeologists) optimistic sample sizes. A more positive way to look at this issue, is to acknowledge that in truly log-normally distributed data, some definable portion of

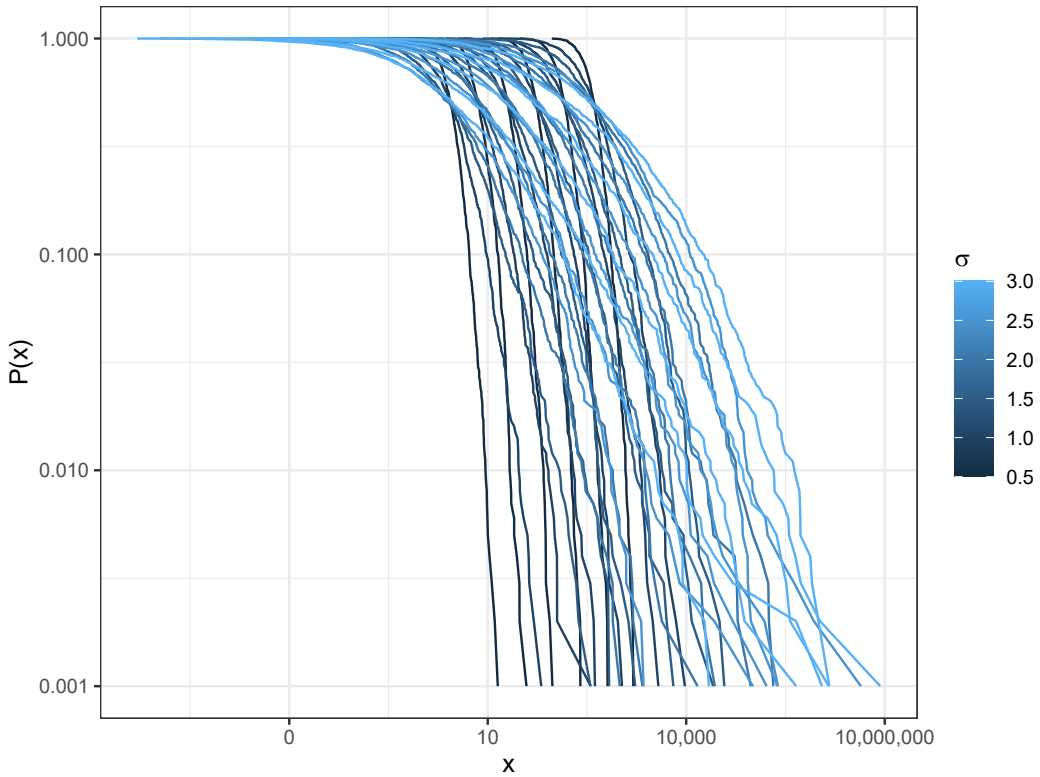


**Figure 5.4:** *cCDF plot of 36 synthetic log-normal distributions with parameter values  $1 \leq \mu \leq 6$  and  $0.5 \leq \sigma \leq 3$ . Each distribution is generated with  $n = 1000$  data points, but rendered here as lines for clarity. Scales are logarithmic*

the upper tail is in many cases indistinguishable from a power law, and actually best modelled as such. There may well be precise mathematical reasons behind this, but further insight to whether such power-law tails are confidently indicative of social hierarchies when observed on material culture proxies such as house sizes, would perhaps require large-scale systematic testing on ethnographically documented cases, which would clearly go beyond the scope of this thesis.

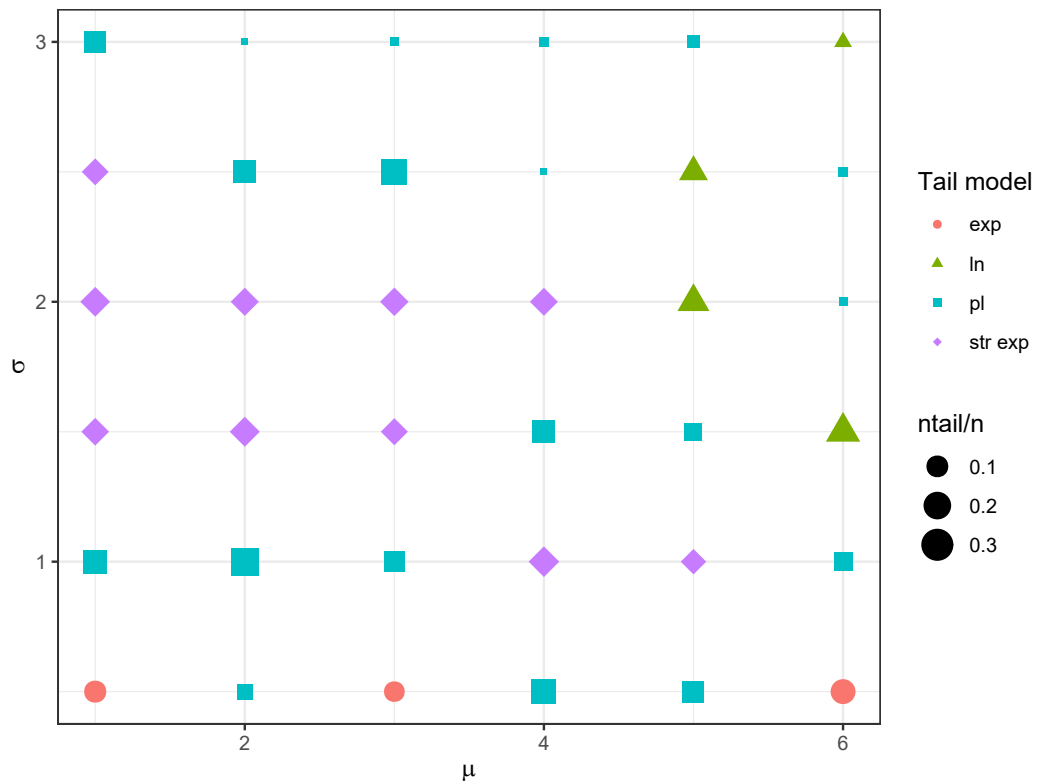


**Figure 5.5:** Interpreted tail models of the same log-normal distributions. 19 of 36 distributions have tails that are best modelled as power laws. Symbol size indicates fraction of the data included in the tail, with  $x_{min}$  parameter set for best possible power law fit. See text for details

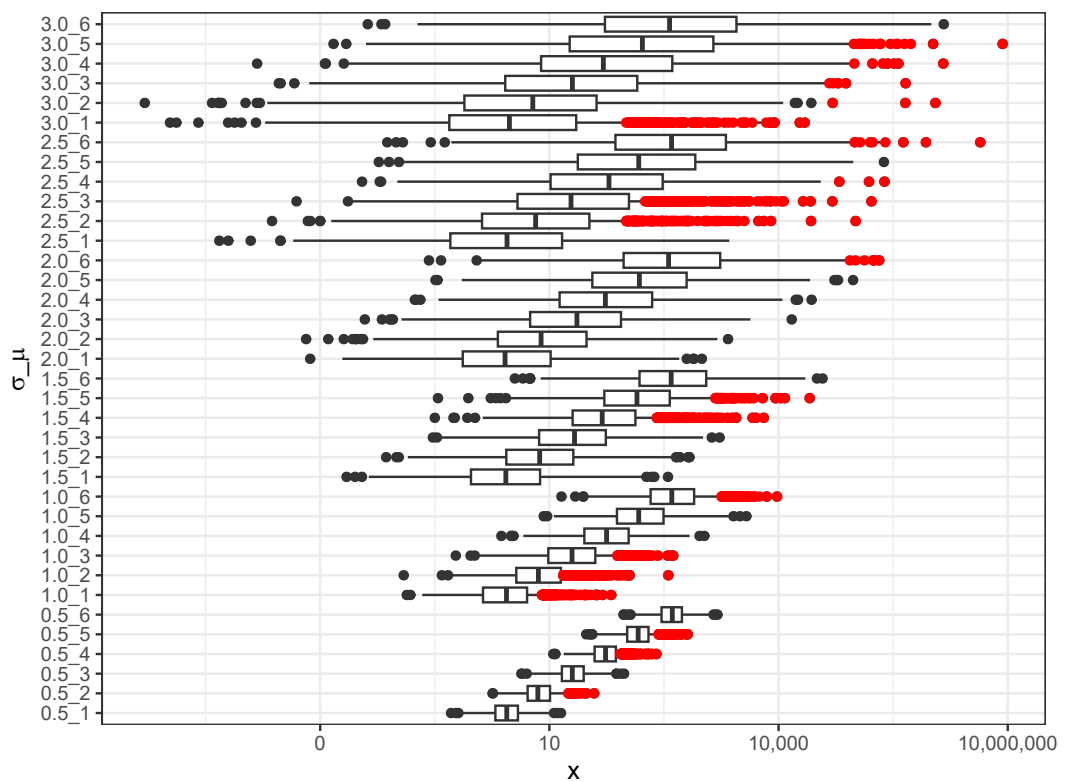


**Figure 5.6:** Boxplot of the same 36 synthetic log-normal distributions, overlaid (in red) with data points included in tails interpreted as power laws. The power-law tails stretch across the log-normal data in a range from 0.3% (3 data points out of 1000) to 23.5%

### 5.3 False positives from data aggregation

Data aggregation or lumping of samples may be done for two main reasons in archaeology. Firstly, when the sample size is too small lumping together several contemporary samples can raise the sample size to an acceptable level (spatial lumping). And secondly, in cases when it is impossible to temporally disentangle elements within a settlement, i.e. to reduce temporal resolution to coeval elements, we are forced to proceed with temporal lumping (accepting a low temporal resolution, Perreault, 2019, pp. 56–61 ff.). The problem can be further broken down to two case types: a) all lumped samples are really drawn from the same underlying distribution (referred to as the i.i.d. condition in the previous chapter), and b) they are not similarly distributed. For spatial lumping this degree of similarity can be assessed, but not necessarily for temporal lumping. But even when it can be assessed, the lumping needs to be justified in social terms. As an example, several spatial samples (e.g. villages in a region) can have house-size distributions in which no significant differences are observed using statistical tests like ANOVA, but at the same time be functionally entirely independent, in which case it is arguably more logical to augment the size of a single sample through simulation and evaluate plausibility through bootstrapping, rather than by lumping of all available samples. On the other hand, house sizes can be significantly different between quarters or suburbs within a city or metropolitan area, or even between cities in a region or country, but if they all function together in a coherent system, they may reflect a spatial segregation between different strata in the society, in which case it can make much sense to lump and analyse them together. When it comes to temporal lumping, given that a settlement does not undergo substantial cultural changes during its timespan (change in archaeological culture), a workaround to evaluate whether the house-size distribution evolves significantly over time may be to target a number of size categories for  $^{14}\text{C}$  dating, and to check that they all stretch over the entire range of the settlement's duration, and if yes, accept to analyse the whole distribution as one.

In order to build an appreciation of the possible effects of data aggregation on the identification of power laws, I constructed a set of 20 synthetic data series in successive steps. The first series consisted of 100 log-normally distributed random numbers with  $\mu = 4.5$  and  $\sigma = 0.4$ , corresponding to sizes of ca. 90 for the mean and 1.5 for the standard deviation when exponentiated. These values were set to be close to realistic values of house-size distributions in Neolithic settlement as presented in the next chapter. The second data series consisted of

the previous plus an additional 100 random numbers with the same parameter values, and so on for 20 iterations, so that the last series consisted of 2000 points. These series were then run through the distribution fitting algorithm for best power-law fits and model selection with AICc (Figures 5.7a and 5.8a). Five of the 20 series were interpreted with power-law tails (1/4), and these were clustered in two groups. The example is only illustrative, and would need larger and more systematic analyses to be considered general, but these results seem to indicate that under these conditions (increasing sample size with identically distributed, though not independent samples) power-law tails appear somewhat randomly, not necessarily as a result of larger or smaller sample sizes. However, once a power-law tail has appeared, it lingers for one or two iterations since the following series are only copies of the previous with some additional data.

It is important to note here that this additive process is not equal to simply constructing random log-normal sequences with gradually increasing sample size, as was done above (Figures 5.2 and 5.3). There it was shown that for log-normal and power-law distributions, data range increases with sample size since larger samples allow for data points with values that have lower probability of occurring. The data series presented here have internally very similar ranges of x values, since for every iteration new data is added *as if* the distribution only had the original sample size of 100, which is closer to what actually happens when we mix together analytically different phases of a settlement. A settlement with a long duration like 20 generations can thus have a house-size distribution that easily appears as a log-normal distribution with an upper truncation when all houses are analysed together. Though this point is not pursued further here, such truncations could then in themselves be seen as indications of temporal depth in a settlement – i.e. if the modelled house-size distribution would be expected, given the sample size, to yield some fraction of data points with markedly higher values than what is observed, it could be a sign of substantial temporal mixing. However, as is shown here, such mixing does not necessarily affect the interpreted model of the data, nor the modelled parameter values, *given that the samples are identically distributed* (see #script in supplementary material for further details).

This situation quickly changes when the samples are made up of differently distributed subsamples. In Figures 5.7b and 5.8b, the same data series are constructed, but allowing for the  $\mu$  and  $\sigma$  values to fluctuate randomly within very small ranges, between 4 and 5 for the mean and 0.3 and 0.5 for the standard deviation. The resulting distributions then become

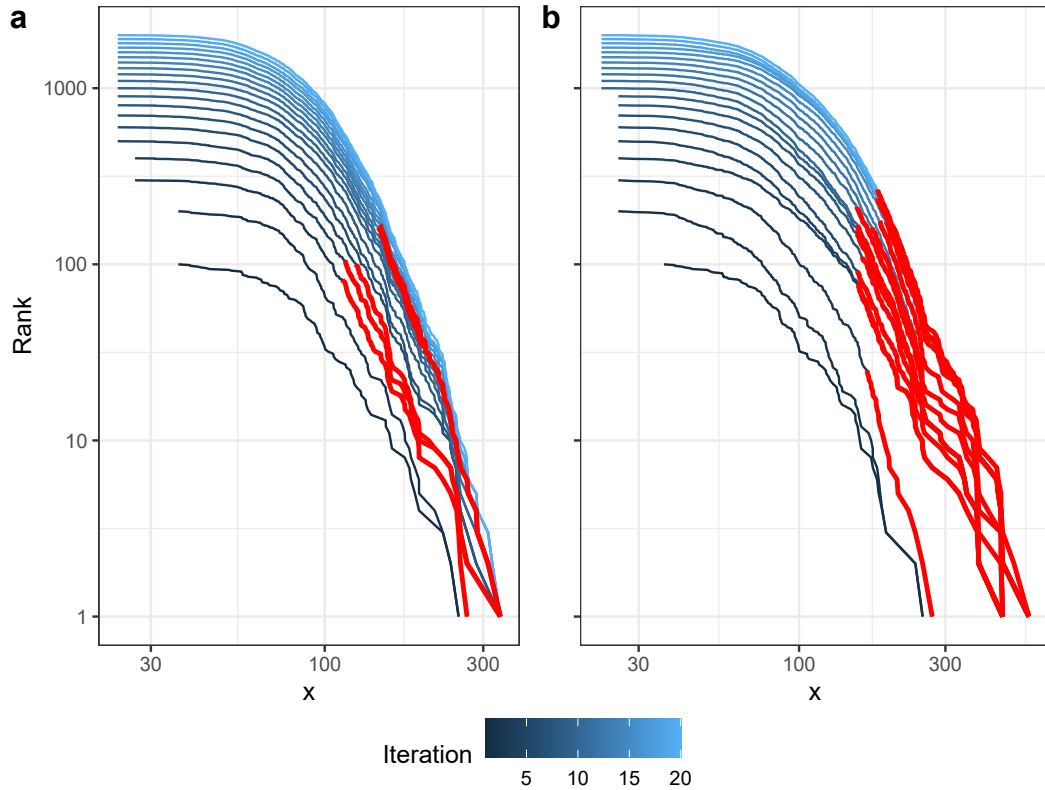


**Figure 5.7:** Twenty series of sequentially aggregated log-normal distributions, starting with 100 data points and 100 more added for each iteration. Parameter values for every group of 100 data points are fixed at  $\mu = 4.5$  and  $\sigma = 0.4$  (a) or uniformly fluctuating between  $4 < \mu < 5$  and  $0.3 < \sigma < 0.5$  (b). Both settings give distributions that resemble those of Neolithic house-size distributions. Red lines indicate power-law tails. The series overlap to a large extent, so y axis is plotted with rank rather than normalised cCDF to facilitate readability. Scales are logarithmic

slightly more skewed over time, and after the first two iterations almost all distributions are modelled to have power-law tails. This is phenomenon of increased variance resulting from analytical lumping is described and further discussed in Perreault (2019, pp. 61–79). In the specific case of house-size distributions, the implication is that if there are significant changes occurring over the time span of the settlement being analysed – e.g. that houses become larger or smaller over time, or that there is growing or reduced inequality over time – this will affect the overall distribution with increased variance, potentially leading to false positive power laws. If individual dating of houses is difficult to achieve, changes in the house-size distribution can to some extent be seen using temporal trends in construction techniques or raw material use as proxies. But if these material factors are stable over time and the change in house-size distribution is induced solely by social factors that are more difficult to observe directly, like post-marital residence patterns or kinship structures, there may be no way of distinguishing trends over time without dating houses individually. The issue of temporal

resolution is a major concern in any social archaeology, and a pragmatic attempt at dealing with it is given in the following chapter.

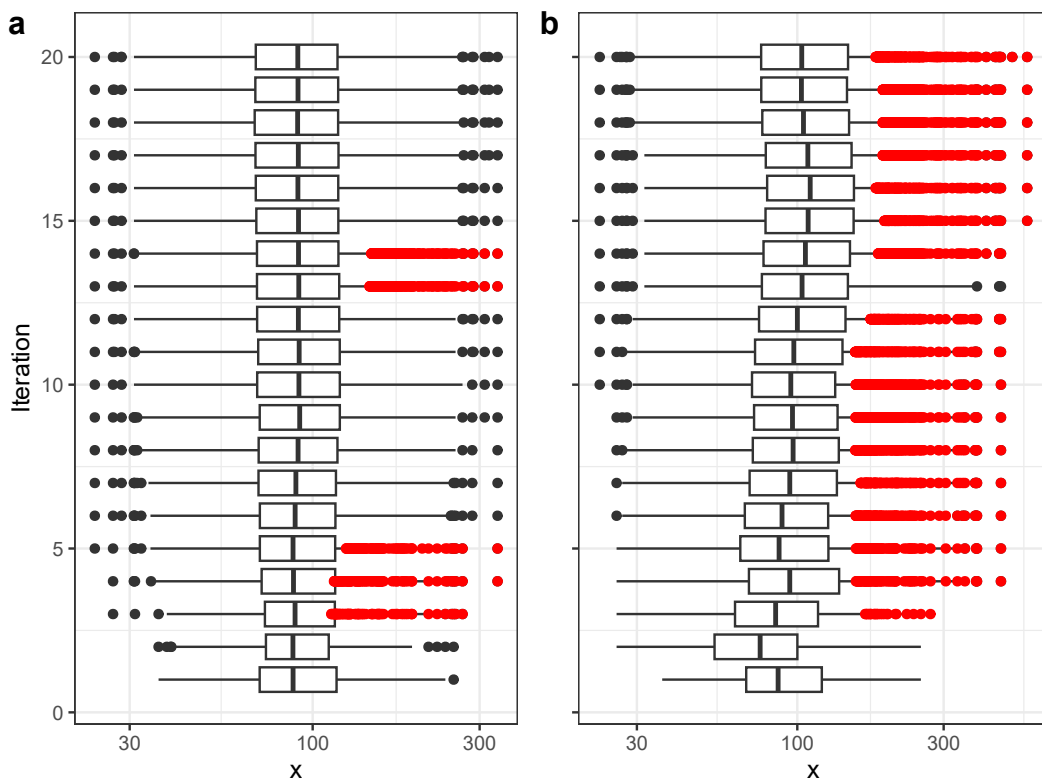


**Figure 5.8:** The same aggregated distributions as above in box-plots, illustrating how the data ranges increase much more slowly with sample size than expected for log-normal distributions. Sample size is 100 for iteration 1 and increases by 100 to 2000 in iteration 20. Fluctuating parameter values (b) increase variance and the probability of finding power-law tails (red points). X axis is logarithmic

## 5.4 Summary of methodological procedure and tests

The overall goal of this part of the thesis is to identify power-law structures in the house-size distributions of the sampled Neolithic settlements of Linear Pottery and Trypillia material culture. As it was shown in the previous chapter, unlike other common size distribution models like the normal, log-normal and exponential, the power law is characteristic of hierarchically scaling structures, and it is assumed here that when such structures are observed in house-size distributions they are indicative of some sort of socially relevant hierarchy, as they are very unlikely to emerge from simple random additive or multiplicative processes like those relating to the Central Limit Theorem or Gibrat's law. However, a number of caveats have been presented so far.

Firstly, a power-law distribution does not suffice to say what *type* of hierarchy is in play, only that there *is* a hierarchy. The idea that hierarchical structure in society equals despotism is a prejudice that should be kept out of the analysis. Rather, the exact political organisation of the society needs to be studied archaeologically through multiple angles. However, distinguishing between cases where there is and where there is not hierarchy remains still very useful.

Secondly, even though I have strived to follow best practice in terms of statistical methodology, some issues remain. One of these is that sample sizes in the following chapter are probably near the lower limit of what is acceptable for the distribution fitting and selection algorithm to be effective. Testing on synthetic data sets indicated that the tail models should ideally include hundreds of data points, and that at  $N \approx 10$  the model selection is unreliable with a high risk of false positive power laws. Furthermore, especially log-normal distributions are known to often produce power-law tails, and in the limited parameter scan provided here there is no obvious pattern between the values of mean and standard deviation and the probability of identifying a power-law tail. The observations done here on synthetic data sets seemingly show that random fluctuations in the tail are sufficient to produce power laws more or less independently of the parameter values. It remains unknown how relevant this issue is for interpreting archaeological house-size data, since the intensity of random fluctuations in house size is difficult to model precisely. It is possible that the frequent (but not constant) power-law behaviour in the tail is a mathematically inherent property of log-normal distributions. The question of the extent to which the presence or absence of power laws in otherwise log-normal house-size distributions confidently translates into presence or absence of social hierarchy should be addressed in future ethnographic or ethnoarchaeological studies.

Lastly, tests on aggregated log-normal distributions with synthetic data indicate that lumping or mixing of data series does not affect the risk of obtaining false positive power laws given that the mixed sub-distributions have identical parameter values. However, if the mixed distributions differ, even by small random fluctuations in the parameter settings, the aggregated data set quickly runs a much higher risk of giving false positive power laws. In the present context, this issue is especially relevant for cases when archaeological settlements are documented primarily through remote sensing, and when a majority of houses lack individual dating, impeding any further separation into coevally existing settlement plans. It should be noted that of all the caveats mentioned here, the main problem is the identification of false positive power laws (so-called “type 1 error”), while failing to recognise actual power laws

(false negative or “type 2 error”) is seemingly much less of an issue.

The applied distribution fitting algorithm can be summed up by the following (see also #script in online supplementary material for further details):

- A lower threshold ( $x_{min}$ ) is selected by fitting power-law models to the data by maximum likelihood estimation. The fitting is done recursively from different threshold values, and the one that gives the model with the lowest K-S statistic is selected.
- Other candidate models for the tail of the distribution are fitted (log-normal, exponential and stretched exponential/Weibull), also by MLE and with the same lower threshold as the power-law model.
- The best tail model is selected by lowest AICc score. The result shows whether a power-law model gives a better fit to the tail than the other models.
- Models are calculated for the whole distribution, without lower bound, excluding the power law and stretched exponential, but including the normal distribution. These are also fitted by MLE and selected based on AICc score.
- Reported values are the selected models for the whole distribution and the tail, as well as model parameter values, sample size (N), size of the tail (N\_tail) and proportion of the data included in the tail (Tail\_P), as well as the Gini index calculated on the whole distribution

In order to test if observed power laws are only resulting from data aggregation, the same analysis is also performed on separate quarters or neighbourhoods for two settlements where this information is available (Nebelivka and Vráble), and on modelled coeval settlement plans for Vráble. In all cases, samples of size 10 or lower are excluded from the analysis, and results for distribution tails that include 10 or less houses are disregarded.



# Chapter 6

## Results: Distribution fitting

### 6.1 Settlements

Running the distribution-fitting algorithm presented in Chapter 5 on the house-size distributions of the 13 settlements in the current sample (settlements with 10 or less houses were excluded), resulted in five settlements being interpreted as having power-law tails. These were the Trypillia sites at Maidanetske, Nebelivka and Moshuriv, as well as the Linear Pottery sites at Vráble and Horný Oháj (Figure 6.1 and Table 6.1). The remaining eight settlements were interpreted as having exponential tails. It is important to note however, that this simply means that the exponential model was the best out of the tested models, on the tail length that gave the best possible power-law fit. In other words, for these eight settlements, the power-law model is effectively excluded, since other models better explain whatever tail could be interpreted as a power law. Analysing the entire distributions the same way without setting a lower threshold value ( $x_{min}$ ) resulted in all settlements but one being interpreted as having log-normally distributed house sizes. Only Úľany nad Žitavou (Linear Pottery) was interpreted as normally distributed (Table 6.1). This result can also be suspected from the logarithmic box-plot, where most distributions are near symmetric (Figure 6.1).

As shown in Figure 6.2a, with the exception of Horný Oháj (Linear Pottery), the power-law tails are much longer than those of the other settlements (b). Even though they do not span two orders of magnitude in size – as predicted earlier due to material and physical limitations of houses as well as the symbolic nature of house size as expression of hierarchy (Section 4.2.4) – they do so on the cCDF which is based on house rank. Two orders of magnitude

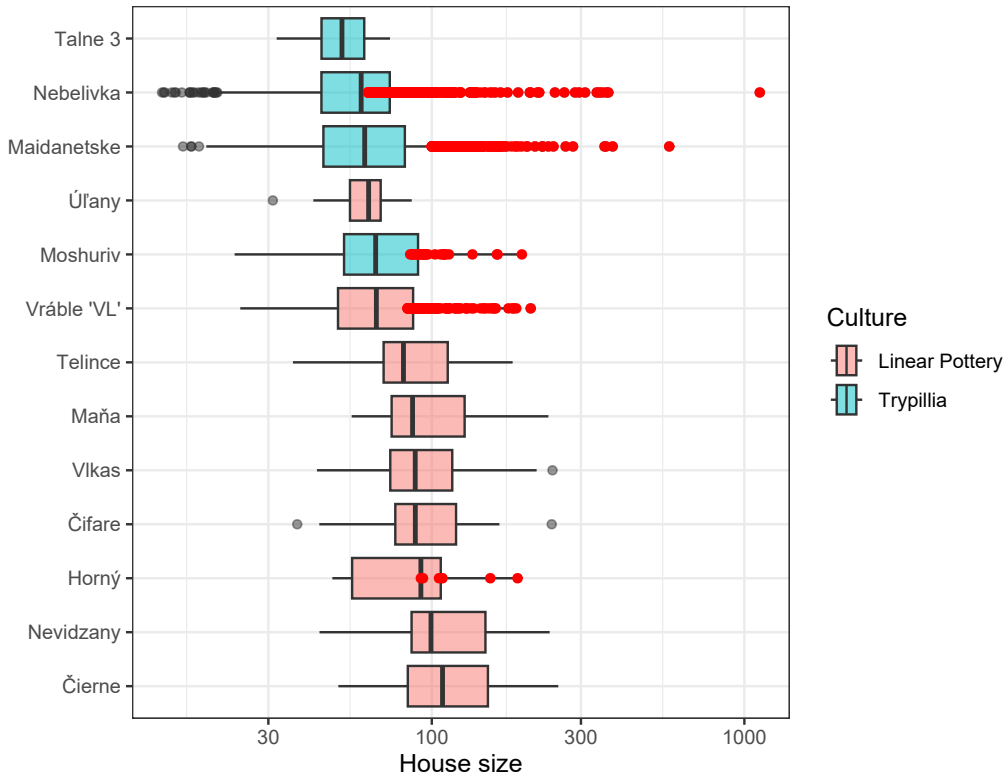


**Figure 6.1:** House sizes of the 13 analysed settlements, arranged according to median house size. Red dots represent houses with size  $\geq x_{min}$  within distribution tails interpreted as power laws. X axis is logarithmic

in rank represents a decreasing proportion of data points as total number increases, meaning that such power-law tails are “easier” to achieve for larger settlements, which is already an indication that this behaviour is inherently connected to settlement size. Table 6.1 shows that the power-law settlements are indeed the largest ones in the sample, again with the exception of Horný Oháj. While these results are not at all surprising when it comes to the two Trypillia mega-sites – indeed the hierarchical scaling of buildings there is already recognised without quantitative analysis – there are two results that may come as more surprising.

Firstly there is a clearly recognised power law in the house-size distribution of Vráble, indicating the probable presence of a hierarchical scaling relationship in its buildings. This is not obvious simply from looking at the site plan, and relates furthermore to the question of social organisation and hierarchy which is much more open and unsettled in Linear Pottery than in Trypillia research. The power-law tail of Horný Oháj should be treated with more caution, as it seems more likely to result erroneously from the very small sample size. Secondly – though the total sample of settlements is admittedly small – the single most relevant predictor for the presence of scaling in house sizes seems not to be cultural attribution but rather

settlement size, since the largest Linear Pottery settlement shows scaling while the smallest Trypillia settlement (Talne 3) does not. This is an indication that social organisation should not be considered as uniform within even well defined archaeological cultures and regions, despite common practice in archaeology. Here, in the case of near contemporary settlements with shared material culture located only some kilometres apart, there are two examples of settlements with deviating size that also deviate in how their houses scale internally, possibly indicating very different structures of social organisation between them and the other settlements in their respective regions (hierarchy seen in Vráble and not the rest of the Žitava valley, and equality seen in Talne 3 and not at other sites in the Bug-Dnieper interfluvium). It should be worthwhile to test whether this relationship – between scaling in house sizes and settlement size – also cross-cut archaeological cultures on larger samples.

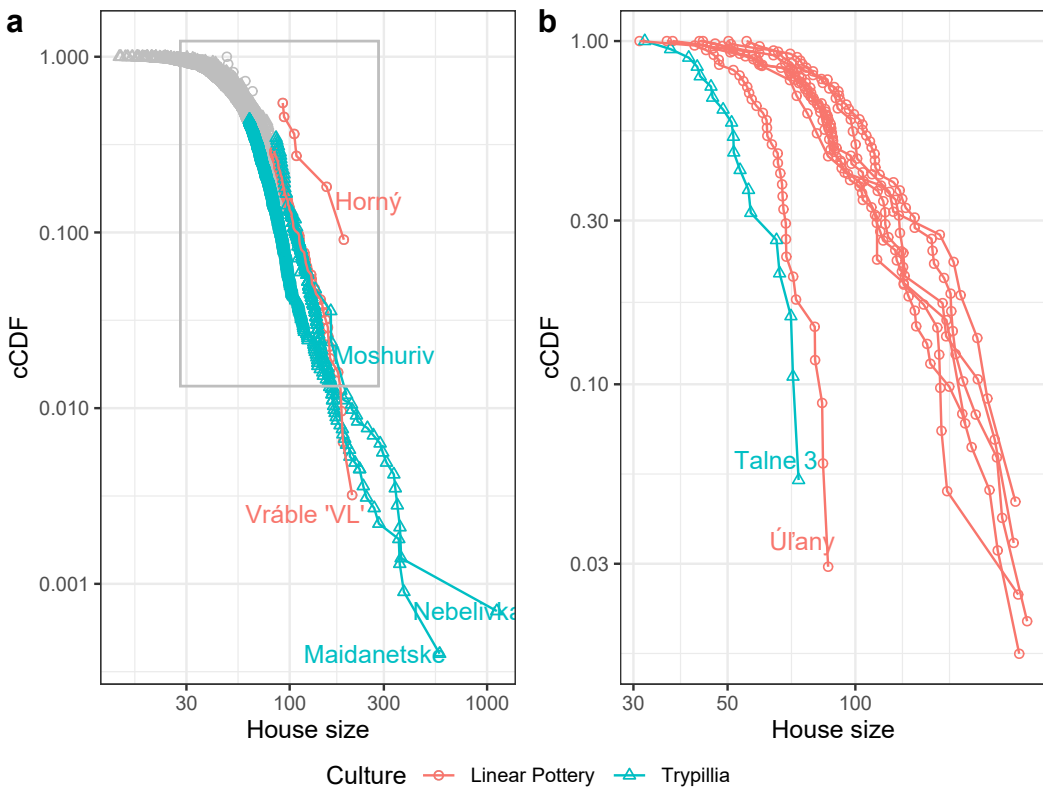


**Figure 6.2:** Analysed house-size distributions for whole settlements. a) Distributions with identified power-law tails. For clarity, only the tails ( $house\ sizes \geq x_{min}$ ) are coloured and connecting lines are added within each settlement. The grey frame represents the extent of panel b. b) House-size distributions without power-law tails. Two settlements are atypical with their absence of large houses. Scales are logarithmic

Figure 6.2b shows that the house-size distributions of both Talne 3 (Trypillia) and Úľany nad Žitavou (Linear Pottery) are clearly different from those of the other settlements without power-law tails. At the same time, only Úľany nad Žitavou was interpreted as normally

distributed – i.e. not skewed but symmetric, with only random differences between houses – when analysed formally. Talne 3 houses were interpreted as a log-normal distribution, but with a very low standard deviation. A Shapiro-Wilk normality test of the house sizes of Talne 3 gives a test statistic  $W = 0.958$  and  $p = 0.541$ , which is far from enough to exclude the null-hypothesis of a normal distribution. In other words, for the practical purpose here of interpreting probable underlying mechanisms of house-size differences, there is no significant difference between houses at Talne 3 and the distribution can be considered normal.

**Table 6.1:** Main results of distribution fitting analysis on settlements, ordered according to retained tail model (Tail) and parameter values (T\_Par1), from steepest to shallowest (see Figure 6.2). Model and Gini are evaluated on the entire distribution for each settlement. Par1 and Par2 represent  $\mu$  (mean) and  $\sigma$  (standard deviation) for normal and log-normal distributions, and T\_Par1 represents  $\lambda$  (rate) for exponential and  $\alpha$  (scaling exponent) for power-law distributions.  $x_{min}$  is the house size from which the tail parameters are estimated. N is the number of houses per settlement, N\_tail is the number of houses in the distribution tail, and Tail\_Pr is the proportion of N being part of the tail, or N\_tail/N

Settlement	Model	Par1	Par2	Tail	T_Par1	xmin	N	N_tail	Tail_P	Gini	Culture
Úľany	norm	62.349	12.542	exp	0.109	63.6	34	17	0.50	0.113	Linear Pottery
Talne 3	ln	3.941	0.226	exp	0.077	45.7	19	14	0.74	0.126	Trypillia
Vlkas	ln	4.534	0.387	exp	0.025	81.2	61	40	0.66	0.221	Linear Pottery
Čifare	ln	4.535	0.398	exp	0.024	70.2	41	34	0.83	0.217	Linear Pottery
Telince	ln	4.452	0.417	exp	0.024	59.3	13	12	0.92	0.228	Linear Pottery
Maňa	ln	4.597	0.381	exp	0.021	65.8	29	27	0.93	0.224	Linear Pottery
Čierne	ln	4.703	0.376	exp	0.021	89.2	49	36	0.73	0.211	Linear Pottery
Nevidzany	ln	4.659	0.434	exp	0.020	86.0	22	17	0.77	0.240	Linear Pottery
Moshuriv	ln	4.211	0.395	pl	6.306	85.3	84	29	0.35	0.219	Trypillia
Maidanetske	ln	4.112	0.443	pl	5.508	100.0	2243	301	0.13	0.249	Trypillia
Vráble 'VL'	ln	4.198	0.389	pl	5.235	83.6	313	91	0.29	0.221	Linear Pottery
Horný	ln	4.423	0.445	pl	4.916	92.3	11	6	0.55	0.253	Linear Pottery
Nebelivka	ln	4.045	0.432	pl	4.764	62.6	1435	629	0.44	0.239	Trypillia

From the table it is clear that the Gini index follows the model type and parameter values closely but not exactly. The advantage of using the Gini index for the purpose of quantifying inequality is that it is more straight-forward to calculate, and it allows for a unified single measure facilitating comparison between different distribution types (Kohler et al., 2017; e.g. Kohler & Smith, 2018). The disadvantage is that there is no clear and reliable way of identifying underlying mechanisms from this index alone – in the present case it would be impossible to single out which settlements show signs of hierarchical scaling in their houses, let alone determining how many of the houses this would concern. My conclusion from this is that the Gini index is useful when the question to be answered relates specifically to inequality within populations, and when cross-cultural comparisons or long temporal trends are more emphasised than the social organisation of specific cultural contexts.

Looking at how the power-law distributed houses are spread spatially within the various settlements allows for further interesting patterns to emerge. At Vráble, the whole range of hierarchically scaling houses is present at each of the neighbourhoods, though apparently somewhat less in the south-west (Figure 6.3). There seems to be a weak tendency for larger houses to cluster throughout, i.e. that large houses tend to be close to other large houses, and with interstices between clusters being filled by regular small houses of size below  $x_{min}$ . However, observing the entire settlement plan in a single block does not allow for further evaluation of whether these clusters actually represent coeval groups of larger houses or if they rather form temporal sequences, following the much discussed “yard model” of Linear Pottery settlement development [Zimmermann (2012a); 3.2]. Either option speaks against an interpretation of house-size differences being only random.

In the much larger Trypillia settlements of Maidanetske (Figure 6.4) and Nebelivka (Figure 6.5) the hierarchical scaling of houses is seen throughout the settlements, indicating that there is no general sector that has obviously more of smaller or larger houses than others. As is widely recognised by the researchers who have studied these settlements in detail (e.g. Hale, 2020, pp. 127–137; Ohlrau, 2020, pp. 61–64), the single and by far largest building is located at around 3 o’clock on the inner house ring (at least for Nebelivka, but most probably also Maidanetske), while other smaller mega-structures or “Assembly Houses” are regularly dispersed throughout the main street and, to a lesser extent and mostly for Nebelivka, outside the outer house ring. The most interesting result from the distribution fitting analysis provided here, is that the scaling behaviour also goes far beyond the typological distinction

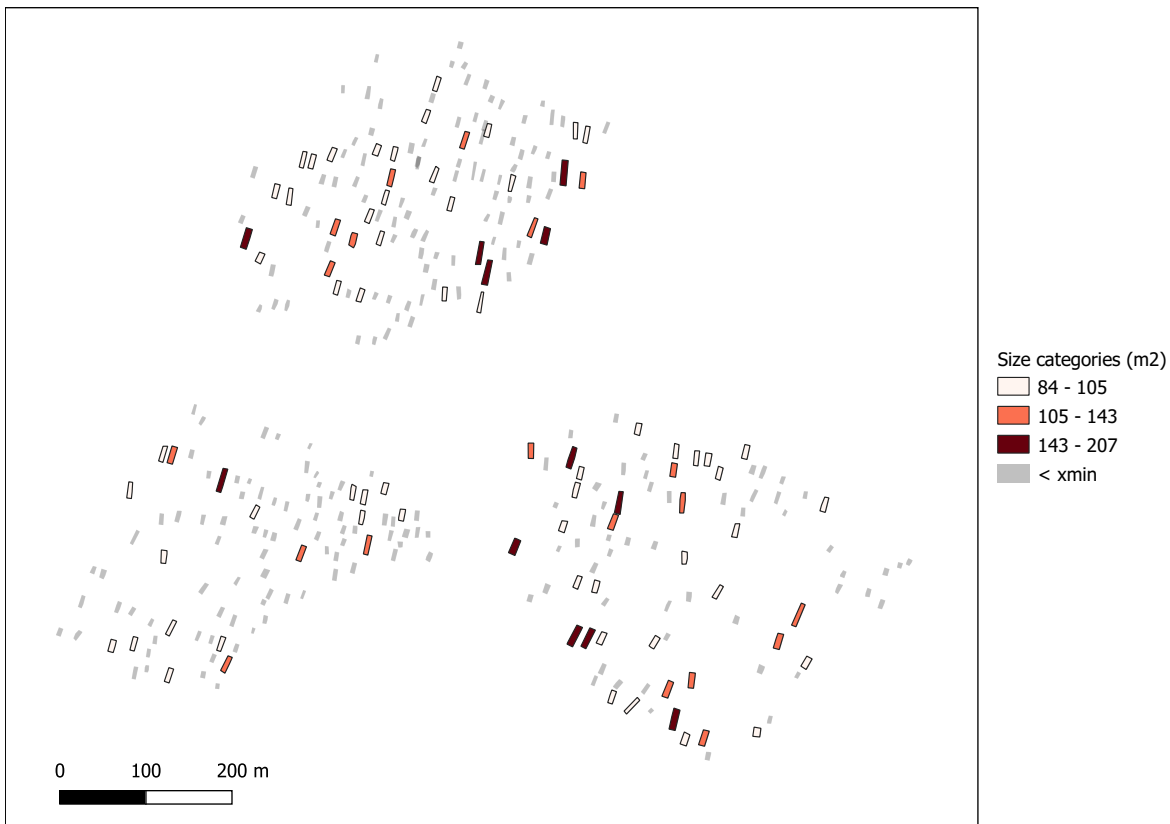


**Figure 6.3:** Power-law distributed houses at Vráble (Linear Pottery), arbitrarily grouped to three levels using the Jenks optimisation method integrated in QGIS for readability. Figure made by author with data from Müller-Scheeßel et al. (2020)

between mega-structures and domestic houses. For both settlements, extra large domestic houses are more concentrated around the main street than in the inner streets and plazas, and while these are quite regularly spaced in Maidanetske, in Nebelivka they seem to cluster near the Assembly Houses, further underlining the size hierarchy. But again it is difficult to know at the present stage to which extent these clusters represent coeval groups of larger houses or temporal sequences, given the duration of the settlement. It does however suggest in any case, that large domestic houses had privileged access to the Assembly Houses by close proximity, while the smaller houses were mostly confined to the inner streets and the borders between Quarters, i.e. the furthest away from the Assembly Houses.

In the small Trypillia settlement of Moshuriv, power-law distributed houses are also spread across the settlement plan, with the largest house situated in the east end of the inner house ring, following the same scheme as the mega-sites, as noted by Ohlrau (2020, pp. 241–243). Here, much like at Maidanetske in miniature, the hierarchically scaling houses are evenly spread without obvious clustering, the only pattern being that the three houses just below the largest one in size also are located on the inner house ring (Figure 6.6).

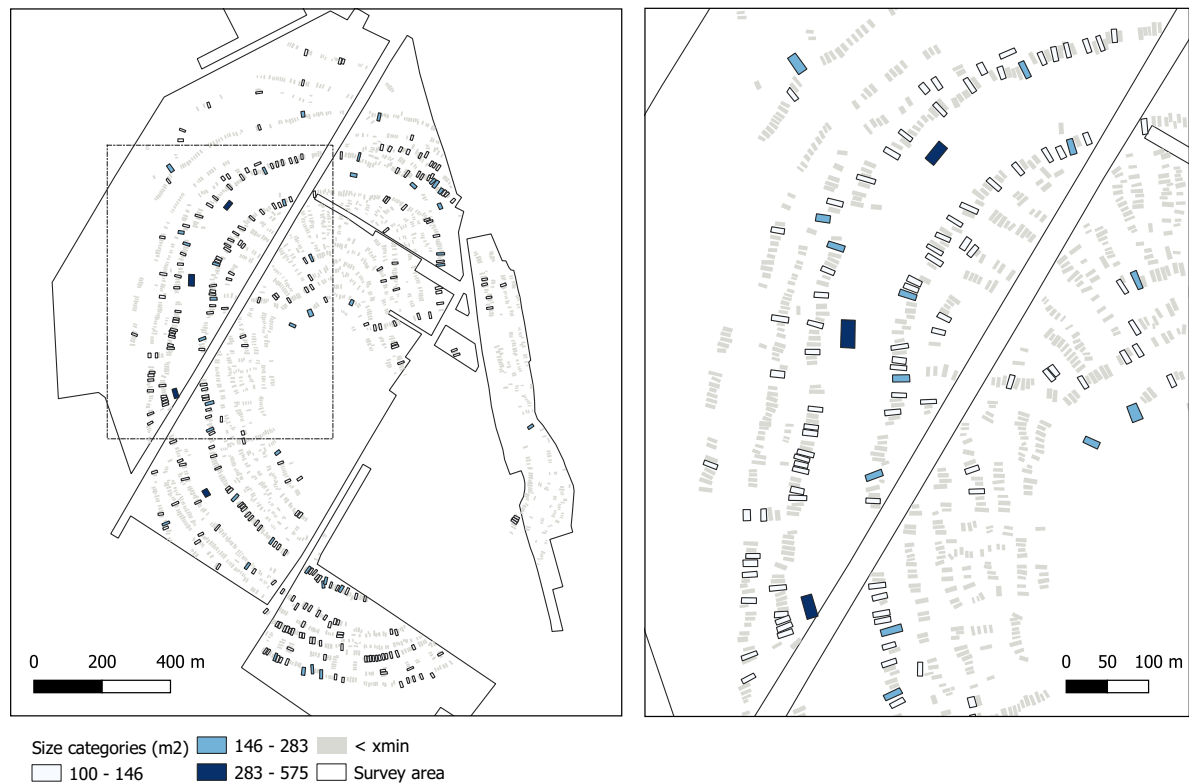


**Figure 6.4:** Power-law distributed houses at Maidanetske (Trypillia), grouped to three levels with Jenks optimisation. The levels are arbitrary but overlap well with the typological distinction between mega-structures (dark blue) and other houses. Hierarchical scaling includes far more houses than the mega-structures, and is distributed across the settlement. Figure made by author with data from Ohlrau (2020)

Since the main goal in this thesis is not only to measure and interpret archaeological data, but also to assess the reliability of the methods and the robustness of the results, in the following sections I propose further iterations of this analysis on gradually more filtered sub-sets of the data, to see whether the power-law interpretations continue to hold. Various factors specifically related to archaeological data could be thought to influence size distributions in ways that would preclude any meaningful interpretations in terms of social organisation. More specifically, if power-law distributed house sizes are to be considered as statistical signatures of social hierarchy, the possibility of them being no more than artefacts resulting from methodological choices like spatial or temporal lumping needs to be excluded.

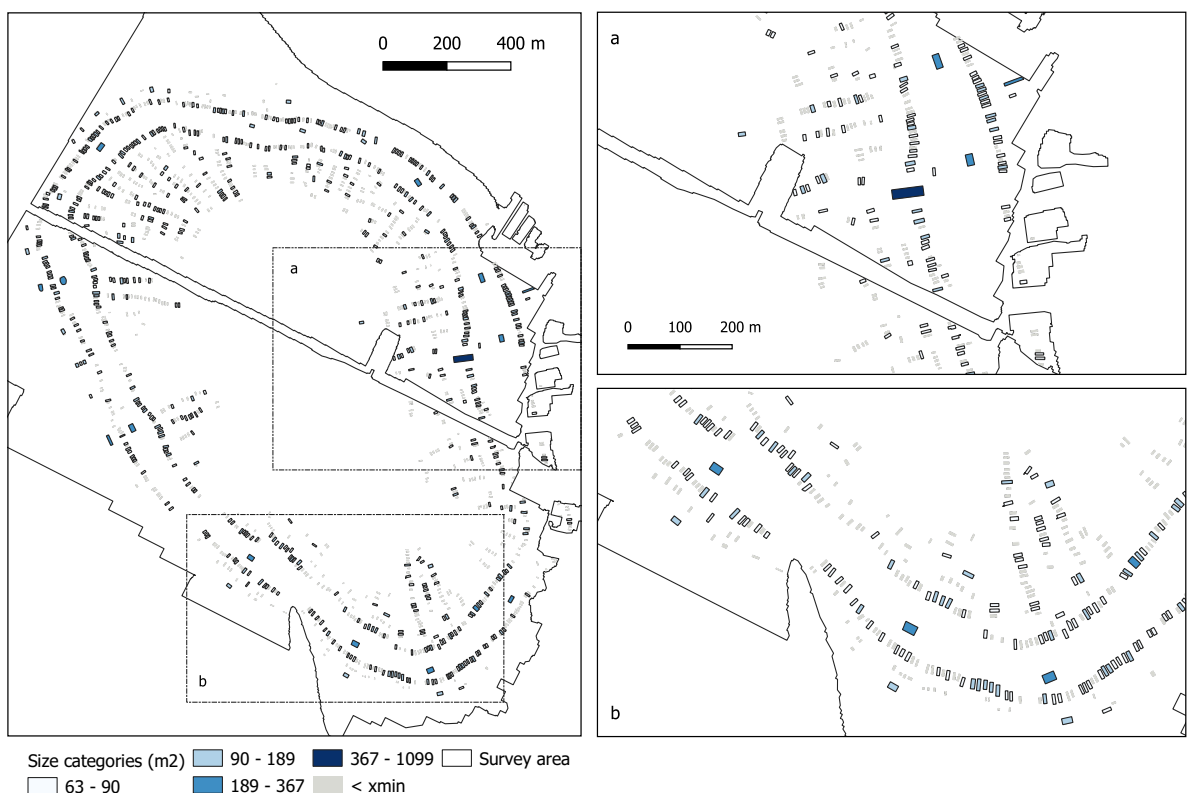


**Figure 6.5:** Power-law distributed houses at Nebelivka (Trypillia), grouped into four arbitrary levels with Jenks optimisation, the two largest of which are overlapping with the typological levels of the “Mega-structure” and the “Assembly Houses”. Figure made by author with data from Hale (2020)

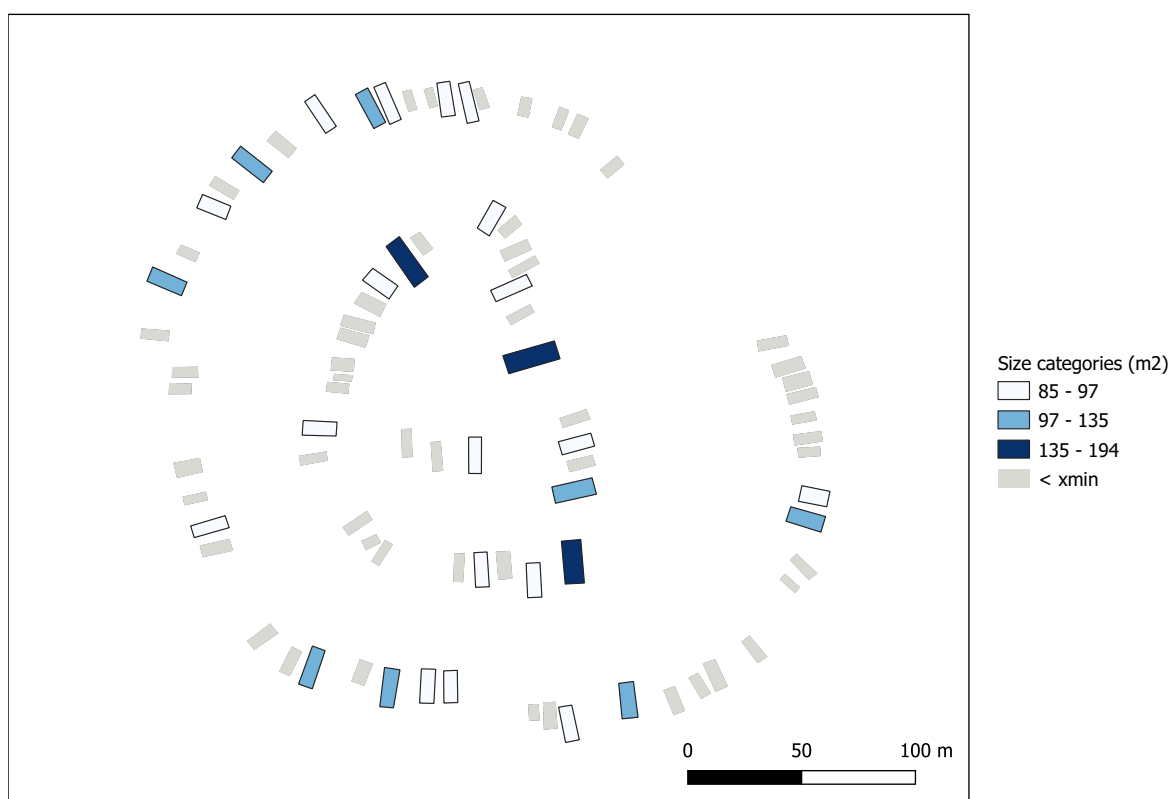


**Figure 6.6:** Power-law distributed houses at Moshuriv (Trypillia), grouped arbitrarily into three size categories using Jenks optimisation. Made by author with data from Ohlrau (2020)

## 6.2 Quarters/neighbourhoods

Two of the large settlements with power-law house-size distribution tails – Nebelivka and Vráble – were selected for further distribution fitting analysis within separate quarters or neighbourhoods. The Linear Pottery site of Vráble is clearly organised into three distinct neighbourhoods, termed North (N), South-West (SW) and South-East (SE) by the research team in the dedicated publications (Furholt, Müller, et al., 2020; Winkelmann et al., 2020). The Trypillia mega-site of Nebelivka has also been subdivided into quarters by its research team (following their terminology here), but the limits between them were set somewhat more arbitrarily based on a series of criteria, including natural topography, placement and orientation of streets and entrance ways, as well as the locations of the large so-called Assembly Houses (Hale, 2020, p. 123). This resulted in a series of 14 defined quarters arbitrarily labelled A–N, which is reused as is here. It should be noted that the single largest building in Nebelivka – the “Mega-structure” of approximately  $1.200\text{ m}^2$  – is not included in any of these quarters, but lies in the interstice between quarters A and B along with a few other houses. Though this delimitation of quarters at Nebelivka could have been done differently, which is clearly recognised by the researchers themselves, I do not pretend that I could make any better judgement. The number of houses per quarter is included in Table 6.2 below.

When analysed separately following the same distribution-fitting algorithm as with the entire settlements, 14 of the 17 data series were recognised as having power-law tails (Figures 6.7 and 6.8). The only deviations were Nebelivka quarters E and N, and the SE neighbourhood of Vráble. This clearly shows that the power laws observed at the total settlement level do not merely result from analytically stacking together separate more lightly skewed distributions like log-normals, but rather from genuinely different scaling patterns in house sizes for these settlements. The  $\alpha$  estimates, between 3.6 and 6.8 (with one outlier for Neb. A), were largely similar to the ones observed for the entire settlements (5.2 for Vráble and 4.8 for Nebelivka; Tables 6.2 and 6.1). Each of the quarters and neighbourhoods were furthermore identified as log-normal when analysed over their entire size range, with  $\mu$  and  $\sigma$  estimates very similar to those observed for the total settlements.

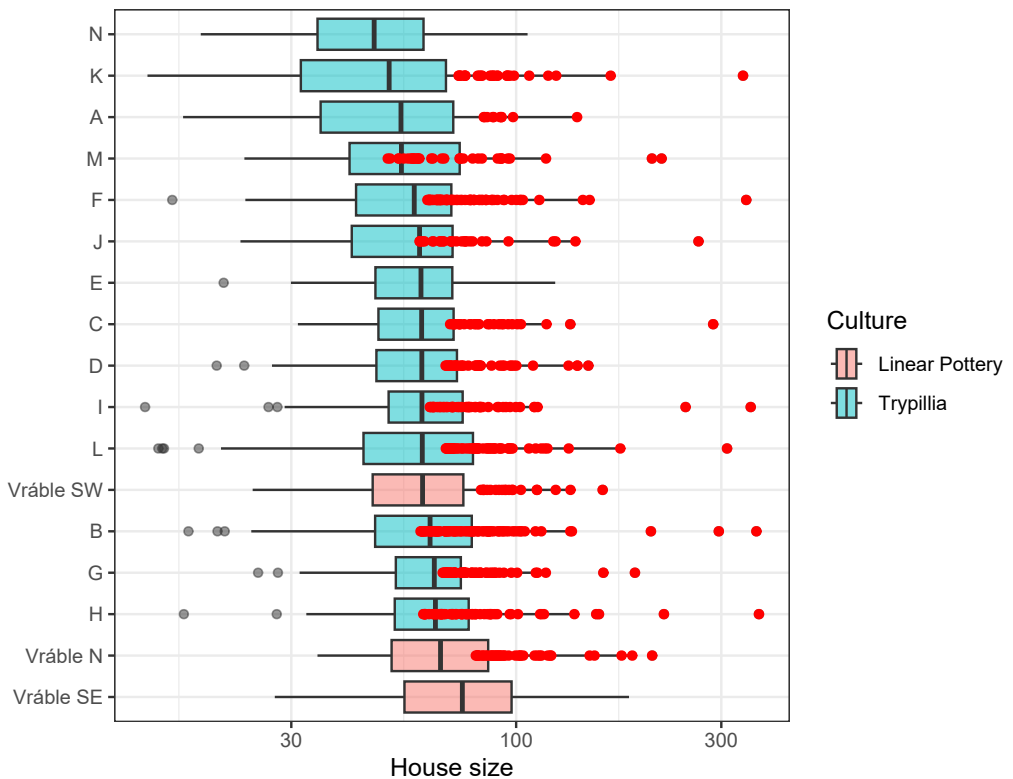


**Figure 6.7:** House-size distributions of individual quarters for Nebelivka and neighbourhoods for Vráble, arranged according to median house size. Red dots indicate houses of size  $\geq x_{min}$  in cases where the distribution tail was interpreted as a power law. X axis is logarithmic

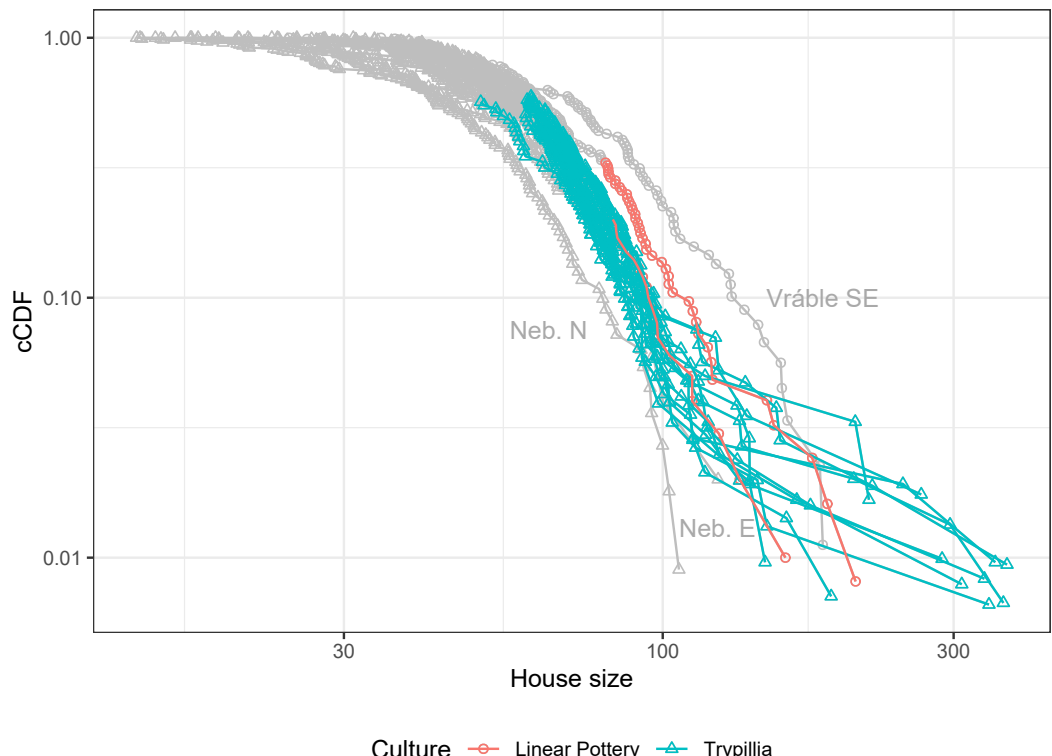


**Figure 6.8:** Survival function of the same house-size distributions of quarters/neighbourhoods. Coloured dots represent houses within power-law tails. Three series were not interpreted as power laws. Scales are logarithmic

**Table 6.2:** Results of distribution fitting on separate quarters at Nebelivka and neighbourhoods at Vráble, arranged by tail model and parameter. Par1 and Par2 indicate  $\mu$  and  $\sigma$  for log-normal distributions, and T\_Par1 is  $\alpha$  for power-law and  $\lambda$  for exponential tail distributions. Gini index is calculated on the entire sample

Quarter	Model	Par1	Par2	Tail	T_Par1	xmin	N	N_tail	Tail_P	Gini	Culture
Neb. N	ln	3.830	0.408	exp	0.063	55.7	111	41	0.37	0.224	Trypillia
Neb. E	ln	4.057	0.333	exp	0.061	59.3	50	27	0.54	0.179	Trypillia
Vráble SE	ln	4.296	0.424	exp	0.034	84.4	89	37	0.42	0.236	Linear Pottery
Neb. A	ln	3.940	0.441	pl	10.490	84.1	51	10	0.20	0.240	Trypillia
Neb. G	ln	4.137	0.295	pl	6.763	67.5	141	60	0.43	0.160	Trypillia
Vráble SW	ln	4.090	0.367	pl	6.704	82.8	100	20	0.20	0.202	Linear Pottery
Neb. D	ln	4.085	0.361	pl	5.684	68.5	104	38	0.37	0.196	Trypillia
Neb. F	ln	4.035	0.385	pl	5.359	62.2	151	69	0.46	0.217	Trypillia
Vráble N	ln	4.215	0.358	pl	5.350	80.6	124	41	0.33	0.208	Linear Pottery
Neb. C	ln	4.097	0.327	pl	5.295	70.2	101	28	0.28	0.191	Trypillia
Neb. L	ln	4.040	0.501	pl	5.285	68.6	126	54	0.43	0.255	Trypillia
Neb. K	ln	3.866	0.548	pl	4.974	73.5	120	27	0.22	0.300	Trypillia
Neb. I	ln	4.113	0.393	pl	4.832	63.0	104	49	0.47	0.218	Trypillia
Neb. J	ln	4.043	0.416	pl	4.620	59.6	57	29	0.51	0.244	Trypillia
Neb. H	ln	4.175	0.390	pl	4.451	60.8	106	63	0.59	0.221	Trypillia
Neb. B	ln	4.112	0.433	pl	4.411	59.9	149	86	0.58	0.241	Trypillia
Neb. M	ln	3.985	0.466	pl	3.614	50.3	60	34	0.57	0.271	Trypillia

In addition to testing whether the power-law interpretations hold when the analysis is done at the quarter rather than settlement level, performing distribution fitting on separate quarters allows for observing intra-site differences between quarters. The immediate interpretation of the two non-power law quarters at Nebelivka would be that their houses are more similar in size and that this could indicate a flatter hierarchical structure, or an absence of hierarchy altogether. The association between settlement size and power-law distributions noted above could also be valid here. With only 50 houses, quarter E is the smallest of the Nebelivka quarters (Table 6.2, Figure 6.9). With a smaller population the inhabitants could possibly do well without a long-range hierarchy beyond the (comparatively small) assembly house located within its section of the central street. However, this interpretation does not fit for quarter N which is in the mid-range of house count with 111 houses. Here the explanation could be taphonomical, as the quarter is lacking an Assembly House which could be located in an unpreserved part of the site (Hale, 2020, p. 123). Interestingly, quarter A also has a small house count (51) *and* is lacking an assembly house, but its house-size distribution is all the same interpreted as a power law, albeit with atypical parameter values –  $x_{min}$  is the highest among the Nebelivka quarters, and  $\alpha$  is by far the highest – indicating that these factors may influence model selection without determining it entirely. For quarter E in particular, another possibility which is linked at least to house count, is that its quarter borders are drawn incorrectly so that the quarter should either be larger or included into one of the neighbouring quarters, which would then probably still be power-law distributed. The explanations based on taphonomy and quarter border definition work under the assumption that since most of the quarters have power-law distributed house sizes, all of them should originally have had this, and that the data is somehow distorted. The social explanation of differing degrees of hierarchical organisation between quarters remains a possibility, but at this stage any of these explanations are difficult to exclude. Given that the Nebelivka mega-site is exceptionally well preserved for its size – the site plan is very nearly complete – this illustrates the difficulty archaeologists face when trying to interpret only partially preserved settlements. I personally see the Nebelivka plan as extremely regular between quarters, and the mentioned deviations in quarters N and A as resulting from taphonomy (missing data) and in quarter E as incorrectly drawn quarter borders. I also question the border drawn between quarters J and K, though this seemingly has not influenced their internal house-size distributions noticeably.

Regarding Vráble SE, in addition to not having a power-law tail, the house-size distribution

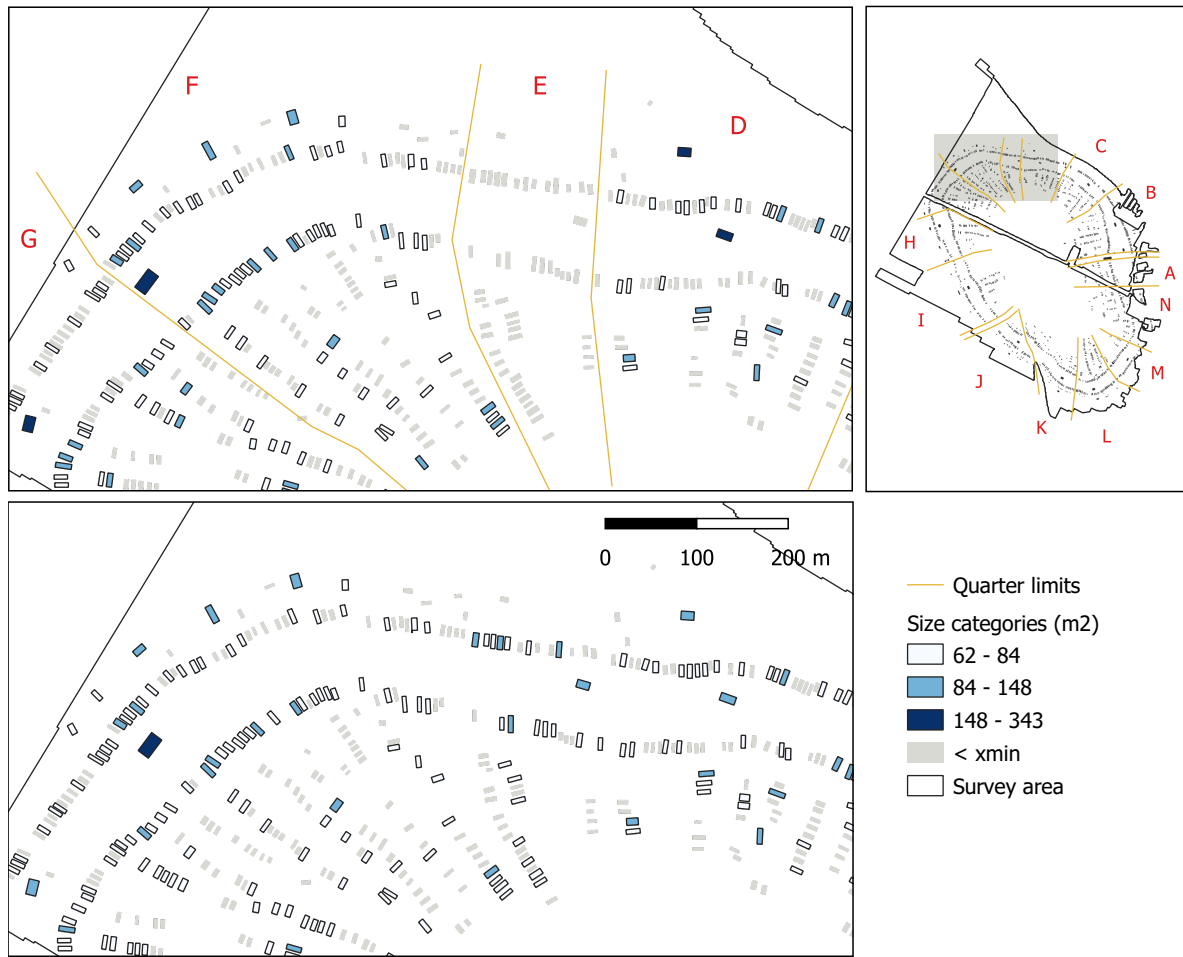


**Figure 6.9:** Power-law distributed houses in quarters D to G in Nebelivka, fitted by quarter (top) and for the settlement as a whole (bottom). Quarter-wise distribution fitting does not identify hierarchical scaling in quarter E, though many of the houses there are included in the power-law model for the whole settlement. Size categories are arbitrary (three levels with Jenks optimisation) and values differ between quarters. Legend values correspond to quarter F. Figure by author with data from Hale (2020)

is also distinguished from the two others with a markedly higher median, i.e. generally larger houses, as well as higher mean and standard deviation (Table 6.2). On the survival function plot on Figure 6.8 this translates to a wider and more regular parabolic curve of house sizes, more typically log-normal, as opposed to the more abruptly descending straight lines of the two other neighbourhoods (in red on the plot). For the N and SW neighbourhoods, the combination of a less skewed log-normal for the main body of the distribution (i.e. regular houses) and an actual power law for the largest 41 and 20 houses respectively (1/3 and 1/5 of the houses), could indicate a more marked difference between these, which could be interpreted either as an emerging social elite or the presence of some large houses with special social functions. However, any further interpretation in social terms depends on how many of these houses were actually coeval, i.e. in use at the same time. If most of these large and hierarchi-

cally scaling houses were in reality spread out through time, so that only a very few existed at any single one moment, it would not make much sense to speak of a social hierarchy, and the distribution should not be interpreted as a power law. For interpreting social relationships between different households and how they function in daily life, it is essential that the studied households be contemporary – a requirement that is often hard to meet in archaeology, but an attempt is done in the following for Vráble only.

### 6.3 Temporal samples (Vráble)

Separating an archaeological settlement plan into samples with temporally coeval structures only is a demanding exercise, and more so the larger the settlement. The best and most reliable method is to date every single structure in the settlement, but this is usually impossible both in theory, since not all structures yield datable material, and in practice when considering the costs involved. The more realistic approach is to sample a smaller amount of structures throughout the settlement for dating and modelling, and then extrapolate the results to get a more or less rough overview of how much, proportionally, of the site was occupied at the same time. This has been done for the Trypillia mega-sites, indicating that the maxima of coeval habitation would be at approximately 33% of houses at Nebelivka (Millard, 2020, pp. 253–256; Müller et al., 2022) and 52% at Maidanetske (Ohlrau, 2020, pp. 233–235; 2022, pp. 86–88). Even though some general tendencies of the spatio-temporal development of these settlement plans have been proposed (Müller et al., 2022, pp. 218–219; Shatilo, 2021, p. 247), it is for now impossible to extract precise temporal samples of coeval house-size distributions here. This also goes for the image analysis presented in Chapter 9 (see also Bruvoll, n.d.). The smaller sites of Moshuriv and Talne 3 are only dated through relative chronology of surface finds and thus attributed as a whole to their chronological phase, though their small sizes and ordered layout would suggest that most houses could be coeval (Ohlrau, 2020, pp. 241–244).

For houses in Linear Pottery settlements, a special dating proxy was recently developed, based on the observation that within this cultural context houses were constructed to be parallel to pre-existing ones, but with a slow and gradual counter-clockwise shift in orientation of approximately 1.3 degrees per decade (Müller-Scheeßel et al., 2020). This shift was hypothesised to be too slow for any conscious intention among the house builders, but rather a result of so-called pseudoneglect, or the tendency of a slight leftwards bias in the perception of parallel

lines, mostly among the right-handed. Müller-Scheeßel et al. (2020) observed this gradual shift in the orientation of 17 houses in Vráble for which construction dates had been estimated based on Bayesian modelling of  $^{14}\text{C}$  dates. Their linear regression model for all these houses only gave a weak correlation however, and they argued for basing the model on the eight houses in the SW neighbourhood only, where the sampling strategy had been the most systematic. This gave a regression model defining house orientation as  $0.129x - 651.016$  with correlation coefficient  $r = 0.84$ ,  $x$  being the modelled construction year BCE, which when applied inversely (solving for  $x$ ) gives modelled construction year as  $\frac{\text{orientation} + 651.016}{0.129}$ . Use-life of houses in Vráble was modelled by Meadows et al. (2019) to a median of 27.5 years, a number which according to the same authors has varied greatly throughout the long history of Linear Pottery research. Extrapolating the model for construction year based on house orientation and adding this median duration onto all known houses in Vráble gives a settlement occupation span from 5297 to 4975 cal. BCE, which is in good agreement with the currently available and modelled  $^{14}\text{C}$  dates (though admittedly a few decades earlier, see Meadows et al., 2019). For the distribution fitting analysis in this section I defined a set of 16 sample dates spaced 20 years apart from 5290 to 4990 within this timespan, and assigned houses to each sample accordingly. Since the duration between time samples is a few years shorter than the duration of houses, some houses were assigned to more than one sample. Furthermore, as with the analyses above, samples with 10 or less houses in them were filtered out, mainly since the distribution method then becomes too unreliable (this is already a quite generous allowance, Chapter 5), but also since it makes little sense to speak of hierarchy in a group of less than 10.

It must be noted that there are several caveats with this procedure of selecting out houses to be considered coeval. Firstly, the dating proxy method proposed by Müller-Scheeßel et al. (2020) is recent and not yet well established. It is based on linear regression of very few data points (8 houses in only one part of the settlement), all of which are not unique certain values but dates that are themselves also modelled. Though the publication does not specify it explicitly, it seems their model was fitted by ordinary least squares (OLS) regression, while systematic measurement uncertainty in the independent variable (the modelled  $^{14}\text{C}$  dates) should warrant more robust methods like orthogonal regression or probabilistic Monte Carlo methods. My use of a single value for house duration rather than the probability distribution that it really is, is also a simplification that could affect the results of the analysis. In general,

longer house durations lead to more of the houses being coeval throughout the timespan of a settlement, while inversely shorter house durations lead to fewer coeval houses. There could also potentially be systematic relationships between house size and duration, e.g. that larger houses were occupied by more temporally stable households for several generations, putting in greater efforts to maintenance. These questions are not further pursued here however, and the results of this analysis must be considered preliminary.

Following this procedure for defining data series with houses in Vráble considered to be coeval at given time samples, these series were analysed through the same distribution fitting algorithms as before. Ten of the 16 time samples had more than 10 houses, and these were situated consecutively in time between 5230 and 5050 cal. BCE, the remaining samples being at the start and end of the settlement's duration. Of these 10 samples, seven had tails in their house-size distributions that were interpreted as power laws (Figures 6.10 and 6.11).

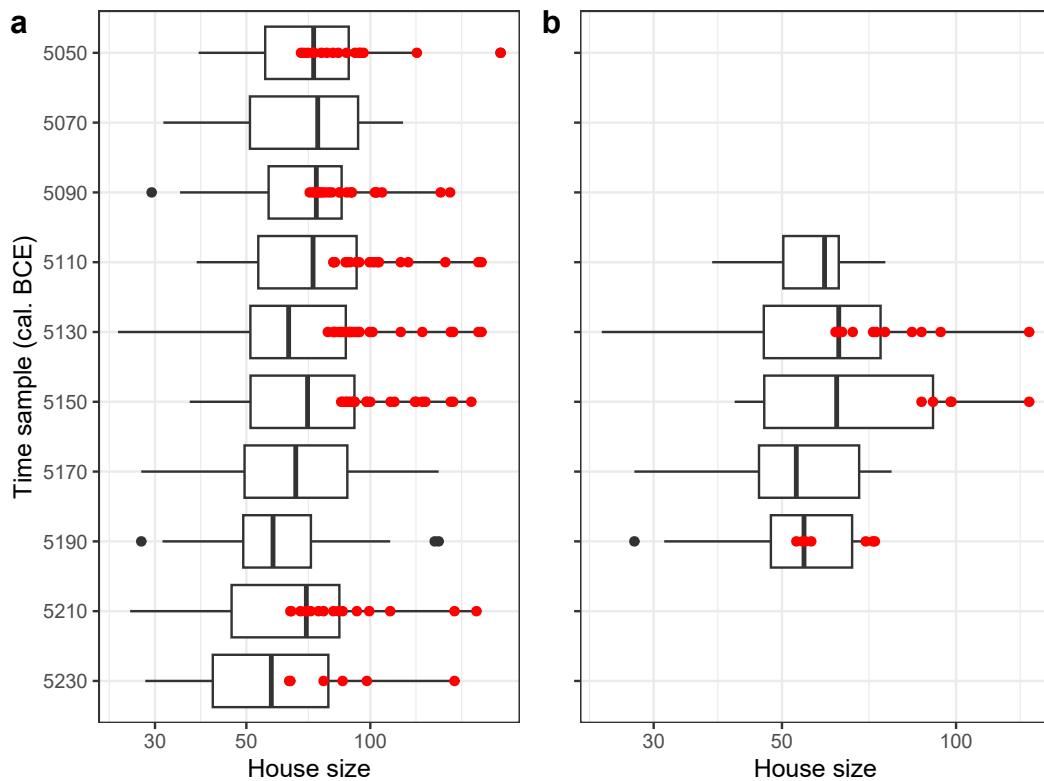


**Figure 6.10:** House-size distributions at single time samples for the entire settlement at Vráble (a) and the South-West neighbourhood only (b). Red dots indicate houses with power-law distributed size. Only distributions including more than 10 houses are represented. In plot b, the single largest house of each sample is also excluded. X axis is logarithmic

A last attempt to test if these power laws were simply statistical artefacts of lumped data sets, was done parting from the following hypothesis: At any given time during Vráble's dura-

tion, the three neighbourhoods were largely independent from each other and there was no hierarchical relationship between them. Within each neighbourhood, household sizes were log-normally distributed, or lightly skewed, as a result of their generalised post-marital residence pattern of patrilocality, and in addition there was always one single building markedly larger than the others, intended for communal ceremonial use. Analysing all houses in Vráble together, even by considering only temporally coeval houses, would be enough to generate a false impression of a hierarchy between the largest houses.

In order to investigate if this was the case, only the houses from the south-west neighbourhood of Vráble were selected out (being the ones for which the construction date model was the most secure), and the single largest house of each time sample was excluded. It then remained only five time samples with more than 10 houses, namely the ones situated between 5190 and 5110. Out of these, three were still interpreted with power-law distributed house-size distributions (Figures 6.10b and 6.11b). These power laws could thus not be explained as resulting from neither spatial nor temporal lumping, nor from the eventuality of a special function of the single largest house, and it seems therefore reasonable to conclude that they represent actual hierarchical scaling which can be further interpreted in terms of social organisation. It also seems plausible that analysing the three neighbourhoods together may be justified, which allows for identifying this scaling behaviour over a larger range of the settlement's duration. Though conclusions should not be taken too far given the many uncertainties related to the temporal modelling applied here, it is interesting to note that power-law tails are identified throughout the duration of the settlement, and are seemingly not a feature that is specifically related to the later phases only. This seemingly contradicts the current understanding of the temporal trajectory of inequality in Linear Pottery society, which is generally seen as increasing towards the later phases, leading to the rising tensions seen in the widely discussed massacre deposits, including in the very same Vráble settlement [Furholt, Müller-Scheeßel, et al. (2020); Müller-Scheeßel et al. (2021); Section 3.2]. Not surprisingly, the more conventional inequality measure of the Gini index draws a similar picture of the temporal development of house sizes at Vráble (6.3). Throughout the phases with 10 or more coeval houses, the index remains rather stable at values between 0.28 and 0.20, and if anything it shows a more decreasing than increasing trend. In other words, the dynamics of changing house sizes at Vráble do not give support to an interpretation of the eventual decline of the settlement as a result of rising inequalities (though this does not exclude the possibility such

inequalities being expressed through other material proxies).

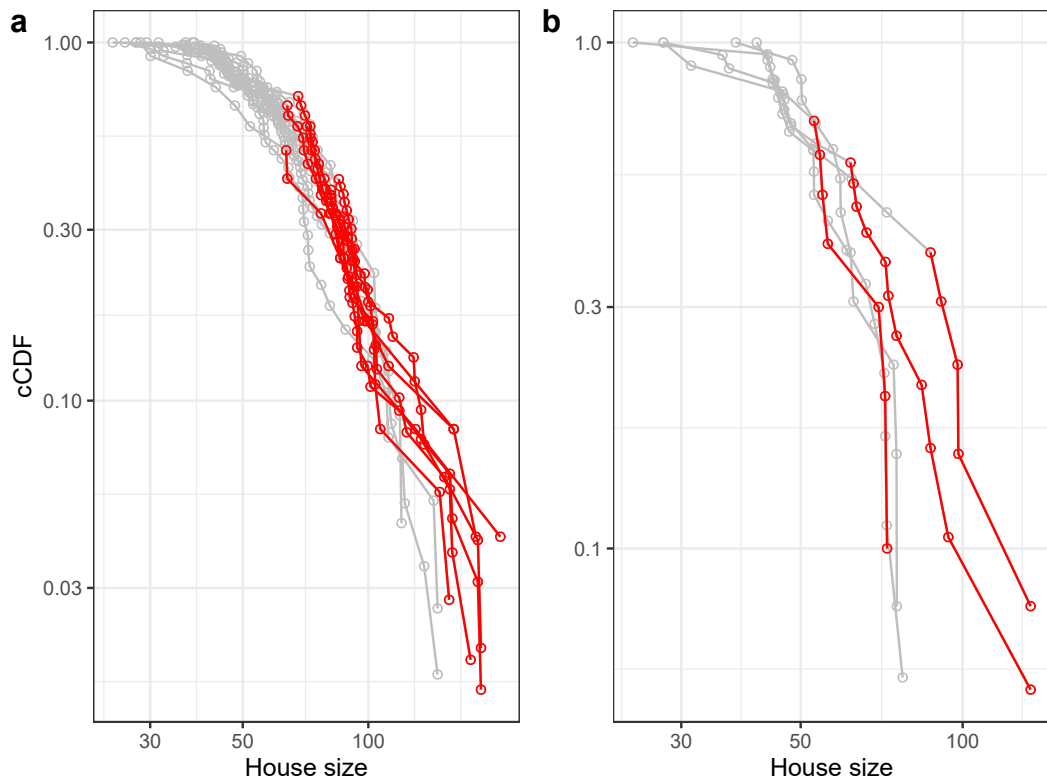


**Figure 6.11:** Survival function of the same house-size distributions of time samples for Vráble (a) and Vráble SW only excluding the largest house of each sample (b). Coloured dots represent houses within power-law tails. Power-law tails persist despite the gradual breaking down of the data set. Scales are logarithmic

**Table 6.3:** Distribution analysis results for Vráble, subdivided into time samples with coeval houses, arranged chronologically. The analysis was also done on the South-West neighbourhood separately, where the single largest house for each sample was excluded. In both series, only samples consisting of 10 houses or more were analysed. Par1 and Par2 are  $\mu$  and  $\sigma$  for log-normal and normal distribution models. T\_Par1 is  $\alpha$  for power-law and  $\lambda$  for exponential tail models. Tail\_P is the proportion of data points (N) in the tail model ( $N_{tail}$ ), or  $N_{tail}/N$ . Gini index is calculated on the entire sample distribution

BCE	Model	Par1	Par2	Tail	T_Par1	xmin	N	N_tail	Tail_P	Gini
<b>Vráble</b>										
5230	ln	4.059	0.487	pl	4.232	63.5	12	6	0.50	0.279
5210	ln	4.188	0.477	pl	4.314	63.9	24	16	0.67	0.258
5190	ln	4.114	0.372	exp	0.041	51.4	38	28	0.74	0.210
5170	ln	4.199	0.360	exp	0.038	60.9	58	35	0.60	0.204
5150	ln	4.288	0.398	pl	5.235	85.0	53	22	0.42	0.228
5130	ln	4.224	0.395	pl	5.041	78.9	64	25	0.39	0.225
5110	ln	4.281	0.368	pl	4.907	81.3	49	19	0.39	0.215
5090	ln	4.224	0.378	pl	5.542	71.3	36	21	0.58	0.206
5070	norm	75.086	25.864	exp	0.044	70.0	22	14	0.64	0.197
5050	ln	4.297	0.357	pl	5.010	67.9	24	17	0.71	0.201
<b>Vráble SW*</b>										
5190	norm	53.755	14.740	pl	7.911	52.9	10	7	0.70	0.151
5170	norm	54.851	13.923	exp	0.063	44.3	18	15	0.83	0.145
5150	ln	4.186	0.375	pl	8.045	87.1	13	5	0.38	0.213
5130	ln	4.100	0.365	pl	5.489	61.9	19	11	0.58	0.196
5110	norm	58.895	10.918	exp	0.074	48.2	13	12	0.92	0.103

Three examples of the spatial distribution of coeval power-law houses is seen in Figure 6.12. Through most of the analysed time samples there is seemingly only one or two very large houses per neighbourhood, and in the first and last of the samples that are large enough for distribution fitting (5230 and 5050 cal. BCE) there is only one for the entire settlement (Figure 6.10a). This further indicates that it would be in the middle phases of Vráble in particular – roughly between 5150 and 5090 following the model – that the three neighbourhoods developed into independently functioning settlements, possibly with increased competition between them, as is also suggested by the construction of the enclosure and palisade around the south-west neighbourhood shortly after and by 5070 BCE (Furholt, Müller, et al., 2020, pp. 493–498). A single house per phase which is clearly larger than the rest is a regular trend in Linear Pottery settlements, though absolute size categories vary between contexts (Coudart, 1998, p. 49). This largest house does not necessarily represent any obvious architectural particularities indicating special function like the Modderman 1a type (1970), though they do tend to have double posts (possible elevated granaries) in the frontal section [Coudart (1998), pp. 41-2; 3.2]. Though this is not yet confirmed through excavation in Vráble (#CHECK), the largest houses are generally upscaled versions of smaller common types, in particular the type 1b, or *Großbau* with ditch in the posterior section only. And though it is difficult to prove with house sizes alone, it seems fully plausible that such largest houses be inhabited by clan leader households. Once the settlement grew large enough for more than one clan to take on a leading role – i.e. too large for one clan to control alone – the settlement would split and crystallise into three more or less independent factions, each with a clan-leading household during the middle phases. Following this model, it would then be the competition between three clan households or Houses that lead to the increased tensions and violence seen in the late phases of the settlement, rather than generally increasing levels of inequality. Given that the above described power-law distributions stretch well beyond these largest houses in the Vráble neighbourhoods, it is furthermore tempting to interpret the placement of subsequent houses in the size hierarchy as a function of their kin proximity to the leading household, with the smallest houses (those outside the power law) representing recently established or otherwise poorly integrated households [Hachem & Hamon (2014); 3.2].

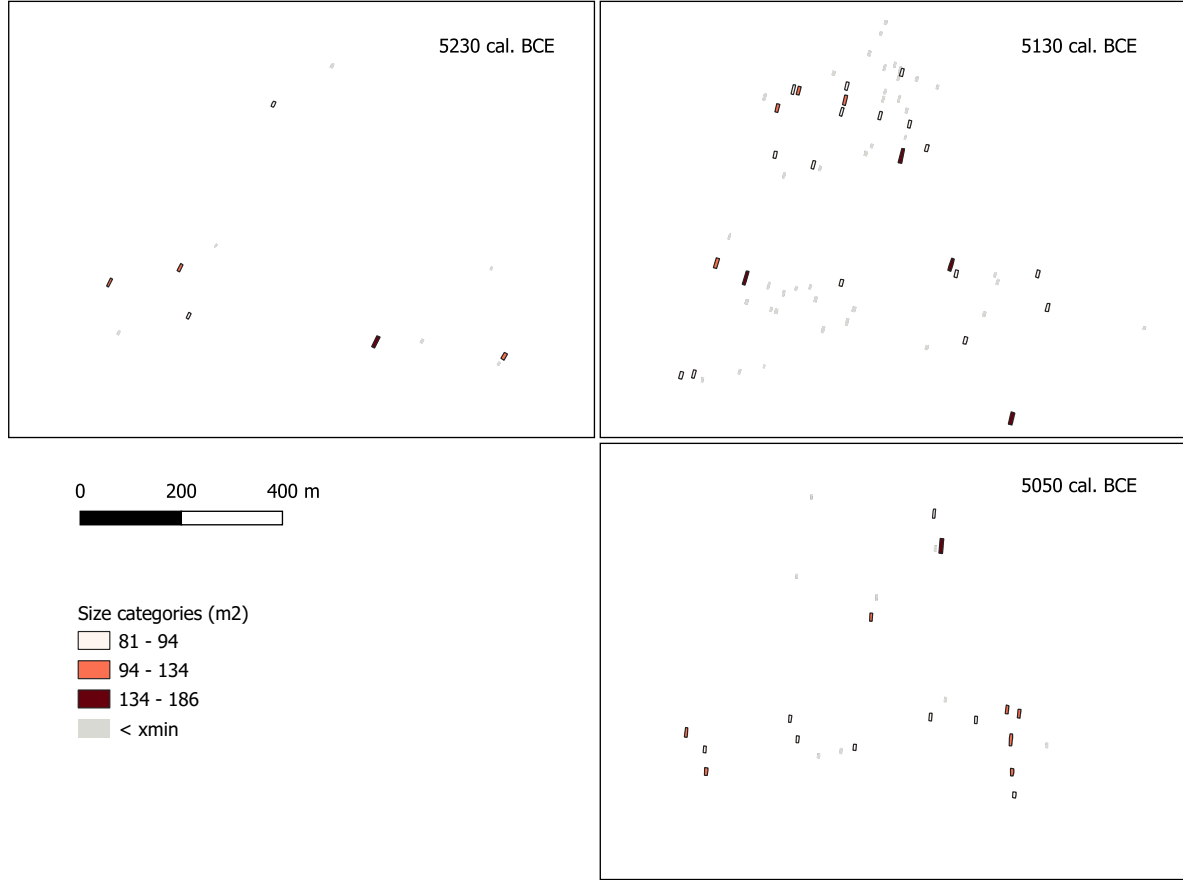


**Figure 6.12:** Vráble at three temporal samples, with house sizes above  $x_{min}$  grouped into three arbitrary classes by Jenks optimisation. Parameter values differ slightly between time samples (see table), and the legend categories refer to the 5130 sample. Counter-clockwise shift in house orientation is used as proxy for construction date

## 6.4 Summary of findings

The distribution fitting analysis on the house sizes of entire settlements resulted in power-law tails being clearly identified in four out of 13 cases. These were the Trypillia mega-sites of Maidanetske and Nebelivka, as well as the smaller Trypillia site of Moshuriv and the Linear Pottery settlement of Vráble. The much smaller Linear Pottery settlement of Horný Oháj was also identified with a power-law tail, but the result was disregarded due to the small sample size. These four settlements were also the largest of the sample of settlements. Furthermore, one Linear Pottery settlement – Úľany nad Žitavou – had normally distributed house sizes, and one Trypillia settlement – Talne 3 – had a log-normal house-size distribution with very little skew which in practice was indistinguishable from a normal distribution. While these two settlements were not the smallest in the sample, they were clearly within the lower end of settlement sizes. While the normal distribution is by definition symmetric, the power-law

distribution is the most asymmetric or unequal of the models compared here. Though the settlement sample used here is small, I see these results as indications that absolute settlement size is more determinant for the shape of the house-size distribution than cultural belonging. Given that settlements within archaeological cultures like the Trypillia and the Linear Pottery vary greatly in size, this has potentially great implications for how we conceptualise their social organisation. In other words, the daily life in large Neolithic settlements may have been more similar across cultures than to small settlements within the same culture, much like urban life of large contemporary cities may have more in common more across nations than it has between a large city and its surrounding rural area. More specifically, the house-size distributions of these large Neolithic settlements show hierarchical scaling which – at least in theory – can be related to preferential attachment processes where the already large have advantages for growing larger. How exactly this may translate to the specific cultural settings of the Trypillia and the Linear Pottery contexts is however open for debate, and other strands of evidence from their material culture indicate that these hierarchies may have been socially quite different. These issues are further discussed in Chapter 10.

Following the methodological tests given in the previous chapter, the distribution fitting was also performed on separate quarters for Nebelivka and neighbourhoods for Vráble. The results were largely similar, with a few exceptions, notably the south-east neighbourhood of Vráble (one of three) and the N and E quarters of Nebelivka (two of 14). For Nebelivka, the result of two non-power-law quarters could largely be questioned with missing data and unclear quarter boundaries, and the hierarchically scaling houses were wildly spread across the site both when analysed as a whole and by quarters. Compared to Maidanetske, for which this spread was seemingly very even and unstructured, in Nebelivka the scaling houses were at the same time spread throughout the quarters as well as clustered, so that large houses tended to be found near other large houses, and small houses near other small houses, seemingly reflecting some level of segregation between privileged and unprivileged households. For Vráble, the picture was somewhat more confusing since the interpretation of house scaling would differ more between the perspective of the whole settlement and that of the separate neighbourhoods. In particular Vráble SE has a scaling of house sizes which is very similar to that of Vráble N when all is analysed together, while it has no scaling when analysed separately. This difference should perhaps not be overstated however, since other parameter values showed that the south-east neighbourhood did not have a markedly more symmetrical house-size distribution than the

other two sections – both its standard deviation and Gini index were actually higher than those of the other two (Table 6.2). Judging from the cCDF plot in Figure 6.8, Vráble SE was seemingly not recognised as having a power-law tail since its two or three largest houses were smaller than what should be expected for a power law given the size of the other large houses.

The houses of the Vráble settlement were furthermore attributed to one or more temporal samples based on modelled construction date and house durations. Sixteen samples of 20 year intervals were defined, 10 of which had more than 10 houses attributed to them and were thus analysed further. Of these, seven were interpreted as having power-law distributed house sizes. These were spread in time, and neither the distribution types nor the more standard Gini index give support to interpretations of increasing inequalities toward the later occupation phases of Vráble. Rather, it was shown that in the early and late phases there was only a single very large house dominating the hierarchy of houses at the whole settlement, while in the middle phases there were usually two or three, and when mapped to the settlement plan, these were situated in the three different neighbourhoods. From this it could be interpreted that it was increasing competition and tension between leading Houses or clan leading households in the three neighbourhoods – rather than increased inequalities in general – that lead to the violence observed in the skeletal material, as well as the construction of the enclosure surrounding the south-west neighbourhood, in the late phases of the settlement shortly before its decline. An additional distribution-fitting and model-selection test was done on coeval houses of the south-west neighbourhood only, and excluding the single largest house for each phase, to ensure that the power-law signal was not a statistical artefact resulting from lumping the three neighbourhoods and from a scenario where a single communal building would dominate otherwise moderately skewed distributions. In this sub-set, only five time samples were large enough for analysis, three of which still gave power-law distributed tails. It was concluded that the observed hierarchies in house sizes were real, at least in the case of Vráble, and that they most probably represent some sort of hierarchical social organisation, which is discussed further in Chapter 10.

# **Part III**

## **Settlement Plans**



# **Chapter 7**

## **Village planning in prehistory**

### **7.1 Settlement layout and social structure**

Or the social organisation of village layout. Research background:

Lit. use Furholt (2016), Fraser (1968), Ensor (2017), Ensor (2013), also check Souvatzi (2017).

For cities, see Kostof (1991)

Space syntax, Hillier (1984)

Visibility Graph Analysis/connectivity: Turner 2001, applied in Buchanan 2020

Viewshed Analysis: applied in Ohlrau 2015?

Materiality of built space??

Artursson et al. (2010) (Bronze Age, descriptive/interpretive approach). Cleuziou et al. (1999) (book in MAE)

Use the Trypillia volumes. Also Müller-Scheeßel (2019), Trebsche et al. (2010)

Access analysis: Fisher (2009)

Viewshed analysis:

Transition from village to urban (again): Birch (2014).

Factors affecting village layout:

- Political structure (but, as with hierarchy, an organised layout does not necessarily equate top-down despotic decision making).
- Kinship, matrimonial and locality structures
- Cosmology (e.g. Linear Pottery house orientations)
- Economic and ritual functions of village elements (constructed and non-constructed)
- Local landscape setting (to be factored out)

## 7.2 The geometries of conscious planning vs. emergent behaviour

- I need to find some references here! Eglash (1999)
- Euclid: grids, lines, circles – how humans think in shapes. Social settings: architect/planner, strong common institutions/ideals (examples?)
- Mandelbrot: irregular, self-similar, scale independent (i.e. fractal) shapes – emergent, not consciously preconceived. Self-organisation. Does the “no pattern” case exist? Emergence from repetitive sequences of simple choices/mechanisms. Examples.
- Binary or continuum? Needs to be studied empirically.

## 7.3 Fractal image analysis in archaeology

END Chapter

# Chapter 8

## Methods: Fractal image analysis

In this chapter I present briefly the techniques for calculating fractal dimension and lacunarity estimates on archaeological and synthetic settlement plans, as applied further on. The chosen procedure for preparing images of these plans for analysis is also detailed. I review some issues related to the interpretation of these measurements, mainly in terms of visual pattern characteristics and textures. In order to evaluate how various parameters influence fractal dimension and lacunarity estimates on images, some tests on synthetically generated images are provided and discussed. Results of analyses on images of archaeological settlement plans are presented in the following chapter. #recheck this intro

### 8.1 Calculating fractal dimension and lacunarity

As noted in the previous chapter, the fractal dimension of spatial patterns was originally estimated by Mandelbrot by deciphering visually the relations of size and frequency of elements between the *initiator* and the *generator* of theoretical (i.e. fully regular) fractal sets like the Koch curve or the Sierpinski triangle (e.g. Mandelbrot, 1982, p. 39 ff.). Empirical fractals on the other hand usually also include some stochastic elements, rendering this technique much more difficult to use in practice, as the generator of the pattern is harder or even impossible to discern. A number of more systematic methods have therefore been developed since the 1980s for estimating the fractal dimension of empirical patterns, the by far most popular being the so-called box-counting method (Klinkenberg, 1994; Li et al., 2009). The principle of the method is quite simple:

- Cover the pattern with a regular square grid of a given mesh (“box”) size, and count the number of boxes that intersect with the pattern.
- Do this for a range of box sizes (usually in exponential steps from the pixel size up to about half of the image length), recording the number of boxes for each size.
- Fit a linear model to the logarithms of box counts to box sizes, and the slope of the line corresponds to an approximation of the fractal dimension of the pattern.

Readers of Section 4.2.4 will recognise that the relationship between box sizes and box count is a power law with fractal dimension being defined as its scaling exponent, and while one may wonder why the log-log fitting method is accepted here when it was banned in previous chapters, there are some differences between the two contexts. Firstly, we are not dealing here with univariate distributions and their underlying generative mechanisms, but rather the relation between two variables. Secondly, the fractal dimension (in the following denoted  $D$ ) is *defined* as this scaling exponent, that is the logarithm of frequency (number of elements) divided by the logarithm of their sizes relative to the whole (#did I remember to add an equation of D in chapter 7?). In theory, the graph of boxes to box sizes should always follow a power law – i.e. a straight line on a log-log plot – but with a fractional slope value when the pattern is fractal and an integer slope value when the pattern is a fully Euclidean shape.

There are some caveats regarding the interpretation of this estimate however. One is that there is nothing preventing a fractal shape of having an integer dimensional value. Its defining characteristic is that unlike Euclidean dimensions it can take on any value from 0 to 3 for spatial patterns and higher for more abstract patterns, and the numbers 0, 1, 2 and 3 are values just like any other in this continuous range. An integer dimension is thus in itself not enough to claim that a pattern is Euclidean and not fractal (though fractals with exactly integer dimensions are rare). But it is more important to consider what exactly is meant by Euclidean shapes in this context, namely a shape that entirely fills its embedding Euclidean dimension like a square or circle in two-dimensional space or a straight line segment in one dimension. An entirely regular grid pattern consisting only of identical squares or circles with some space between them does not fill its embedding space, and will have a fractional dimension when analysed through box counting, even though it can hardly be described as scale-invariant or fractal (examples are given below). For such cases, the total area of the pattern, approximated by the box count times box size, will be unstable down to the image resolution, as if the pattern

were truly fractal. The dimension value obtained through box counting is thus in itself not a guarantee for the pattern being either Euclidean or fractal, which is why it is more accurate to refer to it as the *box-counting dimension* or  $D_{box}$ . This has led to numerous confusions and erroneous interpretations in earlier studies involving box counting Oleschko et al. (2000), and it illustrates the difficulty involved in interpreting the obtained values. This is also largely why I have opted for a more prudent empirical approach using synthetically constructed images to guide interpretation, testing for the effects of different variables one-by-one as presented below.

Some similar issues concern the estimation of lacunarity in empirical patterns. While Mandelbrot mainly relied on regular constructed fractals for estimating lacunarity, empirical patterns involving stochastic processes require more formal methods for analysis. The main method for estimating lacunarity is the so-called gliding-box method (Allain & Cloitre, 1991; Cheng, 1997; Hingee et al., 2019; Plotnick et al., 1996). Similarly to box counting, it involves evaluating the pattern over a range of scales (box sizes), but instead of a grid, a single box is glided incrementally across the image with overlaps (rendering the method computationally heavier). For each increment, the pixel mass (number of foreground or pattern pixels) within the window is recorded, and the average spread of this over all box displacements for a given box size is calculated, giving a lacunarity index (#refer to the equation in chapter 7). This index – i.e. lacunarity for a given box size, is then plotted according to box size, and unlike the fractal (box-counting) dimension, the shape of the lacunarity curve can effectively give an indication of whether or not, or over which scales, the analysed pattern is fractal. For regularly self-similar mono-fractals, the curve of the lacunarity index forms a straight line in log-log scales, with the slope being equal to  $D-E$ , i.e. the fractal dimension of the pattern minus its Euclidean dimension (Allain & Cloitre, 1991; Mandelbrot, 1982, pp. 315–317; Plotnick et al., 1996, p. 5463). Since real-world patterns are rarely self-similar over very large ranges, and even less so for image renderings of them which depend on pixel resolution, this lacunarity index curve tends to follow a power law less strictly than that of box counts, even when the pattern is fractal-like over some scales.

Mandelbrot never gave any single definition of a summary statistic for lacunarity across scales like the fractal dimension, and several such summary measures have subsequently been proposed. The software plugin *FracLac* for *ImageJ* offers principally three of these, namely the exponent and prefactor values of a power-law approximation of the lacunarity index, as well

as its arithmetic mean (Karperien, 2013). There is little literature on the relationship between these, and it is not always clear which one of these is applied. Farías-Pelayo seems to be using exponent lacunarity in (Farías-Pelayo, 2017) and a mixture of this and mean lacunarity in (Farías-Pelayo, 2015). The value range of the power-law exponent should be expected to vary much less than that of the mean or prefactor, and these latter two cannot be below 1, while the exponent can in theory go down to 0 (a full pattern with no gaps and  $D = 2$  for spatial patterns, see also Bruvoll, n.d. for further discussion on this issue). As mentioned above, the power-law exponent is directly correlated to  $D$  in the case of self-similar mono-fractal patterns.

For practical applications, Hingee et al. (2019) recently showed that the lacunarity index is mathematically equivalent to spatial covariance, which has the further advantage of being more tolerant to irregular image outlines as well as missing data. From this they proposed a series of estimators that they showed to give more reliable results than the standard lacunarity estimate, and implemented these in the *R* package *lacunaritycovariance*. While both irregular outlines and missing data are continuously relevant issues in archaeology, I did not pursue these possibilities further here, though I made use of the *gbl()*-function (gliding-box lacunarity) from this package, with its default “GBLcc.pickaH” estimator, for calculating the lacunarity index of images. Fractal dimension was in this thesis calculated in *R* using the *fract2D()*-function from the *fractD* package (Mancuso, 2021). For both analyses, box sizes (widths) were set to the default values in *fractD*, namely 1, 2, 4, 8, 16, 32, 64, 128, 256 and 512 pixels.

The analysed images of empirical settlement plans were prepared in QGIS 3.20.1, from shapefiles that were kindly shared by their creators on behalf of the research projects in which the spatial data was collected [Hale (2020); Ohlrau (2020); Müller-Scheeßel et al. (2020); 3]. In order to focus the analysis on architectural features only, all other spatial features were removed, while house polygons were rendered with black fill and no stroke, and rasterised to a Boolean (black-and-white) image with 0.5 m pixel resolution, and cropped to the minimal extent of the corresponding vector layer. Differences in image processing between the *lacunaritycovariance* and the *fractD* packages made it necessary to store the images in two versions in separate folders, in .jpeg format with greyscale rendering (0 for black and 255 for white) for fractal dimension and in .tiff format with binary values (1 for black and 0 for white) for lacunarity. This preparation process is obviously not ideal, and is due to the lack,

for the time being, of implementation of these methods in a single coherent *R* package. This also makes the use of ready-made image analysis softwares like the above mentioned *FracLac* plugin even more convenient. However, the advantages of still performing the analysis in *R*, include the full transparency and adaptability of the method implementation, as well the increased possibility of combining the analysis with other methods. The analysed images are reproduced in the #appendix, and are available in their original sizes and formats in the #online repository, along with the code for analysing them.

In the following, I attempt to address the difficulty of interpreting fractal dimension and lacunarity measures of spatial patterns by testing the methods on synthetically produced images, designed to isolate relevant variables one by one. The chosen variables are perceived to be of importance specifically in the present context where the images of interest represent architectural features on archaeological settlement plans. While this is not a sufficient analysis for effectively modelling the relative effects that any of these parameters may have on  $D$  and  $L$  measurements in any image, it allows for an intuitive illustration of the complexity involved in analysing spatial textures. The chosen image variables which are selected here for empirical testing are image size, element count, element size, image density, element size distribution, self-similarity/clustering and random noise. While the first three are important for assessing the requirements of the analysed images for the methods to function properly, the latter two are of more direct interest for the hypothesis which is proposed in this part of the thesis, namely that fractal image analysis may allow for quantification of the degrees of hierarchy and conscious planning in a society evident through the layout of its settlement plans. The variables density and size distribution are important aspects of any settlement plan, but say little by themselves about the extent to which the layout is planned or not, and their influence on fractal dimension and lacunarity measurements can thus in this context be regarded more as side effects. As is shown below and further discussed in Chapter 11, while spatial clustering, element size distribution and noise do have effects on both fractal dimension and lacunarity measurements, in many practical settings these effects tend to be drowned by those induced by other variables like image size and density. The possibility remains that these methods may prove useful for comparisons of settlements of similar size and density only, or by defining more formal model by which undesired effects of other variables may be factored out. Here I suggest thresholds from which image size and resolution seem to give stable results, and I provide only some very simple models are tentatively constructed to factor out image

density. While more formal and complete modelling for these purposes would be warranted for obtaining more fine-grained results, this goes beyond the scope of the present study.

For the following tests, all images were constructed in R as data tables with x and y coordinates for each element (“house”), rendered with the *ggplot2* package (Wickham, 2016). More specifically, in each image houses were represented as a `geom_tile()` layer with black fill and given height and width, and the background was set to white, while the `theme_void()` function allowed for removing the axes and grids altogether. With this procedure it was possible to generate incremental changes in a single variable on otherwise identical images. However, as some of the variables are inherently connected, full separation was not always possible. Again, all the generated and analysed images are included in #Make Appendix, and the original files and code for generating them, are available in the #online repository.

## 8.2 Effects from image size, element size and element count

To test the effect from image size on fractal dimension and lacunarity measures, it was necessary to proceed in three steps (Figure 8.1). A first series was created in which a single image was simply scaled up from  $40^2$  to  $420^2$  pixels in 20 steps. The smallest image thus represented four square houses of size  $10 \times 10$  pixels, which with 0.5 m per pixel length (the resolution used with the actual settlement plans in the next chapter) gives houses of  $25 \text{ m}^2$ . Each house filled the lower left quarter of a 4 times larger square, so that image density was kept at 0.25. Density is defined here as fraction of pattern pixels to the whole number of pixels. For the largest version of this pattern, each house thus had a side length of 52.5 m, giving a total surface of ca.  $2.756 \text{ m}^2$  per house, which is far above comparable values for houses in prehistoric settlement plans. Since in reality house sizes do not increase linearly with settlement size, but are more constant, a second series was created where the image size was incremented the same way, but with a constant house size of  $25 \text{ m}^2$ , so that in order to also keep image density constant, house count ( $N$ ) was increased proportionally with image size. For this series, the largest image then had  $N = 21^2 = 441$  houses, thus emulating settlements of different sizes but with similarly sized houses and densities between houses. In other words, different image sizes could not be made keeping both density, house count and house size constant. A third series of 20 images was made where image size was kept constant at  $420^2$  pixels, but with the same range of house count from 4 to 441 as well as house sizes from  $105^2$  to  $10^2$  pixels, or

2.756 to 25 m<sup>2</sup>.

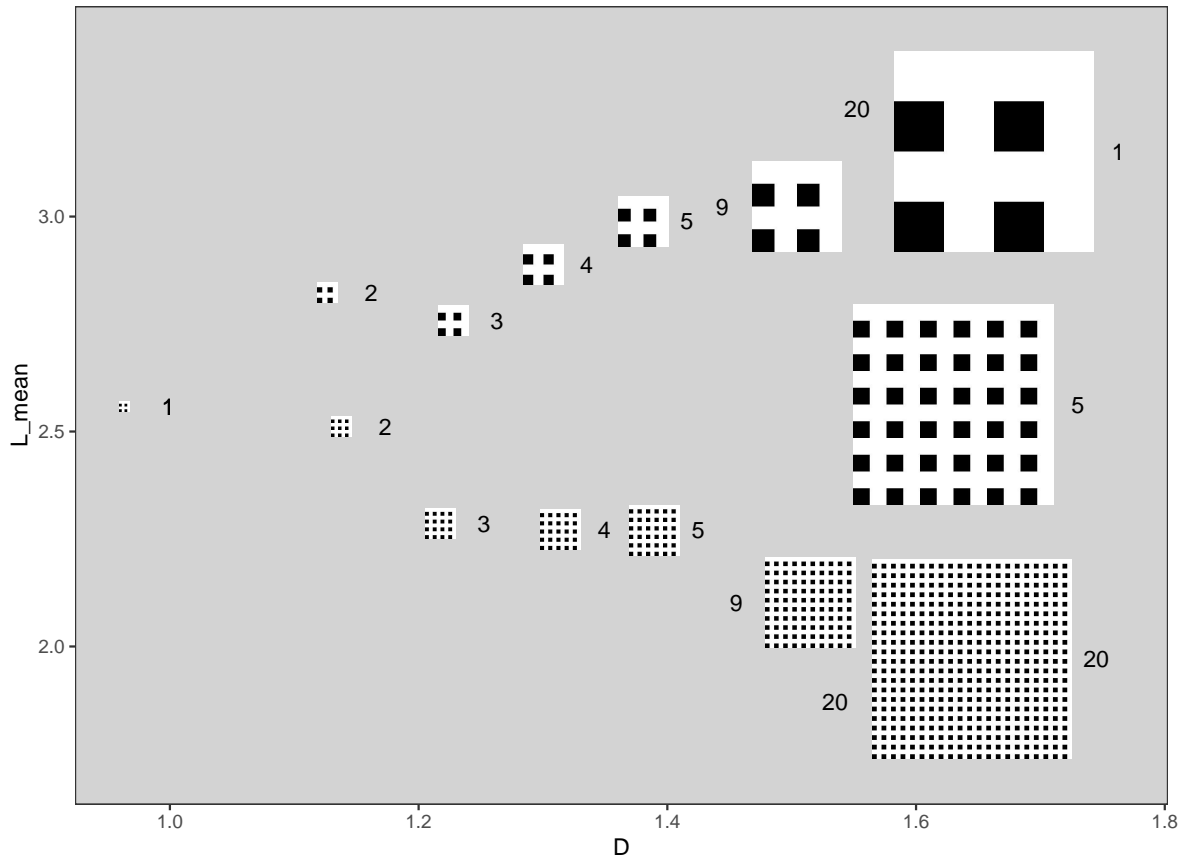


**Figure 8.1:** Effects from image size, element count and element size on fractal dimension and lacunarity. Density is fixed at 0.25 for all images. Number labels represent iteration within each series. Image size is variable in the upper and lower series, house size in the upper and the vertical series, and house count in the vertical and the lower series. The three corner images are identical for two series each. Images are selected here to prevent overlaps

The resulting fractal dimension and lacunarity measures for all images in these three series are shown in Figures 8.2 to 8.4. In all three cases – increased image size and house size, increased image size and house count, and increased house count and decreased house size – there are clear tendencies. In the two first series (upper and lower images in Figure 8.1), fractal dimension increases with image size, seemingly independently from the evolution in the pattern given that density remains constant. In the third case, when image size is kept constant (right side images in Figure 8.1), changes in fractal dimension are much smaller and less systematic, however lacunarity changes with some fluctuation. Regarding the two different summary measures of lacunarity – mean  $L$  and exponent  $L$  (see above) – though not identical, they respond in very similar ways to changes in all three image series. However, it is important to notice that the direction of change in lacunarity is opposite depending of the summary measure in the first and third series, while identical in the second. This difference

is not easy to explain, and underlines the importance of reporting explicitly which lacunarity measure is being used. As seen on these plots, the exponent lacunarity typically has values below or around 1, while the mean lacunarity may have much higher values and cannot be below 1 – an observation that can serve as a rule of thumb for decrypting results where the exact type of measurement used is not explicitly reported.

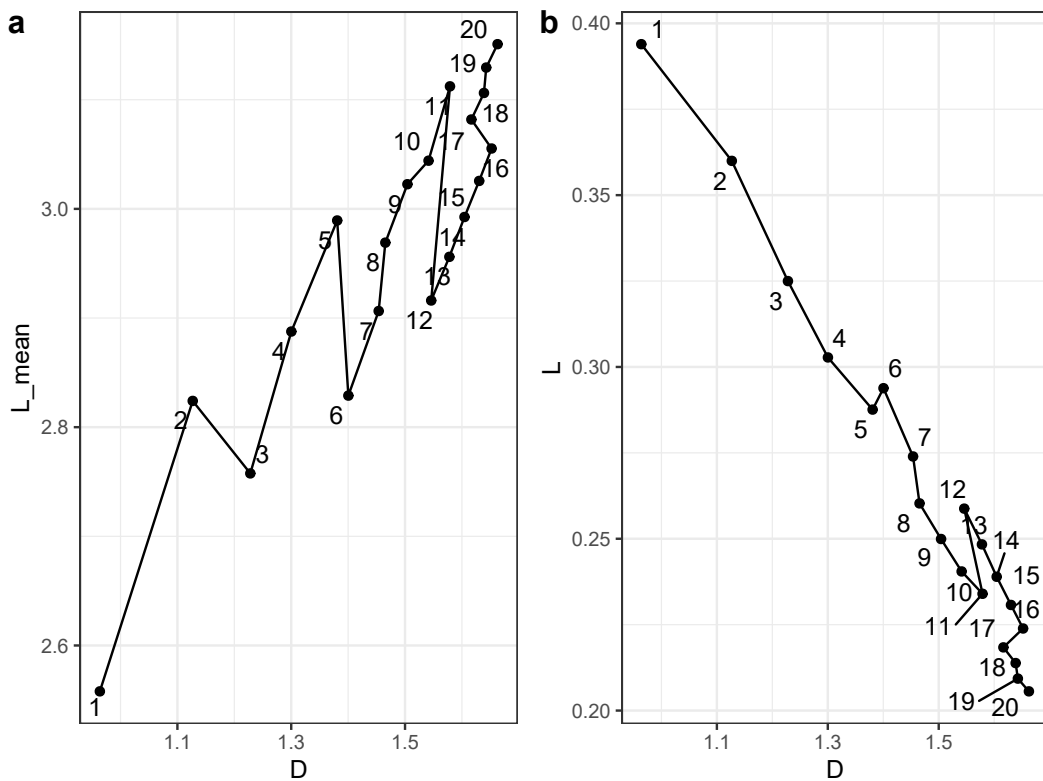


**Figure 8.2:** Different image sizes and house sizes, with  $N = 4$  and density = 0.25. Resulting fractal dimension ( $D$ ) and mean lacunarity ( $L_{\text{mean}}$ , plot a) and exponent lacunarity (plot b). Images are numbered by iteration

In the first two series, where image size is variable, it should furthermore be noted that the changes in  $D$  and  $L$  measures between iterations roughly slow down as image size increases, potentially indicating that they approach the “true” values of the given pattern, and that the measurements of the smallest images are only statistical artefacts. Another parameter which is related to image size is the range of box widths used when analysing the images, and further study could allow for more elaboration on the possible influence this could have on the resulting estimates. In any case, the range of dimension values from 0.96 to 1.66 is considerable given that these images are practically the same besides image size. The range of lacunarity in these series is more moderate compared to the results from other variables presented below. The step-wise decrease in lacunarity seen especially in the image series of increasing  $N$  with

image size (Figure 8.3), is a further indication that the choice of box widths relative to the resolution of the image has a marked influence on the results.

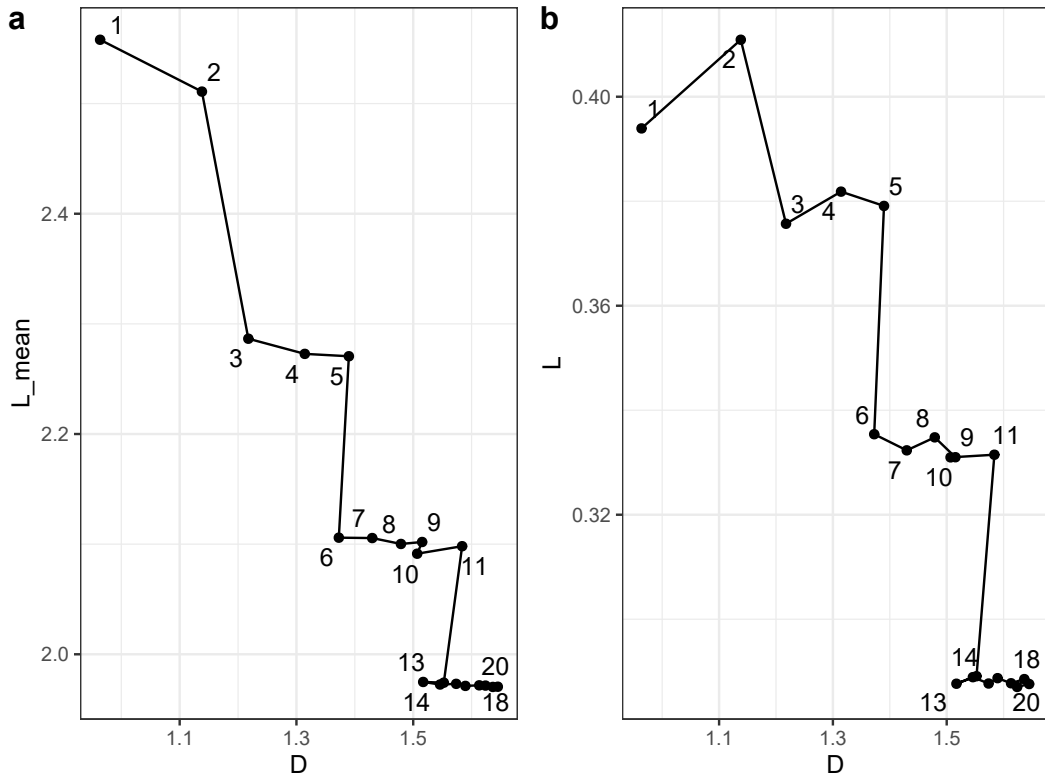


**Figure 8.3:** Variable element count ( $N$ ) and image size, with constant house length of 10 pixels and density at 0.25. Resulting fractal dimension ( $D$ ) and mean lacunarity ( $L_{mean}$ , plot a) and exponent lacunarity ( $L$ , plot b). Images are numbered by iteration

The series with fixed image size and changes in house count and house size also show some convergence in results at higher iterations, though with seemingly more random volatility (Figure 8.4). This indicates that with a given image size, zooming in and out on the pattern has very little influence on the measured fractal dimension (as would be expected from the theory), as long as the pattern is spatially homogeneous. Lacunarity estimates on the other hand, become influenced when zooming in too much, though it quickly stabilises when more of the pattern is included by zooming out. Judging from the results of all three size related image series, there might be some lower threshold of image size and resolution beyond which the box-counting and gliding-box methods become inaccurate, and that the “real” values for this regular square grid pattern of 0.25 density are close to those in the lower right end of Figure 8.1, namely  $D \approx 1.64$  and  $L_{mean} \approx 2.0$ . For image size, the results start to converge at iteration 12 or around 260\*260 pixels (Figure 8.3), given the box size range and fitting method used here. Furthermore, the choice of a 0.5 m per pixel resolution used in this thesis

was arbitrary but came from the acknowledgement that higher resolution would only induce a false sense of accuracy, while lower resolution could potentially lump together archaeological spatial data. In Figure 8.4, estimates begin to stabilise at iteration 7 for mean lacunarity and 5 for exponent lacunarity. Using the more conservative option of 7 (discarding the most inaccurate data), the length of a house is here covered by  $420/8/2 \approx 26$  pixels, which, if this represents 5 metres gives a resolution of  $\approx 0.19$  metres per pixel, which again is about 0.04 or 4% of the house length. In other words, the results presented here indicate that when single pixels represent 4% or less of the smallest features that are being analysed, lacunarity estimates become inaccurate, while fractal dimension estimates remain more unaffected, again given the box widths and fitting method applied here. This sets a tentative upper threshold to image resolution, while the lower threshold should be determined by what gives an acceptable spatial representation of the data. The 0.5 metres per pixel resolution applied in Chapter 9 lets one pixel represent 10% of a 5 metres long wall, thus being within the threshold. The other way around, 0.5 metres is 4% of 12.5 metres, which would be the maximum size of the smallest mapped feature before the resolution would be too high for the lacunarity estimates to be accurate. This threshold value should however at this point only be understood as a rule-of-thumb, as its precision is difficult to quantify any further here. The effect of image resolution on  $D$  and  $L$  estimates of images with other pattern layouts and densities also remains unknown. And again, in these analyses image resolution is only an issue since the analysed pattern is not strictly speaking scale-invariant. Rather it has a clear lower bound, leaving large open spaces in the image when zooming in too much. This is also the case with settlement plans, which, no matter the degree of clustering and self-similarity, will always have a lower bound set by the human scale, since houses can only be so small.

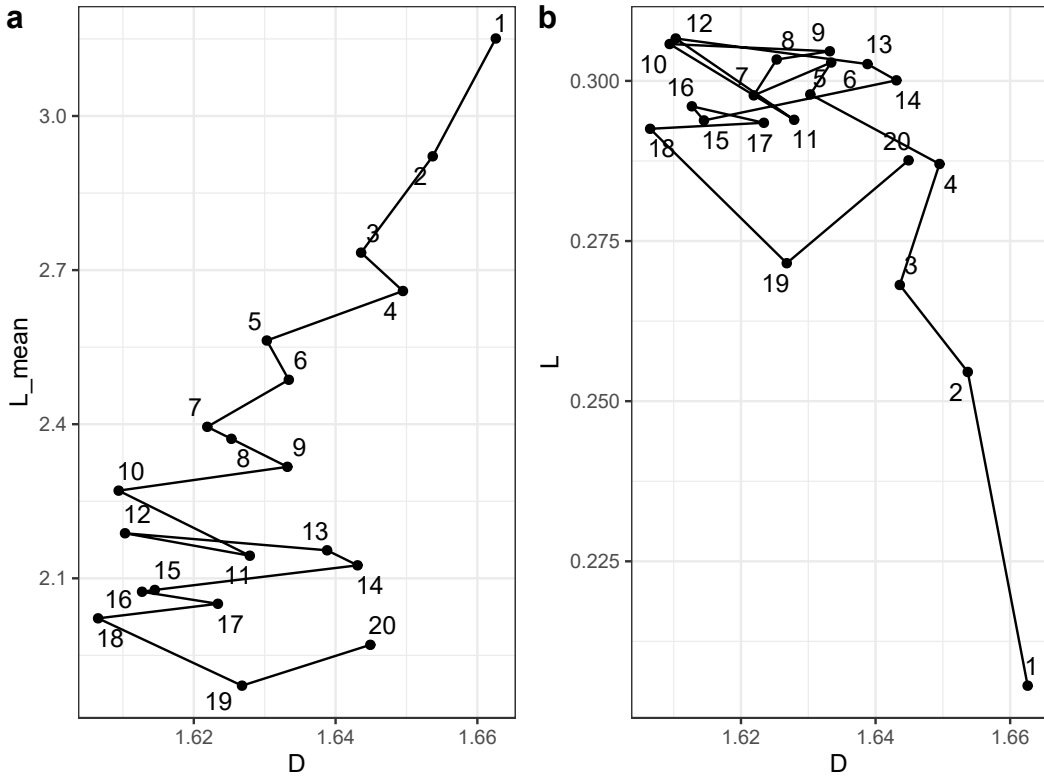


**Figure 8.4:** Variable house count ( $N$ ) and house size, with fixed image size of  $420^2$  pixels and density at 0.25. Resulting fractal dimension ( $D$ ) and mean lacunarity ( $L_{mean}$ , plot a) and exponent lacunarity ( $L$ , plot b). Images are numbered by iteration

### 8.3 Effects from density and size distribution

While density and size distribution of elements are not directly connected to layout type and regularity, as different layouts may have varying degrees of both, they are nonetheless important aspects of settlement plans. Different chrono-cultural contexts give settlement plans of different densities, and this aspect was one of the main differences between the “Anatolian village” and “Balkan village” types of the early Neolithic as shown by Furholt (2016). The density between houses may be highly reflective of the organisation of village life as a whole, as well as of differences between areas of larger settlements. The importance of size distribution of houses for understanding the underlying social system and potential hierarchy between houses was shown in the previous chapters of this thesis.

For both of these variables, a series of 20 images was constructed with internal incremental change between images, keeping other variables constant. In order to avoid the issues related to image size and resolution presented above, image size was set here to  $540 \times 540$  pixels, with a regular grid of  $N = 27^2 = 729$  houses (i.e. corresponding to rather large settlements from

an archaeological point of view). Over the 20 images, density was set to vary incrementally from 0.05 (one pixel per house) to the upper limit where all houses percolate into a single filled square (density = 1, Figure 8.5). Fractal dimension and lacunarity estimates of the images with variable density followed clear and regular trends, with  $D$  and  $L$  being seemingly exponentially correlated to density, as seen in how the step lengths between iteration points in Figure 8.6b decrease at a constant rate.  $L_{mean}$  being already exponentially correlated to  $D$  (see further discussion below), it seems to follow a power-law relationship to density, meaning that low densities get very high values of  $L_{mean}$  and inversely. As should be expected the range in  $D$  values in this series is very wide, from approximately 1.0 (the dimension of a straight line segment with no surface) to above 1.8. In theory the single black box of which the last iteration image consists should have a dimension of 2, illustrating the limits of the box-counting method. This wide range also shows clearly that a fractional dimension value obtained from an image through box counting does not in itself mean that the analysed pattern is actually fractal (i.e. exhibiting self-similarity at a range of different scales). The observed lacunarity values of the last image of this series (no space between points) were, however, arbitrarily close to the theoretical values of 0 for  $L$  and 1 for  $L_{mean}$ .

The exponential relationship between fractal dimension and density of spatial patterns was noted by Thomas et al. (2007), who – based on the layouts of different suburbs of modern Brussels – argued that  $D$  gave additional information on texture and clustering that density could not give. The constant relationship between  $D$  and density here shows that the two measures are largely equivalent, *given a constant layout*. To further investigate whether  $D$  and  $L$  measurements actually capture anything more than density, in the remaining image series density was kept constant at 0.25.

A natural follow-up from the preceding chapters is to test to which extent different size distributions of houses are reflected in fractal dimension and lacunarity of settlement plans, all other things being equal. A series of 20 images were generated with gradually increased inequality between house sizes, with image size kept at  $540^2$  pixels and  $N = 729$  (27 rows and columns in a square grid). The size distribution was defined as a log-normal with an arbitrary mean at  $\mu = 3.5$  and standard deviations varying in linear increments between  $0 < \sigma < 0.9$ . The first image was thus uniform with identical house sizes, while the last image had some sizes that were much larger than most of the others. For each image, the size distribution was normalised to 1 and multiplied with the desired fraction of the total image area so that den-

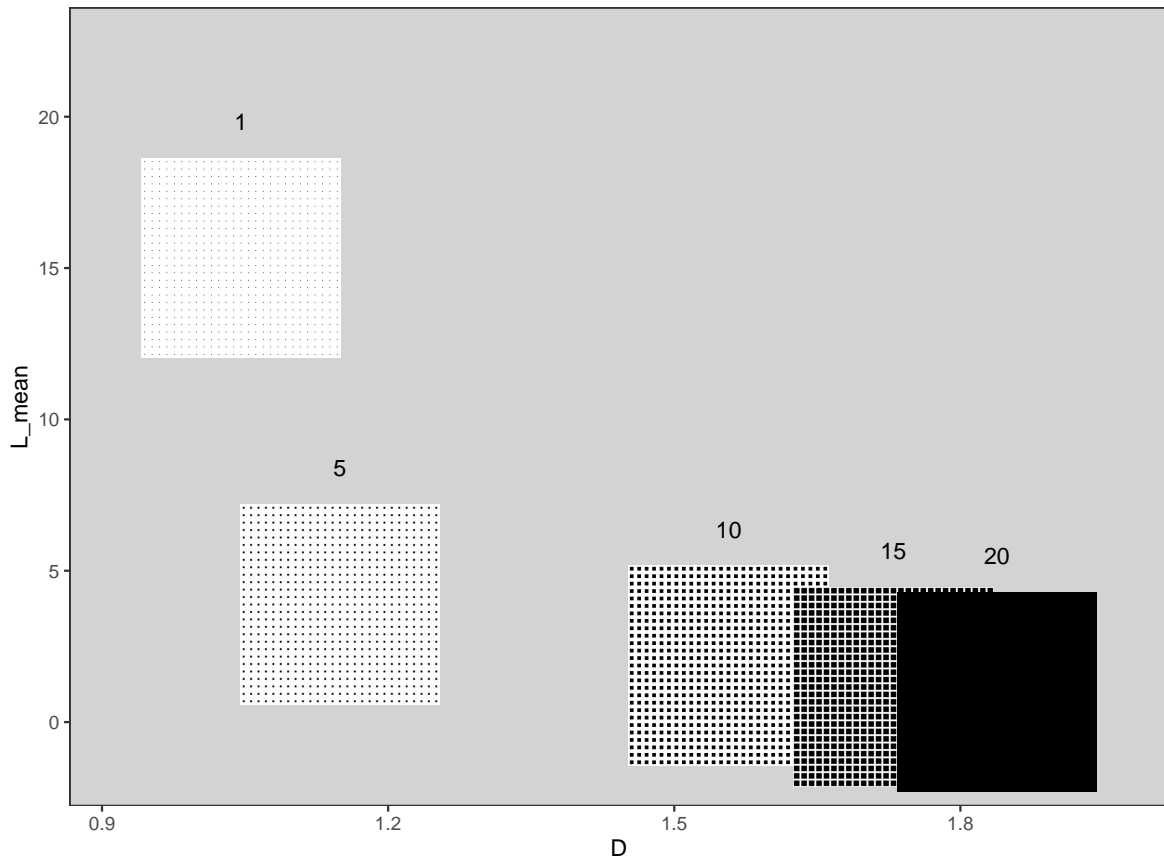


**Figure 8.5:** Fractal dimension and mean lacunarity of images with identical size and layout, but with densities varying with linear increments from 0.05 to 1. Number labels represent iteration, and images are selected to prevent overlaps

sity was kept at 0.25 (with small deviations due to occasional overlaps between neighbouring houses). This series thus illustrates settlements of identical size and layout, but where the size distribution of houses range from (nearly) identical to very unequal (Figure 8.7).

The fractal dimension of the images with variable house-size distributions dropped from the value of the first iteration ( $D \approx 1.56$ ) to around 1.52 where it fluctuated with no clear pattern for the remaining iterations (Figure 8.8). Lacunarity – both the mean and exponent summary measures – increased gradually for almost every iteration, showing how this measure quantifies the increasing irregularity of the gaps between elements, and not only the sum of the gap sizes (i.e. density). Though this trend seems clear enough, the range of lacunarity values on this series remains moderate compared to those obtained from the series with variable density.

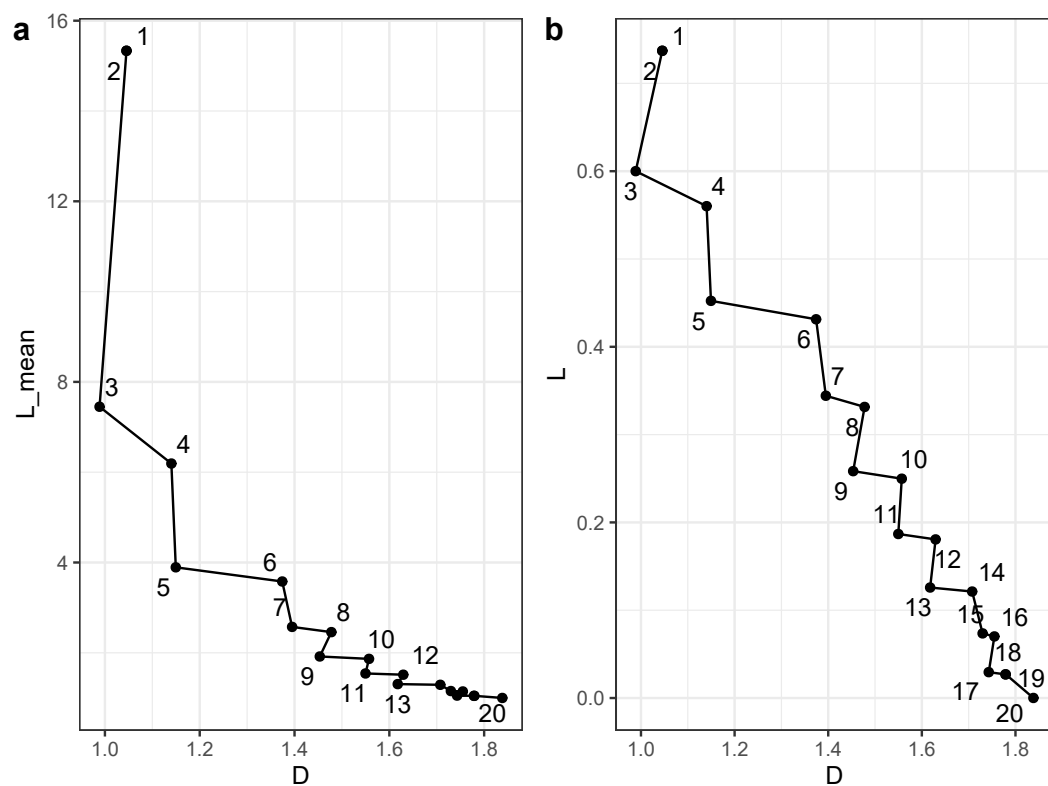


**Figure 8.6:** Fractal dimension and lacunarity measures on the same 20 images with varying density. Because of pixelation the first image was rounded up to be identical to the second, with density = 0.01. Number labels represent iterations

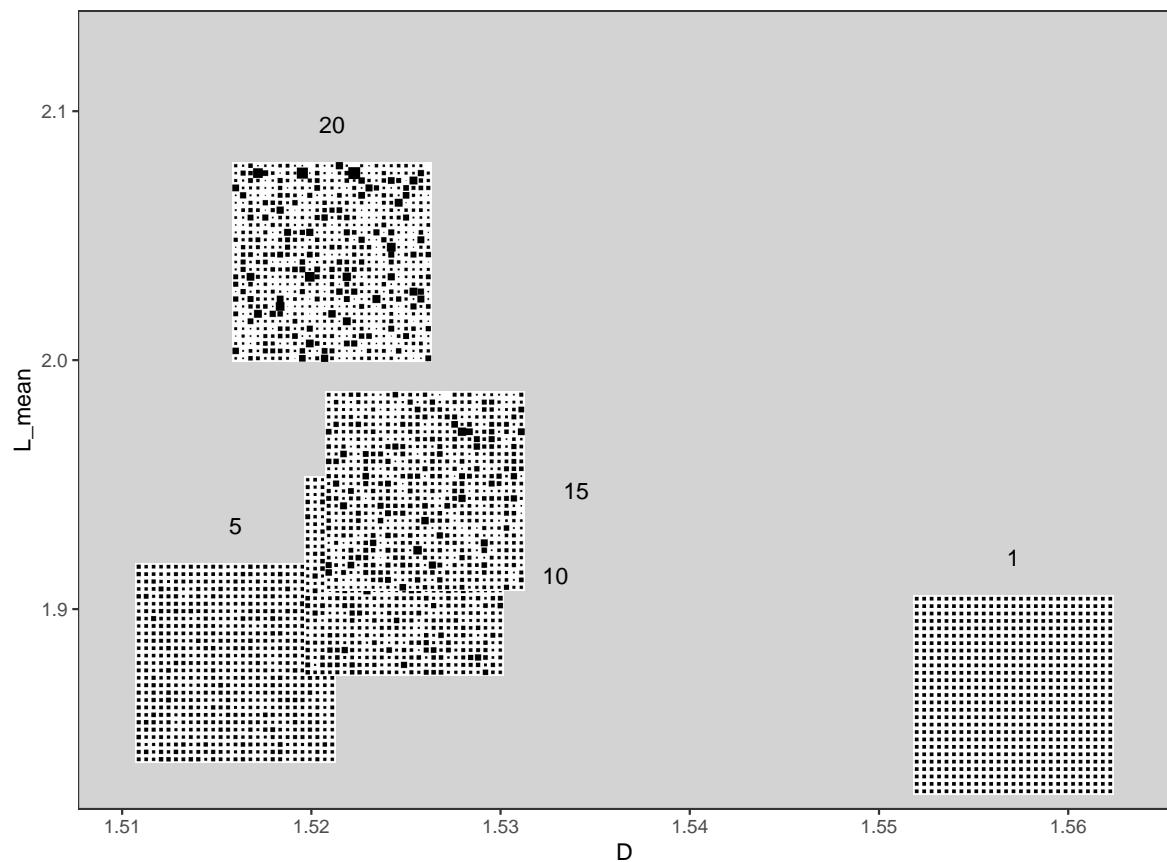


**Figure 8.7:** Fractal dimension and mean lacunarity of images with identical size, layout and density but with varying size distributions of single elements, from uniform (image 1) to log-normal with  $\sigma = 0.9$  (image 20), in linear increments of  $\sigma$  from 0. Number labels represent iteration, and images are selected here to prevent overlaps

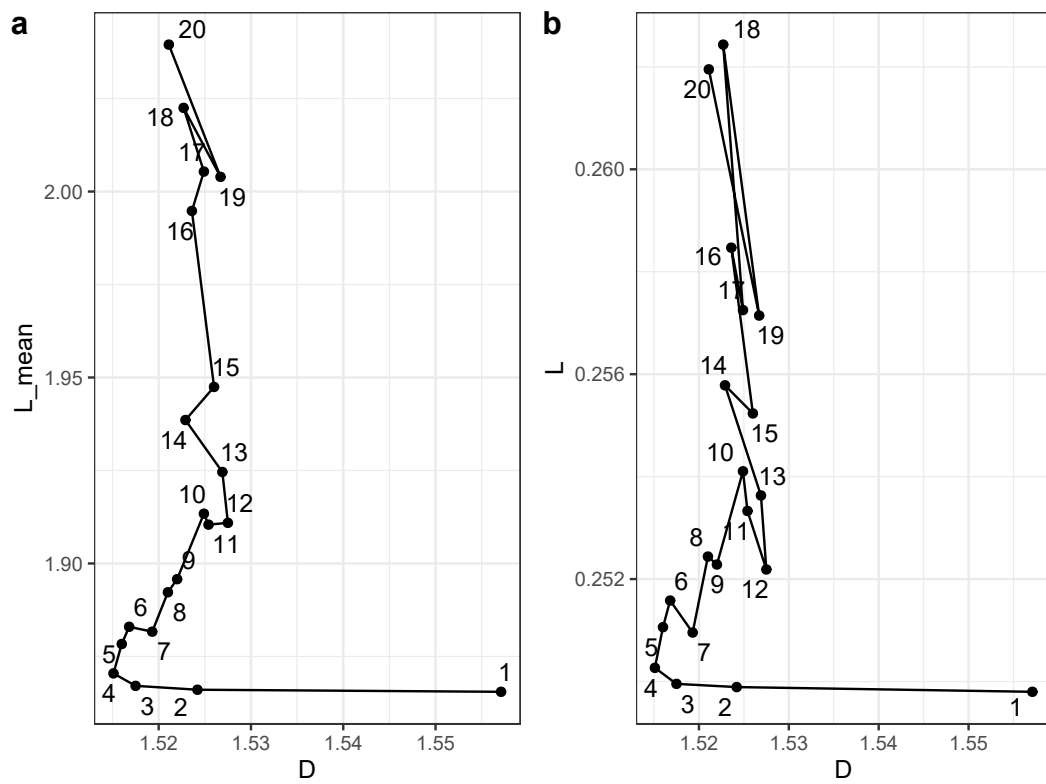


**Figure 8.8:** Fractal dimension and lacunarity estimates of the whole image series, with 729 square points varying in size distribution from uniform (log-normal with  $\sigma = 0$ ) to log-normal with  $\sigma = 0.9$ . For each image, sizes were normalised so that they together covered 25% of the total image area, notwithstanding some overlaps causing image density to descend to a minimum of 0.242. Label numbers indicate iteration

## 8.4 Quantification of self-similarity and random noise

To assess the effect of spatial self-similarity or hierarchical clustering, an image series was generated where, as before, image size, N and density were kept constant, and the size distribution was kept uniform, but where the spaces between houses were gradually increased or reduced so that houses increasingly would form hierarchical clusters. This can be done in a number of ways – in this case two levels of clusters were generated (a third being the settlement as a whole), the lower consisting of 3\*3 houses and the upper of 3\*3 lower clusters (Figure 8.9). This configuration was the reason for choosing 27 rows and columns in the first place for all these image series, since it can conveniently allow for such hierarchical clustering without having non-integer numbers of houses (or houses of different sizes). The first image in this series was thus an entirely regular grid identical to the first image in the size distribution series described above, but the last image here represents a rather different layout, illustrating settlements where hierarchical organisational levels result in self-similar clustering of the overall plan, as described by Brown and Witschey for classical and post-classical Maya urban settlements (2003, pp. 1625–1628). As they argue, the underlying hierarchical levels of social organisation (e.g. family, lineage, clan, state) have been widely observed and described by ethnographers and historians, while the materialisation of such hierarchies in settlement plans is far more rarely recognised, and even less so in terms of fractal geometry.

The resulting fractal dimension and lacunarity estimates on these images show a very similar trend as the one observed on the size distributions image series (Figure 8.10). However, in this case  $D$  continues to drop from the first until the last iteration, albeit with some seemingly random fluctuations. Furthermore, after the first five iterations (which are in reality quite close to the entirely regular grid, see Figure 8.9), both lacunarity measures given here start to increase and do so regularly until the end of the series. Though again the ranges in both dimension and lacunarity are rather moderate here compared to those seen for density and image size above, the trend seen here is clear enough to conclude that hierarchical clustering is reflected in both these measures, in good accordance with the theory.

As a last test series of images to facilitate interpretation of fractal dimension and lacunarity estimates of settlement plans, 20 images were generated from the same point of departure as before – i.e. image size of 540\*540 pixels, 27\*27 houses each of 10\*10 pixel size, giving 0.25 image density – but where an increasing amount of spatial noise was added for each iteration.

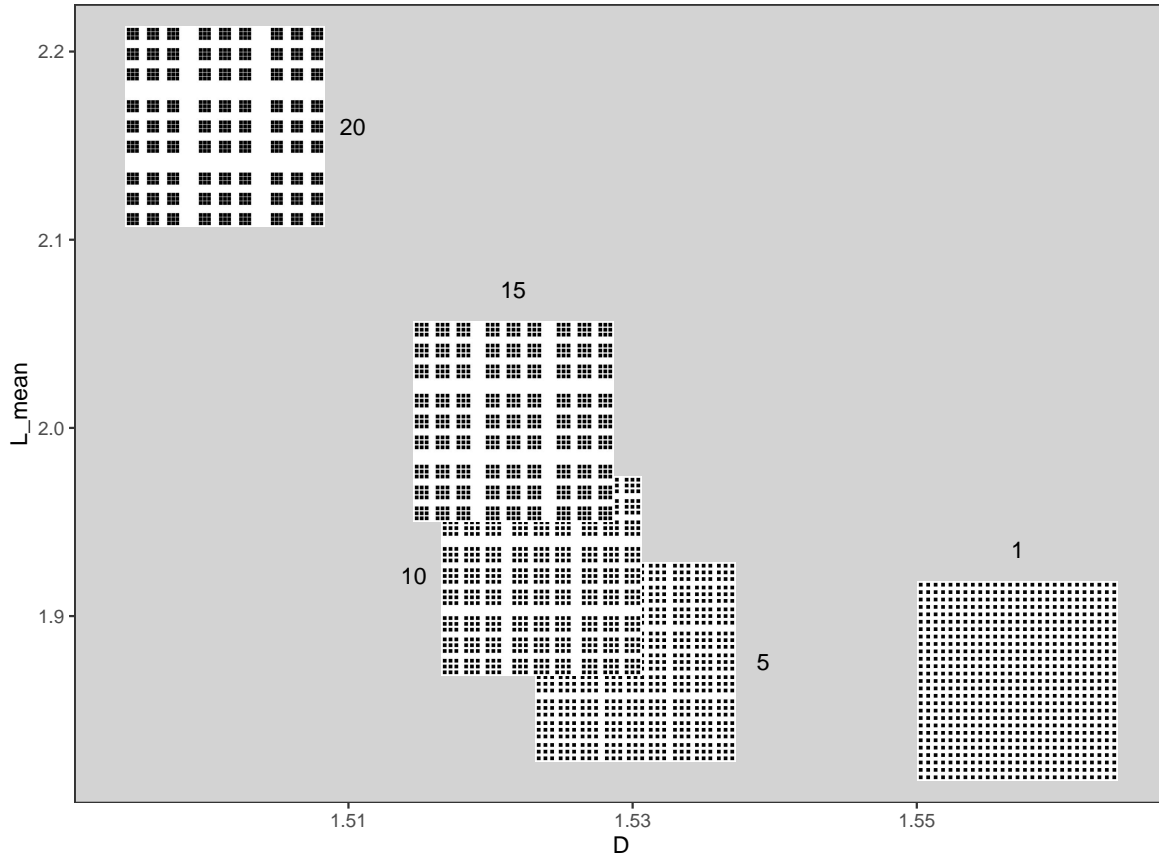


**Figure 8.9:** Fractal dimension and mean lacunarity of images of identical size, layout and density, but with degrees of hierarchical clustering, from no clustering (image 1) to high clustering in two levels, where the space between clusters represent 8% of the superior level's total length and the points start to percolate (image 20). Number labels represent iteration, and images are selected to prevent overlaps

Again, this could be done in a number of ways. In this case, each house was allowed to do an independent random walk with a step length of 2.4 pixel equivalents in one out of 12 circular directions (this caused some greyscaling in the resulting images, but the applied box-counting and gliding-box functions round such values to 0 and 1). Each random-walk step represented one iteration in the series (see Bruvoll, n.d. for a similar approach). An advantage of using square synthetic images for this test rather than simulations of actual settlement plans, is that the effect from such spatial noise can be more easily isolated from density. When elements walk in random directions, some will inevitably walk out and away from the initial pattern, thus decreasing image density no wether the image is extended to include them or not. To solve this issue and making sure that density remained as constant as possible given how it was shown above to influence the resulting estimates, the image size was here kept constant and houses that walked beyond the boundaries were moved across the image to the opposite side. Some decrease in image density was however difficult to avoid given the frequent overlaps

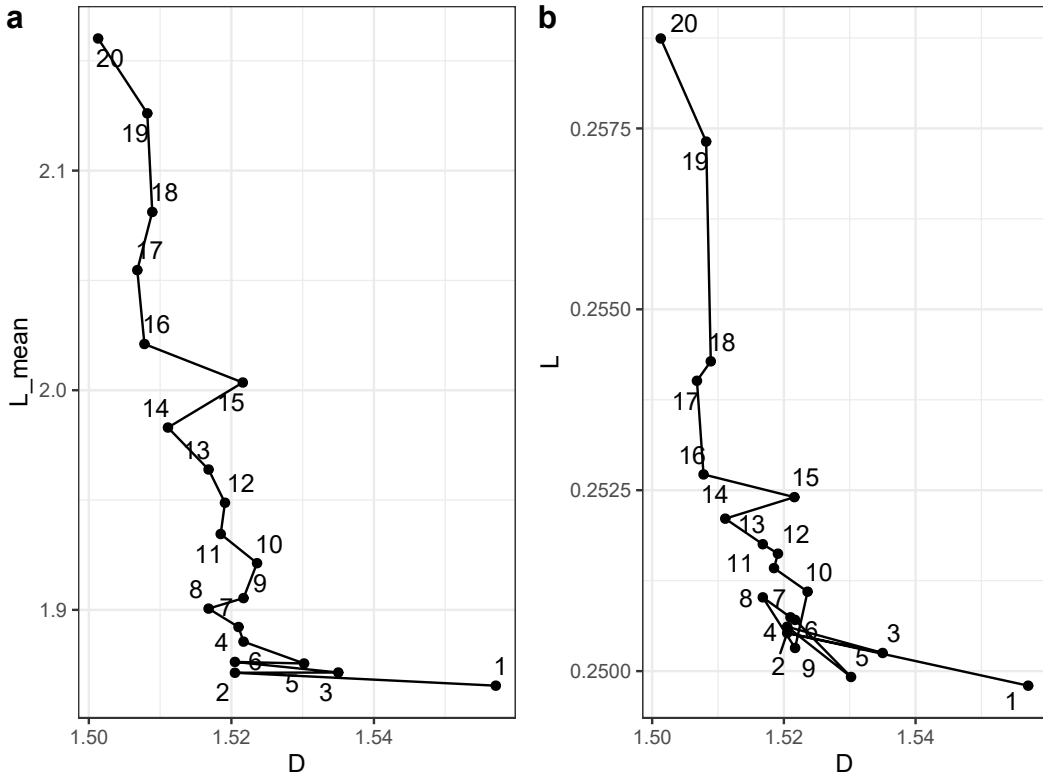


**Figure 8.10:** Fractal dimension and lacunarity measures on the same images with varying degrees of spatial clustering, and fixed image size, density, element count and size distributions. Number labels represent iteration

of the areas of houses that walked very close to each other. As a result, the lowest density in this series extended to 0.232, which is still fairly close to the goal of 0.25. The resulting more or less noisy images in this series thus illustrate the range of possible settlement layouts from one where every house is strictly allotted to a predefined place following a simple geometric grid, to one where houses are constructed completely without any regard to the placement of surrounding houses (Figure 8.11). Neither of these extremes are of course very likely for any real archaeological setting, but it seems obvious that the former case will be more characteristic of societies with strong overarching institutions that regulate everyday life while the latter case is more representative of very loose social ties between independent households and an absence of any overarching decision-making authority. #Ref?

The resulting  $D$  and  $L$  measures from these images follow the same general trajectory as the images with variable clustering and size distribution, with lower fractal dimension and higher lacunarity for each step of added noise (Figure 8.12). The fractal dimension estimates oscillate in a few cases, possibly because of sudden random correspondence between the initial pattern grid and the box sizes used in the calculations. The lacunarity estimates – both the

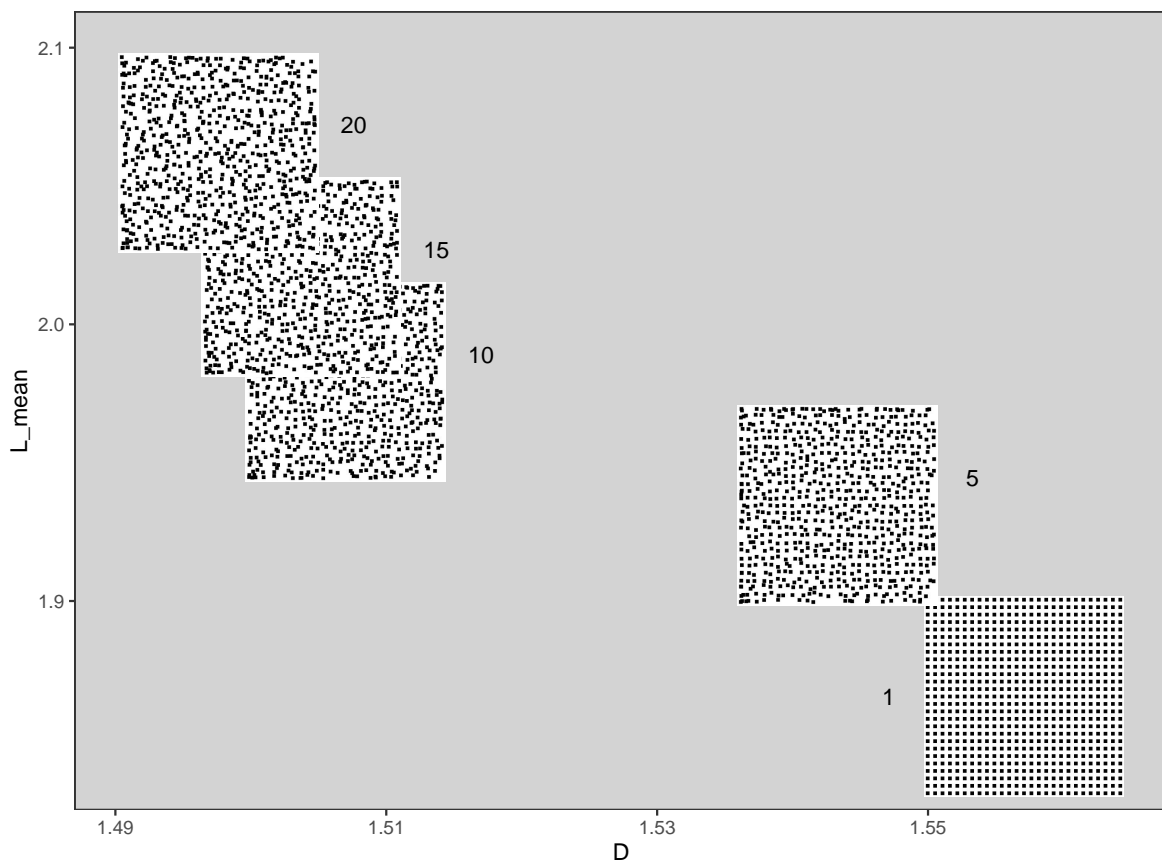


**Figure 8.11:** Different degrees of random spatial noise

mean and the exponent lacunarity – followed very regular increase after the second iteration. Here again, the trend seems sufficiently regular to conclude that random noise is effectively quantified by both fractal dimension and lacunarity, in a similar way to the other changes in pattern presented above.

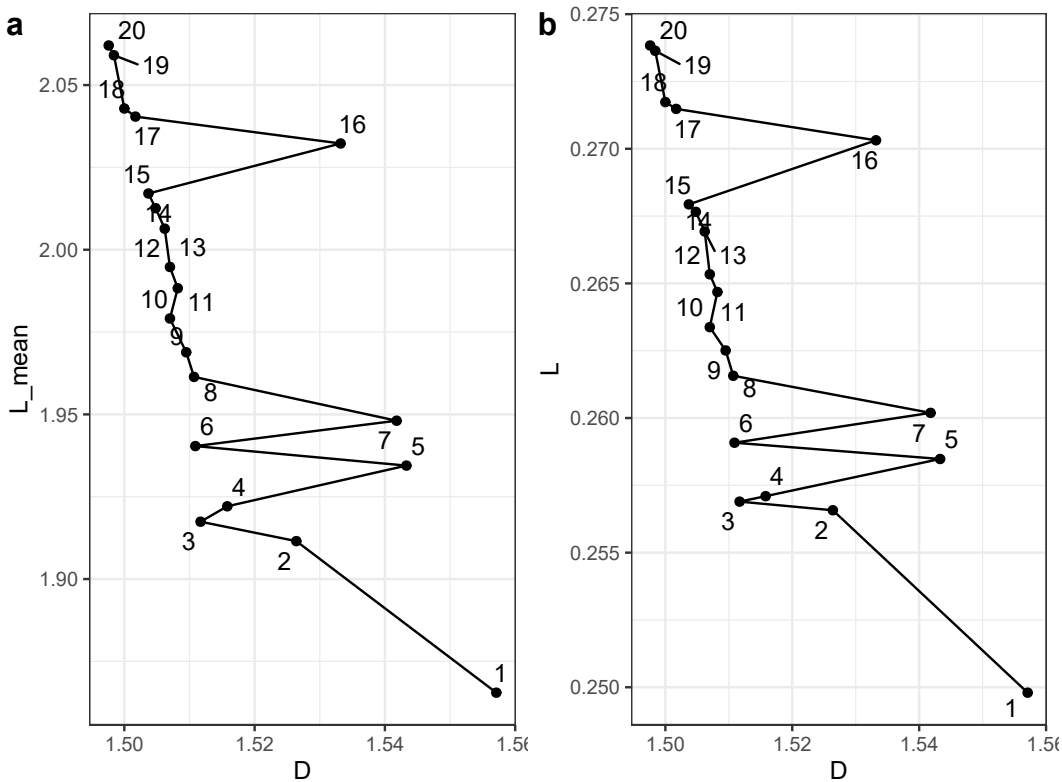


**Figure 8.12:** Estimates of fractal dimension ( $D$ ) and mean lacunarity (plot a) and exponent lacunarity (plot b), of 20 images with increasing degrees of added random spatial noise. Number labels represent iteration

## 8.5 Summary of procedure and tests

Calculations of fractal dimension and lacunarity on synthetically generated test images provide useful clarifications on how these measures respond to changes in some crucial variables. The tests on image series with varying image sizes and zooms on a regular square grid pattern indicate that both  $D$  and  $L$  measures become increasingly inaccurate when estimated on images smaller than about 260\*260 pixels, given the box sizes used here in the analyses. The values were calculated from bi-logarithmic linear fits to results for box sizes ranging from 1 to 512 pixel lengths, where null values were excluded from the fit whenever the analysed images were smaller than the box size. Reducing the maximum box sizes remains a possibility that could allow for more accurate estimates from small images, which again could prove useful whenever run time becomes an issue, since larger images are computationally much heavier to analyse. With the test images analysed here, too small images gave too low fractal dimension estimates, while lacunarity was seemingly less affected (Figure 8.1).

Another requirement for reaching acceptable accuracy in fractal dimension and lacunarity

results, is that the image resolution should seemingly not exceed pixel sizes smaller than about 4% of the side length of the smallest mapped features. Letting pixels be smaller than this (i.e. *higher* image resolution) only adds a false sense of accuracy given that the analysed patterns are not strictly speaking scale independent but rather bound to the scales that are relevant for human agency. A too high resolution thus generates too large void spaces between elements, leading to too high lacunarity values, while fractal dimension in this case remains less affected.

Other variables, which were more related to the visual appearance of the pattern, also gave characteristic results. Size distribution of pattern elements, level of hierarchical clustering and random spatial noise all affected  $D$  and  $L$  measures in a similar way, in that larger deviations from homogeneity drew the former values down and the latter up in a consistent way. Density on the other hand, had a different effect on  $D$  and  $L$  estimates in two ways. Firstly, increased image density gave consistently *higher* fractal dimension and *lower* lacunarity values, and secondly – though the intensity of the different variables are difficult to compare – the effect from density appeared here as much stronger than that of the others. Figures 8.13 and 8.14 illustrate how a minor adjustment in image density made more difference in both fractal dimension and lacunarity than the whole range of variation in noise, clustering and size distribution. One caveat here though, is that these variables are often in practice combined in empirical settlement plans – there is usually both some level of clustering, noise and inequality in sizes – and it remains unknown whether these factors combined give stronger signals compared to that of density. In any case, it seems clear that image density must be taken into consideration when interpreting the layout of settlement plans from their fractal dimension and/or lacunarity.

From the results presented above, another trait seemed characteristic of the link between density, fractal dimension and lacunarity. All other things being equal, density was exponentially correlated to both  $D$  and  $L$ , and power-law correlated to  $L_{mean}$  (Figure 8.6). In fact, for a regular square grid pattern with given density, these fractal analysis measures can seemingly be very well predicted with simple linear models on log-transformed density (Table 8.1). These models can be used tentatively to compare  $D$  and  $L$  values of images with varying density, by first subtracting the values expected from density alone. However, it must again be stressed such an analysis probably is premature at this stage, since several factors remain unaccounted for. For example, regarding the Neolithic settlement plans compared in the next chapter, the

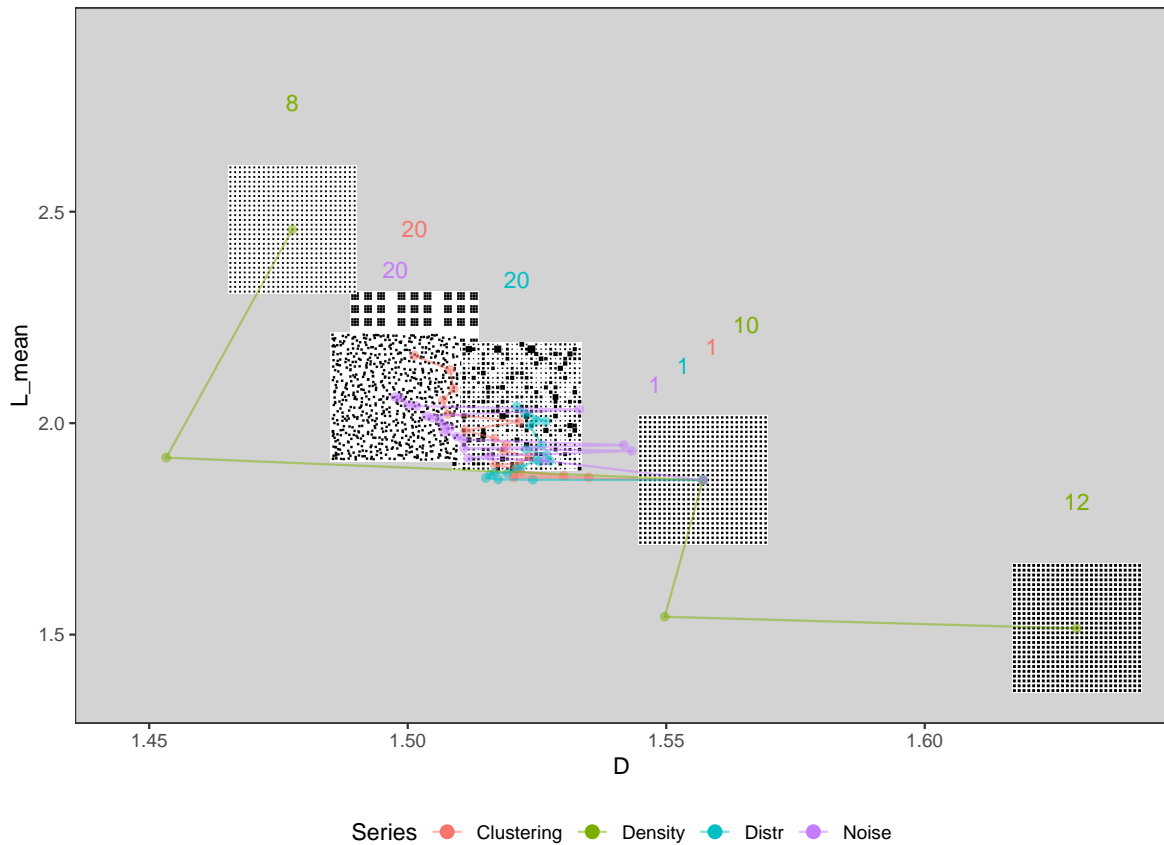


**Figure 8.13:** The first and last images of the clustering, size distribution and noise series, as well as images 8, 10 and 12 of the density series, showing how only small increments in density – here from 0.16 (im. 8) to 0.36 (im. 12) – generate changes in fractal dimension and lacunarity that are larger than those induced by the whole range of the other variables. Density image 10 is identical to image 1 of the three other series, and has density value 0.25

effects on  $D$  and  $L$  from different settlement layouts remain untested (the standard Trypillia layout is radial and not a grid). Also, effects from size distribution, clustering and noise have only been evaluated here at a single given density value, and these may behave very differently at other density levels. As mentioned, these factors are usually mixed to some extent and may have cocktail effects that for now remain unstudied. In empirical settings grid orientation and edge effects quickly become issues of their own that are also not further investigated here.

Lastly, in this chapter I have largely opted for presenting results for both exponent lacunarity (here denoted simply  $L$ ) and mean lacunarity ( $L_{mean}$ ), since both are found in the literature as summary measures of lacunarity, but not always with explicit mention of what they represent mathematically (Fariás-Pelayo, 2015; as in Fariás-Pelayo, 2017). The results here show that they are largely equivalent, a part from the differing value ranges. For two image series – varying image size and house size (Figure 8.2), and varying house size and house

**Table 8.1:** Linear models of fractal dimension (D), exponent lacunarity (L) and mean lacunarity ( $L_{\text{mean}}$ ) with the log-transformations that give the best fit, evaluated by the coefficient of determination ( $R^2$ ). The third model can be written in power-law form as  $L_{\text{mean}} = 0.862 * \text{density}^{-0.61}$

Model	coeff.
$D = 0.188 * \log(\text{density}) + 1.792$	0.931
$L = -0.166 * \log(\text{density}) + 0.008$	0.994
$\log(L_{\text{mean}}) = -0.610 * \log(\text{density}) - 0.148$	0.995

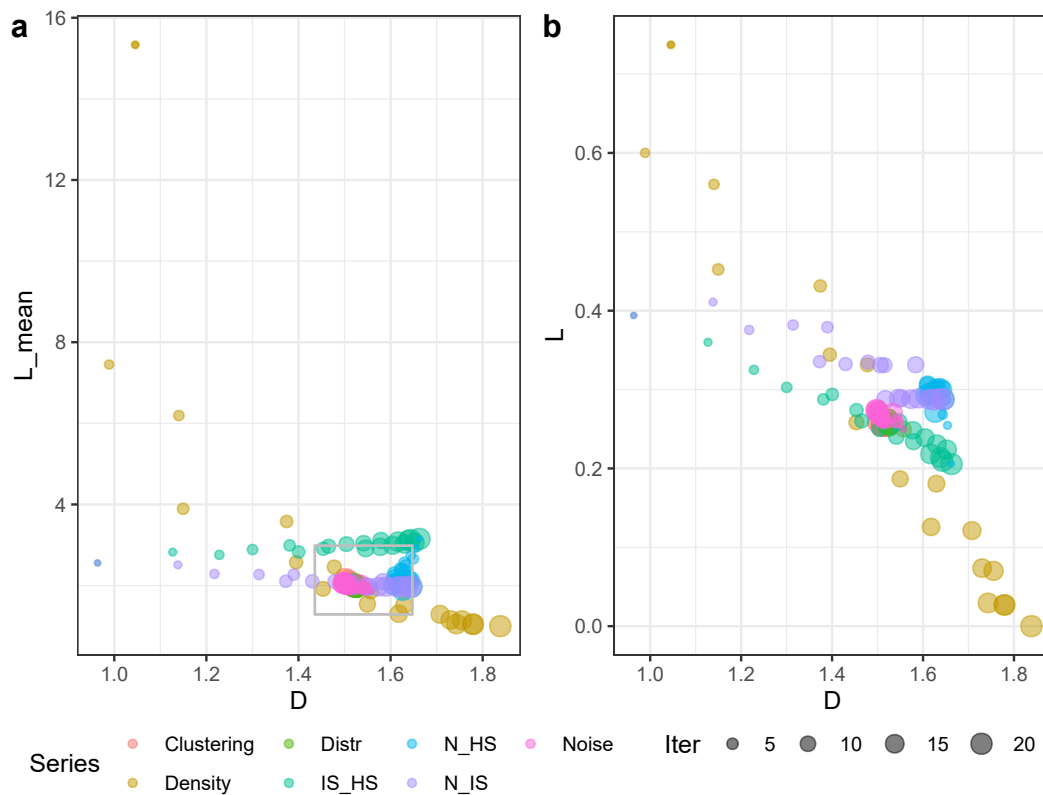


**Figure 8.14:** Fractal dimension and lacunarity estimates of all synthetic images analysed in this chapter.  $L_{\text{mean}}$  and L show largely similar distributions but with some marked differences. See text for details. The grey frame in plot a shows the extent of Figure 8.13

count (Figure 8.4) – the results followed similar but reverse trajectories, without any obvious reason. And for density, as mentioned,  $L_{mean}$  was power-law correlated while  $L$  was only exponentially correlated (Figure 8.6). I have elsewhere shown how prefactor lacunarity is very closely correlated to mean lacunarity, arguing that these two are practically linearly equivalent (Bruvoll, n.d.; see also Karperien, 2013). While studies in various fields refrain from using summary measures of lacunarity at all, preferring to rather show the full distribution of lacunarity to box sizes (e.g. in ecology, see Hingee et al., 2019), my impression here is that any of these summary measures may be used, as long as it remains clear which one it is. This relative equivalence being demonstrated, and for ease of presentation, in the following chapter I will largely focus on mean lacunarity values, while exponent and prefactor lacunarity values are given in the full data table in #ref appendix.

In the following chapter, the same methods of analysis are applied to images of archaeological settlement plans, in series consisting of total settlement plans, single quarters/neighbourhoods and temporally coeval sub-samples. The goal is then primarily to investigate how they perform with real archaeological spatial data, and to which extent they quantify different spatial layouts and textures that can be interpreted in terms of social organisation.

END Chapter



# Chapter 9

## Results: Image analysis

The same Neolithic settlements that were analysed in Chapter 6 were here analysed with image renderings of their plans following the procedure presented in Section 8.1. Resulting estimates of fractal dimension and lacunarity (summarised by power-law exponent and mean) are shown for all images in Figure 9.1. The spread of results in the scatter plot is very similar to that of the synthetic images analysed in the previous chapter (Figure 8.14), with a strong linear correlation between  $D$  and  $L$ , and exponential correlation between  $D$  and  $L_{mean}$ . Fractal dimension estimates are however much lower and lacunarity estimates are higher for the empirical settlement plans than for the synthetic ones, possibly resulting from the generally lower image densities (see Appendix ref(add ref) for the complete results). Settlements with higher house counts are also consistently situated towards the lower right of the plot, while the temporal samples of Vráble, with fewer houses and large voids between them, fall towards the upper left. The image of Vráble 1, showing only a single house, is a clear outlier. It also violates the minimal image size prerequisite suggested previously, and will be excluded from the further analysis. The clear separation between the temporally coeval and the cumulative settlement plans illustrates how these are not easily comparable, which is a very common problem in archaeology. It shows how crucial it is to take into consideration the temporal resolution of the data both when formulating research questions and when interpreting results [#ref with pages, perrault]. In the following, the results are further discussed by image series, starting with whole settlements, followed by quarters and neighbourhoods for Nebelivka and Vráble, and lastly by temporal samples for Vráble. The results presented in this chapter are also partially presented in Bruvoll (n.d.).

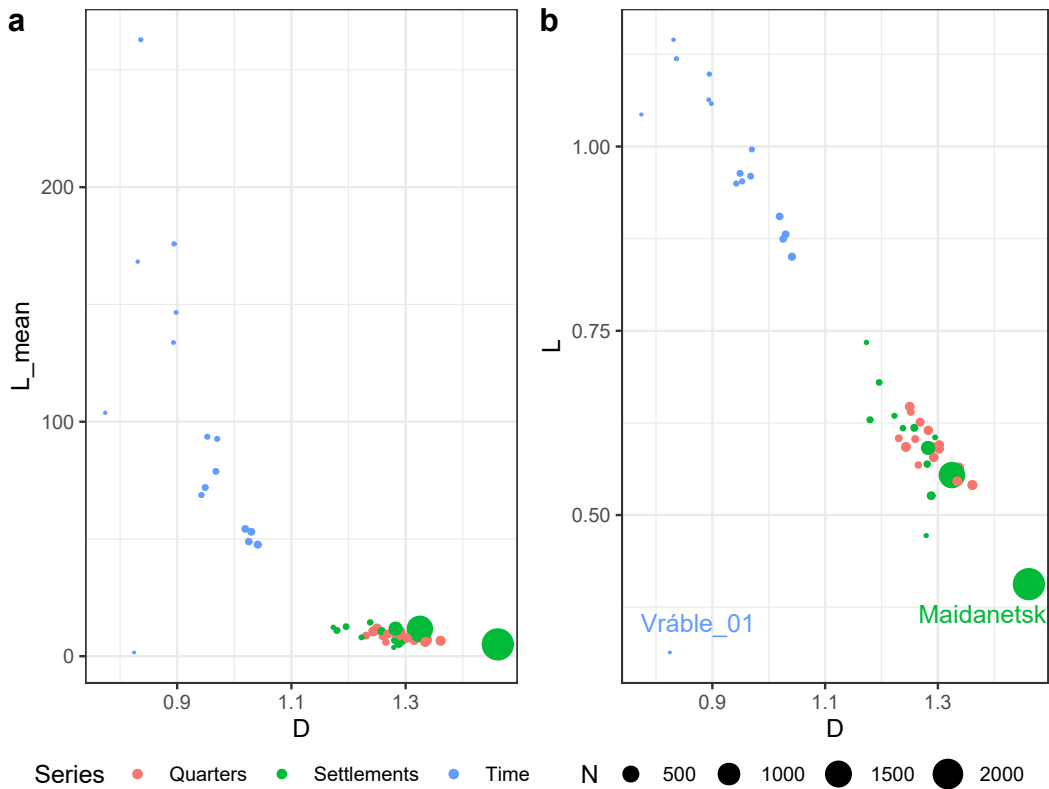


**Figure 9.1:** Fractal dimension and mean lacunarity (plot a) and exponent lacunarity (plot b) for all 46 images analysed in this chapter. Values are presented as a data table in Appendix #add ref

## 9.1 Settlements

Fractal dimension and mean lacunarity of the plans of whole settlements are shown in Figure 9.2a. Lacunarity values divide the images into two distinct groups, cross-cutting cultural adherence, while dimension values seem closely correlated to settlement size (proxied through house count  $N$ ). The plot can to some extent be reproduced directly by replacing  $D$  with  $N$  and  $L_{mean}$  with density, also setting both axes in logarithmic scales and reversing the y axis (Figure 9.2b). In this image series, the small Linear Pottery settlement of Horný Oháj and the Trypillia settlement of Talne 3 had image sizes that were below the threshold proposed in the previous chapter, meaning that their fractal dimensions are possibly underestimated. When comparing these values to the visual appearance of the settlement plans, at least for the Linear Pottery settlements it seems clear that the upper group of settlements (those with high lacunarity values) are subdivided into more or less separate neighbourhoods with open spaces between them, i.e. more clustered, while the lower group – specifically Nevidzany and Čierne – only consist of one more dense and regular grid-like layout (Figure 9.3). For the two Trypillia mega-sites, Nebelivka and Maidanetske, this separation is somewhat less obvious,

since they both follow the characteristic radial layout. Nebelivka does arguably have more open space between quarters than Maidanetske, which in turn is more homogeneously “filled”, and the higher overall density of the latter (0.084 to 0.031 of Nebelivka) may contribute to its higher fractal dimension. The smaller circular settlement of Moshuriv is also highly regular in its distribution of open spaces, leading to lower lacunarity.

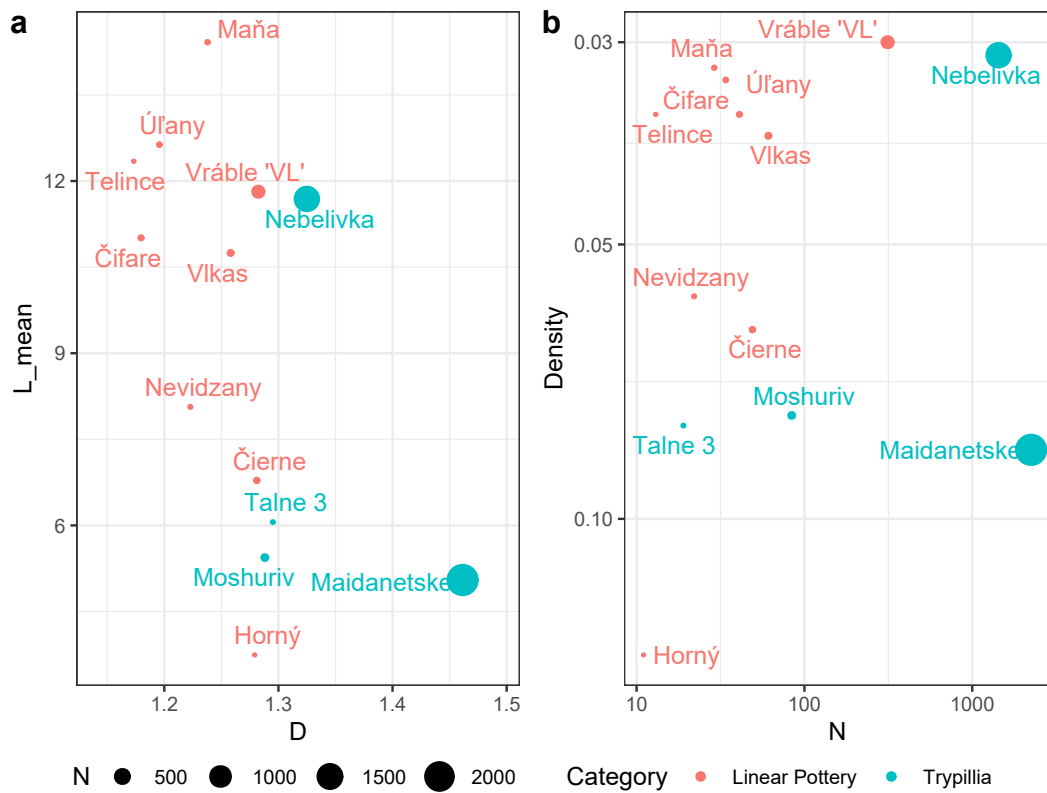


**Figure 9.2:** Settlements plans quantified through their fractal dimension ( $D$ ) and mean lacunarity ( $L_{\text{mean}}$ , plot a) and house count ( $N$ ) and density (plot b). In plot b, scales are logarithmic, and the y axis is reversed, in order to obtain as similar results as possible to those shown in plot a. The settlements of Talne 3 and Horný Oháj had images that were smaller than the lower threshold proposed in the previous chapter

The models formulated in the preceding chapter for  $D$ ,  $L$  and  $L_{\text{mean}}$  as functions of density on regular grids (Table #add ref) were tentatively applied to these results, and the residuals – i.e. the differences between the modelled and the empirical values for each image – are shown on Figure 9.4. The residual values do not show actual values of  $D$  and  $L$ , ( $D$  values are below 1 and close to 0) but value points of how much the empirical values differ from the modelled ones. The plot thus gives an idea of fractal dimension and lacunarity estimates that could be obtained for these settlement plans if they all had the same density. However, as already mentioned, these results are only illustrative, since the analysis does not take into account a number of relevant factors, like the different layout concepts differentiating Trypillia and

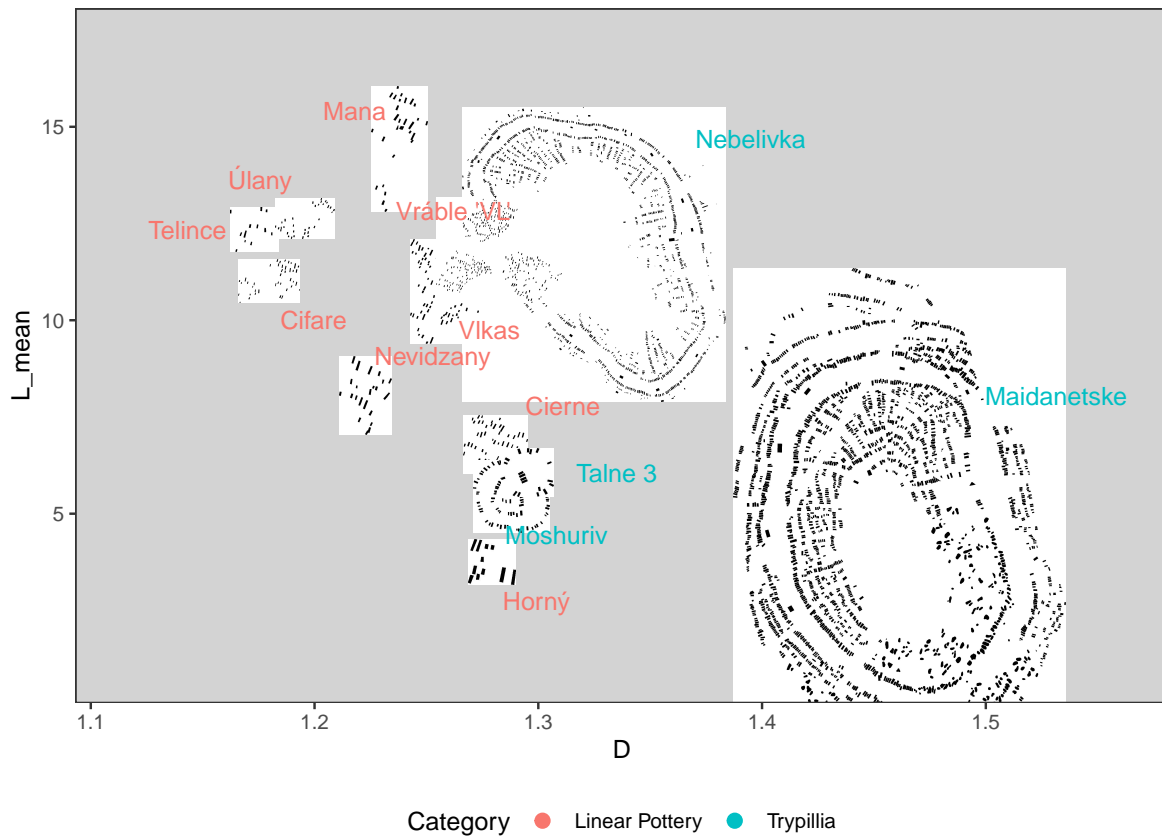


**Figure 9.3:** Plans of the same settlements, plotted by D and L\_mean. Image sizes are not internally to scale – size differences are reduced to facilitate readability, as the mega-sites are in reality orders of magnitude larger than the smallest ones

Linear Pottery settlement plans. The resulting scatter plot shows similarities to both plots in Figure 9.2. The differentiation by lacunarity between clustered and less clustered settlements is maintained, while fractal dimension separates the three largest settlements – the two Trypillia mega-sites as well as Vráble – more clearly from the remainder. These were also the ones showing the clearest power-law distributions of house sizes in Chapter 6. In the synthetic images analysed earlier, clustering, noise and unequal size distributions resulted in lower fractal dimension for images with the same density, while here almost all settlements have *higher* dimension than what would be expected from a regular grid with the same density. Comparing the values in relative rather than absolute terms, and following the conclusions from the analysis on synthetic images, the three largest settlements here could be interpreted as being overall more regular, less clustered and noisy (though with more unequal size distributions) than the other settlements. Since fractal dimension here is seemingly correlated to settlement size, it could also be that the effects from noise, clustering and size distribution be weaker relative to the overall plan, though this effect does not appear on the results for lacunarity.

Any attempt of interpreting these results in terms of social organisation is not self-evident. However, some points can be made. Firstly, it is clear that fractal dimension and lacunarity are not sufficient for distinguishing Trypillia and Linear Pottery settlement plans quantitatively. Neolithic specialists may find this result disappointing, pointing to the visually very obvious difference between grid and radial layouts. On the other hand, it could be objected that these cultures do share concepts in spatial organisation that are quite close – houses are largely free-standing, often organised in rows, and overall densities are similar – and it remains quite possible that these methods could distinguish more easily between more differentiated plans like early Neolithic Anatolian villages, Alpine wetland sites or Bronze or Iron Age semi-urban or urban settlements. Secondly, the results do seem to differentiate effectively between clustered and non- (or at least less) clustered settlements, which again points to the social coherence within the settlement. Villages that are clearly clustered into separate neighbourhoods may show signs of higher levels of inter-group competition and potentially violent tensions, as seen in the skeletal material at Vráble. Contrarily to the results obtained from synthetic images, household inequality proxied through house sizes seems not to be effectively reflected in fractal dimension nor lacunarity, since the settlements that previously have been shown to exhibit the highest levels of inequality also have the highest fractal dimension values, especially when controlled for effects from density. Expected effects from size distribution as well as spatial noise probably drowned from the size of the largest settlements. More sophisticated modelling could possibly also control for a larger range of disturbing factors such as image size, house count, grid orientations etc. Lastly, even though the quantitative distinction between clustered and non-clustered settlements is interesting, the results obtained here (Figures 9.2a and 9.4) are not substantially better than those that could be obtained more directly through house count and density (Figure 9.2b), which are far easier to calculate.

## 9.2 Quarters/neighbourhoods

The quarters of Nebelivka and the neighbourhoods of Vráble were analysed in the same way, and their fractal dimension and lacunarity estimates are shown in Figure 9.5a, while for comparison, house count and image density are shown on Figure 9.5b. For this image series, the spread of estimates was rather moderate, and again no clear distinction was observed between Linear Pottery and Trypillia layouts, even though they are visually organised in strikingly dif-

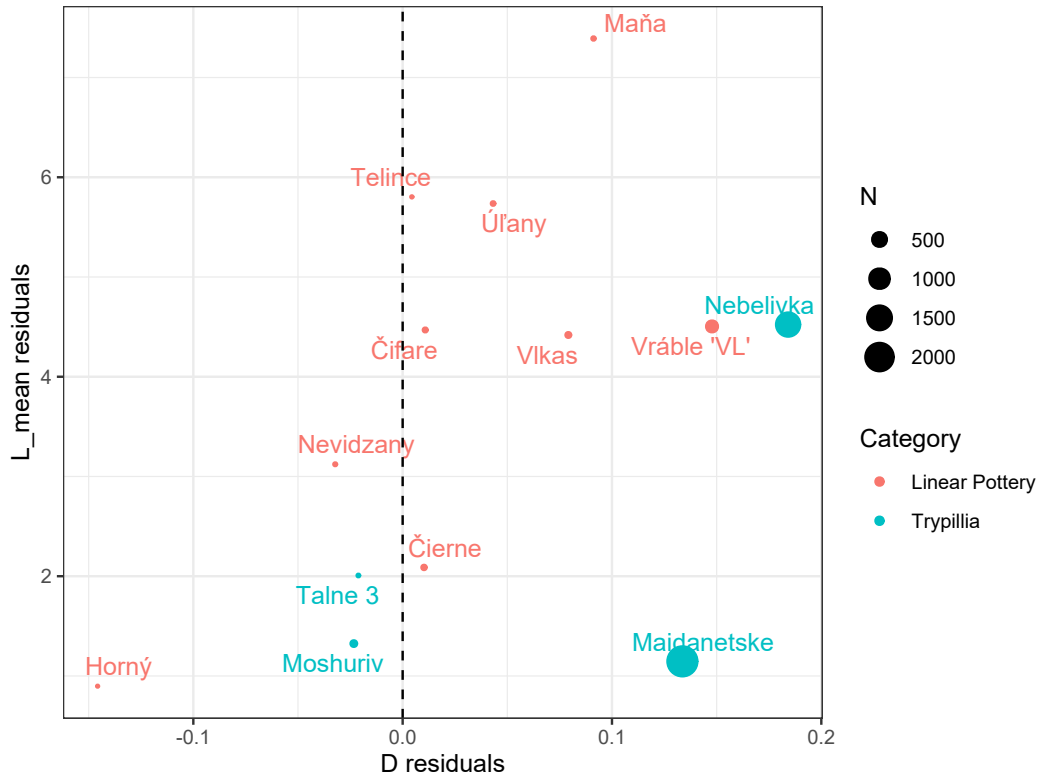


**Figure 9.4:** D and L\_mean residuals for the same settlements after subtracting expected values due to image density alone, modelled on the synthetic images with variable density presented in Chapter 8. See #table for details

ferent ways (Figure 9.6). For both settlements, there was no clear partition of sections into separate groups – rather, the whole series formed a continuous spread across the plot. It is clear that density was correlated to lacunarity for these images, since the relative order of images on the y-axis is nearly the same in plots a and b of Figure 9.5. However, fractal dimension was in this case less obviously correlated to house count than for the total settlement plans – or, this correlation had a lesser effect since the various quarters and neighbourhoods were of more uniform sizes (both by image size and house count).

If some distinction is still to be made between images on opposite ends of the scatter plot, for both settlements the most compact sections were plotted towards the lower right end of the plot, while the most patchy or stretched-out images were towards the upper left. For example, quarters L, F, D and G at Nebeliyka are all dominated by inner more or less parallel streets, and have relatively high D and low L\_mean values, while quarters N, A and K are more patchy or dusty – one could even say lacunar – and are evaluated to correspondingly low D and high L\_mean values. Interestingly, the results here do seem to reflect those obtained from the distribution fitting analysis in Chapter 6, where quarters N and A were judged as

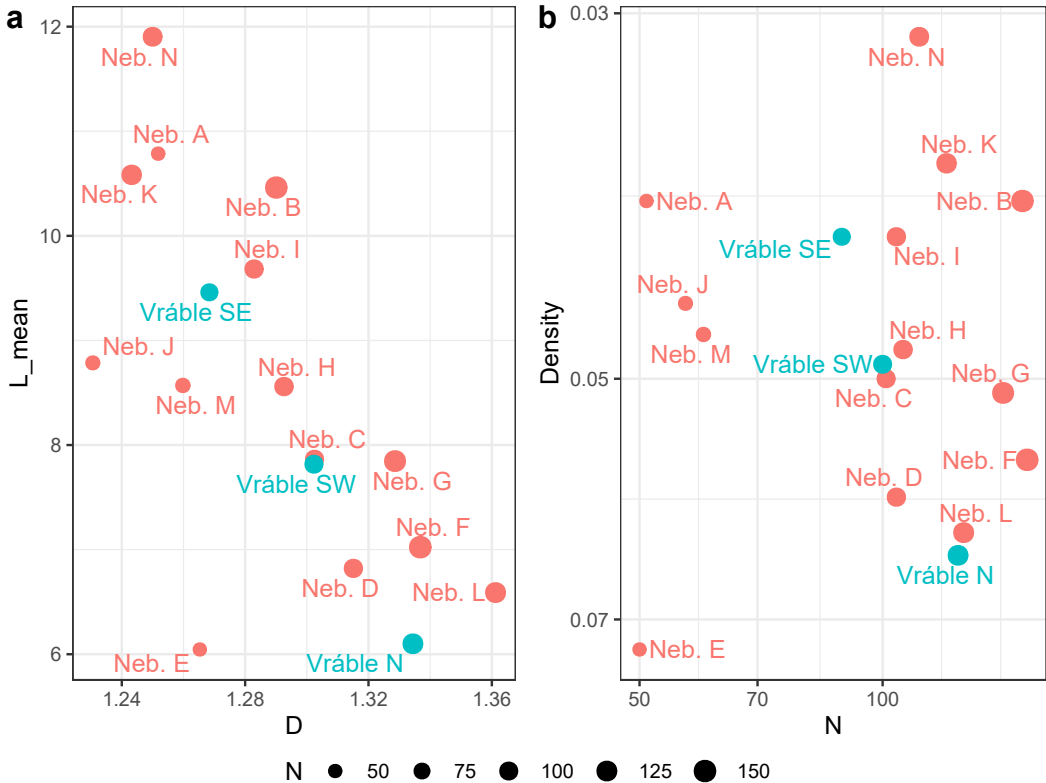


**Figure 9.5:** Fractal dimension (D) and mean lacunarity (L\_mean, plot a) and house count (N) and density (plot b) of the plans of separate Nebelivka quarters and Vráble neighbourhoods. The image size of Nebelivka E was below the lower threshold of 260\*260 pixels. Axes in plot b are logarithmic, with the y-axis reversed, in order to reproduce the spread in plot a

suffering from missing data (notably lacking Assembly Houses). Quarters K and J, which here have the lowest fractal dimension values, were there interpreted as having quarter borders erroneously drawn by the researchers – in any case their outlines are irregular compared to the other quarters. Quarter E was also speculated to be wrongly interpreted as a separate quarter, causing it to “lack” the power-law distribution of house sizes which characterised the other quarters. Here, quarter E is an outlier regarding both fractal dimension and lacunarity, but the analysed image is also the only one falling below the size threshold of 260\*260 pixels previously proposed. Taking these methodological caveats into account, it would seem the Nebelivka quarters had an even smaller spread in fractal dimension and lacunarity, since all the quarters with the most atypical values can seemingly be explained away as non-representative of their original layouts. Despite this, the observation still holds, that quarters dominated by dense inner street grids are placed to the lower right of the plot, while those dominated by the open main street are to the upper left.

For Vráble, the three neighbourhoods also show similar results, with differences being ap-

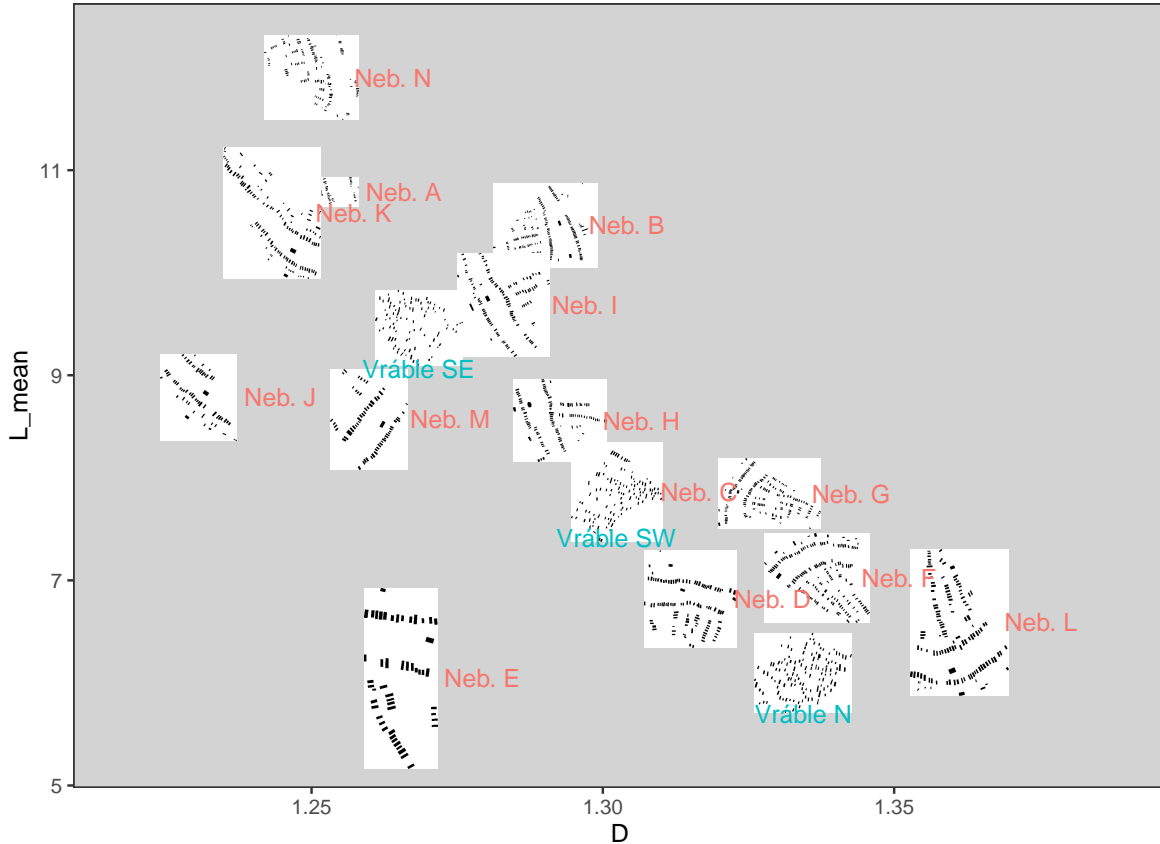


**Figure 9.6:** Plans of Nebelivka quarters and Vráble neighbourhoods, placed according to fractal dimension ( $D$ ) and mean lacunarity ( $L_{mean}$ ). Image sizes are transformed to allow for better visibility of smaller images. The two layout types representative of Trypillia (Nebelivka) and Linear Pottery (Vráble) settlements largely overlap

parently gradual rather than categorical. Also here, the image with the most densely packed and grid-like layout – the northern neighbourhood – also had the highest  $D$  and the lowest  $L_{mean}$ , and inversely for the most patchy image of Vráble South-East. This latter neighbourhood was also the one of the three that was shown to not have a power-law tail to its house-size distribution in Chapter 6, similarly to Nebelivka quarter N. However, the perhaps most surprising result from analysing this series, is that these rather subtle differences in plan regularity had a greater effect on the fractal dimension and lacunarity estimates than the more obvious differences in layout between Linear Pottery and Trypillia settlements. Again, it should be worthwhile to test these analyses on other and more different data sets, to see whether they capture other types of layout differences more accurately.

Lastly, when  $D$  and  $L_{mean}$  estimates are controlled for effects from density, as was done with whole settlements above, residual  $D$  values become somewhat more randomly distributed, while lacunarity remains more unaffected (Figure 9.7). Even though the caveats already men-

tioned for this modelling must be repeated here, it would thus seem that there is very little to no significant difference between quarters and neighbourhoods in these two large settlements, further suggesting that there is no noticeable intra-site socio-economic differentiation either, which is in agreement with current understanding of Linear Pottery and Trypillia social organisation (see Chapter 3). Further analysis on more recent settlements (e.g. Bronze Age tell settlements or Iron Age *oppida*) could potentially contribute to our understanding of when such intra-site differentiation first became important factors for urban or semi-urban life.

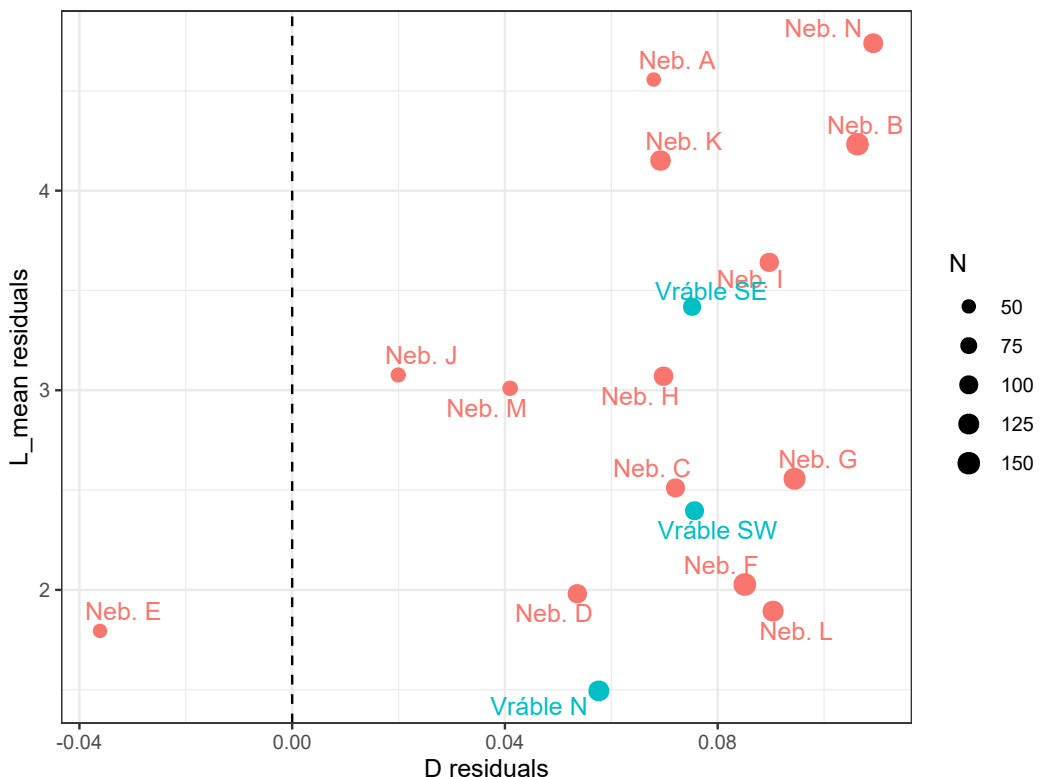


**Figure 9.7:** Fractal dimension and mean lacunarity estimate residuals after controlling for effects from density, on the same quarter and neighbourhood images. Values expected from density are modelled on the density series of synthetic images in the previous chapter, see #table

## 9.3 Temporal samples (Vráble)

The partitioning of the Vráble settlement plan into 16 coeval plans separated in time by 20 year intervals was done following the same procedure as in Chapter 6, and an image for each plan was generated, setting the image size to the minimal x and y extent, as with the total settlement and quarter images analysed above. As before, the first time sample consisted of a single house, which by any standards would not be representative of a settlement plan, and

for the purpose of this analysis was excluded for having a too small image size (its deviating results are shown on Figure 9.1). Samples two and 16, representing Vráble at 5270 and 4990 BCE according to the model, were different in that they only included houses from two of the three neighbourhoods, resulting in relatively smaller image sizes, while all the remaining images included houses from all three neighbourhoods and thus had similar sizes. Thus, as the village grew over time and subsequently declined, it follows that it effectively also densified until its peak around 5110 before thinning out again until its abandonment. Given how image density was already shown to be determinant of an image's fractal dimension and lacunarity estimated by box-counting and gliding-box algorithms, and since in this case image density would be furthermore highly dependent on house count, it is not surprising that  $D$  and  $L$  results of these images can be largely predicted by density and  $N$  (Figure 9.8).

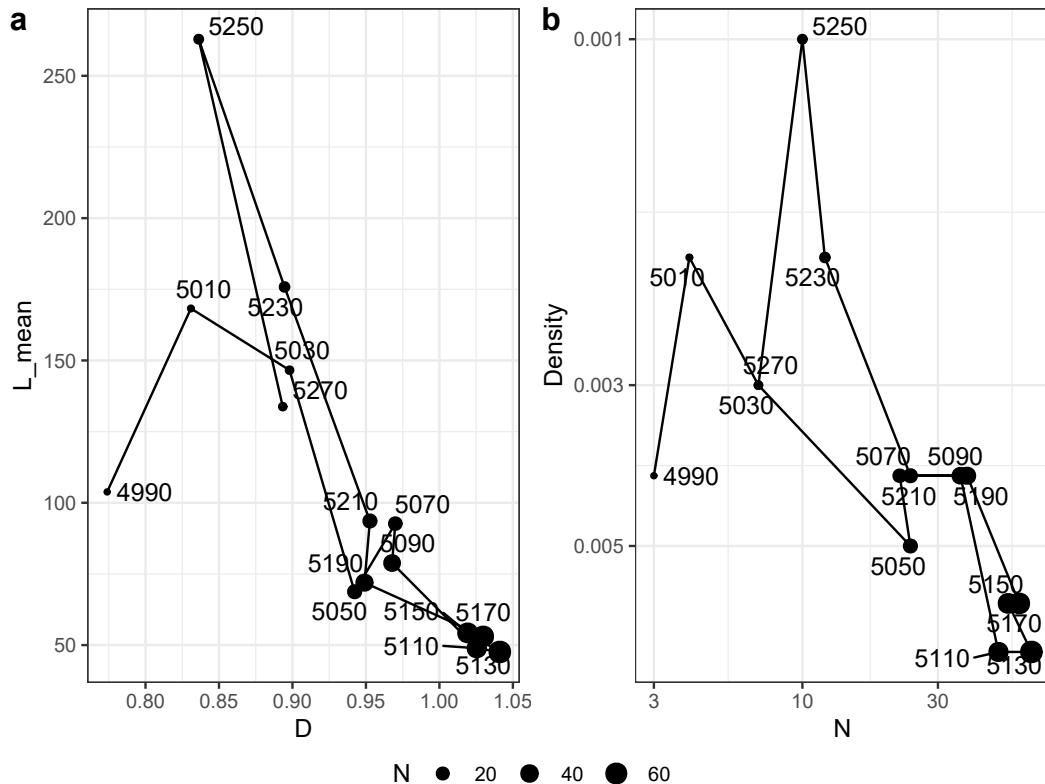


**Figure 9.8:** Fractal dimension ( $D$ ) and mean lacunarity ( $L_{\text{mean}}$ , plot a) and house count ( $N$ ) and image density (plot b) of the site plan of the Linear Pottery settlement of Vráble, subset into 15 coeval time samples with 20 year intervals. Axes in plot b are logarithmic and with reversed y axis in order to emulate plot a

While the fractal dimension and lacunarity results of these images are inversely proportional, in accordance with the results of the previously analysed series, it is then not clear if they simply reflect this temporal trend of density or add any other information on grid regularity or clustering (the house-size distribution was shown in Chapter 6 to be stable over time in

Vráble). However, when looking at the visual aspects of the different images, the first and last few images of the series among those that include houses from all neighbourhoods – i.e. samples 3, 4, 14 and 15 (representing model years 5250, 5230, 5030 and 5010 BCE) – do not exhibit the clear clustering into three neighbourhoods seen in the middle phases of the settlement (Figure ??, all images are included in #Appendix ref). These are also the images that get exceedingly high lacunarity values.

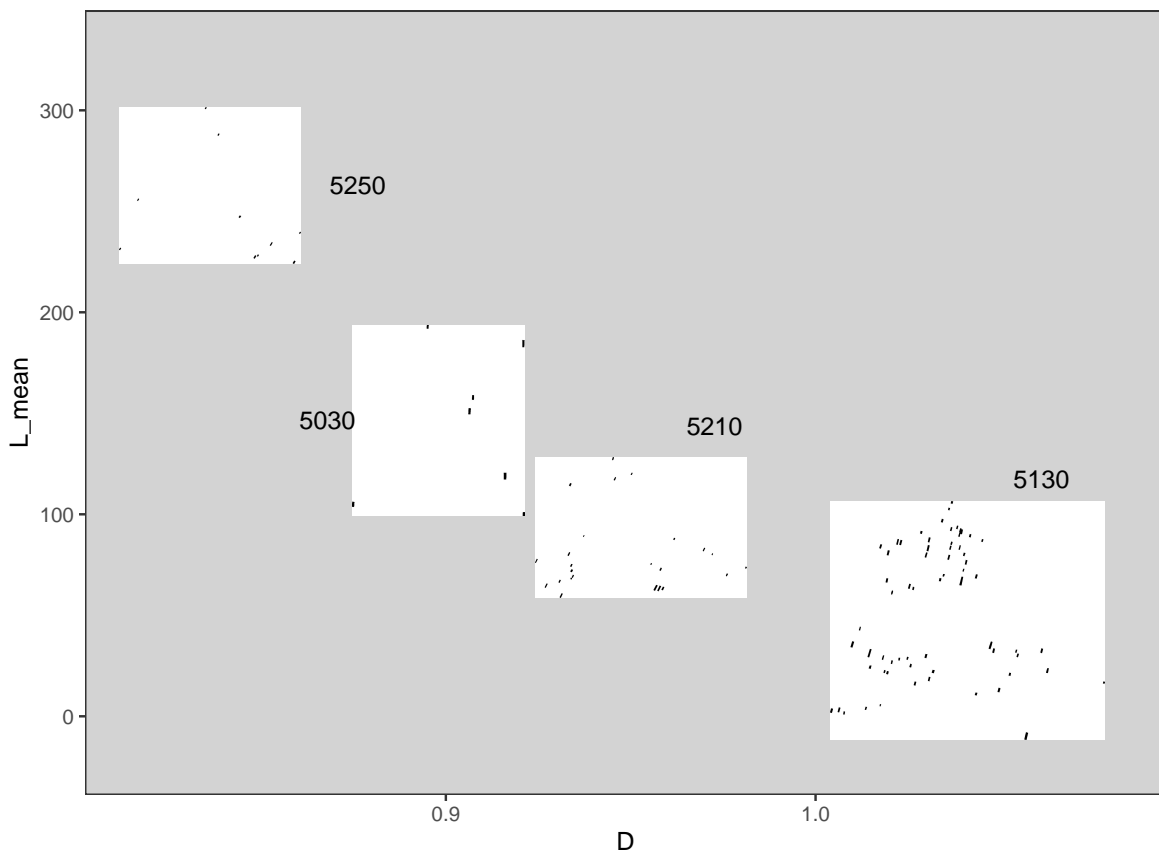


**Figure 9.9:** The temporal development of Vráble (Linear Pottery), as seen through the fractal dimension ( $D$ ) and mean lacunarity ( $L\_mean$ ) of coeval samples of its settlement plan. Images are selected here to prevent overlaps

When subtracting  $D$  and  $L\_mean$  values following the models that were made on synthetic images with varying density (in #Table),  $D$  residuals show no clear pattern besides a seemingly random (normal) spread around a mean of 0.19, i.e. a slightly higher value than would be expected from a perfectly regular grid (Figure 9.10). Residual values of  $L\_mean$  on the other hand do still show some spread for the same deviating time samples, possibly indicating that lacunarity in this case captures the crystallisation of three distinct neighbourhoods in the settlement between approximately 5210 and 5050 BCE. If this were to be interpreted as a higher level of clustering in the middle phases however, from the experimental results

in the previous chapter we should expect higher rather than lower lacunarity in these phases. Another way of looking at it is to remark that the distribution of gap sizes becomes more equal with increased clustering in the middle phases of Vráble because of the overall densification, while in the synthetic images clustering was generated with increased gap differences (Figure 8.9). Such apparently trivial differences in how clustering is generated may thus seemingly determine the direction of change in lacunarity values, illustrating once again the difficulty of interpreting this variable directly. But again, these results are to be taken with a particular pinch of salt, considering the many uncertainties (house orientation as proxy for construction date, modelled house duration,  $D$  and  $L$  values modelled from density of regular grid images) that had to be accepted in order to generate them.

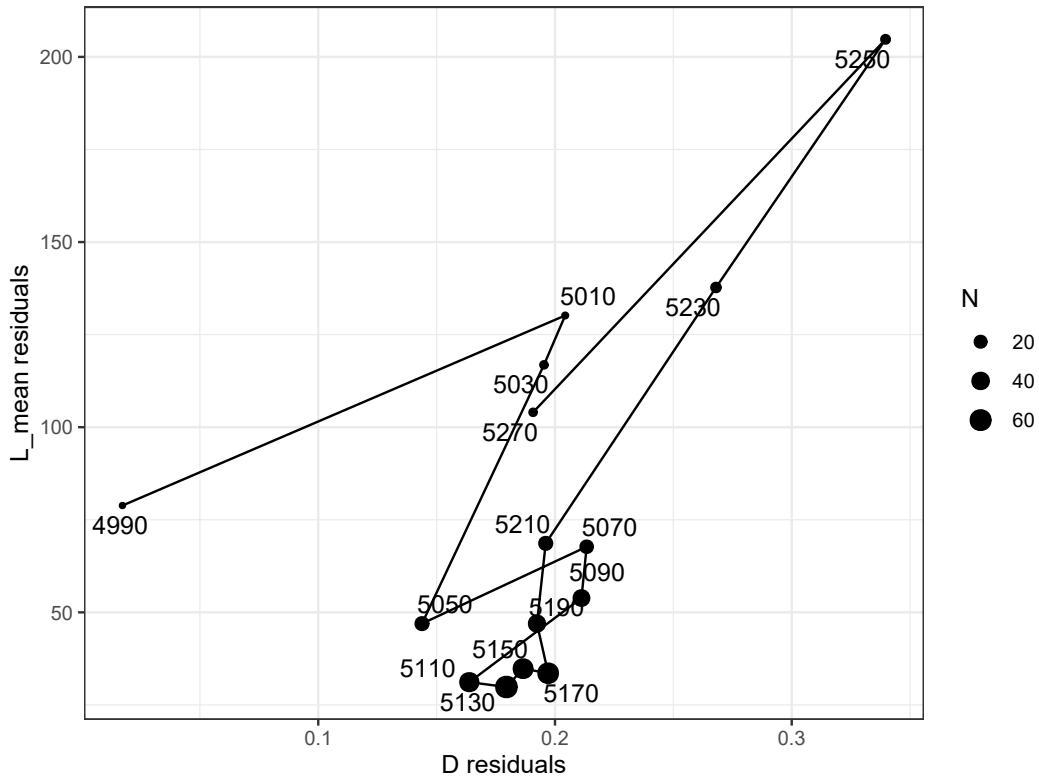


**Figure 9.10:** Fractal dimension and mean lacunarity residuals after controlling for effects from image density, following the models presented in #Tab. in the previous chapter.

## 9.4 Summary of findings

In this chapter, fractal dimension and mean lacunarity estimates were calculated by the box-counting and gliding-box methods on binary images of the 13 settlements, 17 single quarters/neighbourhoods and 16 time samples analysed in Chapter 6, in total 46 images. The

results for all three series were shown to be strongly correlated to other known variables like image size, house count and density, as expected from the tests on synthetic images, and the scatter plots of  $D$  and  $L\_mean$  could in all three cases be largely emulated by plotting  $N$  (house count, as proxy of settlement and image size) and density on logarithmic scales. The goal of this analysis being to quantify and compare different levels of spatial irregularity and clustering between these plans, the question must then be asked whether fractal analysis in the end brought any more insights than what could be obtained much more easily – both with far less code and far shorter computing time – through other and more direct variables. The patterns that were seen in fractal dimension and, especially, lacunarity results also persisted when modelling away the effects that would be expected from the variation in density between images, and it may seem that while lacunarity and density do not measure the exact same things, they are in practice also correlated, so that the plans that show higher lacunarity also consistently show lower density. These variables are thus difficult to separate analytically in empirical data.

The results for the image series of cumulative settlement plans gave an apparent partitioning by lacunarity into two groups of settlements which cross-cut size categories as well as cultural adherence (Figures 9.2 and 9.3). Settlements with low lacunarity like Maidanetske, Moshuriv and Čierne were more homogeneously compact, while those with higher lacunarity like Nebelivka, Vráble and Úľany nad Žitavou were more clearly clustered into separate neighbourhoods. However, this clustering also gave them lower density since the space between clusters was also included in the images, which would explain the similarity between these results, and why this partition remained after subtracting the effects from density alone. Fractal dimension was also more sensitive to either house count or image size (which were closely connected in these images), and this tendency was strengthened in the  $D$  residuals after removing effects from density (Figure 9.4). Considering the results from the analysis of synthetic images, it is possible that any spatial irregularities (noise) would be similar in the small and large settlements, but that the effects of these on fractal dimension estimates become relatively smaller in larger images/settlements with the same resolution (see Bruvoll, n.d. for further discussion on similar observations with synthetic images of variable sizes).

Results on separate quarters did not yield a partition between different types, but rather a continuum from regular, compact and grid-like to loose, dusty or irregular spatial patterns. The most interesting observation here was perhaps that images of typical Linear Pottery and Tryp-

illia layouts – i.e. grid-like and radial with perpendicular streets – that are visually very easy to distinguish, were not differentiated by the fractal analysis, but rather overlapped with larger spread within each group than between them (Figures 9.5 and 9.6). However, the analysed images also did overlap in image size, house count and density, and the gradient in results did seem to capture another difference between the images, more difficult to spot, in compactness. But again the results are difficult to separate analytically from the differences in density and size.

The fractal dimension and lacunarity results of temporally coeval plans at the Linear Pottery settlement of Vráble showed very close resemblance to those of house count and density. In this image series, image size was much more constant than in the quarters and settlements series, but density and house count followed a clear trajectory of growth by concentration followed by dilution after the peak of the settlement, as seen in Chapter 6. Here, fractal dimension and lacunarity estimates thus followed the same trajectory, but when effects from density were modelled out, some of the variability in lacunarity remained (Figure 9.10). This seemingly contradicted the previous observation that increased clustering gives higher lacunarity, since the three neighbourhoods at Vráble were most visible in the images with the *lowest* lacunarity. However, lacunarity did in this case probably capture the subtlety that the *distribution* of gap sizes after all became more equal in the middle phases of the settlement when density was highest. In the early and late phases, the few present houses were already located in what would become or had been the separate neighbourhoods, and these were then, relatively speaking, much more separated in space than when the village was more fully settled.

Overall these results were perhaps less satisfying than those obtained through distribution fitting, and little more insight is gained regarding Trypillia and Linear Pottery social organisation. The fractal dimension and lacunarity estimates obtained here could be largely reproduced by log-transformed house count and density, meaning that the utility of these methods is not clearly demonstrated. More careful modelling on larger synthetic data sets, accompanied with more in-depth theoretical exploration as well as tackling of methodological issues like edge effects, image orientation and missing data, all seem like necessary requirements for luring out the positive correlation seen between fractal dimension and lacunarity on the one hand, and clustering, size inequality and spatial noise seen on the synthetic images.

END Chapter

## **Part IV**

### **Synthesis**



# Chapter 10

## Discussion: Social complexity in Linear Pottery and Trypillia settlements

(Results from size distributions and settlement plans, for Trypillia and Linear Pottery settlements.)

- Restate the research questions: Social hierarchy. Was there any, how important was it, and at which scale did it operate?
  - Restate the status quo of research:
    - \* Oscillations in general opinion over time for Linear Pottery
    - \* Geographical/national research traditions for Trypillia
- The question of urbanity for Trypillia. Sindbæk (2022): Anomalocivitas or low-density urbanism, also Ohlrau (2022) for neither.
  - No visible spatial differentiation between quarters in Nebelivka – not filling the classic requirement for urbanism
  - But clear hierarchisation between households – beyond the house typology. Evidence of social hierarchy, though the specific social content of it is hard to say from house sizes alone. This analysis cannot decide between the two main competing hypotheses of democratic assemblies or more clan-based autocracy #check again#

## CHAPTER 10. DISCUSSION: SOCIAL COMPLEXITY IN LINEAR POTTERY AND TRYPILLIA SETTLEMENTS

---

- Draw in previous house-size analyses of Nebelivka and Maidanetske
- For Linear Pottery, evidence of hierarchical scaling between households, corroborating current argumentations based on grave goods and skeletal remains.
  - Linear Pottery society was not simply egalitarian, as that could hardly account for the large inequalities in house sizes.
  - Inequality does not seem to have increased markedly over time at Vráble. Rather there seems to have been a (at least moderately) hierarchical social system in place from early expansion phases of the settlement, possibly with clan leaders present in each of the three neighbourhoods, as well as competitive behaviours among lower levels households as well. While tensions may well have increased over time, the social hierarchy seems to have been in place long before the massacres of the late phases.
- For both: Results from both approaches cross-cut the distinction between Trypillia and Linear Pottery cultural belonging. There are homogeneously compact vs. heterogeneously clustered settlements from either group, as well as power-law vs. non-power-law house size distributions. These two differentiations do not overlap either, leaving a complex overall impression.
  - Despite methodological challenges (effectively distinguishing between log-normal and power-law distributions) power-law distributed house sizes seem inherently

END Chapter

# Chapter 11

## Discussion: Fractal Analysis and Archaeological data

Draw conclusions based on comparison of results from the synthetic data series and the empirical ones, both for distribution and for image analysis.

Also mention here fractals or related concepts used as a metaphor, with no mathematics involved (e.g. Chapman et al., 2006; Sherratt, 2004; Sindbæk, 2022; Whitridge, 2016).

### 11.1 Distribution fitting

- Multiplicative processes: power laws vs. log-normal, long debates Sheridan & Onodera (2018). Does it really matter in the end?
  - The most characteristic difference between power-law and non-power-law tails (log-normal distributions) for settlements, was the proportion of the distribution included in the tail (Table 6.1). Tails that were interpreted as power laws consisted of a maximum of 44% of the data (at Nebelivka, and excluding Horný which was too small for confident results). Log-normal distributions without power-law tails on the other hand (interpreted as exponentials) had a minimum of 66% and up to 93% of the data in them. All tail  $x_{min}$  values were set where they gave the best possible power-law fit. This may indicate that the distinction *is* meaningful after all.
    - The power laws identified for whole settlements were largely persistent when the

distributions were subdivided into separate quarters, neighbourhoods and time samples – sub-samples that often had lower house counts than settlements that did not have power law tails.

- Tests on synthetic data series indicated that aggregated data series (settlement data with low temporal resolution) would not generate false positive power-law distributions, as long as the data aggregation did not involve stacking of essentially differently distributed sub-sets (i.e. different settlements or phases with marked shifts in material culture).
  - Small sample sizes were shown to increase the risk of false positive power laws, while large sample sizes reduced the risk. Only the small settlement of Horný seems to have given a false positive power-law tail, the other ones being the largest settlements in the sample.
  - Together, these arguments further indicate that the settlements with identified power-law tails were indeed different from the rest, and that this difference was linked to settlement size.
- Power-law distribution in house sizes were identified for the largest settlements only,
    - Also the whole settlements without power-law tails would have even smaller co-eval plans than Vráble, further strengthening the argument of a correlation between settlement size and hierarchy.
  - Conclusion of these observations: Social hierarchy emerges as a result of social groups growing beyond a critical threshold, while cultural specifics are of less importance.
    - This is completely uncontroversial from a dynamical systems point of view, and there are several social (Alberti, 2014; De Landa, 2006; G. A. Johnson, 1982) and psychological (Dunbar, 2023; Zhou et al., 2005) explanations for how such emergence takes place.
    - In archaeology, such explanations are often unpopular, since we like to believe that social organisation is culture-specific and largely determined by human agency. However, this view can paradoxically lead to seeing archaeological cultures as monolithic in how their society is organised, while there might well be more intra-culture variation than what is often recognised.

- From this I argue that we must be open to the possibility that social life could have been as different between small and large settlements within single archaeological cultures as it would be between settlements of different cultures within the same period.
- Lots of caveats:
  - \* The possibility of seasonality of Trypillia mega-sites – which is not necessarily contradictory to the above conclusion. Discussion in Graeber & Wengrow (2021) on seasonality also in social organisation.
  - \* These emerging hierarchies would not explain the subsequent disintegration of neither Linear Pottery nor Trypillia culture groups, since the largest settlements are rather atypical for each of them (#recheck this after chap 3).
- Settlement size hierarchies are seemingly much more difficult to observe for prehistoric contexts, since the contemporaneity of settlements and their coeval sizes must first be established. Much of earlier attempts of doing this have been flawed both by their use of theory and method (see review in Grove, 2011), but current developments – framed as Settlement Scaling Theory (Bettencourt, 2021; Lobo et al., 2020; Smith et al., 2021) – show promising results, albeit for more recent periods than what is considered in this study.
  - In addition to the problem of contemporaneity of settlements, their total size often remains unknown since in the majority of cases, neolithic settlements are known through surface finds and partial excavations.
  - The ongoing revolution in the use of remote sensing imagery (quality of documentation and price/availability) may change this situation soon.
  - More theoretical and methodological studies are needed to determine the necessary requirements, specifically of spatial and temporal resolution, for settlement scaling to give accurate results.

## 11.2 Image analysis

The relationship between image density (built-up area) and fractal dimension was evaluated by Thomas et al. (2007), where they showed that these two parameters, under certain conditions (constant observation window, prefactor values close to 1), are exponentially correlated. They furthermore showed that observation window size and shape, as well as centroid placement, have little influence on  $D$ , while they have more influence on density when the pattern is not homogeneous. They do show, however, that images with the same density may have quite much variation in  $D$ , which is reflected in the layouts. Judging from their examples, more clustered layouts give higher  $D$  values, while more dispersed or dusty layouts give lower  $D$ , when density is constant. I ignore the use of prefactor values. According to Thomas et al. (2007), density is a crude measure of the overall intensity of the pattern, while fractal dimension is characterises the morphological structure, though it is not directly descriptive.

### 11.3 Concluding remarks?

Check for “fractal + archaeology” in WorldCat.

END Chapter

# **Chapter 12**

## **Conclusion and Outlook**

### **12.1 Things I would like to have done, but that didn't fit into this study**

- Ethnoarchaeology: Measure house sizes and settlement layouts in contemporary settings, and relate to social organisation (largely overlooked by ethnographers)
- Test distributions and settlement layout analysis on other settings: Lake dwellings, later/historic periods, other materials (e.g. megaliths)... Add more complex distribution models, add observation windows on images. Try on remote sensing imagery.
- Settlement Scaling on Neolithic settings
- Time series: Hurst exponent and scale invariance in temporal development of e.g. regional settlement or population
- Integrate – bridge the gap – between opposite theoretical (nat. and soc./hum.) approaches to the same phenomena
- Chaos and strange attractors in Archaeology
- More?

### **12.2 Concluding remarks**

END Thesis



# References

- Alberti, G. (2014). Modeling Group Size and Scalar Stress by Logistic Regression from an Archaeological Perspective. *PLOS ONE*, 9(3), e91510. <https://doi.org/10.1371/journal.pone.0091510>
- Allain, C., & Cloitre, M. (1991). Characterizing the lacunarity of random and deterministic fractal sets. *Physical Review A*, 44(6), 3552–3558. <https://doi.org/10.1103/PhysRevA.44.3552>
- Arshad, S., Hu, S., & Ashraf, B. N. (2018). Zipf's law and city size distribution: A survey of the literature and future research agenda. *Physica A: Statistical Mechanics and Its Applications*, 492, 75–92. <https://doi.org/10.1016/j.physa.2017.10.005>
- Artursson, M., Bech, J.-H., Earle, T., Fuköh, D., Kolb, M. J., Kristiansen, K., Ling, J., Mühlenbock, C., Prescott, C., Sevara, C., Tusa, S., Uhnér, C., & Vicze, M. (2010). Settlement Structure and Organisation. In K. Kristiansen & T. Earle (Eds.), *Organizing Bronze Age Societies: The Mediterranean, Central Europe, and Scandinavia Compared* (pp. 87–121). Cambridge University Press. <https://doi.org/10.1017/CBO9780511779282.005>
- Auerbach, F. (1913). Das Gesetz der Bevölkerungskonzentration. *Dr. A. Petermanns Mitteilungen aus Justus Perthes' Geographischer Anstalt*, LIX, 73–76. <http://archive.org/details/Auerbach1913>
- Augereau, A. (2021). *Femmes néolithiques - Le genre dans les premières sociétés agricoles* (Illustrated édition). Cnrs.
- Baden, W. W., & Beekman, C. S. (2016). *Nonlinear models for archaeology and anthropology: Continuing the revolution*. Routledge. <https://doi.org/10.4324/9781315247908>
- Bak, P. (2013). *How Nature Works: The Science of Self-Organized Criticality*. Springer.
- Bak, P., Tang, C., & Wiesenfeld, K. (1987). Self-organized criticality: An explanation of the 1/f noise. *Physical Review Letters*, 59(4), 381–384. <https://doi.org/10.1103/PhysRevLett.59.381>

- Bánffy, E., & Höhler-Brockmann, H. (2020). Burnt daub talking: The formation of the LBK longhouse (a work hypothesis). *Quaternary international*, 560-561, 179196. <https://doi.org/10.1016/j.quaint.2020.06.007>
- Barabási, A.-L., & Albert, R. (1999). Emergence of Scaling in Random Networks. *Science*, 286(5439), 509–512. <https://doi.org/10.1126/science.286.5439.509>
- Barley, N. (2011). *The Innocent Anthropologist: Notes from a Mud Hut*. Eland.
- Batty, M. (2005). *Cities and complexity: understanding cities with cellular automata, agent-based models, and fractals*. MIT Press.
- Batty, M., & Longley, P. (1994). *Fractal cities - a geometry of form and function*. Academic Press.
- Baxter, M. (2003). *Statistics in archaeology*. Arnold.
- Beck, R. A. (Ed.). (2007). *The Durable House: House Society Models in Archaeology*. Center for Archaeological Investigations, Southern Illinois University.
- Bee, M., Riccaboni, M., & Schiavo, S. (2011). Pareto versus lognormal: A maximum entropy test. *Physical Review E*, 84(2), 026104. <https://doi.org/10.1103/PhysRevE.84.026104>
- Bentley, R. A., & Maschner, H. D. G. (2001). Stylistic Change as a Self-Organized Critical Phenomenon: An Archaeological Study in Complexity. *Journal of Archaeological Method and Theory*, 8(1), 35–66. <https://doi.org/10.1023/A:1009521915258>
- Bentley, R. A., & Maschner, H. D. G. (2008). *Complexity Theory* (R. A. Bentley, H. D. G. Maschner, & C. Chippindale, Eds.). AltaMira Press.
- Bettencourt, L. M. A. (2021). *Introduction to Urban Science: Evidence and Theory of Cities as Complex Systems*. MIT Press.
- Bickle, P., & Whittle, A. (2013). *The first farmers of central europe: Diversity in LBK lifeways*. Oxbow Books.
- Birch, J. (2014). *From prehistoric villages to cities: settlement aggregation and community* (Vol. 10). Routledge.
- Blanton, R. E. (1994). *Houses and households*. Springer US. <https://doi.org/10.1007/978-1-4899-0990-9>
- Bradley, R. (2001). Orientations and origins: a symbolic dimension to the long house in Neolithic Europe. *Antiquity*, 75(287), 5056. <https://doi.org/10.1017/S0003598X00052704>
- Bradley, R. (2013). Houses of Commons, Houses of Lords: Domestic Dwellings and Monumental Architecture in Prehistoric Europe. *Proceedings of the Prehistoric Society*, 79,

- 1–17. <https://doi.org/10.1017/ppr.2013.1>
- Brink, K. (2013). Houses and hierarchies: Economic and social relations in the late neolithic and early bronze age of southernmost scandinavia. *European Journal of Archaeology*, 16(3), 433–458. <https://doi.org/10.1179/1461957113Y.0000000033>
- Brown, C. T., Witschey, W. R., & Liebovitch, L. S. (2005). The Broken past: Fractals in Archaeology. *Journal of archaeological method and theory*, 12(1), 3778. <https://doi.org/10.1007/s10816-005-2396-6>
- Brown, C., & Liebovitch, L. (2010). *Fractal analysis*. SAGE Publications, Inc. <https://doi.org/10.4135/9781412993876>
- Brown, C., Watson, A., Gravlin-Beman, A., & Liebovitch, L. (2012). *Poor mayapán* (pp. 306–324). Equinox Publishing.
- Brown, C., & Witschey, W. (2003). The fractal geometry of ancient Maya settlement. *Journal of Archaeological Science*, 30(12), 1619–1632. [https://doi.org/10.1016/S0305-4403\(03\)00063-3](https://doi.org/10.1016/S0305-4403(03)00063-3)
- Bruvoll, H. (n.d.). Quantifying spatial complexity of settlement plans through fractal analysis. *Journal of Archaeological Method and Theory*.
- Cafazzo, S., Lazzaroni, M., & Marshall-Pescini, S. (2016). Dominance relationships in a family pack of captive arctic wolves (*Canis lupus arctos*): the influence of competition for food, age and sex. *PeerJ*, 4, e2707. <https://doi.org/10.7717/peerj.2707>
- Carneiro, R. L. (1986). On the relationship between size of population and complexity of social organization. *Journal of Anthropological Research*, 42(3), 355–364. <http://www.jstor.org/stable/3630039>
- Carsten, J., & Hugh-Jones, S. (1995). *About the house: Lévi-Strauss and beyond*. University Press.
- Chapman, J., Higham, T., Slavchev, V., Gaydarska, B., & Honch, N. (2006). The social context of the emergence, development and abandonment of the Varna cemetery, Bulgaria. *European journal of archaeology*, 9(2-3), 159183. <https://doi.org/10.1177/1461957107086121>
- Chen, Y. (2011). Fractal systems of central places based on intermittency of space-filling. *Chaos, Solitons & Fractals*, 44, 619–632.
- Cheng, Q. (1997). Multifractal Modeling and Lacunarity Analysis. *Mathematical geology*, 29(7), 919932. <https://doi.org/10.1023/A:1022355723781>

- Clauset, A., Shalizi, C. R., & Newman, M. E. J. (2009). Power-law distributions in empirical data. *Society for Industrial and Applied Mathematics Review*, 51(4), 661–703.
- Cleuziou, S., Braemer, F., & Coudart, A. (1999). *Habitat et société*. APDCA.
- Costin, C. L. (1991). Craft specialization: Issues in defining, documenting, and explaining the organization of production. *Archaeological Method and Theory*, 3, 1–56. <https://www.jstor.org/stable/20170212>
- Coudart, A. (1998). *Architecture et société néolithique : L'unité et la variance de la maison danubienne*. Éditions de la Maison des Sciences de l'Homme.
- Coudart, A. (2015). *The bandkeramik longhouses: A material, social, and mental metaphor for small-scale sedentary societies* (C. Fowler, J. Harding, & D. Hofmann, Eds.; pp. 309–325). Oxford University Press.
- Crabtree, S. A., Bocinsky, R. K., Hooper, P. L., Ryan, S. C., & Kohler, T. A. (2017). How to make a Polity (in the Central Mesa Verde Region). *American Antiquity*, 82(1), 71–95. <https://doi.org/10.1017/aaq.2016.18>
- Crumley, C. L. (1995). Hierarchy and the Analysis of Complex Societies. *Archaeological Papers of the American Anthropological Association*, 6(1), 1–5. <https://doi.org/https://doi.org/10.1525/ap3a.1995.6.1.1>
- D'Acci, L. (Ed.). (2019). *The Mathematics of Urban Morphology*. Springer International Publishing. <https://doi.org/10.1007/978-3-030-12381-9>
- Daems, D. (2021). *Social complexity and complex systems in archaeology*. Routledge.
- De Landa, M. (2006). *A new philosophy of society: assemblage theory and social complexity*. Continuum.
- Devaney, R. L. (2020). *A First Course In Chaotic Dynamical Systems: Theory And Experiment*. CRC Press.
- Diachenko, A. (2018). *Fractal models* (S. López Varela, Ed.). John Wiley & Sons.
- Diachenko, A., & Sobkowiak-Tabaka, I. (2022). Self-Organized Cultural Cycles and the Uncertainty of Archaeological Thought. *Journal of Archaeological Method and Theory*. <https://doi.org/10.1007/s10816-022-09548-8>
- Dohm, K. (1990). Effect of population nucleation on house size for pueblos in the American Southwest. *Journal of anthropological archaeology*, 9(3), 201239. [https://doi.org/10.1016/0278-4165\(90\)90007-Z](https://doi.org/10.1016/0278-4165(90)90007-Z)
- Dubreuil, B. (2010). *Human evolution and the origins of hierarchies: the state of nature*.

- University Press.
- Duffy, P. R. (2015). Site size hierarchy in middle-range societies. *Journal of Anthropological Archaeology*, 37, 85–99. <https://doi.org/10.1016/j.jaa.2014.12.001>
- Dunbar, R. (2023). The social brain hypothesis thirty years on: Some philosophical pitfalls of deconstructing dunbar's number. *Annales - Academiae Scientiarum Fennicae*, I, 8–27.
- Earle, T. (2002). *Bronze Age Economics: The Beginnings of Political Economies*. Westview Press.
- Earle, T. K. (1997). *How chiefs come to power: the political economy in prehistory*. Stanford University Press.
- Eglash, R. (1999). *African Fractals: Modern Computing and Indigenous Design*. Rutgers University Press.
- Ensor, B. E. (2013). *The archaeology of kinship: Advancing interpretation and contributions to theory*. University of Arizona Press. <https://www.jstor.org/stable/j.ctt183pcj3>
- Ensor, B. E. (2017). Testing Ethnological Theories on Prehistoric Kinship. *Cross-Cultural Research*, 51(3), 199–227. <https://doi.org/10.1177/1069397117697648>
- Ensor, B. E. (2021). Making aDNA useful for kinship analysis. *Antiquity*, 95(379), 241–243. <https://doi.org/10.15184/aqy.2020.234>
- Ensor, B. E., Irish, J. D., & Keegan, W. F. (2017). The bioarchaeology of kinship: Proposed revisions to assumptions guiding interpretation. *Current Anthropology*, 58(6), 739–761. <https://doi.org/10.1086/694584>
- Falconer, K. (2013). *Fractals: A very short introduction*. Oxford University Press.
- Farías-Pelayo, S. (2015). *La Cultura Xajay. Los otomíes al sur de la frontera norte de Mesoamérica. Caracterización por medio de su firma fractal* [PhD thesis]. [https://www.academia.edu/43740443/La\\_Cultura\\_Xajay\\_Los\\_otom%C3%A3Des\\_al\\_sur\\_de\\_la\\_frontera\\_norte\\_de\\_Mesoam%C3%A3rica](https://www.academia.edu/43740443/La_Cultura_Xajay_Los_otom%C3%A3Des_al_sur_de_la_frontera_norte_de_Mesoam%C3%A3rica)
- Farías-Pelayo, S. (2017). *Characterization of Cultural Traits by Means of Fractal Analysis* (F. Brambila, Ed.). IntechOpen. DOI: 10.5772/67893
- Fisher, K. D. (2009). Placing social interaction: An integrative approach to analyzing past built environments. *Journal of Anthropological Archaeology*, 28(4), 439–457. <https://doi.org/10.1016/j.jaa.2009.09.001>
- Flannery, K. V., & Marcus, J. (2012). *The creation of inequality: how our prehistoric ancestors set the stage for monarchy, slavery and empire*. Havard University Press.

- Fontijn, D., & Brück, J. (2013). The Myth of the Chief: Prestige Goods, Power, and Personhood in the European Bronze Age. In *The Oxford Handbook of the European Bronze Age*. Oxford University Press. <https://doi.org/10.1093/oxfordhb/9780199572861.013.0011>
- Fraser, D. (1968). *Village planning in the primitive world*. George Braziller. <http://archive.org/details/VillagePlanningInThePrimitiveWorld>
- Furholt, M. (2016). Settlement layout and social organisation in the earliest european neolithic. *Antiquity*, 90(353), 1196–1212.
- Furholt, M., Grier, C., Spriggs, M., & Earle, T. (2020). Political Economy in the Archaeology of Emergent Complexity: a Synthesis of Bottom-Up and Top-Down Approaches. *Journal of Archaeological Method and Theory*, 27(2), 157–191. <https://doi.org/10.1007/s10816-019-09422-0>
- Furholt, M., Müller, J., Bistákova, A., Wunderlich, M., Cheben, I., & Müller-Scheeßel, N. (2020). *Archaeology in the zitava valley I - the LBK and zeliezovce settlement site of vráble*. Sidestone Press.
- Furholt, M., Müller-Scheeßel, N., Wunderlich, M., Cheben, I., & Müller, J. (2020). Communality and discord in an early neolithic settlement agglomeration: The LBK site of vráble, southwest slovakia. *Cambridge Archaeological Journal*, 30(3), 469–489.
- Gaydarska, B., Rebay-Salisbury, K., Valiente, P. R., Fries, J. E., Hofmann, D., Augereau, A., Chapman, J., Mina, M., Pape, E., Ialongo, N., Nordholz, D., Bickle, P., Haughton, M., Robb, J., & Harris, O. (2023). To Gender or not To Gender? Exploring Gender Variations through Time and Space. *European journal of archaeology*, 128. <https://doi.org/10.1017/eaa.2022.51>
- Gibrat, R. (1930). Une loi des répartitions économiques : L'effet proportionnel. *Bulletin de La Statistique Générale de La France*, 19(3), 469–513.
- Gillespie, C. S. (2015). Fitting heavy tailed distributions: The poweRlaw package. *Journal of Statistical Software*, 64(2).
- Gleick, J. (1987). *Chaos: Making a new science*. Viking.
- Godelier, M. (1986). *The making of great men: male domination and power among the New Guinea Baruya* (Vol. 56). University Press.
- Gomez-Lievano, A., Youn, H., & Bettencourt, L. (2012). The statistics of urban scaling and their connection to zipf's law. *PloS One*, 7, e40393. <https://doi.org/10.1371/journal.pone.0040393>

- Goodale, N., Quinn, C. P., & Nauman, A. (2021). Monumentality of houses: Collective action, inequality, and kinship in pithouse construction. In L. B. Carpenter & A. M. Prentiss (Eds.), *Archaeology of Households, Kinship, and Social Change* (pp. 177–203). Routledge.
- Gould, S. J. (2007). *Punctuated equilibrium*. Belknap Press of Harvard University Press.
- Graeber, D., & Wengrow, D. (2021). *The dawn of everything: a new history of humanity*. Farrar, Straus; Giroux.
- Gronenborn, D., Strien, H.-C., Dietrich, S., & Sirocko, F. (2014). ‘Adaptive cycles’ and climate fluctuations: a case study from Linear Pottery Culture in western Central Europe. *Journal of Archaeological Science*, 51, 73–83. <https://doi.org/10.1016/j.jas.2013.03.015>
- Grove, M. (2011). An archaeological signature of multi-level social systems: The case of the Irish Bronze Age. *Journal of Anthropological Archaeology*, 30(1), 44–61. <https://doi.org/10.1016/j.jaa.2010.12.002>
- Haas, W. R., Klink, C. J., Maggard, G. J., & Aldenderfer, M. S. (2015). Settlement-Size Scaling among Prehistoric Hunter-Gatherer Settlement Systems in the New World. *PLoS One*, 10(11), e0140127. <https://doi.org/10.1371/journal.pone.0140127>
- Hachem, L., & Hamon, C. (2014). *Linear pottery culture household organisation* (A. Whittle & P. Bickle, Eds.). British Academy Oxford University Press.
- Hale, D. (2020). *Geophysical investigations and the nebelivka site plan* (B. Gaydarska, Ed.; pp. 122–148). De Gruyter.
- Hamilton, M., Milne, B., Walker, R., Burger, O., & Brown, J. (2007). The complex structure of hunter-gatherer social networks. *Proceedings of the Royal Society B*, 274, 2195–2202.
- Harper, T. K., Diachenko, A., Ryzhov, S. N., Rassamakin, Y. Y., Eccles, L. R., Kennett, D. J., & Tsvek, E. V. (2023). ASSESSING THE SPREAD OF ENEOLITHIC AGRICULTURAL COMMUNITIES IN THE FOREST-STEPPE OF UKRAINE USING AMS RADIOCARBON DATING. *Radiocarbon*, 1–21. <https://doi.org/10.1017/RDC.2023.28>
- Harrison, A. (1981). A tale of two distributions. *The Review of Economic Studies*, 48(4), 621–631.
- Harte, D. (2001). *Multifractals: Theory and applications*. Chapman; Hall/CRC. <https://doi.org/10.1201/9781420036008>
- Haude, R., & Wagner, T. (2019). *Herrschaftsfreie Institutionen : Texte zur Stabilisierung staatsloser, egalitärer Gesellschaften*. Verlag Graswurzelrevolution. <http://www.herrschaftsfreie-institutionen.de>

- deutsche-digitale-bibliothek.de/item/7WYRGHTXGAOZOF5JUQ5JQCONFJKLTBIE
- Hillier, B. (1984). *The social logic of space*. University Press.
- Hingee, K., Baddeley, A., Caccetta, P., & Nair, G. (2019). Computation of Lacunarity from Covariance of Spatial Binary Maps. *Journal of Agricultural, Biological and Environmental Statistics*, 24(2), 264–288. <https://doi.org/10.1007/s13253-019-00351-9>
- Hodder, I. (1979). *Simulating the Growth of Hierarchies* (C. Renfrew & K. L. Cooke, Eds.; pp. 117–144). Academic Press. <https://doi.org/10.1016/B978-0-12-586050-5.50015-4>
- Hofmann, D., & Smyth, J. (Eds.). (2013). *Tracking the Neolithic House in Europe*. Springer New York. <https://doi.org/10.1007/978-1-4614-5289-8>
- Honoré, E. (2022). Différences de richesse et inégalités sociales au Paléolithique: éléments pour une discussion. *Paléo (Les Eyzies de Tayac-Sireuil)*, 5059.
- Hrnčíř, V., Duda, P., Šaffa, G., Květina, P., & Zrzavý, J. (2020). Identifying post-marital residence patterns in prehistory: A phylogenetic comparative analysis of dwelling size. *PLOS ONE*, 15(2), e0229363. <https://doi.org/10.1371/journal.pone.0229363>
- Hrnčíř, V., Vondrovský, V., & Květina, P. (2020). Post-marital residence patterns in LBK: Comparison of different models. *Journal of Anthropological Archaeology*, 59, 101190. <https://doi.org/10.1016/j.jaa.2020.101190>
- Jahanmiri, F., & Parker, D. C. (2022). An Overview of Fractal Geometry Applied to Urban Planning. *Land*, 11(4), 475. <https://doi.org/10.3390/land11040475>
- Jeunesse, C. (2022). *Vertical social differentiation and social competition in the Lbk: “rich” and “poor” cemeteries* (M. Dębiec, J. Górska, J. Müller, M. Nowak, A. Pelisiak, T. Saile, & P. Włodarczak, Eds.; pp. 33–42). Verlag Dr. Rudolf Habelt GmbH. [https://www.academia.edu/95075660/Vertical\\_social\\_differentiation\\_and\\_social\\_competition\\_in\\_the\\_Lbk\\_rich\\_and\\_poor\\_cemeteries](https://www.academia.edu/95075660/Vertical_social_differentiation_and_social_competition_in_the_Lbk_rich_and_poor_cemeteries)
- Johnson, A., & Earle, T. (1987). *The evolution of human societies : From foraging group to agrarian state*. Stanford University Press.
- Johnson, G. A. (1982). *Organizational structure and scalar stress* (C. Renfrew, M. J. Rowlands, & B. A. Segraves, Eds.; pp. 389–421). Academic Press.
- Johnson, N. L. (1994). *Continuous univariate distributions: Vol. 1: Vols. Vol. 1* (2nd ed.). Wiley.
- Joyce, R. A., & Gillespie, S. D. (2000). *Beyond kinship: social and material reproduction in house societies*. University of Pennsylvania Press.

- Kadrow, S. (2013). *Social organization and change* (A. Gardner, M. Lake, & U. Sommer, Eds.; p. 0). Oxford University Press. <https://doi.org/10.1093/oxfordhb/9780199567942.013.023>
- Kahn, J. G. (2021). Houses of power: Community houses and specialized houses as markers of social complexity in the pre-contact Society Island chiefdoms. In L. B. Carpenter & A. M. Prentiss (Eds.), *Archaeology of Households, Kinship, and Social Change* (pp. 82–110). Routledge.
- Karperien, A. (2013). *FracLac for ImageJ*. <http://rsb.info.nih.gov/ij/plugins/fraclac/FLHelp/Introduction.htm>
- Kienlin, T. L., & Zimmermann, A. (2012). *Beyond Elites - Alternatives to Hierarchical Systems in Modelling Social Formations: International Conference at the Ruhr-Universität Bochum, Germany, ... zur prähistorischen Archäologie*). Habelt, R.
- Klinkenberg, B. (1994). A review of methods used to determine the fractal dimension of linear features. *Mathematical Geology*, 26(1), 23–46. <https://doi.org/10.1007/BF02065874>
- Kohler, T. A., & Smith, M. E. (2018). *Ten thousand years of inequality: The archaeology of wealth differences*. University of Arizona Press.
- Kohler, T. A., Smith, M. E., Bogaard, A., Feinman, G. M., Peterson, C. E., Betzenhauser, A., Pailes, M., Stone, E. C., Marie Prentiss, A., Dennehy, T. J., Ellyson, L. J., Nicholas, L. M., Faulseit, R. K., Styring, A., Whitlam, J., Fochesato, M., Foor, T. A., & Bowles, S. (2017). Greater post-Neolithic wealth disparities in Eurasia than in North America and Mesoamerica. *Nature*, 551(7682), 619–622. <https://doi.org/10.1038/nature24646>
- Kostof, S. (1991). *The city shaped: urban patterns and meanings through history ; original drawings by Richard Tobias*. Thames; Hudson.
- Kramer, C. (1982). *Village ethnoarchaeology: rural Iran in archaeological perspective*. Academic Press.
- Kuijt, I. (2018). Material Geographies of House Societies: Reconsidering Neolithic Çatalhöyük, Turkey. *Cambridge Archaeological Journal*, 28(4), 565–590. <https://doi.org/10.1017/S0959774318000240>
- Květina, P., & Řídký, J. (2019). Traditional and archaic societies - problems linked to the search for social and power attributes in the archaeological record. In J. Řídký, P. Květina, P. Limburský, M. Končelová, P. Burgert, & R. Šumberová, *Big men or chiefs? Rondel builders of neolithic Europe* (pp. 7–14). Oxbow Books.

- Lagarias, A., & Prastacos, P. (2021). Fractal dimension of European Cities: A comparison of the patterns of built-up areas in the urban core and the peri-urban ring. *Cybergeo: European Journal of Geography*. <https://doi.org/10.4000/cybergeo.37243>
- Laherrère, J. (2000). Distribution of field sizes in a petroleum system: Parabolic fractal, lognormal or stretched exponential? *Marine and Petroleum Geology*, 17, 539–546.
- Laherrère, J., & Sornette, D. (1998). Stretched exponential distributions in nature and economy: “fat tails” with characteristic scales. *The European Physical Journal B - Condensed Matter and Complex Systems*, 2(4), 525–539. <https://doi.org/10.1007/s100510050276>
- Last, J. (2015). *Longhouse lifestyles in the central european neolithic* (C. Fowler, J. Harding, & D. Hofmann, Eds.; p. 0). Oxford University Press. <https://doi.org/10.1093/oxfordhb/9780199545841.013.009>
- Lévi-Strauss, C. (1982). *The way of the masks*. University of Washington Press.
- Li, J., Du, Q., & Sun, C. (2009). An improved box-counting method for image fractal dimension estimation. *Pattern Recognition*, 42(11), 2460–2469. <https://doi.org/10.1016/j.patcog.2009.03.001>
- Lobo, J., Bettencourt, L. M., Smith, M. E., & Ortman, S. (2020). Settlement scaling theory: Bridging the study of ancient and contemporary urban systems. *Urban Studies*, 57(4), 731–747. <https://doi.org/10.1177/0042098019873796>
- Lund, J., Furholt, M., & Austvoll, K. I. (2022). Reassessing power in the archaeological discourse. How collective, cooperative and affective perspectives may impact our understanding of social relations and organization in prehistory. *Archaeological Dialogues*, 1–18. <https://doi.org/10.1017/S1380203822000162>
- Madella, M. (2013). *The archaeology of household*. Oxbow books.
- Mancuso, F. P. (2021). *fractD: Estimation of fractal dimension of a black area in 2D and 3D (slices) images*. <https://CRAN.R-project.org/package=fractD>
- Mandelbrot, B. (1967). How long is the coast of britain? Statistical self-similarity and fractional dimension. *Science*, 156(3775), 636–638. <https://www.jstor.org/stable/1721427>
- Mandelbrot, B. (1982). *The fractal geometry of nature*. Freeman.
- Mandelbrot, B. B. (1975). *Les objets fractals: forme, hasard et dimension*. Flammarion.
- Mandelbrot, B. B. (1997). *Fractals and scaling in finance: discontinuity, concentration, risk : selecta volume E*. Springer.
- Mandelbrot, B. B. (2021). *The fractal geometry of nature*. Echo Point Books & Media, LLC.

- Maschner, H., & Bentley, A. (2003). *The power law of rank and household on the north pacific* (A. Bentley & H. Maschner, Eds.; pp. 47–143). The University of Utah Press.
- Mazerolle, M. J. (2023). *AICmodavg: Model selection and multimodel inference based on (q)AIC(c)*. <https://cran.r-project.org/package=AICmodavg>
- Meadows, J., Müller-Scheeßel, N., Cheben, I., Agerskov Rose, H., & Furholt, M. (2019). Temporal dynamics of Linearbandkeramik houses and settlements, and their implications for detecting the environmental impact of early farming. *The Holocene*, 29(10), 1653–1670. <https://doi.org/10.1177/0959683619857239>
- Mech, L. D. (1999). Alpha status, dominance, and division of labor in wolf packs. *Canadian Journal of Zoology*, 77(8), 1196–1203. <https://doi.org/10.1139/z99-099>
- Merton, R. K. (1968). The matthew effect in science. *Science*, 159(3810), 56–63. <https://www.jstor.org/stable/1723414>
- Midlarsky, M. I. (1999). *The evolution of inequality: War, state survival, and democracy in comparative perspective*. Stanford University Press.
- Millard, A. (2020). *The AMS dates* (B. Gaydarska, Ed.; pp. 246–255). De Gruyter.
- Mitzenmacher, M. (2004). A brief history of generative models for power law and lognormal distributions. *Internet Mathematics*, 1(2), 226–251. <https://doi.org/10.1080/15427951.2004.10129088>
- Modderman, P. J. R., Newell, R. R., Brinkman, J. E., & Bakels, C. C. (1970). *Linearbandkeramik aus Elsloo und Stein* (Vol. 3). Leiden University Press. <http://hdl.handle.net/1887/2720923>
- Müller, J., Hofmann, R., Videiko, M., & Burdo, N. (2022). *Nebelivka – Rediscovered: A Lost City* (M. Dębiec, J. Górska, J. Müller, M. Nowak, A. Pelisiak, T. Saile, & P. Włodarczak, Eds.; pp. 33–42). Verlag Dr. Rudolf Habelt GmbH. [https://www.academia.edu/95075660/Vertical\\_social\\_differentiation\\_and\\_social\\_competition\\_in\\_the\\_Lbk\\_rich\\_and\\_poor\\_cemeteries](https://www.academia.edu/95075660/Vertical_social_differentiation_and_social_competition_in_the_Lbk_rich_and_poor_cemeteries)
- Müller-Scheeßel, N. (2007). Further thoughts on the hidden settlement structures of the hallstatt period in southern germany: Testing for auto-correlation. *Archäologisches Korrespondenzblatt*, 37(1), 57–66.
- Müller-Scheeßel, N. (2019). *A new approach to the temporal significance of house orientations in European Early Neolithic settlements*. <https://doi.org/10.17026/DANS-XU6-C6YR>

- Müller-Scheeßel, N., Hukeľová, Z., Meadows, J., Cheben, I., Müller, J., & Furholt, M. (2021). New burial rites at the end of the Linearbandkeramik in south-west Slovakia. *Antiquity*, 95(379), 65–84. <https://doi.org/10.15184/aqy.2020.103>
- Müller-Scheeßel, N., Müller, J., Cheben, I., Mainusch, W., Rassmann, K., Rabbel, W., Corradini, E., & Furholt, M. (2020). A new approach to the temporal significance of house orientations in european early neolithic settlements. *PLoS ONE*, 15(1), e0226082.
- Murdock, G. P. (1949). *Social structure*. Macmillan.
- Muro, C., Escobedo, R., Spector, L., & Coppinger, R. P. (2011). Wolf-pack (*Canis lupus*) hunting strategies emerge from simple rules in computational simulations. *Behavioural Processes*, 88(3), 192–197. <https://doi.org/10.1016/j.beproc.2011.09.006>
- Netting, R. McC. (1982). Some Home Truths on Household Size and Wealth. *American Behavioral Scientist*, 25(6), 641–662. <https://doi.org/10.1177/000276482025006004>
- Newman, M. E. J. (2005). Power laws, pareto distributions and zipf's law. *Contemporary Physics*, 46(5), 325–351. <https://doi.org/10.1080/00107510500052444>
- Nordquist, P. (2001). *Hierarkiseringsprocesser: om konstruktion av social ojämlikhet i Skåne, 5500-1100 f.Kr.* [PhD thesis].
- Ohlrau, R. (2020). *Maidanets 'ke - development and decline of a trypillia mega-site in central ukraine*. Sidestone Press.
- Ohlrau, R. (2022). Trypillia mega-sites: Neither urban nor low-density? *Journal of Urban Archaeology*, 5, 81–100. <https://doi.org/10.1484/J.JUA.5.129844>
- Oleschko, K., Brambila, R., Brambila, F., Parrot, J.-F., & López, P. (2000). Fractal Analysis of Teotihuacan, Mexico. *Journal of Archaeological Science*, 27(11), 1007–1016. <https://doi.org/10.1006/jasc.1999.0509>
- Packard, J. (2003). Wolf behavior: Reproductive, social and intelligent. In L. D. Mech & L. Boitani (Eds.), *Wolves: Behavior, ecology, and conservation* (pp. 35–65). The University of Chicago Press.
- Pareto, V. (1896). *Cours d'économie politique* (Éd. F. Rouge, Vol. 1). <http://archive.org/details/fp-0148-1>
- Perreault, C. (2019). *The quality of the archaeological record*. The University of Chicago Press.
- Peters, R., & Zimmermann, A. (2017). Resilience and Cyclicity: Towards a macrohistory of the Central European Neolithic. *Quaternary International*, 446, 43–53. <https://doi.org/>

- 10.1016/j.quaint.2017.03.073
- Pickartz, N., Hofmann, R., Dreibrodt, S., Rassmann, K., Shatilo, L., Ohlrau, R., Wilken, D., & Rabbel, W. (2019). Deciphering archeological contexts from the magnetic map: Determination of daub distribution and mass of Chalcolithic house remains. *The Holocene*, 29(10), 1637–1652. <https://doi.org/10.1177/0959683619857238>
- Pickartz, N., Hofmann, R., Wunderlich, T., Rassmann, K., Müller, J., Ohlrau, R., Wilken, D., & Rabbel, W. (2021). Magnetization Patterns as Indicator of Settlement Structures. *ArcheoSciences*, 45-1(1), 187–190. <https://www.cairn.info/revue-archeosciences-2021-1-page-187.htm>
- Plotnick, R. E., Gardner, R. H., Hargrove, W. W., Prestegaard, K., & Perlmutter, M. (1996). Lacunarity analysis: A general technique for the analysis of spatial patterns. *Physical Review E*, 53(5), 5461–5468. <https://doi.org/10.1103/PhysRevE.53.5461>
- Porcic, M. (2010). House Floor Area as a Correlate of Marital Residence Pattern: A Logistic Regression Approach. *Cross-cultural research*, 44(4), 405424. <https://doi.org/10.1177/1069397110378839>
- Porčić, M. (2012). Effects of Residential Mobility on the Ratio of Average House Floor Area to Average Household Size: Implications for Demographic Reconstructions in Archaeology. *Cross-Cultural Research*, 46(1), 72–86. <https://doi.org/10.1177/1069397111423889>
- Price, T. D., & Feinman, G. M. (1995). *Foundations of social inequality*. Plenum Press.
- Price, T. D., & Feinman, G. M. (2010). *Pathways to Power: New Perspectives on the Emergence of Social Inequality*. Springer.
- Pumain, D. (2006). Introduction. In D. Pumain (Ed.), *Hierarchy in Natural and Social Sciences* (pp. 1–12). Springer Netherlands. [https://doi.org/10.1007/1-4020-4127-6\\_1](https://doi.org/10.1007/1-4020-4127-6_1)
- R Core Team. (2023). *R: A language and environment for statistical computing*. R Foundation for Statistical Computing. <https://www.R-project.org/>
- Rathje, W. L., & McGuire, R. H. (1982). Rich Men... Poor Men. *American Behavioral Scientist*, 25(6), 705–715. <https://doi.org/10.1177/000276482025006008>
- Redhead, D., & Power, E. A. (2022). Social hierarchies and social networks in humans. *Philosophical Transactions of the Royal Society B: Biological Sciences*, 377(1845), 20200440. <https://doi.org/10.1098/rstb.2020.0440>
- Rodríguez, L., Castillo, O., Soria, J., Melin, P., Valdez, F., Gonzalez, C. I., Martinez, G. E., & Soto, J. (2017). A fuzzy hierarchical operator in the grey wolf optimizer algorithm.

- Applied Soft Computing*, 57, 315–328. <https://doi.org/10.1016/j.asoc.2017.03.048>
- Ross, J. C., & Steadman, S. R. (2017). *Ancient complex societies*. Routledge.
- Roussot-Larroque, J. (2022). Relations sud-nord en Europe occidentale au Néolithique ancien. In C. Guillaume (Ed.), *Le Néolithique du nord-est de la France et des régions limítrophes : Actes du XIIIe colloque interrégional sur le Néolithique* (p. 10-40). Éditions de la Maison des sciences de l'homme. <https://doi.org/10.4000/books.editionsmsh.39018>
- Sahlins, M. (2013). *What kinship is - and is not*. University of Chicago Press.
- Sahlins, M. (2020). *Stone Age Economics*. Routledge.
- Saile, T. (2020). On the Bandkeramik to the east of the Vistula River: At the limits of the possible. *Quaternary international*, 560-561, 208227. <https://doi.org/10.1016/j.quaint.2020.04.036>
- Scheidel, W. (2017). *Great leveler: violence and the history of inequality from the stone age to the twenty-first century*. University Press.
- Schiesberg, S. (2010). *Von häusern und menschen. Das beispiel bandkeramik* (E. Claßen, T. Doppler, & B. Ramminger, Eds.; Vol. 1, pp. 53–69). Welt und Erde.
- Schiesberg, S. (2016). *Post-marital residence patterns and descent rules in prehistory* (T. Kerig, K. Nowak, & G. Roth, Eds.; Vol. 285). Dr. Rudolf Habelt.
- Schreier, A. L., & Swedell, L. (2009). The fourth level of social structure in a multi-level society: ecological and social functions of clans in hamadryas baboons. *American Journal of Primatology*, 71(11), 948–955. <https://doi.org/10.1002/ajp.20736>
- Service, E. (1971). *Primitive social organization : An evolutionary perspective* (2nd ed.). Random House.
- Shatilo, L. (2021). *Tripolye typo-chronology. Mega and smaller sites in the sinyukha river basin*. Sidestone Press. <https://library.oapen.org/handle/20.500.12657/50807>
- Shennan, S. (2008). *Quantifying archaeology* (Second edition.). University Press.
- Shennan, S. (2018). *The first farmers of Europe: an evolutionary perspective*. University Press.
- Sheridan, P., & Onodera, T. (2018). A Preferential Attachment Paradox: How Preferential Attachment Combines with Growth to Produce Networks with Log-normal In-degree Distributions. *Scientific Reports*, 8(1), 2811. <https://doi.org/10.1038/s41598-018-21133-2>
- Sherratt, A. (2004). *Fractal farmers: Patterns of neolithic origin and dispersal* (J. Cherry, C. Scarre, & S. Shennan, Eds.; pp. 53–63). McDonald Institute for Archaeological Research.

- Shimoji, H., & Dobata, S. (2022). The build-up of dominance hierarchies in eusocial insects. *Philosophical Transactions of the Royal Society B: Biological Sciences*, 377(1845), 20200437. <https://doi.org/10.1098/rstb.2020.0437>
- Simon, H. A. (1955). On a Class of Skew Distribution Functions. *Biometrika*, 42(3-4), 425440. <https://doi.org/10.1093/biomet/42.3-4.425>
- Sindbæk, Søren M. (2022). Weak ties and strange attractors: Anomalocitas and the archaeology of urban origins. *Journal of Urban Archaeology*, 5, 19–32. <https://doi.org/10.1484/J.JUA.5.129841>
- Smith, M. E. (1987). Household possessions and wealth in agrarian states: Implications for archaeology. *Journal of Anthropological Archaeology*, 6(4), 297–335. [https://doi.org/10.1016/0278-4165\(87\)90004-3](https://doi.org/10.1016/0278-4165(87)90004-3)
- Smith, M. E. (Ed.). (2011). *The Comparative Archaeology of Complex Societies*. Cambridge University Press. <https://doi.org/10.1017/CBO9781139022712>
- Smith, M. E., Ortman, S. G., Lobo, J., Ebert, C. E., Thompson, A. E., Prufer, K. M., Stuardo, R. L., & Rosenswig, R. M. (2021). The Low-Density Urban Systems of the Classic Period Maya and Izapa: Insights from Settlement Scaling Theory. *Latin American Antiquity*, 32(1), 120–137. <https://doi.org/10.1017/laq.2020.80>
- Souvatzi, S. (2017). Kinship and Social Archaeology. *Cross-cultural research*, 51(2), 172195. <https://doi.org/10.1177/1069397117691028>
- Strauss, E. D., Curley, J. P., Shizuka, D., & Hobson, E. A. (2022). The centennial of the pecking order: Current state and future prospects for the study of dominance hierarchies. *Philosophical Transactions of the Royal Society B: Biological Sciences*, 377(1845), 20200432. <https://doi.org/10.1098/rstb.2020.0432>
- Strawinska-Zanko, U., Liebovitch, L., Watson, A., & Brown, C. (2018). *Capital in the First Century: The Evolution of Inequality in Ancient Maya Society* (U. Strawinska-Zanko & L. Liebovitch, Eds.; pp. 161–192). Springer International Publishing. [https://doi.org/10.1007/978-3-319-76765-9\\_9](https://doi.org/10.1007/978-3-319-76765-9_9)
- Stumpf, M. P. H., & Porter, M. A. (2012). Critical truths about power laws. *Science*, 335(6069), 665–666. <https://doi.org/10.1126/science.1216142>
- Tannier, C., & Pumain, D. (2005). Fractals in urban geography: A theoretical outline and an empirical example. *Cybergeo : European Journal of Geography*. <https://doi.org/https://doi.org/10.4000/cybergeo.3275>

- Testart, A. (1982). *Les chasseurs-cueilleurs ou L'origine des inégalités*. Société d'ethnographie.
- Testart, A. (2005). *Eléments de classification des sociétés*. Éditions Errance : ill. en noir, tabl., cartes, schémas, couv. ill. en coul.
- Testart, A. (2012). *Avant l'histoire: l'évolution des sociétés, de Lascaux à Carnac*. Gallimard.
- Thomas, I., Frankhauser, P., & De Keersmaecker, M.-L. (2007). Fractal dimension versus density of built-up surfaces in the periphery of Brussels. *Papers in Regional Science*, 86(2), 287–308. <https://doi.org/10.1111/j.1435-5957.2007.00122.x>
- Trebsche, P., Müller-Scheeßel, N., & Reinhold, S. (2010). *Der gebaute Raum: Bausteine einer Architektursoziologie vormoderner Gesellschaften*. Waxmann.
- Venables, W. N., & Ripley, B. D. (2002). *Modern applied statistics with s* (Fourth). Springer. <https://www.stats.ox.ac.uk/pub/MASS4/>
- West, B., Dunbar, R., Garland, C., & Grigolini, P. (2023). *Fractal structure of human and primate social networks optimizes information flow*. <https://doi.org/10.1101/2023.02.23.529431>
- West, G. B. (2017). *Scale: the universal laws of growth, innovation, sustainability, and the pace of life in organisms, cities, economies, and companies*. Penguin Press.
- Whitridge, P. (2016). Fractal Worlds: An Archaeology of Nested Spatial Scales. *ARCTIC*, 69(5), 1–10. <https://doi.org/10.14430/arctic4659>
- Whittle, A. (2022). The Danube in Prehistory. *European Journal of Archaeology*, 25(1), 133137. <https://doi.org/10.1017/eaa.2021.59>
- Whittle, A., & Bickle, P. (2014). *Early farmers: the view from archaeology and science* (First edition., Vol. 198). Published for the British Academy by Oxford University Press.
- Wickham, H. (2016). *ggplot2: Elegant graphics for data analysis* (2nd ed. 2016). Springer International Publishing : Imprint: Springer. <https://doi.org/10.1007/978-3-319-24277-4>
- Wilk, R. R. (1983). Little house in the jungle: The causes of variation in house size among modern Kekchi Maya. *Journal of anthropological archaeology*, 2(2), 99116. [https://doi.org/10.1016/0278-4165\(83\)90009-0](https://doi.org/10.1016/0278-4165(83)90009-0)
- Wilk, R. R., & Rathje, W. L. (1982). Household Archaeology. *American Behavioral Scientist*, 25(6), 617–639. <https://doi.org/10.1177/000276482025006003>
- Winkelmann, K., Bátorá, J., Hohle, I., Kalmbach, J., Müller-Scheeßel, N., & Rassmann, K. (2020). *Revealing the general picture: Magnetic prospection on the multiperiod site of*

- vráble 'fidvár'/'velké lehemby'/'farské' (M. Furholt, I. Cheben, J. Müller, A. Bistáková, M. Wunderlich, & N. Müller-Scheeßel, Eds.; pp. 33–52). Sidestone Press.
- Yoffee, N. (1993). *Too many chiefs? (or, Safe texts for the '90s)* (N. Yoffee & A. Sherrett, Eds.; 1st ed., pp. 60–78). Cambridge University Press. <https://doi.org/10.1017/CBO9780511720277.007>
- Yoffee, N. (2005). *Myths of the archaic state : Evolution of the earliest cities, states, and civilizations*. Cambridge University Press.
- Yule, G. U. (1925). A mathematical theory of evolution, based on the conclusions of dr. J. C. willis. *Philosophical Transactions of the Royal Society of London. Series B*, 213(402-410), 21–87. <https://doi.org/10.1098/rstb.1925.0002>
- Zhou, W.-X., Sornette, D., Hill, R. A., & Dunbar, R. I. M. (2005). Discrete hierarchical organization of social group sizes. *Proceedings of the Royal Society B: Biological Sciences*, 272(1561), 439–444. <https://doi.org/10.1098/rspb.2004.2970>
- Zhukov, D. S., Kanishchev, V. V., & Lyamin, S. K. (2016). Application of the Theory of Self-Organized Criticality to the Investigation of Historical Processes. *SAGE Open*, 6(4), 2158244016683216. <https://doi.org/10.1177/2158244016683216>
- Zimmermann, A. (2012a). *Das hofplatzmodell - entwicklung, probleme, perspektiven* (S. Wolfram & H. Stäuble, Eds.; pp. 11–19). Universität Leipzig; Landesamt für Archäologie - Freistaat Sachsen.
- Zimmermann, A. (2012b). Cultural cycles in Central Europe during the Holocene. *Quaternary International*, 274, 251–258. <https://doi.org/10.1016/j.quaint.2012.05.014>
- Zipf, G. K. (1949). *Human behavior and the principle of least effort: an introduction to human ecology*. Addison-Wesley Press.



# **Appendix A**

## **This is my first appendix**

Something from the distfit analyses?? Are there enough results in the tables in chapters?

APPENDIX A. THIS IS MY FIRST APPENDIX

## **Appendix B**

### **This is my second one**

Things to include here: D\_L results table Images used in analysis, both synthetic and empirical